

Bacterial and fungal biofilms contribute enormously to the persistence of many life-threatening infections, causing millions of deaths annually. In addition, bacteria and fungi growing as biofilms are up to 1.000 times more resistant to conventional antimicrobial treatments, resulting in a significant economic burden and challenging diagnosis and treatment. Therefore, there is a need to search for new reliable tools to study biofilm formation dynamics to improve treatment strategies.

This doctoral thesis aims to set up an impedance-based system to study biofilm formation and dynamics of bacterial (gram-positive and gram-negative) and fungal species, as well as complex multi-species biofilms such as subgingival plaque collected from patients with chronic periodontitis.

After the impedance system is set up, the specific objectives of the doctoral thesis are its application as a tool in the identification of effective treatment against persistent biofilms, testing new antimicrobial and anti-biofilm compounds, and the evaluation of novel self-propelled nanoparticles on the eradication of multi-resistant *S. aureus* biofilms. Finally, a clinical application of the impedance system is proposed, aiming at determining the best individual antibiotic therapy in dental clinics (personalized use of antibiotics).

Towards personalized medicine in antibiotic treatment:
The development of a Real-Time Cell Analysis system for biofilm studies

Miglė Žiemytė

Doctoral Thesis

Towards personalized medicine in antibiotic treatment: Development of a Real-Time Cell Analysis system for biofilm studies

Author: Miglė Žiemytė

Thesis directors: Alejandro Mira Obrador and
María Desamparados Ferrer García

Valencia, May 2023



UNIVERSITAT
POLITÈCNICA
DE VALÈNCIA

Towards personalized medicine in antibiotic treatment: Development of a Real-Time Cell Analysis system for biofilm studies

MIGLĖ ŽIEMYTĖ

Doctoral Thesis



UNIVERSITAT
POLITÈCNICA
DE VALÈNCIA

The Polytechnic University of Valencia, Doctoral School in Biotechnology
Genomics & Health Department, FISABIO Foundation, Oral Microbiome Laboratory



GENERALITAT
VALENCIANA



Fundació
Fisabio



OralMicrobiomeLab

Directors: Alejandro Mira Obrador and María Desamparados Ferrer García

Work performed at Genomics & Health Department at FISABIO Foundation and described in this doctoral thesis was supported by the Spanish Ministry of Science, Innovation and Universities scholarship **FPU17/01302** to Miglė Žiemytė and a grant **RTI2018-102032-B-I00** to Alex Mira Obrador.

ACKNOWLEDGEMENTS

First of all, I would like to thank my supervisors, *Alex Mira* and *Mariam Ferrer*, for their guidance and persistent support. *Alex*, it has been a pleasure to form a part of your team. No words can describe how thankful I am for everything I have learned from you. Special thanks for embracing me to grow as a scientist and independent researcher, and hopefully, you know that you are the best boss a PhD student can ask for. *Mariam*, thank you for your invaluable help with all our experiments, great ideas, for colouring every single day with your contagious smile, and for just being there for me all these years (it is pretty amazing to have a boss and a friend in the same person and I will always appreciate all the great memories we shared)... and of course, I couldn't be happier to be your first PhD student. **THANKS!**

I am also very grateful for *Oral Microbiome Lab* (OML) members – you all are so unique, and I could not ask for a better team ever! Thank you for your companionship and for providing a friendly work atmosphere, smarties. I will always cherish the moments that we share!

Beyond thankful to *Miguel* for all the bioinformatic analyses, great personal and academic advice, and constant support. No words can describe how grateful I am for our friendship, for you always lifting me up and having my back. Cheers to those four great papers we worked on together and to all the amazing memories we shared throughout time (and, of course, to many more even greater ones to come)! **ZCS and AT1m visada!**

Special thanks to *Elena* - for all your help in the lab, for caring about me daily, for all the great conversations and unforgettable memories! I am thrilled to have met you! You are a gem! Keep going!

Oscar, los miércoles siempre serán para ti! ¡Gracias por todo!

I would also like to thank *Contxa* and *Sandra* for making lab work way easier, *Alejandro Artacho* for bioinformatic analyses, and all the great scientists from Genomics and Health Area for their help and advice during these years.

Sincere “**AČIŪ**” to prof. *Rimantas Daugelavičius* (Vytautas Magnus University) who sparked my interest in microbiology. Thank you very much for always believing in me. “**Gracias**” to *Baltasar Mayo* (IPLA, Asturias) and his research team for teaching me my very first microbiology assays. It was a pleasure to stay in your lab in the summer of 2014. **Thanks to Maria Angeles Tormo-Mas** for three great years in Instituto investigación Sanitaria La Fe. It's been an absolute pleasure to learn and grow as a scientist in your lab.

Special mention to *Alicia Ros* for helping with all the legal stuff.

Thanks to my academic supervisor *Maria Antonia Ferrus* and for *Rosa Montes* for making UPV feel at home and for giving great academic advice.

Beyond thankful to *Peter Zilm* and *Stephen Kidd* and their research teams for a unique collaboration and three unforgettable months in Adelaide at the end of 2022. I can't wait to see all of you again (Especially you, *Kev*! **Thank you for everything!**)

Special thanks to the greatest collaborators that I could ever ask for – *Juan Carlos Rodriguez* and *Mari Paz Ventero* (ISABIAL, Alicante), *Jaione Valle* and her research group (Pamplona), perio team from the University of Valencia and, of course, an enormous **THANKS** for the NANOteam led by *Ramon Martinez-Manez*. It is pretty amazing what we have done with those nanoparticles, isn't it?

Given that my Ph.D. journey had various ups and downs, I would like to thank my family and friends for their unconditional support and encouragement. It is incredible to be surrounded by amazing people who truly encourage and inspire me daily.

Special thanks to:

Miglė II – AČIŪ už paguodą, supratimą, sugebėjimą patarti ir už visus prisiminimus, kuriais dalinomės, dalinamės ir dalinsimės. Niekada nemaniau, kad Valencijoje surasiu ne tik geriausią draugę, bet ir sesę. Neįsivaizduoju viso šio “tezės kelio” be tavęs, mūsų kelionių, juokų ir istorijų. “Dabar geriausi mūsų vakarai” arba ***“The sweet life of Miglė and Miglė”!***

Neringa – už visus nesuskaičiuojamus pokalbius, paskatinimus, AT analizes ir draugystę kuria dalinamės daugiau negu 15 metų. Nes kai kurie skirtumai yra visai ne skirtumai, o tik tai ko reikia, kad papildytume viena kitą. I love you, my favorite ENFP.

To *Mercedes* – my first and the best lab mate ever. Thank you for showing me how to prepare my first PCR MIX, for invaluable advice and support, for listening to all my stories, and for all the unforgettable moments we shared since the summer of 2015. It was and still is a pleasure to grow as a person (and as a scientist) having a friend like you by my side. Big kiss for *Margarita*!

Salome – it is pretty amazing how time has this extraordinary manner to show who really matters. Thank you for EVERYTHING and cheers to all the battles that we have won!

Merve, civciv, thank you for sticking by my side since 2011. It is a blessing to have a friend like you. “Tree or three?”

Katy, thank you for being in my life since day one in Valencia! So many great memories and I couldn't be happier to have you in my life!

To “MAYONESA LUNCH” team for all the amazing coffee breaks, lunches, pixwords, and lots of laughs over these years. It is such a blessing to have friends like you.

Ally, thanks for bringing so many (very needed) colours into my life! There is a saying that some friends are like family and for me, you have been one of those friends since the first day we met at FISABIO. Thanks for being the one who always sees things from the bright side, for coping with all ups and downs, for unforgettable coffee breaks and of course, “*Grazie*” for the incredibly delicious Italian food that you cooked for all of us over these years! Cheers to all the

great memories (there are so many of them that I can't even put them into words) and all the amazing things to come! Thank you! Ci vediamo dopo.

Dani, I am so thankful for your funny stories and all the great moments that we shared together! Keep being awesome and “tell me something funny, MY FRIEND”. (Confirmation to what you have already told me: “no hay nanopartículas que destruyen este biofilm de amistad y love que tenemos”)!

Marta, it is not easy to adapt to a new country, language, and workplace, but I am beyond thankful to you for being so friendly since the first day we met at FISABIO. Thanks for all the great conversations, vocal messages, laughter, memories, brunches, and support during these years. You are such a gem, and I couldn't be happier that we ended up having this great friendship! Cheers to FPU'17.

Ivan, a huge **thank YOU** for always sticking around! I could say so many great things about our friendship, which started preparing bacterial growth media and successfully bloomed after you left FISABIO! I am so blessed to have a personal make-up artist and a friend like you!

Bea Neves, thank you for all the unforgettable moments, laughter, chats, and understanding. So many kilometers away, but always in my heart.

Valeria, thank you for showing up at FISABIO when I really needed a friend. You are a truly fantastic scientist (and even more fantastic person), and I can't wait to see you having your lab one day. See you soon! *Salute!*

To *Oliver* for proofreading the dalba paper and just for being you. Cheers!

Raz, Thanks for showing me what and who really matters. “Korčula”.

To *Alex* for our endless friendship, amazing “*Santorini*” days and all the great moments, dreams, hopes and conversations we have shared throughout all these years. You are so unique, and thanks to you, I will always have a piece of Greece in my heart. Ευχαριστώ.

Nishadi, I can't believe how lucky I am to have a friend like you. Thanks for the fantastic moments in Adelaide and see you soon (“*not related at all*”).

Henkiui, Tučkui ir visiems kurie prisidėjo prie to kokia esu dabar.

It is pretty challenging to mention everyone but **THANK YOU** so much to every person I met during my Ph.D. journey. You are all the reason why my days were so colourful and full of great and unforgettable moments.

Ir žinoma pats didžiausias AČIŪ– *mamai* – nes tik stipri moteris gali užauginti kitą tokią pat stiprią moterį. **Ačiū TAU už viską.**

Table of Contents

ABBREVIATIONS USED IN THE CURRENT THESIS.....	9
ORIGINAL PUBLICATIONS	11
SUMMARY	12
RESUMEN – Castellano.....	15
RESUM – Valencià.....	18
OBJECTIVES	21
INTRODUCTION	22
1. Microbial biofilms	22
2. Biofilm formation	24
3. Biofilms and quorum sensing	27
4. Biofilm forming microorganisms of clinical relevance	28
4.1. <i>Staphylococcus</i> spp.....	28
4.2. <i>Pseudomonas</i> spp.....	29
4.3. <i>Candida</i> spp.	30
5. Oral biofilms	31
6. Biofilm study methodologies	34
6.1. <i>In vitro</i> biofilm models	34
6.2. Microscopy	38
6.3. Real-Time Cell Analyzer by impedance measurements	39
6.4. <i>In vivo</i> biofilm models	41
7. Biofilm treatment	44
7.1. Prevention of biofilm formation.....	45
7.2. Biofilm weakening.....	46
7.3. Biofilm disruption.....	46
7.4. Biofilm killing.....	47
8. Nanotechnology and biofilms	48
9. The problem of persistence in biofilm cells.....	49
10. Rationale of this thesis	50
CHAPTER I	
Effect of dalbavancin on staphylococcal biofilms when administered alone or in combination with biofilm-detaching compounds.....	52
ABSTRACT.....	52

INTRODUCTION	53
MATERIALS AND METHODS	55
RESULTS	58
DISCUSSION	68
CHAPTER I SUPPLEMENTARY INFORMATION	72
CHAPTER II	
Real-time monitoring of <i>Pseudomonas aeruginosa</i> biofilm growth dynamics and persister cell's eradication.....	75
ABSTRACT	75
INTRODUCTION	76
MATERIALS AND METHODS	77
RESULTS	82
DISCUSSION	96
CHAPTER II SUPPLEMENTARY INFORMATION	98
CHAPTER III	
Real-time monitoring of biofilm growth identifies andrographolide as a potent antifungal compound eradicating <i>Candida</i> biofilms	103
ABSTRACT	103
INTRODUCTION	104
MATERIALS AND METHODS	106
RESULTS	110
DISCUSSION	120
CHAPTER III SUPPLEMENTARY INFORMATION	124
CHAPTER IV	
Personalized antibiotic selection in periodontal treatment improves clinical and microbiological outputs	128
ABSTRACT	128
INTRODUCTION	129
MATERIALS AND METHODS	130
RESULTS	137
DISCUSSION	147
CHAPTER IV SUPPLEMENTARY INFORMATION	152
CHAPTER V	
Self-propelled nanoparticles for bacterial biofilm eradication.....	177

ABSTRACT.....	177
INTRODUCTION	178
MATERIALS AND METHODS.....	179
RESULTS	184
Effect of H ₂ O ₂ on planktonic and biofilm growth.....	184
DISCUSSION	191
CHAPTER V SUPPLEMENTARY INFORMATION	195
GENERAL DISCUSSION	197
1. The challenge of studying and combating biofilms	197
2. Are all biofilms the same?	198
3. Antibiotic susceptibility tests for biofilms	200
4. Conventional therapies against biofilms	202
5. Novel strategies against biofilms	206
6. Future prospects for biofilm studies.....	210
CONCLUSIONS.....	217
ANNEX A – Published version of CHAPTER I	220
ANNEX B – Published version of CHAPTER II	221
REFERENCES	222

ABBREVIATIONS USED IN THE CURRENT THESIS

AFM – atomic force microscopy

bCD – β -cyclodextrins

BOP – bleeding on probing

CAL – clinical attachment level

CAZ – ceftazidime

CIP – ciprofloxacin

CFU – colony forming unit

CI – cellular index

CLSM – confocal laser scanning microscopy

COL – colistin

CSLI – clinical and laboratory standards institute

CV – crystal violet

EUCAST - European Committee on Antimicrobial Susceptibility Testing

eDNA – extracellular DNA

EPS –extracellular polymeric substances

F – protease ficin

FISH – fluorescence in situ hybridization

IMP – imipenem

NAC – N-acetyl-L-cysteine

MBIC – Minimum Biofilm Inhibitory Concentration

MEM – meropenem

NMs – mesoporous silica nanoparticles

MIC – minimum inhibitory concentration

MRSA – methicillin-resistant *Staphylococcus aureus*

MRSE – methicillin-resistant *Staphylococcus epidermidis*

QS – quorum sensing

PD – periodontal pocket depth

Pt – platinum

RT-Culture – real-time culture

RTCA – real-time cell analysis

SEM – scanning electron microscopy

SCVs – small colony variants

TSB-glu – TSB supplemented with 0.25% of glucose

TOB – tobramycin

TZP -piperacillin-tazobactam

V – vancomycin

V-Rh B – rhodamine B-functionalized vancomycin

wt – wild type

ORIGINAL PUBLICATIONS

This doctoral thesis is based on the following publications:

Žiemytė M, Rodríguez-Díaz JC, Ventero MP, Mira A, Ferrer MD. Effect of Dalbavancin on Staphylococcal Biofilms When Administered Alone or in Combination with Biofilm-Detaching Compounds. *Front Microbiol.* 2020 Apr 17;11:553. Doi: 10.3389/fmicb.2020.00553. PMID: 32362877; PMCID: PMC7180179

Žiemytė M, Carda-Diéguez M, Rodríguez-Díaz JC, Ventero MP, Mira A, Ferrer MD. Real-time monitoring of *Pseudomonas aeruginosa* biofilm growth dynamics and persister cells' eradication. *Emerg Microbes Infect.* 2021 Dec;10(1):2062-2075. Doi: 10.1080/22221751.2021.1994355. PMID: 34663186; PMCID: PMC8583918.

Žiemytė M, Escudero A, Díez, P, Ferrer MD, Murguía JR, Martí-Centelles V, Mira A and Martínez-Mañez R. Ficin-Cyclodextrin-Based Docking Nanoarchitectonics of Self-Propelled Nanomotors for Bacterial Biofilm Eradication. *Chem. Mater.* 2023 (*IN PRESS*). Doi: 10.1021/acs.chemmater.3c00587.

Other publications:

Matilla-Cuenca L, Gil C, Cuesta S, Rapún-Araiz B, **Žiemytė M**, Mira A, Lasa I, Valle J. Antibiofilm activity of flavonoids on staphylococcal biofilms through targeting BAP amyloids. *Sci Rep.* 2020 Nov 3;10(1):18968. Doi: 10.1038/s41598-020-75929-2. PMID: 33144670; PMCID: PMC7641273

Lee J, Carda-Diéguez M, **Žiemytė M**, Vreugde S, Cooksley C, Crosby HA, Horswill AR, Mira A, Zilm PS, Kidd SP. Functional *mgrA* Influences Genetic Changes within a *Staphylococcus aureus* Cell Population over Time. *J Bacteriol.* 2022 Sep 26:e0013822. doi: 10.1128/jb.00138-22. Epub ahead of print. PMID: 36154359.

SUMMARY

Background: Bacterial and fungal biofilms contribute enormously to the persistence of many life-threatening infections, causing millions of deaths annually. In addition, bacteria and fungi growing as biofilms are up to 1.000 times more resistant to conventional antimicrobial treatments, resulting in a significant economic burden and challenging diagnosis and treatment. Therefore, there is a need to search for new reliable tools to study biofilm formation dynamics to improve treatment strategies.

Objectives: This doctoral thesis aims to set up an impedance-based system to study biofilm formation and dynamics of bacterial (gram-positive and gram-negative) and fungal species, as well as complex multi-species biofilms such as subgingival plaque collected from patients with chronic periodontitis. After the impedance system is set up, the specific objectives of the doctoral thesis are its application as a tool in the identification of effective treatment against persistent biofilms, testing new antimicrobial and anti-biofilm compounds, and the evaluation of novel self-propelled nanoparticles on the eradication of multi-resistant *S. aureus* biofilms. Finally, a clinical application of the impedance system is proposed, aiming at determining the best individual antibiotic therapy in dental clinics (personalized use of antibiotics).

Methods: Real-Time cell analyzer (RTCA) or CELLigence system was used to study bacterial (*Staphylococcus aureus*, *Staphylococcus epidermidis* and *Pseudomonas aeruginosa*) and fungal (*Candida* spp.) biofilm formation growth dynamics and eradication patterns. Different conventional antibiotics, antifungals, and anti-biofilm compounds alone and in combination were tested to assess their *in vitro* effect on biofilm prevention and disruption. Furthermore, real-time impedance measures were used to test the effect of novel self-propelled nanoparticles on pre-formed and mature *S. aureus* biofilms. The results obtained using the xCELLigence system were confirmed by standard end-point methodologies for biofilm study, such as crystal violet staining, viable cell counts, and different microscopic techniques. In addition, genomic analyses were carried out to study persistent cell fractions within *P. aeruginosa* biofilms. Lastly, a randomized, double-blind clinical trial of two parallel groups of patients with chronic periodontitis was performed. The clinical and microbiological improvement observed in patients after the antibiotic treatment suggested by the impedance system and by standard methods based on the

quantification of periodontal pathogens using PCR-hybridization was compared. Therefore, patients were randomly divided into two groups (xCELLigence and classical method of antibiotic selection) and treated with an antibiotic suggested by each methodology. The improvement in clinical parameters (periodontal pocket depth, clinical attachment level, bleeding on probing and plaque presence), as well as changes in oral microbiota (by 16S rRNA gene sequencing of periodontal samples), were evaluated after one and two months of treatment.

Results and discussion: This doctoral thesis comprehensively assessed biofilm growth dynamics and eradication patterns of gram-positive bacterial biofilms (Staphylococcal), gram-negative (*Pseudomonas aeruginosa*), fungal (*Candida* spp.) and complex multispecies biofilms (subgingival plaque biofilms collected from patients with periodontal disease) using the xCELLigence system based on impedance measurements in real-time. Specifically, the inhibitory properties of a new lipoglycopeptide group antibiotic, dalbavancin, were proven, both alone and in combination with biofilm anti-aggregation compounds against staphylococcal biofilms. Secondly, the effect of different conventional antibiotics on biofilm prevention and disruption was tested on *P. aeruginosa* biofilms and persister cell fractions were identified after the exposure of mature pseudomonas biofilms to some antibiotics. Identified persister cells were eradicated using mannitol and subinhibitory ciprofloxacin combination. This suggests that the combined use of mannitol together with conventional antibiotics could be a good alternative in the treatment of biofilm-associated infections and prevent the appearance of persister cell populations. In addition, fungal biofilm formation of different *Candida* spp. isolates was studied for the first-time using impedance measures in real-time. Moreover, the impedance system allowed to study the effect of andrographolide, the main bioactive compound of the medicinal plant *Andrographis paniculata* and this compound showed an extraordinary anti-biofilm agent against fungal biofilms. In addition, novel mesoporous silica nanoparticles with movement, propelled by low levels of H₂O₂, were revealed to be effective in pre-formed and mature *S. aureus* biofilm. Finally, the randomized, double-blind clinical trial showed that the impedance-based system is a reliable, cheap and effective tool for studying complex periodontal biofilms in real time. Besides, it enabled a selection of individualized antibiotic treatment for patients with periodontal disease as better clinical and microbiological outcomes were observed when compared to the conventional PCR-hybridization method.

The overall results of this thesis suggest that this impedance system could be used as a fast and reproducible tool in biofilm research to test the effect of new antimicrobial compounds and nanomaterials with anti-biofilm properties, as well as in clinical settings for the evaluation of antibiotic susceptibility of biofilm-associated infections.

RESUMEN – Castellano

Antecedentes: Las biopelículas bacterianas y fúngicas contribuyen enormemente a la persistencia de muchas infecciones graves y potencialmente mortales, las cuales anualmente provocan millones de defunciones. Además, estas bacterias y hongos que crecen adheridas formando biopelículas son hasta 1.000 veces más resistentes a los tratamientos antimicrobianos convencionales, generando una carga económica significativa y dificultando su diagnóstico y tratamiento. Por tanto, es necesario buscar nuevas herramientas fiables para estudiar la dinámica de formación de biopelículas con el fin de mejorar las estrategias de tratamiento.

Objetivos: El objetivo general de la tesis doctoral es la puesta a punto de un sistema basado en medidas de impedancia eléctrica para el estudio de la formación y dinámica de crecimiento de las biopelículas bacterianas (gram-positivas y gram-negativas) y fúngicas, así como de biopelículas complejas multi-especie como las de la placa dental subgingival de muestras periodontales humanas. Tras la puesta a punto del sistema, los objetivos específicos de la tesis doctoral son su aplicación como herramienta en la identificación de tratamientos efectivos contra biopelículas persistentes, la búsqueda de nuevos compuestos antimicrobianos con actividad anti-biofilm, así como la evaluación de novedosas nanopartículas autopropulsadas para la erradicación de biofilms multirresistentes. Finalmente, se ha evaluado su aplicación clínica directa en la selección de la terapia antibiótica para el tratamiento personalizado de pacientes con enfermedad periodontal.

Métodos: Para el estudio de las dinámicas de crecimiento y los patrones de erradicación de la formación de biopelículas bacterianas (*Staphylococcus aureus*, *Staphylococcus epidermidis* y *Pseudomonas aeruginosa*) y fúngicas (*Candida* spp.) se ha utilizado el sistema xCELLigence de análisis celular en tiempo real (del inglés RTCA). Diferentes antibióticos convencionales, antifúngicos y compuestos anti-biofilm han sido testados, solos y en combinación, para determinar su efecto *in vitro* en la prevención y erradicación de las biopelículas. Además, el sistema también ha sido empleado para evaluar el efecto de nuevas nanopartículas autopropulsadas en la eliminación de biopelículas de *S. aureus* maduras. Por otro lado, para la confirmación de los resultados obtenidos con el sistema xCELLigence se han empleado diferentes metodologías estándares de estudio de los biofilms a tiempo final como son la tinción con cristal violeta, los recuentos de células viables y diferentes técnicas de microscopía. Además,

se han realizado análisis genómicos para el estudio de las variantes bacterianas persistentes de *P. aeruginosa*. Por último, se ha llevado a cabo un ensayo clínico aleatorizado doble ciego de dos grupos paralelos en pacientes con periodontitis crónica donde se comparó la mejora clínica y microbiológica observada en los pacientes tras el tratamiento antibiótico sugerido por el sistema de impedancia o por los métodos actuales basados en la cuantificación de patógenos periodontales mediante PCR-hibridación. Los pacientes fueron divididos aleatoriamente en 2 grupos (xCELLigence vs. método actual de selección de antibiótico), y fueron tratados con el antibiótico sugerido en cada caso. Al mes y a los dos meses tras el tratamiento, se evaluó en ambos grupos la mejora observada en los parámetros clínicos (profundidad de las bolsas periodontales, sangrado al sondaje, pérdida de inserción clínica y la presencia de placa) así como los cambios en microbiota oral, mediante secuenciación del gen 16S rRNA de las muestras periodontales

Resultados: En esta tesis doctoral se ha evaluado exhaustivamente las dinámicas de crecimiento y los patrones de erradicación de biopelículas bacterianas gram-positivas (estafilocócicas) y gram-negativas (*Pseudomonas aeruginosa*), fúngicas (*Candida* spp.) y de biopelículas complejas multiespecies (placa dental subgingival de pacientes con enfermedad periodontal) utilizando el sistema xCELLigence basado en mediciones de valores de impedancia en tiempo real. Específicamente, se ha demostrado que un nuevo antibiótico del grupo de los lipoglucopeptidos, la dalbavancina, tiene propiedades inhibitorias sobre las biopelículas estafilocócicas, testado solo y en combinación con otros compuestos antiagregación. En segundo lugar, se ha evaluado el efecto de diferentes antibióticos convencionales tanto en la prevención como en la erradicación de las biopelículas en *P. aeruginosa*. Además, tras la exposición de las biopelículas maduras de *P. aeruginosa* a determinados antibióticos, se han podido identificar una fracción de células persistentes que mediante el uso combinado con manitol se consiguieron erradicar. Lo que sugiere que el uso combinado del manitol junto con los antibióticos convencionales podría ser una buena alternativa en el tratamiento de infecciones asociadas a biopelículas y evitar la aparición de células persistentes. Por otro lado, se ha estudiado la formación de biopelículas fúngicas de *Candida* spp. en tiempo real por primera vez, utilizando medidas de impedancia. Con este sistema, se ha podido evaluar el efecto anti-biofilm del compuesto natural andrografolida, que es el principal componente bioactivo de la planta medicinal *Andrographis paniculata*, y que ha resultado ser un extraordinario agente anti-biofilm. Además, se ha testado el

efecto de novedosas nanopartículas porosas de sílice con movimiento, impulsadas por concentraciones bajas de H_2O_2 , que han mostrado ser eficaces para la erradicación de biopelículas maduras de *S. aureus*. Finalmente, el ensayo clínico aleatorizado doble ciego llevado a cabo ha demostrado que el sistema basado en medidas de impedancia es una herramienta rápida, barata y eficaz para el estudio en tiempo real de las biopelículas multiespecie de muestras periodontales, al permitir una selección del tratamiento antibiótico individualizado con mejores resultados clínicos en pacientes con enfermedad periodontal comparado con los métodos actuales.

En conclusión, los resultados de la tesis doctoral sugieren que este sistema de impedancia podría usarse como herramienta rápida y reproducible en la investigación de biopelículas, tanto para testar el efecto de nuevos compuestos o nanomateriales antimicrobianos con propiedades anti-biofilms, así como en entornos clínicos para la evaluación de la susceptibilidad a los antibióticos de infecciones causadas por biopelículas.

RESUM – València

Antecedents: Les biopel·lícules bacterianes i fúngiques contribueixen en gran manera a la persistència de moltes infeccions greus i potencialment mortals les quals provoquen anualment milions de morts. A més, estes bactèries i fongs que creixen adherides en forma de biopel·lícules son fins a 1000 vegades més resistents als tractaments antimicrobians convencionals, generant una càrrega econòmica significativa i dificultant el diagnòstic i tractament. Per això, es necessari trobar noves eines fiables per a estudiar la dinàmica de formació de biopel·lícules amb l'objectiu de millorar les estratègies de tractament.

Objectius: El objectiu general de la tesis doctoral es la posta a punt de un sistema basat en mesures d'impedància elèctrica per al estudi de la formació i dinàmica de creixement de les biopel·lícules bacterianes (gram-positives i gram-negatives) i fúngiques, així com de biopel·lícules complexes mutiespècie com les de la placa dental subgingival de mostres periodontals humanes. Una vegada posat a punt el sistema, els objectius específics de la tesis doctoral son la aplicació com a eina de la identificació de tractaments efectius contra biopel·lícules persistents, la recerca de nous compostos antimicrobians amb activitat antibiopel·lícula, així com la avaluació de noves nanopartícules autopropulsades per a l'eliminació de biofilms multiresistents. Finalment, s'ha avaluat l'aplicació clínica directa en la selecció de la teràpia antibiòtica per al tractament personalitzat de pacients amb periodontitis.

Mètodes: Per al estudi de les dinàmiques de creixement i els patrons d'erradicació de la formació de biopel·lícules bacterianes (*Staphylococcus aureus*, *Staphylococcus epidermidis* y *Pseudomonas aeruginosa*) y fúngiques (*Candida* spp.) s'ha utilitzat el sistema xCELLigence de anàlisi cel·lular en temps real (del anglès RTCA). Diferents antibiòtics convencionals, antifúngics i compostos antibiofilm han sigut testats per si mateixos o en combinació per a determinar el seu efecte *in vitro* en la prevenció i erradicació de les biopel·lícules. A més, el sistema també ha sigut utilitzat per a avaluar l'efecte de noves nanopartícules autopropulsades en l'eliminació de biopel·lícules de *S. aureus* madures. Per un altre lloc, per a la confirmació dels resultats obtinguts amb el sistema xCELLigence s'han utilitzat diferents metodologies estàndards d'estudi dels biofilms a temps final com ara la tinció amb cristall violeta, els recomptes de cèl·lules viables i diferents tècniques de microscòpia. A més, s'han realitzat anàlisis genòmics per al estudi de variants bacterianes persistents de *P. aeruginosa*. Per últim, s'ha dut a terme un

assaig clínic aleatoritzat doble cec de dos grups paral·lels en pacients amb periodontitis crònica on es va comparar la millora clínica i microbiològica observada en els pacients després del tractament antibiòtic suggerit per el sistema d'impedància o per els mètodes actuals basats en la quantificació de patògens periodontals mitjançant PCR-hibridació. Els pacients varen ser dividits aleatòriament en dos grups (xCELLigence vs mètode actual de selecció d'antibiòtics) i varen ser tractats amb el antibiòtic suggerit en cadascun del casos. Després d'un i dos mesos de tractament es va avaluar en ambos grups la milloria observada en els paràmetres clínics (profunditat de les bosses periodontals, sagnat al sondatge, pèrdua de inserció clínica i la presència de placa dental) així com els canvis en la microbiota oral mitjançant la seqüenciació del gen 16S rRNA de les mostres periodontals.

Resultats: En aquesta tesis doctoral s'ha avaluat exhaustivament les dinàmiques de creixement i els patrons d'erradicació de biopelícules bacterianes gram-positives (estafilocòccies) i gram-negatives (*Pseudomonas aeruginosa*), fúngiques (*Candida spp.*) i de biopelícules complexes multiespècies (placa dental subgingival de pacients amb periodontitis) utilitzant el sistema xCELLigence basat en mesures de valors de impedància en temps real. Específicament, s'ha demostrat que un nou antibiòtic del grup dels lipoglucopeptids, la dalbacancina, té propietats inhibidores sobre les biopelícules estafilocòccies, tant per si sol com en combinació amb altres compostos antiagregadors. En segon lloc, s'ha avaluat el efecte de diferents antibiòtics convencionals tant en la prevenció com en l'erradicació de les biopelícules en *P. aeruginosa*. A més, després de l'exposició de les biopelícules madures de *P. aeruginosa* a determinats antibiòtics s'han pogut identificar una fracció de cèl·lules persistents que mitjançant l'ús combinat amb manitol es van poder erradicar. Per lo tant l'ús combinat del manitol amb els antibiòtics convencionals podria ser una bona alternativa per al tractament d'infeccions associades a biopelícules i evitar així l'aparició de cèl·lules persistents. D'altra banda, s'ha estudiat la formació de biopelícules fúngiques de *Candida spp.* en temps real per primera vegada utilitzant mesures d'impedància. Amb aquest sistema, s'ha pogut avaluar l'efecte antibiofilm del compost natural andrografolida, que es el principal component bioactiu de la planta medicinal *Andrographis paniculata*, i que ha resultat ser un extraordinari agent antibiofilm. A més, s'ha avaluat l'efecte de noves nanopartícules poroses de sílice amb moviment impulsades per concentracions baixes de H₂O₂ que han mostrat ser efectives per a l'erradicació de biopelícules madures de *S. aureus*. Finalment, l'assaig clínic aleatoritzat doble cec portat a terme ha

demostrat que el sistema basat en mesures d'impedància es una eina ràpida, barata i eficaç per al estudi en temps real de les biopelícules mutiespècie de mostres periodontals, al permetre una selecció del tractament antibiòtic individualitzat amb millors resultats clínics en pacients amb periodontitis comparat amb mètodes actuals.

En conclusió, els resultats de la tesis doctoral suggereixen que el sistema d'impedància podria ser útil com a eina ràpida i reproduïble en la investigació de biopelícules tant per a testar l'efecte de nous compostos o nanomaterials antimicrobians amb propietats antibiofilms així com en ambients clínics per a l'avaluació de la susceptibilitat als antibiòtics d'infeccions causades per biopelícules.

OBJECTIVES

The main objective of this doctoral thesis is to set up a non-invasive, impedance-based, *in vitro* system to quantify biofilm growth in real-time for (a) gram-positive, (b) gram-negative, (c) fungal and (d) polymicrobial (oral) biofilm studies with different purposes:

1. To study biofilm formation and dynamics.
2. To test new antimicrobials and anti-biofilm compounds.
3. To optimize treatment strategy in clinical settings (personalized use of antibiotics).

The specific aims of the work, which will be addressed in each chapter of the present thesis, are:

- I-** To assess staphylococcal biofilm growth dynamics in real-time and test the effect of a new lipoglycopeptide antibiotic (dalbavancin) on biofilm formation and eradication alone and in combination with anti-biofilm compounds.
- II-** To set up the impedance system to measure *Pseudomonas aeruginosa* biofilm growth and dynamics, evaluate the effect of conventional antibiotics on biofilm formation and disruption, and detect dormant persister cells and evaluate their possible eradication.
- III-** To study *Candida* spp. capacity to form biofilms using different growth media, as well as to evaluate the effect of different antifungals and novel natural compounds on biofilm formation and eradication.
- IV-** To study multi-species (subgingival plaque) biofilm growth in real-time, in order to select the best individual antibiotic treatment strategy for patients with chronic periodontal disease, and clinically evaluate the improvement of impedance-based measurements compared to standard antibiotic selection methodologies.
- V-** To set up the impedance system for *in vitro* testing novel nanoparticles against microbial biofilm infections.

INTRODUCTION

1. Microbial biofilms

Generally speaking, microorganisms can be found in two distinct states: planktonic and sessile cells. Planktonic cells are defined as “free-floating” cells, while sessile cells are generally associated with surfaces and can form biofilms¹⁻³. Thus, biofilms are described as bacterial or fungal cell aggregates immobilized in a self-produced extracellular matrix composed of different biopolymers such as proteins, polysaccharides, and extracellular DNA (eDNA)^{4,5}. Extracellular polymeric substances (EPS) matrix provides structural stability and allows biofilm-embedded microorganisms to survive in extreme conditions and different environments^{6,7}. Therefore, biofilms are widely distributed in water (for example, attached to aggregated material), soil, sediment, and other abiotic or biotic surfaces and can consist of a single (mono-species biofilms) or various bacterial or fungal species (multispecies biofilms)^{8,9}.

Most medically important microorganisms, such as pathogenic gram-positive and gram-negative bacteria, mycobacteria, and fungi, including molds and yeast can grow forming biofilms^{1,5,10}. For this reason, biofilm growth mode is linked to more than 80% of persistent and chronic recurrent infections with enhanced resistance to conventional treatment, higher medical costs, prolonged stay in hospitals and healthcare facilities, and increased morbidity and mortality rates¹¹⁻¹³. In the human body, biofilms are often found on biomaterials such as indwelling medical devices and prostheses, intravenous and urinary catheters, contact lenses, prosthetic heart valves, cardiac pacemakers, and others (**Fig. 1**) and can act as reservoirs for spreading into new infection sites^{1,14,15}. In addition, tissue-associated biofilms contribute enormously to recurrent infections such as bacterial vaginosis or urinary tract infections. On the other hand, in the case of oral biofilms, the dysbiosis caused in the composition of the surface-associated oral biofilms is a triggering factor for the development of oral diseases, including dental caries and periodontal and peri-implant-related infections, which can all lead to serious health complications¹⁵⁻¹⁷ (**Fig. 1**).

Besides surface-attached biofilms, chronic biofilm-related infections are also common in different tissues in the human body, including the airways of cystic fibrosis and obstructive pulmonary disease patients, infected mucous membranes, and wounds^{1,18,19}. These biofilms are

found as cell aggregates encased in the macromolecular matrix and embedded in host material (for example, mucus in the case of cystic fibrosis) and contribute to host tissue damage as they enhance host proinflammatory responses^{2,15,20}.

It is well known that biofilm-grown bacteria and fungi represent increased resistance to conventional treatment and host immune system attacks compared to free-floating bacteria^{1,21,22}. Several factors contribute to biofilm resilience to conventional treatment, including the synthesis of different EPS matrix elements that act as a barrier for antimicrobial drugs, upregulation of efflux pumps, horizontal gene transfer, and changes in metabolic activity of bacterial or fungal cells within biofilms, including the appearance of small colony variants (SCVs) and dormant cell fractions called persister cells^{18,23–26}. For this reason, biofilm-related infections should be carefully studied in order to understand their occurrence and development and predict efficient treatment, which would lead to the best possible clinical outcomes.

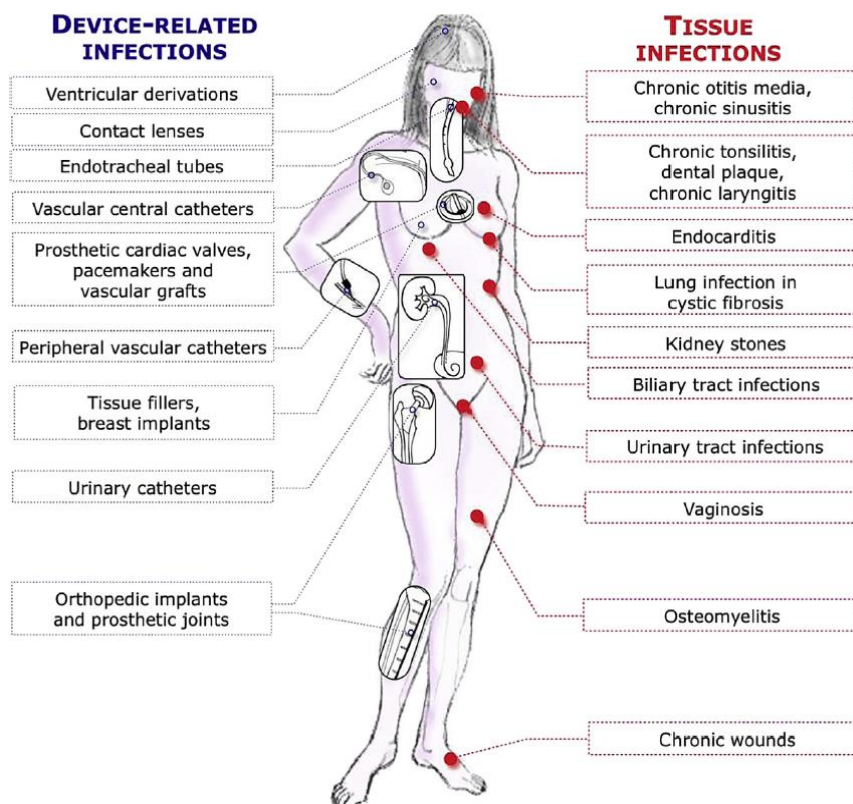


Figure 1. Microbial biofilm infections in the human body. Figure illustrates various types of indwelling medical device-associated and tissue associated biofilm infections caused by bacterial and fungal pathogens. Adapted from ¹⁴.

2. Biofilm formation

The transition from “free floating” to sessile growth mode is a complex process which involves different stages and results in phenotypic changes^{27,28}. Both bacteria and fungi form biofilms as a response to different environmental stress, including nutrient deprivation, temperature or pH changes, the presence of antimicrobial agents, UV exposure, high salt concentrations, and others^{29,30}. Although the molecular and spatial attributes involved in biofilm formation may vary amongst bacterial and fungal species or even strains, it is generally assumed that it involves four different steps for both bacteria and fungi: initial attachment to a vacant surface (I), irreversible attachment (II), biofilm accumulation and mature biofilm development (III) and biofilm dispersal or detachment (IV)^{31–33} (**Fig.2**).

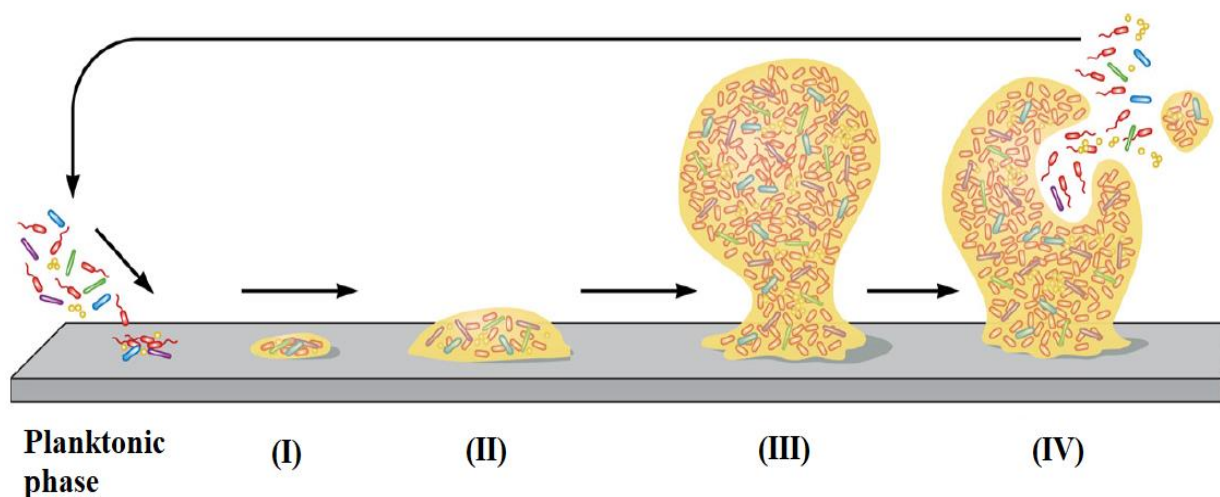


Figure 2. Biofilm formation stages. Planktonic bacteria (single or various species) reversibly attach on vacant abiotic or biotic surfaces (I); subsequently, irreversible attachment (II) is facilitated by extracellular organelles (pili, curli, fimbriae), and biofilm maturation phase (III) includes microcolony formation and EPS matrix development (IV). Finally, some biofilm-embedded cells are dispersed (IV) to the environment, where they can colonize new vacant surfaces. Modified from³¹.

The first stage of biofilm formation involves the interaction and adherence of biofilm-forming microorganisms on the surface³⁰. Reversible adhesion (I) is usually influenced by thermodynamics and physicochemical and electrostatic interactions, including Van der Waals

forces, while (irreversible) adhesion on the surfaces (II) is facilitated by extracellular organelles such as flagella, fimbriae, and pili, surface proteins (adhesins) and cell-cell interactions^{34,35}. Moreover, environmental factors such as pH or salinity and surface properties such as hydrophobicity, topography, oxygen concentration, and charge enhance the permanent attachment of the microorganisms on vacant surfaces^{30,36-39}. Some studies have already concluded that microorganisms are more likely to bond on hydrophobic surfaces like polystyrene, silicone, and polystyrene, among others, compared to hydrophilic ones such as stainless steel^{38,40}. Moreover, it has been shown that surface features could influence the proteome of some bacteria, suggesting that they can sense different surface characteristic^{19,41,42}. Eventually, in most cases, after irreversibly bonding on the surfaces, microorganisms lose their motility and activate genes involved in EPS matrix synthesis⁴³.

Thereafter, the biofilm maturation phase (III) involves EPS matrix development, and its morphology can vary depending on microorganisms and macromolecules present in the biofilm, shear forces, pH, temperature, and available nutrients^{24,30,44,45}. EPSs in the biofilm matrix act as a scaffold for other biomolecules, such as proteins, nucleic acids, lipids, and other polysaccharides, to adhere^{9,22,27,46}. Once established, the EPS matrix immobilizes microorganisms within the biofilm and keeps them in close proximity, allowing cell-cell communication, horizontal gene transfer and long-term coexistence⁴⁷⁻⁴⁹.

In addition, EPS acts as a protective barrier and limits the penetration of conventional antimicrobials and immune system components through the biofilm structure^{4,50-52}. For example, various studies concluded that biofilm-embedded bacteria are protected from polymorphonuclear leucocytes, as they fail to phagocytose and disrupt biofilms^{53,54}. Thus, during the biofilm maturation stage, bacteria and fungi replicate within the EPS matrix and form microcolonies, and some important changes in gene expression patterns and metabolic pathways can be detected^{30,48,55,56}. For example, the down-regulation of flagella biosynthesis was observed in different bacteria as a response to environmental signals of the surface⁵⁶⁻⁵⁸. On the other hand, while cell motility genes are downregulated, Tuson and Weibel in 2014 assessed that biofilm-embedded cells turn on the genes responsible for EPS matrix production⁵⁹. In addition, eDNA was shown to induce the expression of drug-resistance genes by chelating cations and increasing antibiotic resistance in *Pseudomonas aeruginosa* biofilms⁶⁰. Eventually, EPS matrix maturation

is followed by water channels formation, which are responsible for conveying oxygen and nutrients for biofilm-embedded bacteria and fungi and help eliminate unwanted products from established biofilms⁶¹. In most cases biofilm reaches its thickness limit during its maturation phase, and after that, some bacterial and/or fungal cells are sloughed from biofilms^{29,30,62}.

Once the microorganisms are dispersed from the biofilm (IV), they are able to colonize new surfaces resulting in continuous biofilm accumulation and spread^{38,63}. For example, biofilm dispersion within the human body can cause severe infections in surrounding tissues and subsequently reach the bloodstream, resulting in worsened clinical outcomes⁶³⁻⁶⁵. Thereby, environmental conditions, including chemical, oxygen or c-di-CAMP gradients can influence biofilm dispersion^{39,63,66}. For instance, low concentrations of nutrients, oxygen, or general stress, especially in interior biofilm levels, might lead to increased motility and subsequently to biofilm dispersion⁶⁷.

Recently, the general idea that planktonic cells initiate biofilm formation has been challenged by several authors. In oral biofilms, for example, it has been shown that over 95% of bacteria in saliva are not in planktonic form, but forming multi-species aggregates, either among themselves or attached to buccal epithelial cells⁶⁸. When planktonic, individual cells, adhere to the teeth, they hardly grow, whereas multi-cellular aggregates act as “nucleating agents” that seed the biofilm structure and whose growth accounts for over 99% of the final biofilm mass. The interpretation of these results is that in multi-species aggregates, the metabolic output of some bacteria facilitates the growth of others, via synergistic interactions that outcompete the slow growth of attached single cells. These interactions could be especially relevant for anaerobic bacteria, that would not be able to start growing until oxygen has been consumed by aerobic or facultative anaerobic companions. This aggregates-dependent biofilm formation process has already been proposed for some single-species and complex environmental biofilms^{69,70}. However, whether this phenomenon applies to other, non-oral biofilms, remains to be determined by future studies.

Environmental cues might also contribute to microorganism dispersion from biofilms⁷¹. This process is mediated by self-produced signaling molecules and involves only specific biofilm parts (linked to biofilm thickness and diameter, but not to biofilm lifetime)^{63,64,67}. Inducer molecules involved biofilm dispersion are pyruvate, oxygen, high iron concentrations, nitric

oxide and others^{39,64}. For example, rhamnolipids were found to be crucial in *P. aeruginosa* biofilm dispersion, suggesting that biofilm dispersion is a complex process and involves various molecular pathways and environmental cues^{64,5,68,69}. In addition, environment-induced biofilm dispersion depends on signals within cells embedded in the biofilms and can be linked to cell-cell interactions and quorum sense (QS) systems^{67,74}.

3. Biofilms and quorum sensing

Bacterial and fungal cells embedded in biofilms often communicate with each other using QS systems depending on the population density³⁰. This cell-cell communication is based on the use of small chemical molecules called autoinducers that were shown to be involved in the regulation of microbial behavior^{19,75}. For example, QS based cell communication was found to be important in transfer of genetic material between cells, gene expression, modulation of different cell functions and synthesis of secondary metabolites in many pathogenic bacteria and fungi^{54,76}. While gram-positive bacteria use peptide-based QS, gram-negative pathogens usually employ acyl-homoserine lactonases as their signal molecules⁷⁵. Therefore, different authors have concluded that QS systems play a key role in biofilm formation, development and pathogenicity in both bacteria and fungi^{77,78}. For example, QS systems in *P. aeruginosa* were shown to be essential for biofilm maturation or differentiated architecture⁷⁶ and were suggested to play an important role in biofilm dispersion⁷⁴. Similarly to these results, QS systems were found to be responsible for cell detachment from established *S. aureus* biofilms, allowing this bacterium to spread and colonize new niches⁷⁹. Additionally, QS molecules such as farnesol and tyrosol appeared to have an impact on biofilm morphogenesis and were implicated in the transition from yeast to hyphae in *Candida* spp⁵¹.

Thus, given that QS systems help bacterial and fungal pathogens survive under stress conditions and are responsible for switching to a biofilm lifestyle when the population reaches a specific density, they should be intensively studied as potential drug targets in order to treat biofilm-associated infections successfully.

4. Biofilm forming microorganisms of clinical relevance

4.1. *Staphylococcus* spp.

Staphylococcus aureus (*S. aureus*) and *Staphylococcus epidermidis* (*S. epidermidis*) are gram-positive human opportunistic pathogens that commonly colonize skin and represent a leading cause of nosocomial and chronic biofilm-associated infections in the urinary tract and soft tissues, including cystic fibrosis, endocarditis, and others^{6,21,80}. In addition, both *S. aureus* and *S. epidermidis* are often isolated from the surfaces of indwelling medical devices, including catheters and prosthesis, as the surface proteins of these bacteria can bind to host extracellular matrix proteins such as collagen, fibronectin, fibrinogen and immunoglobulins, whose coatings are often found on these surfaces^{15,21,81,82}. Whereas *S. aureus* contains various virulence factors necessary to infect and persist in the host organisms, *S. epidermidis* pathogenicity is mostly related to biofilm formation^{83,84}. Usually, staphylococcal biofilms are divided into two groups: biofilms that consist mostly of polysaccharidic material and those of proteinaceous matrix^{4,82,85}. Proteinaceous biofilms are mostly found in methicillin resistant *S. aureus* (MRSA) isolates and most of *S. epidermidis* strains, while methicillin susceptible *S. aureus* strains (MRSE) usually have polysaccharidic biofilm matrix^{82,86,87}.

Nevertheless, both categories of *S. aureus* and *S. epidermidis* are highly recalcitrant to host immune system response. In addition, antimicrobial agents and biofilm formation of these bacteria can often lead to bacteremia, which represents high morbidity and mortality rates, especially in patients undergoing immunosuppressive therapy or those representing any other health condition related to the weakened immune system^{6,55,80}. For this reason, indwelling device-associated staphylococcal infections usually require implant removal or prolonged therapy which may result in the development of multi-resistance^{32,88}. Therefore, considering the widespread use of implantable medical devices and the difficulties of treating multi-resistant infections, studying biofilm formation and dynamics of both *S. aureus* and *S. epidermidis* and testing of new anti-biofilm therapies against these bacteria are of great interest.

4.2. *Pseudomonas* spp.

Pseudomonas aeruginosa (*P. aeruginosa*) is a gram-negative bacterium that causes acute and chronic infections in the urinary tract, wounds, mucus membranes or in patients undergoing chemotherapy or any other clinical condition related to the weakened immune system, such as HIV or cystic fibrosis^{23,89}. Moreover, this bacterium is considered a notorious pathogen due to its ability to undergo many genetic adaptations and synthesize numerous virulence factors and metabolites, including elastase, pyocyanin, exotoxin A, or phospholipase B, among others, in order to evade the host immune system^{76,90-92}. In addition, *P. aeruginosa* infections are extremely difficult to eradicate because this bacterium is resistant to most conventional treatments commonly used in clinical practice and can easily survive on abiotic and biotic surfaces such as medical equipment even after disinfection⁹³⁻⁹⁵.

Besides all the features mentioned above, different QS systems and biofilm formation capacity of *P. aeruginosa* contribute enormously to infection development because the EPS matrix protects biofilm embedded bacterial cells from immune system attack and acts as a barrier limiting penetration of antibiotics^{76,96}. For instance, three different extracellular polysaccharides are present in *P. aeruginosa* biofilms: Pel, Psl, and alginate, which are essential for biofilm matrix stability⁴³. Several studies related to *P. aeruginosa* EPS matrix polysaccharides concluded that while alginate enhances bacterial adhesion to surfaces and protects biofilm embedded bacteria from leucocyte-mediated killing⁹⁷⁻⁹⁹, the overexpression of Pel and Psl has been linked to their tolerance to various first-line antibiotics, including polymyxin B, colistin, tobramycin, ciprofloxacin and others¹⁰⁰⁻¹⁰². In addition, *P. aeruginosa* is able to tolerate high antibiotic concentrations due to changes in population heterogeneity where a dormant cell population can survive, regrow and form even thicker biofilms once the antibiotic is ceased (see section “Biofilms and persistence”)^{103,104}. Therefore, all these *P. aeruginosa* biofilm-related features highlight that new therapies and technological advances are required in order to understand and successfully cope with pseudomonal infections.

4.3. *Candida* spp.

In contrast to bacterial biofilms, *Candida* spp. (mainly *C. albicans*, *C. krusei*, *C. parasilopsis*, *C. glabrata* and *C. auris*) biofilms usually consist of round-shaped yeast and hyphae cells, both of which are essential for EPS matrix development^{33,105}. Round yeast cells attach and proliferate on the surface followed by the induction of hyphae formation, which is considered a biofilm initiation step. Further, cell attachment is followed by proliferation and maturation¹⁰⁶ (**Fig. 3**). During this phase, *Candida* spp. biofilms consist of yeasts, hyphae and pseudohyphae and EPS matrix, which mainly consists of glycoproteins (55%), carbohydrates (25%), lipids (15%) and eDNA (5%)^{33,107}. The last stage of fungal biofilm formation is cells' detachment from the biofilm in order to colonize favorable niches for new biofilm formation^{108,109}.

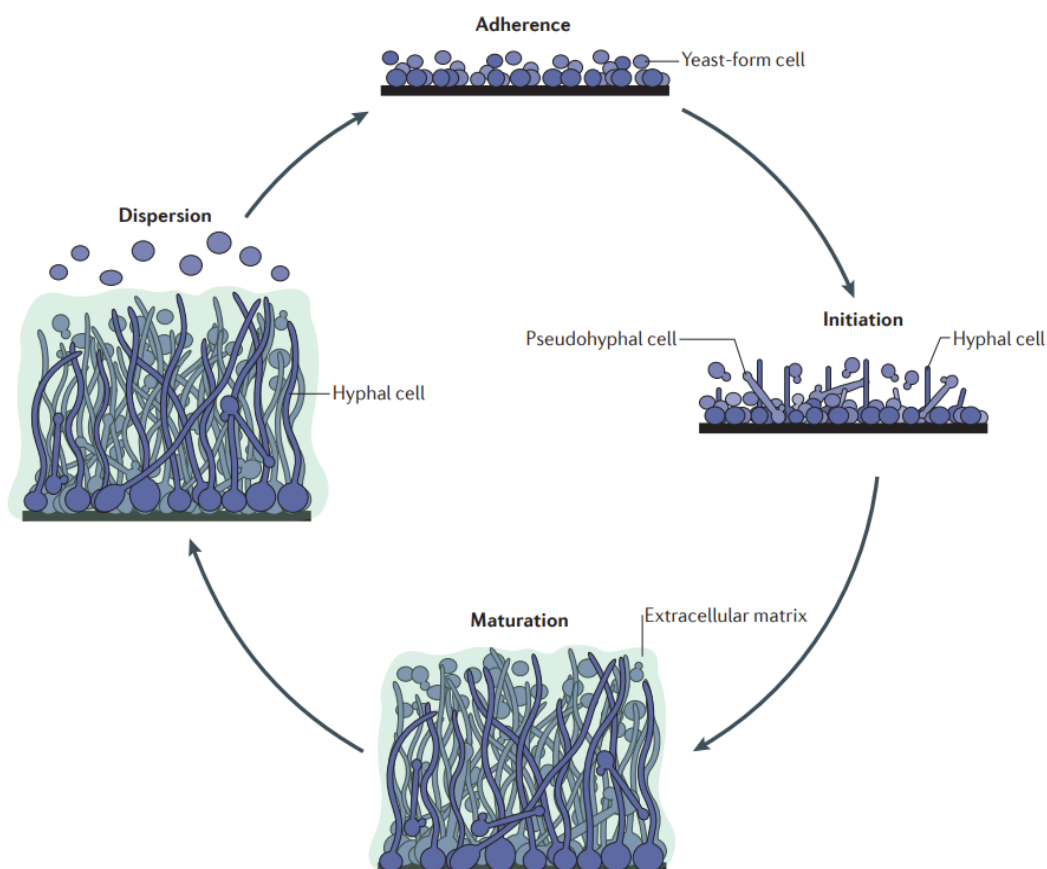


Figure 3 *Candida* spp. biofilm formation. Round yeast cells adhere to the surface and start to proliferate. During the initiation stage, biofilm consists of round yeast cells, pseudohyphae and

hyphal cells. Later, the EPS matrix is formed, and then yeast cells are dispersed from the biofilms to seed new niches. Adapted from¹⁰⁷.

Several studies have described the differences among *Candida* spp. biofilms, concluding that some of the species present differences in biofilm architecture¹¹⁰. For instance, *C. krusei*, *C. parasilopsis*, and *C. glabrata* seem to produce less EPS matrix compared to *C. albicans* or *C. auris*¹¹¹. Nevertheless, the biofilm formation of all *Candida* spp. generally leads to acute and chronic infections being the fourth most common nosocomial and bloodstream infections with high mortality rates, especially in immunocompromised or critically ill patients^{106,107,112}. *Candida* spp. biofilms are often associated with indwelling medical devices such as urinary and vascular catheters, joint prostheses, or cardiac devices that act as perfect niches for fungal cell attachment^{112–116}. For instance, it is well concluded that established fungal biofilms are extremely difficult to eliminate and, in many cases, attribute increased resistance to conventional treatment by changing cell metabolic activity (e.g. forming persister cells), overexpressing efflux pumps or employing QS systems^{114,117,118}.

Thus, the primary strategy to fight fungal biofilm-related infections consists of both indwelling device removal, which usually results in large skeletal defects, and systemic treatment using conventional antifungals^{119,120}. A limited number of antifungals exist to treat *Candida* spp. infections including polyenes and azoles that interfere with ergosterol synthesis leading to damage in the cell membrane, and fungicidal echinocandins that inhibit fungal cell wall synthesis^{121–123}. However, in many cases, antifungal therapy is responsible for adverse effects such as nephrotoxicity, cardiotoxicity, arrhythmias, hepatic toxicity, and gastrointestinal tract disturbances^{124–126}. This emphasizes the need to investigate new approaches to treat *Candida* spp. infections that would be efficient against biofilm-embedded fungal cells.

5. Oral biofilms

The oral cavity contains many different free-floating bacteria and aggregates that eventually deposit to teeth or dental implant surfaces, forming biofilms that usually consist of up to 200 different bacterial, fungal species and archaea (with more than 700 species being identified in different individuals)^{127–129}. Thus, oral biofilm formation and development on the teeth above

(supragingival dental plaque biofilm) or below the gum line (subgingival dental plaque biofilm) play an important role in oral diseases including dental caries, gingivitis and periodontitis^{130–133}. Moreover, biofilms can also be formed on the tongue dorsum, giving rise to a polymicrobial community that is responsible for oral malodor (halitosis)¹³⁴. On the other hand, other niches in the oral cavity such as the cheek mucosa do not sustain biofilms due to the continuous turnover of buccal epithelial cells, that impedes the maturation of biofilms.

Oral biofilm formation has traditionally been proposed to start with the interaction of microorganisms with host-derived saliva proteins or glycoproteins and the deposition of gram-positive bacteria such as *Streptococcus* spp. followed by *Actinomyces* spp., *Fusobacterium nucleatum*, and others on the teeth/implant surface (early colonizers)^{135–137}. These bacteria act as substrates for the adhesion of other bacteria which are called late colonizers. This group includes *Porphyromonas gingivalis*, *Treptonema denticola*, *Eubacterium* spp., and others (**Fig. 4**)^{49,129,138,139}. Sequentially, this adhesion is followed by the appearance of gram-negative bacteria, rods, vibrios, and spirochetes^{136,140}. Therefore, the maturation and accumulation of oral biofilms composed of periopathogens plays a key role in the inflammation of the gingiva leading to gingivitis and periodontitis development^{130,141}. While gingivitis is a reversible deregulated immune system inflammatory response to excessive formation of biofilm without loss of bone support, periodontitis is characterized by the destruction and loss of tooth/implant-supporting tissue which can eventually lead to its exfoliation^{142,143}.

Despite the significant advances in the treatment of periodontal disease, this pathology continues to increase being the sixth-most common prevalent condition in the world. Additionally, the lack of adequate treatment and proper personal hygiene have been suggested as the potential causes for the aggravation of the disease¹⁴⁴. In addition, even though dental plaque elimination by radicular scrapping reduces inflammation, this effect is transient, and inflammation usually returns with time, especially in high-risk individuals^{142,145,146}. Thus, in these cases, different additional periodontal therapy which includes antibiotics and antiseptics can be used.^{143,147} In this regard, although policies about the use of antibiotics in periodontal pathogens vary in different countries, there is substantial evidence that the use of antibiotics improves clinical features after non-surgical periodontal treatment^{142,148,149}. However, it is well established that bacterial and fungal species extensively interact in complex multi-species

biofilms in the oral cavity and this coexistence and cell-cell interactions might lead to greater antimicrobial resistance compared to single-species biofilms^{150,151}. Given that multidrug resistance negatively contributes to patient wellbeing and usually results in increased treatment costs, it is important to comprehensively study oral biofilm formation and the role that different species interactions within biofilms can play in antibiotic susceptibility in order to efficiently treat oral biofilm-related diseases^{152,153}.

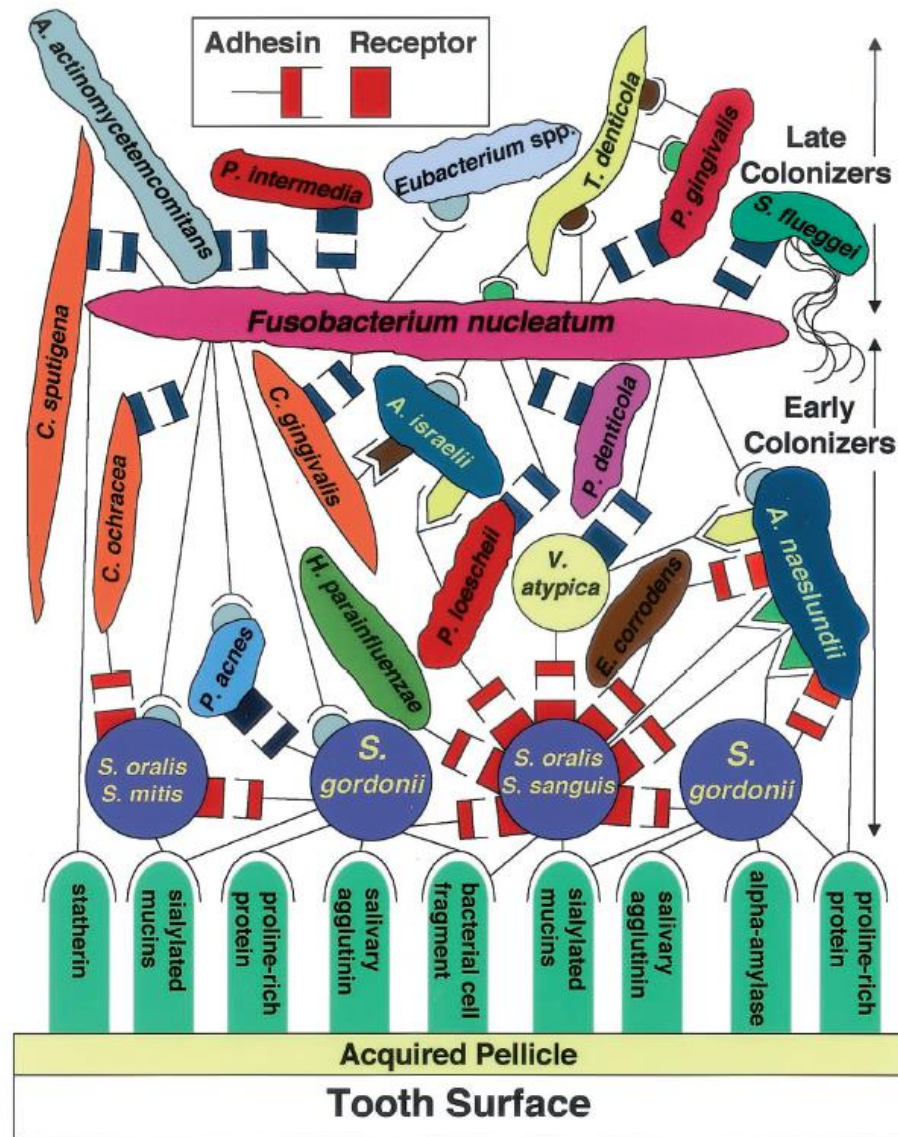


Figure 4. Traditional schematic representation of oral biofilms on the tooth surface. According to this model, oral biofilm formation starts when early colonizers adhere to the acquired enamel pellicle (derived from saliva) on the tooth surface by recognizing salivary

glycoproteins using receptor-specific adhesins. Later, different bacteria (late colonizers) co-aggregate to the existing community and a mature oral biofilm is established. Adapted from¹³⁹.

6. Biofilm study methodologies

6.1. *In vitro* biofilm models

Versatile behavior and high resistance of bacterial and fungal biofilms to conventional treatment make it necessary to develop reliable biofilm detection and study methodologies that could provide information about biofilm growth, persistence, and dissemination¹⁵⁴. Classical laboratory methods include antimicrobial susceptibility testing on agar plates (*E*-test) and microdilution following CSLI and EUCAST normative^{155,156}. However, these tests determine the susceptibility of bacteria and fungi to different antibiotics/antifungals when they are grown in planktonic (not sessile biofilm) mode or forming colonies in agar plates, and do not consider the presence of an EPS matrix, which is rich in macromolecular components and is linked to augmented resistance to antimicrobial/antifungal compounds^{155,157}. For this reason, antibiotic and antifungal susceptibility testing on planktonic bacteria and fungi often results in treatment failure and persistent recurring infections¹⁵⁸.

Currently, the most common models to study bacterial biofilms and their susceptibility to antimicrobial drugs are classified into static and dynamic models¹⁵⁹. The most common static assays are based on biofilm studies in microtiter plates (**Fig. 5A**) and Calgary biofilm devices that consist of 96 or more pegs that perfectly fit in 96 well microplates (**Fig. 5B**)^{14,160}. For instance, both biofilm assays are commonly used for testing cell viability (XTT reduction assay), antibiotic and antifungal susceptibility and for biofilm biomass accumulation assessment by staining using crystal violet (CV), resazurin, safranin or other dyes^{14,161}. CV staining is a rapid, inexpensive and straightforward procedure that helps evaluate the biofilm formation capacity of different microorganisms, including biofilm thickness¹⁶². However, this methodology involves many manipulation steps, which lead to high standard deviations. In addition, CV staining provides information about a single end-point rather than biofilm growth dynamics and cannot distinguish between viable and dead cells^{163,164}. For this reason, plating of viable colony counts (CFUs) is often undertaken to reveal live bacterial or fungal cells without dyes or manipulation

after the use of the ultrasound in order to avoid the appearance of cell aggregates in biofilm matrix^{161,165}. Besides standard 96-well microplates, there are other systems such as the Calgary device that consist of 96 pegs where the biofilms attach during their growth (**Fig. 5B**). In addition, other microtiter plates with removable polystyrene or silicone disk can be used to facilitate biofilm formation and further staining and examination, for instance using microscopic techniques^{156,160}.

Dynamic biofilm systems are commonly used for continuous or batch cultivation of biofilms with constant nutrient supply for biofilm-embedded microorganisms and monitor the factors related to biofilm microenvironments such as temperature and pH changes. These systems include continuous culture in flow-cell systems, rotating-disk reactors, and drip flow reactors, among others^{9,14,31,135}.

Flow-cell systems (**Fig. 5C**) are usually used to observe biofilm formation, including spatial distribution, evaluate the effect of different compounds on biofilm eradication, and investigate biofilms' tolerance to host immune system components^{31,129,156}. Rotating-disk reactors consist of a disk holding several removable coupons for biofilm growth (**Fig. 5D**)^{79,166}. This system allows continuous and non-invasive 3D biofilm observation using confocal laser scanning microscopy (CLSM)¹⁶⁶. Disk rotation creates a similar increase in shear forces across all coupons, and for this reason, this system is used to test biofilm resistance to stress and nutrient limitations^{14,166,167}. Given that the coupons in rotating disk reactors are removable and can be made of different materials, including those commonly used in the production of the prosthesis and other implantable medical devices, rotating-disk reactors are used to test the capability of different bacterial and fungal strains to attach on their surfaces^{31,79,167}. Similarly to rotating disc reactors, drip-flow reactors are used to study biofilms under stress conditions (limited nutrients, oxygen, exposure to anti-biofilm compounds, and others) (**Fig. 5E**)¹⁶⁷. These reactors consist of four equal test channels that hold standard microscope slide-sized coupons, where high biofilm biomass can be produced⁷⁹. For this reason, similarly to rotating-disk reactors, drip flow reactors are commonly used to test medical materials widely used in indwelling medical devices, such as stainless steel, copper, titanium and others¹⁶⁸.

Numerous *in vitro* biofilm systems for studying oral biofilms exist^{1,161,169}. Regarding the complexity of oral biofilm models, static biofilms can be grown on hydroxyapatite and titanium

disks in microtiter plates for further observation by microscopic techniques or staining^{135,170}. On the other hand, dynamic biofilm systems such as bioreactors, where up to six species can grow simultaneously, and Robbins device, which helps to recreate an ideal microenvironment by replicating the physiological effects of unstimulated salivary flow, are used^{16,135}. For instance, Yassin and colleagues used modified Robbins device to assess the impact of fluoride on mixed species biofilms¹⁷¹. In addition, other studies indicated the advantages of using high throughput microfluidics for oral biofilms studies, as this methodology does not require high sample volume and permits biofilm culturing and microscopic analysis (usually by CSLM) and bioinformatics¹⁷²⁻¹⁷⁴. Indeed, bioinformatic analysis became an essential tool in oral biofilm studies in past years as the use of 16s rRNA gene sequencing of hypervariable regions helps to assign a taxonomic rank to genus or species level^{146,175,176}. This methodology is often used to describe microbial communities within biofilms^{177,178}. For example, Johnston and colleagues compared microbial diversity changes after mechanical biofilm elimination in periodontitis¹⁴⁶. Another study by Bizzarro et al. described the effect of periodontal therapy on microbial communities and assessed how interactions between different bacteria within subgingival plaque biofilms could result in clinical outcomes¹⁷⁷.

Overall, both static and dynamic systems have their advantages and disadvantages^{169,179}. While static systems are cheap and highly reproducible and allow to perform a large number of tests simultaneously, they cannot recreate biofilm and host microenvironments^{164,180}. On the other hand, dynamic biofilm models are more expensive and require specialized equipment but continuously supply nutrients for biofilm-embedded bacteria, which allows the possibility of long-term biofilm analysis^{31,179}. Thus, besides static and dynamic biofilm assays, various *ex vivo* models, such as microcosms or the use of host tissues including keratinized, respiratory, gastrointestinal, bone tissue and others, that can recreate host-like microenvironment, could help to provide more reliable and robust results which might be compared with those obtained using *in vivo* assays^{170,181}.

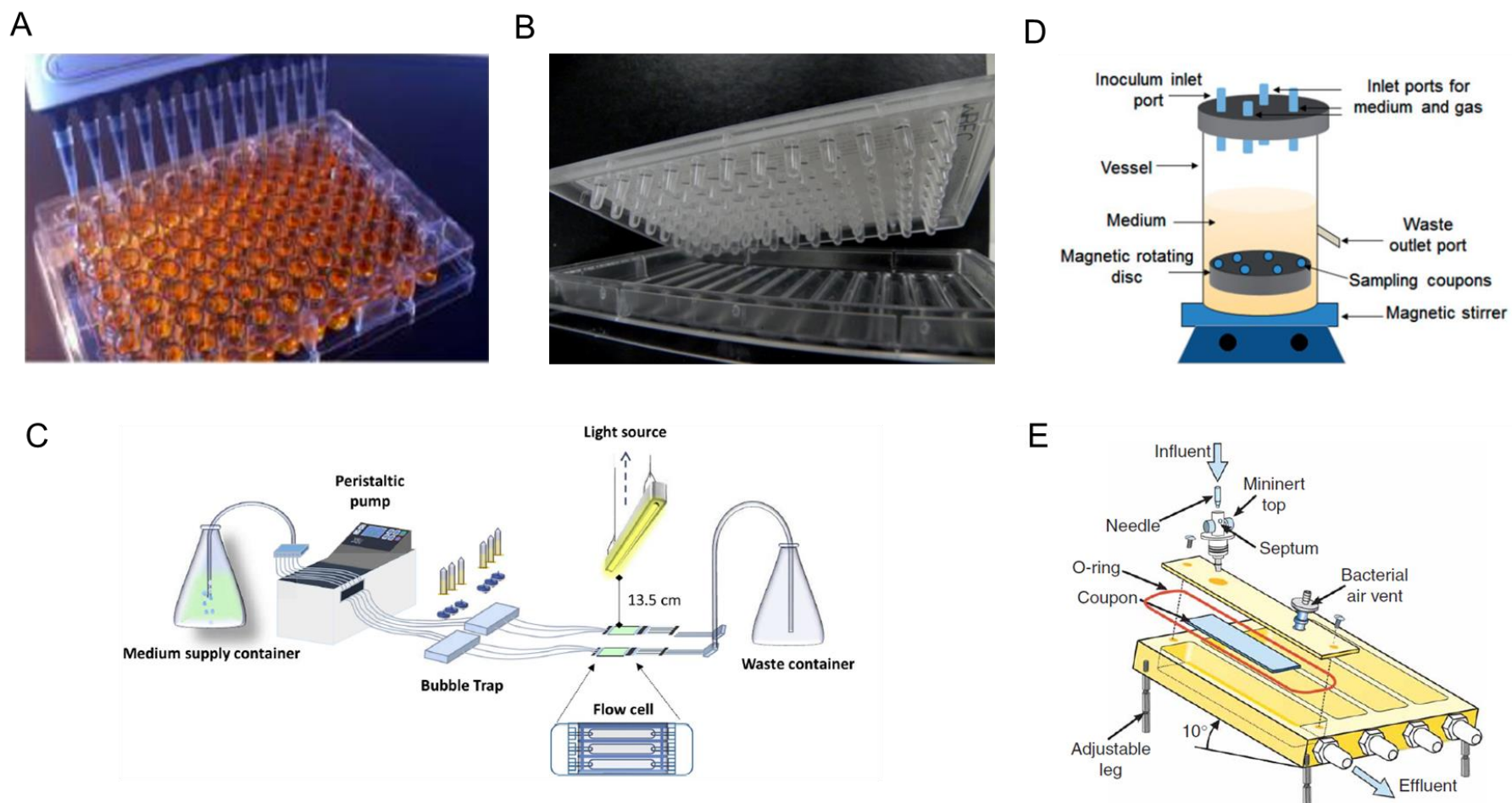


Figure 5. Laboratory setups for biofilm studies. (A) 96-well microtiter plate³¹, **(B)** Calgary biofilm device with 96 pegs¹⁸² **(C)** flow-cell system¹⁸³, **(D)** rotating-disk reactor¹⁶⁶, **(E)** drip-flow reactor¹⁸⁴.

6.2. Microscopy

Biofilms are very heterogeneous in their structure and topography. For this reason, microscopy techniques are also commonly undertaken in order to study bacterial and fungal biofilms¹⁸⁵. For instance, light microscopy is inexpensive, easy to perform and helps identify biofilm's presence. In contrast, confocal laser scanning microscopy (CLSM) can be used to study biofilm development, including its spatial distribution and three-dimensional (3D) structure. In addition, CLSM is commonly employed to quantify live and dead cells within biofilms before and after treatment with different antimicrobials, antifungals or biofilm-detaching compounds¹⁸⁵⁻¹⁸⁷ (**Fig. 6A**). Moreover, specific fluorescent probes can provide information about the biofilm matrix and its thickness, enable differentiation between live and dead cells within different biofilm layers, protein quantification and pathogen-specific labelling within biofilms. Thus, this type of microscopy is also utilized to study complex biofilms^{151,169}. For example, Welch and colleagues have labelled dental plaque using a modified method for fluorescence in situ hybridization (CLASI-FISH), utilizing ten different rRNA probes labelled with fluorophores (each one for different bacteria), enabling the visualization and analysis of multiple bacteria interactions and spatial distribution¹⁸⁸ (**Fig. 6B**).

Biofilm analysis using scanning electron microscopy (SEM) allows various magnifications of the sample and enables high resolution, including the 3D view of the sample, which is very important when studying biofilm surface, spatial distribution, and EPS matrix elements (**Fig 6C**)^{185,189,190}. Given that biofilms can consist of up to 97% of water, sample preparation for SEM examination can be challenging as it consists of various dehydration steps and heavy metal coating, which can destroy the sample^{169,185,191,192}. Nevertheless, SEM is a very powerful technique used to study the effect of different anti-biofilm compounds on biofilm matrix elements and cell viability¹⁸⁵.

Besides CLSM and SEM, atomic force microscopy (AFM) is a powerful emerging technique that helps assess and analyze biofilm surface and adhesion forces between biofilm and the substratum it is attached to. In contrast to other microscopic techniques, AFM permits *in situ* imaging in liquid without labeling, fixing or coating with heavy metals and permits to observe samples to molecular level^{193,194}.

To sum up, various microscopic techniques exist for biofilm studies. Although all of the former methods have several advantages and limitations, at the same time, they provide valuable insights into different aspects related to biofilms and their structure. Thus, combining different microscopy approaches would help better understand biofilms and their interaction with abiotic and biotic surfaces.

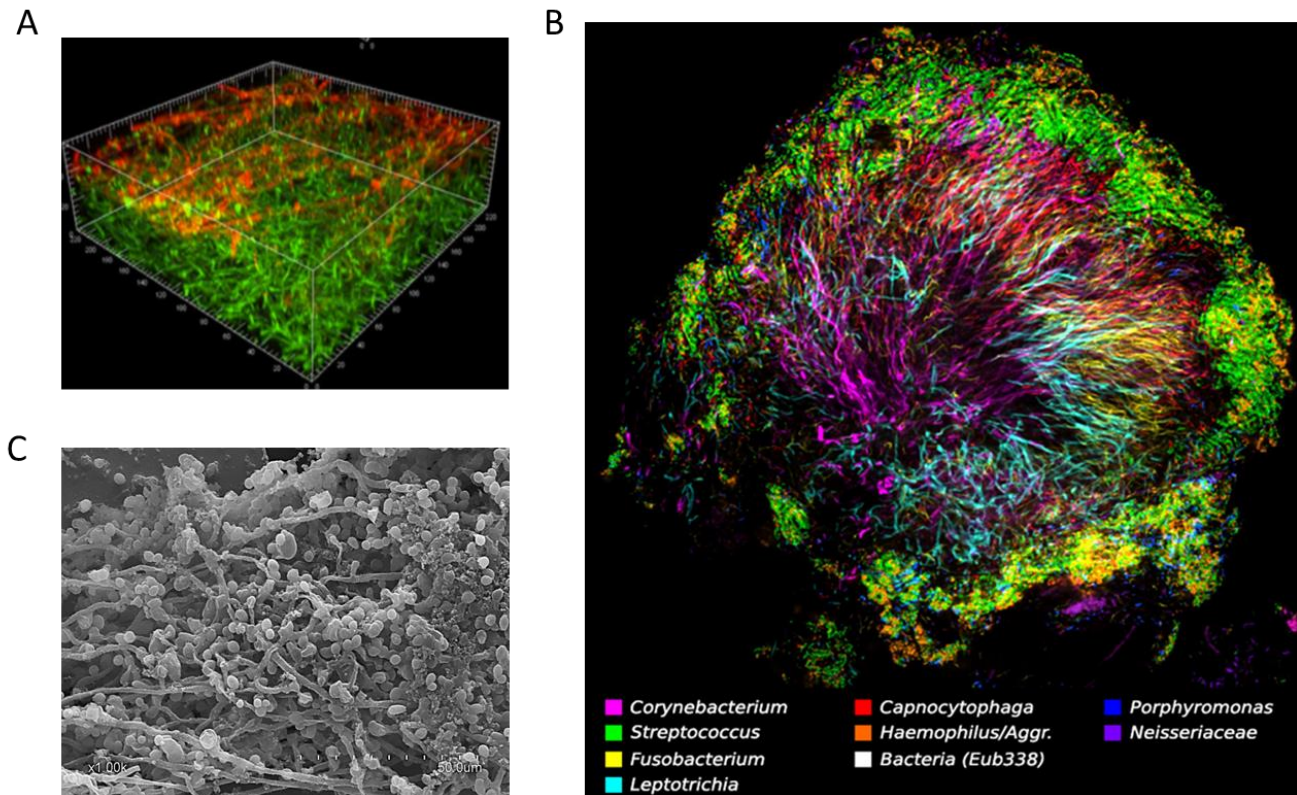


Figure 6. Different microscopy techniques for biofilm observation **A** – CLSM image of spatial distribution of 48h *C. albicans* biofilms after live-dead staining with SYTO9 and propidium iodide. Modified from ¹⁹⁵; **B** – Spatial organization of dental plaque visualized using CLASI-FISH. Different colors indicate different bacteria present in the dental plaque sample. Adapted and modified from ¹⁸⁸. **C** – SEM of 48h *Candida albicans* biofilms (Żiemytę et al., unpublished data);

6.3. Real-Time Cell Analyzer by impedance measurements

The impedance-based xCELLigence Real-Time Cell Analyzer (RTCA) allows continuous biofilm growth quantification without manipulation or labelling. This assay is based

on the ability of biofilm-producing bacteria or fungi to impede an electric current when they physically attach to the surface of electrodes^{196,197}. In detail, gold electrodes that act as biosensors in microtiter E-plates are fused at the bottom of each well in modified microtiter plates and measure the electric current passing through them when the electrodes are submerged in conductive solution such as buffer or bacterial/fungal growth media¹⁹⁸.

Therefore, when microorganisms attach and grow on the bottom of E-plates forming biofilms, they impede the electric current, whereas this current is not altered when bacteria grow planktonically in the culture medium¹⁹⁶. This current is subsequently expressed as a non-dimensional Cellular Index (CI) value that has been shown to be correlated with the biofilm mass¹⁹⁶ (higher CIs – stronger biofilm formation capacity) (**Fig. 7**). The main advantage of this system in contrast to standard biofilm tests methods is that impedance measurements permit biofilm growth dynamics observation over time at different time points (typically every 10 minutes)^{133,196,197}.

In addition, impedance system was recently shown to be suitable for studying complex biofilms such as those associated to oral infections¹⁹⁹. In fact, oral biofilms grown in real time impedance system were also shown to be similar when compared to initial inoculums, suggesting that impedance measures can reliably predict biofilm growth dynamics of both mono- and polymicrobial biofilms^{133,199}. Thus, this method would allow monitoring biofilm growth dynamics and could facilitate antibiotic or antifungal selection by identifying truly efficient treatment against bacterial and fungal biofilm, as well as facilitate the study of complex polymicrobial biofilms.

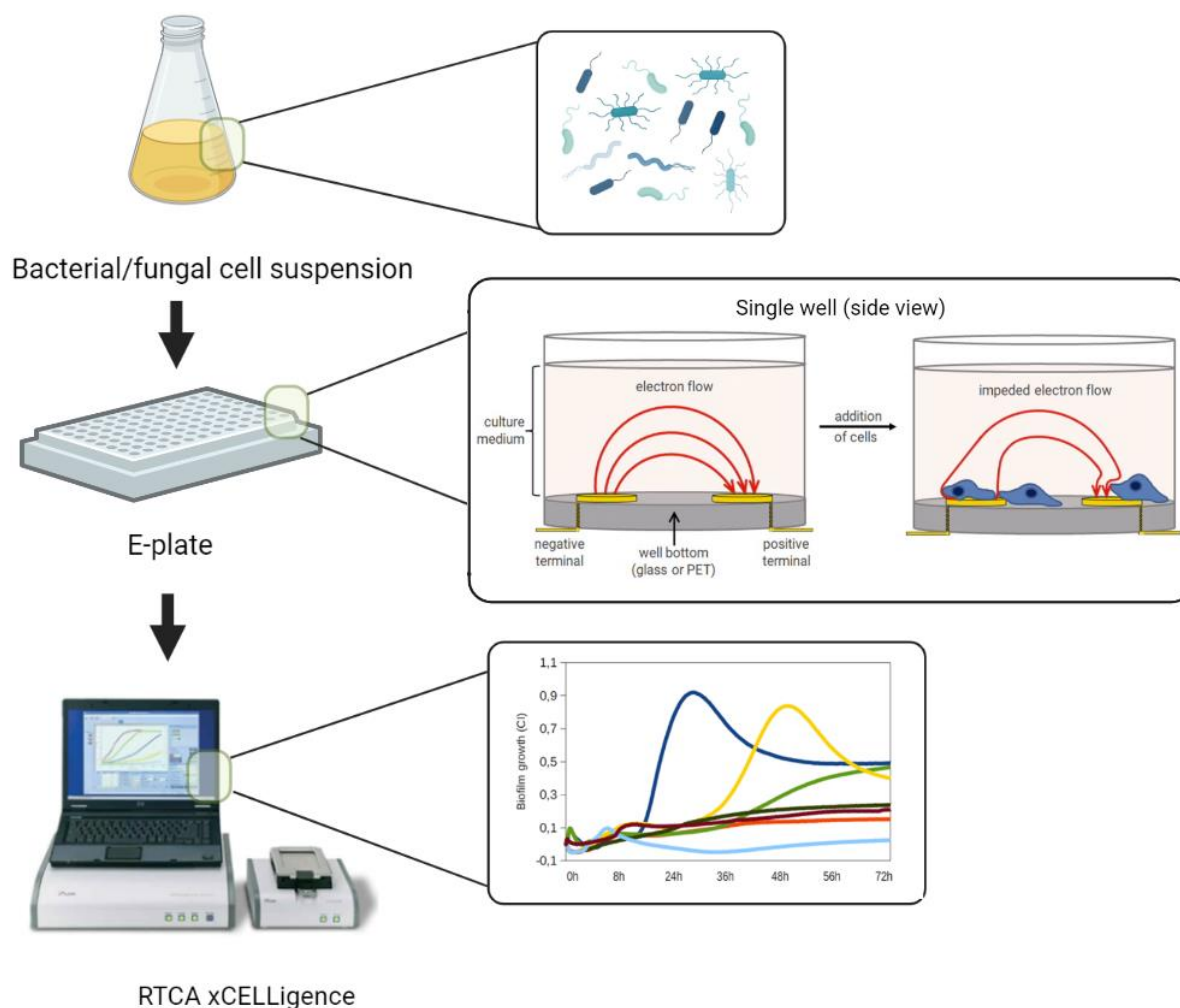


Figure 7. Schematic overview of Real-Time biofilm analysis by impedance measurements using the xCELLigence equipment. Bacterial/fungal overnight cultures are diluted to optimal optical density and added into corresponding E-plate wells. When microorganisms bind to the gold electrodes at the bottom of E-plate wells' surface, the electron flow is impeded and this impedance is expressed as Cellular Index (a proxy for biofilm growth). Higher biofilm formation capacity results in higher CI values, while biofilm non-forming microorganisms tend to give relatively low CIs. Image represents biofilm growth dynamics of seven *P. aeruginosa* strains measured through impedance for 72h.

6.4. *In vivo* biofilm models

Despite numerous biofilm studies *in vitro*, it is not fully understood whether these assays fully resemble biofilm formation and development *in vivo*, as they probably lack the ability to recreate host-like microenvironment and cell-cell interactions^{169,170} (**Fig. 8**). Therefore, during

past decades, several non-mammalian and mammalian animal models, including those in *C. aenorhabditis elegans*, zebrafish, rabbits, mice, rats, and others, have been extensively used in order to investigate biofilm-related infections and validate the results obtained using *in vitro* biofilm models^{125,179}. In addition, *in vivo* biofilm models act as an intermediate step for testing new treatments or devices before they can be applied in clinical practice⁶².

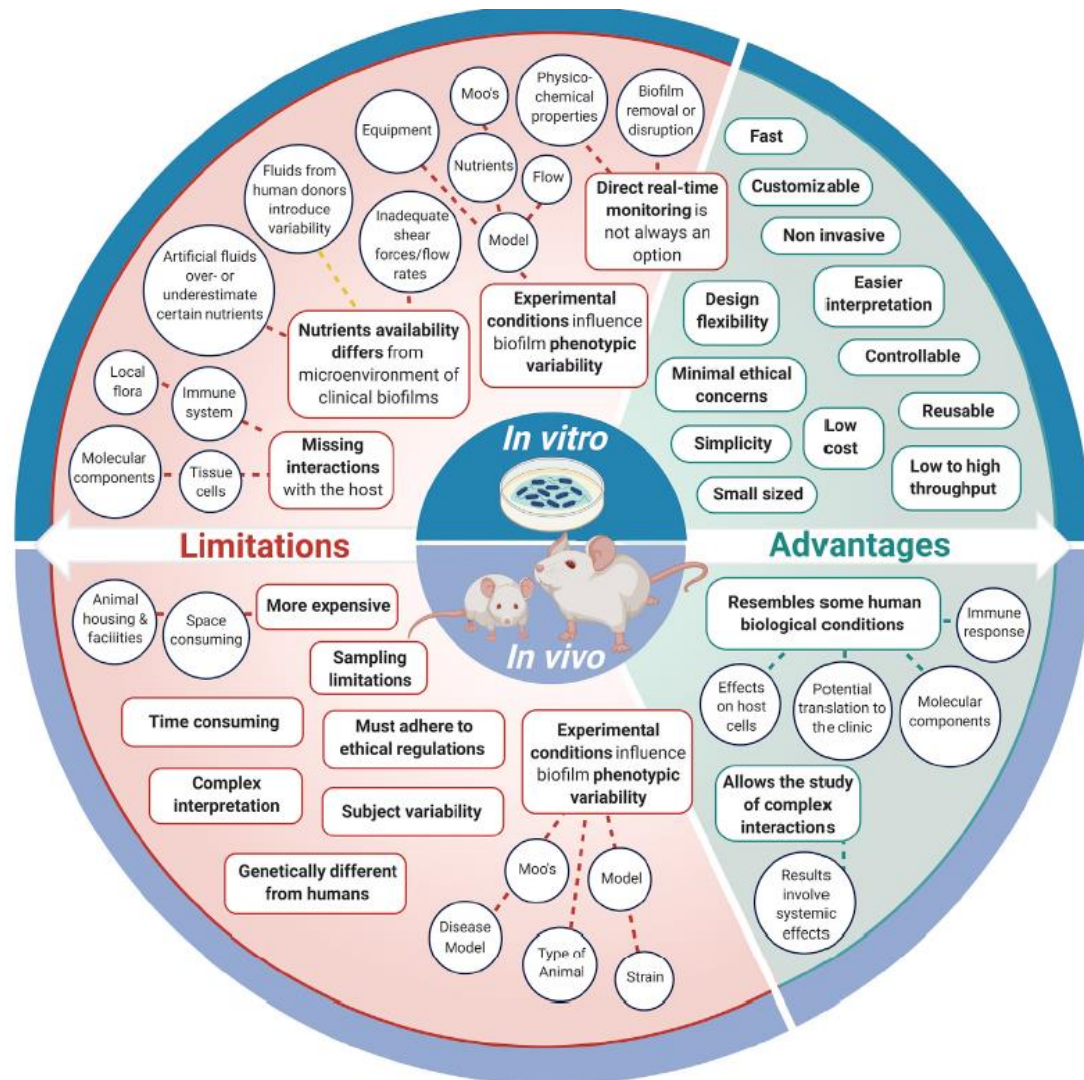


Figure 8. Comparison of *in vitro* and *in vivo* study methodologies, including their advantages and limitations. Adapted from Guzman-Soto et. al⁶².

Although non-mammalian models are cheaper and organisms used for these assays reproduce quickly, the inability to represent the complex immune system needed to investigate different biofilm-related infections reduces their applicability^{170,179}. Thus, several mammalian models were developed to study bacteria-bacteria, bacteria-fungi and host-pathogen interactions and immune response to the infection^{21,108,200,201}. In addition, these models are indispensable when studying indwelling device-related infections. For instance, vascular catheter models were developed to study *S. aureus*, *S. epidermidis* and *C. albicans* biofilm-associated infections in rats and rabbits²⁰²⁻²⁰⁴. In addition, several studies developed different urinary tract infection models using gram-negative bacteria such as *Escherichia coli* and *Klebsiella pneumoniae*^{205,206}. Orthopedic implant models are also extensively studied, as recent studies described the ability of different bacteria to attach to the foreign material surfaces *in vivo* and discovered new approaches that could be used against indwelling-device-associated bacteria²⁰⁷⁻²⁰⁹. For example, Tran and colleagues found that selenium nanoparticles can be used as implant coatings against both *S. aureus* and *S. epidermidis*^{209,210}.

In addition, *in vivo* biofilm models are very important when studying soft tissue-related infections, including cystic fibrosis^{170,211}. These models help to study bacterial persistence in lungs, their long-time coexistence and interactions and respiratory tract inflammatory responses.^{14,212,213}

Moreover, *in vivo* mammalian biofilm models help to evaluate combination therapies, such as synergistic and antagonistic effects of different antibiotics/antifungals or antibiofilm compounds^{62,180,181,214,215}. For instance, Pletzer and colleagues developed and described a murine model for subcutaneous infections. This model can be used to test already existing and new antibiofilm compounds and their toxicity against a wide range of gram-negative pathogens²¹⁴. Other studies used mouse and rabbit models to study keratitis and investigate novel compounds to prevent corneal infection^{216,217}.

In vivo models are also common in fungal biofilm studies²⁰⁴. Some of them concentrate on host-pathogen interaction analysis. For example, Nash and colleagues developed a model for studying vaginal biofilm-associated infections caused by both *C. albicans* and *C. glabrata* and concluded that the immune response to both of these species is different²¹⁸. Meanwhile, other *in*

vivo studies have been undertaken to study the host's response to mucosal and device-associated *Candida* spp. infections^{118,201,219}.

In the case of oral biofilms, a murine model and quantitative PCR assay are commonly used as rodents have been shown to have a similar gingival area to humans^{135,220}. For instance, a rat model has been used to study periodontitis, including the effect of so-called “Red-complex” periodontal pathogens such as *P. gingivalis*^{221,222}. The oral caries model in hamsters and rats with high-sugar diets also indicated the importance of studying interactions between different bacteria within polymicrobial biofilms^{220,221,223}.

Although biofilm studies help to better understand biofilm physiology, development, and prevention, animal welfare is a growing concern in society and academic research^{14,169,200}. For this reason, *ex vivo* models may recreate the corresponding microenvironment for biofilm growth. They are considered a midway between *in vitro* and *in vivo* models and rely on the use of host tissues when possible (usually murine or porcine)^{170,181,219}. These models are cheaper than those *in vivo* and permit predicting treatment outcomes before they can be tested in animals⁶². Nonetheless, the development of *in vivo* and *ex vivo* methodologies is crucial to understand both soft tissues and indwelling device-related biofilm infections^{62,170,204}. Despite the fact that all described *in vivo* and *ex vivo* biofilm models have some disadvantages, they also help to mimic host-like conditions and cell-cell interactions during coinfection and help to assess the clinical efficacy of novel compounds targeting both bacterial and fungal biofilms.

7. Biofilm treatment

Treatment of biofilm-related infections poses a considerable challenge in clinical practice given that, unlike their planktonic counterparts, sessile biofilm-embedded microorganisms withstand chemical and mechanical stresses leading to haltered resistance to conventional treatment and host defense^{11,169}. Currently, besides surgical or mechanical removal when applicable, antibiotics and antifungals are the only options to treat biofilm-related infections³⁷. In fact, it is well known that the minimum inhibitory concentration (MIC) of common antibiotics is between 10 and 1,000 times higher for biofilms and these concentrations are very difficult to reach *in vivo*¹⁷⁹. Several recent investigations concluded that EPS plays a vital role in biofilm

resistance to antimicrobials, as they cannot penetrate deep biofilm layers^{25,140,224}. On the other hand, it is also known that different microorganisms inside biofilms undergo metabolic changes, which might also influence the response of these cells to conventional treatment, emphasizing that identification and development of new anti-biofilm strategies are of great interest^{43,225–227}.

For this reason, there exist four main strategies to cope with biofilm-associated infections: (I) prevention of biofilm formation, (II) biofilm weakening, (III) disruption of pre-formed and mature biofilms, and (IV) biofilm killing^{1,167}.

7.1. Prevention of biofilm formation

To avoid bacterial adhesion on abiotic and biotic surfaces, the prevention of biofilm formation is regularly used as a preventative strategy in clinical practice, for example, during the implantation of different medical devices^{32,65}. This strategy is based on inhibiting bacterial attachment on the surfaces at the initial stage, blocking biofilm development and EPS matrix formation²²⁸. If initial adhesion of biofilms is prevented, host defenses and suitable antimicrobial therapy successfully eliminate biofilm-forming microorganisms¹⁶². For example, various indwelling-medical device coatings with antibacterial properties help inhibit or delay bacterial attachment growth on catheters and implantable medical device surfaces^{229,230}. For these coatings, several antimicrobials, anti-biofilm compounds or surfactants alone or in combination can be applied in order to inhibit biofilm formation on indwelling-medical devices^{206,209,230}. For instance, selenium coating inhibited *S. aureus* biofilm formation in hemodialysis catheters *in vivo*, whilst silver nanoparticles (AgNPs) decreased bacterial attachment on titanium surfaces and were effective against mixed biofilms of *C. albicans* and MRSA *S. aureus*^{210,231,232}. Similarly, accessible devices such as catheters can also be non-invasively treated with ultraviolet light before their implantation, to sterilize the surface and prevent biofilm growth²³³.

In the case of inaccessible surfaces most common strategies to prevent biofilm formation include specific targeting surface properties, inhibition of extracellular organelles such as pili or flagella that facilitate the attachment, and inhibition of eDNA and EPS synthesis pathways^{15,54,59,234,235}. This also includes specific targeting of c-di-GMP metabolism, which was shown to designate the initiation of biofilm formation in different bacteria¹⁶².

7.2. Biofilm weakening

Biofilm weakening includes various strategies that interrupt EPS matrix maturation, such as inhibition of the amyloid fiber synthesis, destabilizing biofilm architecture, and disarming bacteria or fungi embedded in the biofilms by targeting their virulence factors, QS systems, small RNAs (sRNAs), which were found to promote biofilm formation, and others^{1,15,75,95,236}. These strategies are usually strain-specific and are effective only in the early stages of biofilm formation⁸².

Given that QS systems are involved in biofilm formation, many natural and synthetic compounds were derived to inhibit these systems^{75,159,162}. For example, furanone c30, ajoene, and aspirin were shown to interfere with QS systems and inhibit some virulence factors in *P. aeruginosa*, leading to reduced biofilm matrix formation^{76,162}. In addition, biofilm weakening also involves the inhibition of efflux pumps which were shown to be responsible for biofilm-forming bacteria and fungi tolerance to antimicrobials and antifungals²³⁷¹.

7.3. Biofilm disruption

Various biofilm dispersion strategies exist, including compounds that directly interfere with macromolecules in the EPS matrix^{30,38,194}. Additionally, biofilm-embedded bacteria and fungi use chemical signals and self-produced molecules in order to disperse cells from the biofilms and colonize new niches and tissues⁶³. For example, c-di-GMP concentration changes were found to be crucial in active biofilm dispersion in various bacterial pathogens^{39,63}. Moreover, sudden changes in carbon source concentration, oxygen exhaustion and increased heavy metal concentrations in biofilm environment were shown to trigger biofilm disassembly and dispersion⁶³. Recent studies also highlighted the importance elevated levels of nitric oxide (NO) in active biofilm dispersion^{72,238,239}. For instance, NO was shown to disperse mature *P. aeruginosa* biofilms and could be combined with conventional therapy in order to treat pseudomonal biofilm-associated infections^{238,240}. Similarly, another study found that L-arginine was capable to destabilize oral biofilms developed in human saliva, showing its potential against complex biofilms, that consist of many different species²⁴¹.

Additionally, biofilm disruption by the degradation of EPS matrix components such as proteins, polysaccharides and/or eDNA could be exploited^{52,162,242}. For example, eDNA can be targeted using deoxyribonuclease I (DNase I), which interferes with eDNA and inhibits biofilm development on abiotic surfaces, including titanium²⁴³. Moreover, EPS matrix proteins could be targeted with enzymes with proteolytic activity, such as proteinase K, which has been shown to effectively disrupt *S. aureus*, *S. epidermis* and other biofilms^{85,87,244}. In addition, hydrolase dispersin B was shown to be effective in dispersing Staphylococcal biofilms both *in vitro* and *in vivo*^{245,246}.

However, biofilm dispersal agents should be combined with appropriate antibiotics or antifungals, as they usually only detach bacterial/fungal cells from the biofilms without killing them¹. In fact, biofilm dispersion without a conventional drug might lead to even more severe health complications, including recurrent infections in different sites and bacteremia⁸⁸.

On the other hand, disruption of biofilms can be based on mechanical biofilm removal, such as tooth brushing, radicular scrapping and root planning in dental practice^{34,150}. Similarly, infected indwelling medical devices require their removal and replacement³⁴. Nevertheless, there are many cases when the removal of foreign material is not possible, especially in critically ill and immunocompromised patients, highlighting the need to investigate new approaches for biofilm disruption and removal.

7.4. Biofilm killing

Mature biofilms are extremely difficult to eradicate as the exposure of bacterial and fungal biofilms to subinhibitory concentrations of conventional antibiotics and antifungals not only fail to kill biofilm-embedded bacteria but usually promotes and enhances biofilm formation^{247–249}. Moreover, higher antibiotic/antifungal concentrations often result in health complications, including renal failure, hepatotoxicity and others and stimulate the development of antibiotic/antifungal resistance^{24,250}. Therefore, the last biofilm treatment strategy involves combining biofilm detaching or natural compounds that could work in synergy with conventional antibiotics/antifungals^{162,215,235}. This implies using lower, non-toxic antibiotic concentrations together with promising anti-biofilm molecules. Some of these molecules have a direct antimicrobial effect, while some of them only detach bacterial or fungal cells embedded inside of

the biofilm without killing them^{38,52,162}. However, bacterial or fungal cell detachment from pre-formed or mature biofilms was shown to make them more susceptible to conventional therapy^{1,251,252}. For example, encapsulated DNase disintegrates biofilms and increases ciprofloxacin efficiency²⁵³. Similar to these findings, pyruvate-depletion conditions enhanced tobramycin killing in *P. aeruginosa*, while aspartyl proteases combined with conventional antifungals resulted in significant eradication and killing of biofilm-embedded *C. albicans*^{120,254}. Even though synergy between various compounds might lead to complete biofilm elimination, the effect of these compounds in many cases is species or even strain-specific^{102,255}. For this reason, it is important to evaluate the effect of these compounds for each bacterial/fungal strain individually in order to reach the best clinical outcomes and successfully treat established biofilms.

8. Nanotechnology and biofilms

Given that biofilm-related infections are extremely difficult to treat, there is a need to search for new therapeutic approaches which could potentially increase the efficiency of conventional therapy^{256–258}. Therefore, nanomaterials recently emerged as a potential approach in biomedicine, including clinical diagnostics and biofilm treatment, as they can be used as drug carriers to the infection site^{259–261}. Nanoparticles are usually classified according to their size, morphology, and physicochemical properties, and their main advantages of use are a small size (20–200 nm), a large surface area assuring a high loading capacity (for example, mesoporous silica nanoparticles) and the ability to functionalize them with antimicrobials or other therapeutic compounds^{240,256,262,263}. For instance, in addition to their reduced size, metal nanoparticles have a direct antimicrobial effect against different bacteria²⁶⁴. For example, silver nanoparticles have been used for central venous catheter coatings and chronic sinusitis treatment^{265–267}.

Although nanomaterials with antimicrobial properties were shown to prevent biofilm formation by several studies, inhibition of pre-formed or mature biofilms is considerably more challenging as complete eradication of established biofilms can only be reached using nanoparticles that could reach biofilm network, penetrate inside of EPS matrix, and successfully release therapeutic compounds loaded inside of them *in situ*^{268–271}. For example, no significant

differences were found when gentamicin-carrying gold nanoparticles were compared to gentamycin alone²⁷². On the other hand, topical ferumoxytol nanoparticles were shown to disrupt *Streptococcus mutans* biofilms and resulted in being effective *in vivo*, preventing tooth decay. However, they were not able to completely kill all bacterial cells embedded within biofilms, as small separate cell clusters were detected after biofilm treatment²⁷³. Similarly, metal nanoparticles such as CuO, ZnO, and MnO were shown to have a potential effect against various gram-positive, and gram-negative bacteria, spores and viruses^{258,264,274}. Although some metal nanoparticles were also able to reduce mature biofilm biomass, the effect was limited, showing the need to increase nanoparticle concentration. Overall, this suggests the need to develop novel nanomaterials that would be able to uniquely interact and kill bacterial and fungal cells embedded in established biofilms.

Currently, the toxicity of nanomaterials is poorly understood. However, several studies indicated that some nanoparticles could produce multiple organ toxicity as they were found in the liver, spleen, colon, and others²⁷⁵. Other animal model studies also suggested that the interaction of nanoparticles with human cells might lead to nephrotoxicity and hepatotoxicity^{262,275,276}. Therefore, the use of nanoparticles for biomedical applications is providing encouraging results *in vitro* but requires considerable research and safety improvements to be clinically implemented. Regardless, nanoparticles are a promising tool to cope with biofilm-associated infections, and their effect on bacterial and fungal biofilms should be further investigated in the future.

9. The problem of persistence in biofilm cells

Biofilm growth mode is closely related to the appearance of “persister” cells as biofilm-embedded cells are metabolically active in outer layers, while deeper biofilm layers present dormant cell fractions^{248,277}. Moreover, the formation of these cells can be triggered by environmental stress, including exposure to antibiotics or other spatial and nutrient constraints within biofilms^{96,278}. Therefore, persister cells can be described as dormant cell subpopulations exhibiting a non-dividing state, reduced translation, low proton moving force, and decreased

ATP levels^{104,248,279}. In addition to the features mentioned above, these cells can arrest their growth, tolerate high antibiotic concentrations, and regrow once the antibiotic is ceased²⁷⁷.

Many bacterial species such as *Mycobacterium tuberculosis*, *P. aeruginosa*, *Helicobacter pylori*, *Clostridium difficile*, *E. coli*, *S. aureus* and others have been linked to persistent infections^{277,280–282}. Moreover, persistent biofilm-associated infections were also linked to some heterogeneous fungal populations that showed altered resistance to conventional treatment²⁸³. Therefore, prolonged and repetitive use of different antibiotics and antifungals not only leads to the recalcitrance or relapse of persistent infections but has many adverse effects on the patient, including increased treatment expenses and depletion of resident microflora^{278,281,284,285}. For this reason, numerous studies try to investigate environment cues involved in this processes and how actively growing bacteria switch to dormancy by identifying genes involved in dormancy and assessing metabolic profiles of persisters^{45,227,286,287}. For instance, whole genome sequencing and transcriptomic analysis showed different pathways involved in persister cell formation in *M. tuberculosis*²⁸⁸. Another study performed by Pu and colleagues in 2016 showed enhanced activity of efflux pumps within persister cell populations, revealing a possible target for persistent infection treatment²⁸⁹. However, as previous studies showed, some strains can have identical genomes but represent totally different transcriptomic profiles, which suggests that dormant cells need to be studied in detail^{288,290}. Moreover, it is necessary to improve the development of new approaches that could help to diagnose and treat persistent infections within biofilms more efficiently.

10. Rationale of this thesis

As described above, although different advanced static and dynamic models exist for studying bacterial and fungal biofilms, most of them are expensive, include various manipulation steps, require labelling or provide information about a single end-point only. Therefore, this doctoral thesis originates from a need to develop a reliable, fast, inexpensive, and labelling-free system for biofilm studies. Thus, this thesis intends to set up an impedance-based monitoring system in order to study biofilm formation and eradication patterns of gram-positive (staphylococcal), gram-negative bacteria (pseudomonal), fungal (*Candida* spp.) and complex

(periodontal) biofilms. From an applied point of view this work aims to comprehensively describe the effect of already existing and new antimicrobial therapies against biofilm formation and disruption in real-time and to identify new strategies against biofilm-embedded bacteria and fungi.

As mentioned in the above introduction, persistent infections are closely related to biofilm formation and development, but their identification and treatment is extremely difficult. Thus, the current thesis also aims to develop a method to successfully identify, study and treat dormant cell fractions using an impedance-base system for the first time.

Moreover, given that conventional therapy against biofilms fails to eradicate established biofilms, leading to treatment failure, this doctoral thesis also intends to study novel self-propelled nanoparticles as a new approach for pre-formed and mature *S. aureus* biofilm disruption and killing, using measurements in real-time to monitor the effect, confirming it later by more classical techniques.

Finally, as explained in the introduction, it is well-known that oral biofilms are instrumental in the occurrence and development of oral diseases. However, current methods to evaluate the effect of antibiotics on oral biofilms are based on pure cultures or on the levels of pathogenic bacteria, which has been proven to be limited to predict antibiotic efficacy efficiently. Thus, complex periodontal biofilms of subgingival plaque will be analyzed in real-time in the present PhD thesis, with the hope of developing a protocol to select the best individual treatment for periodontal disease and comparing this methodology to traditional antibiotic selection tools.

Overall, this doctoral thesis aims to fill the gap in studying biofilm growth dynamics in real-time, providing a method to monitor biofilm growth dynamics and to evaluate anti-biofilm compounds, and intends to develop a new, rapid, and reliable protocol for antimicrobial selection which could be used in clinical settings.

CHAPTER I

Effect of dalbavancin on staphylococcal biofilms when administered alone or in combination with biofilm-detaching compounds

This chapter has been published in *Frontiers in Microbiology*, April 2020, DOI: 10.3389/fmicb.2020.00553

ABSTRACT

Microorganisms grown in biofilms are more resistant to antimicrobial treatment and immune system attacks compared to their planktonic forms. In fact, infections caused by biofilm forming *Staphylococcus aureus* and *Staphylococcus epidermidis* are a large threat to public health, including patients with medical devices. The aim of the current manuscript was to test the effect of dalbavancin, a recently developed lipoglycopeptide antibiotic, alone or in combination with compounds contributing to bacterial cell disaggregation, on staphylococcal biofilm formation and elimination. We used real-time impedance measurements in microtiter plates to study biofilm growth dynamics of *S. aureus* and *S. epidermidis* strains, in absence or presence of dalbavancin, linezolid, vancomycin, cloxacillin and rifampicin. Further experiments were undertaken to check whether biofilm detaching compounds such as N-acetylcysteine (NAC) and ficin could enhance ficin efficiency. Real-time dose-response experiments showed that dalbavancin is a highly effective antimicrobial, preventing staphylococcal biofilm formation at low concentrations. Minimum biofilm inhibitory concentrations were up to 22 times higher compared to standard *E*-test values. Dalbavancin was the only antimicrobial that could halt new biofilm formation on established biofilms compared to other four antibiotics. The addition of NAC decreased dalbavancin efficacy while the combination of dalbavancin with ficin was more efficient than antibiotic alone in preventing growth once biofilm was established. Results were confirmed by classical biofilm quantification methods such as crystal violet (CV) staining and viable colony counting. Thus, our data support the use of dalbavancin as a promising antimicrobial to treat biofilm-related infections. Our data also highlight that synergistic and antagonistic effects between antibiotics and biofilm-detaching compounds should be carefully

tested in order to achieve an efficient treatment that could prevent both biofilm formation and disruption.

INTRODUCTION

Increased drug resistance of different bacteria is significantly reducing the therapeutic efficacy of antibiotics¹¹. Commonly, this resistance is augmented in bacterial biofilms, which can be described as bacterial communities adhering to biotic or abiotic surfaces and encased in a self-produced extracellular matrix^{242,291}. This matrix is composed of polysaccharides, proteins and extracellular DNAs and plays an important role in persistent chronic infections, resulting in serious health complications. In fact, bacterial cells embedded in a matrix are up to 1,000 times more resistant to antibacterial compounds compared to their planktonic form, leading to increased morbidity and mortality rates of various diseases, like those associated with implantable medical devices^{4,228}.

A mayor cause of medical device-associated and chronic infections, resulting in both economical and clinical burden, is the biofilm formation capacity of *Staphylococcus aureus* and *Staphylococcus epidermidis* bacteria^{21,80}. This capacity, in addition to widespread dissemination of methicillin resistant *S. aureus* (MRSA) and *S. epidermidis* (MRSE), emphasizes the necessity to investigate new antimicrobial compounds and combine different treatment strategies for increasing the therapeutic potential of conventional antibiotics¹. For instance, several agents for cell detachment and breaking down of biofilm matrix have already been reported. Some of them cleave the essential components of the biofilm matrix, like polysaccharides, proteins or extracellular DNAs, destroying its architecture^{64,65}. Ficin, a non-specific fig tree plant protease belongs to this group of anti-biofilm compounds, and it is able to disperse staphylococcal biofilms via enzymatic lysis¹⁹⁴. Others employ microbial signals that disperse bacterial cells embedded inside the biofilm exopolymeric matrix, like nitric oxide in *Pseudomonas* biofilms or certain quorum sensing inhibitors^{159,238}. Other anti-biofilm agents, like N-acetyl-L-cysteine (NAC) besides the ability to impair matrix architecture, have also antimicrobial properties against different pathogenic bacteria, making this molecule an interesting tool to confront biofilms^{292–294}. In addition, a combination of biofilm-detaching compounds together with

antibiotics could represent an alternative strategy for effective treatment of biofilm-associated infections.

Dalbavancin is a new lipoglycopeptide class antibiotic used against many gram-positive pathogens including staphylococcal strains in clinical practice²⁹⁵. It is also a long-action antibiotic which interferes with bacterial wall cell synthesis and does not require frequent administration, allowing weekly dosing and earlier patient discharge from the hospital²⁹⁶. Although dalbavancin has been proposed as a promising agent in biofilm-mediated infections, susceptibility to this antibiotic has mainly been tested using traditional microbiological tests such as microdilution or agar-based tests. However, it is well established that bacteria behave differently in a planktonic state or when forming biofilms, and there is currently limited information on its efficacy on biofilm-embedded bacteria with only a few studies available²⁹⁷⁻²⁹⁹, some of them in animal model^{300,301}. In some cases, the efficacy of dalbavancin or vancomycin has been shown to be low, with less than an order-of-magnitude decrease in viable counts of staphylococci³⁰². Thus, recent work has proposed the combination of antibiotics and biofilm-detaching compounds to treat biofilm-mediated infections^{162,234}, but this strategy has not currently been tested with dalbavancin. In addition, there is conflicting evidence about the comparative efficacy of dalbavancin and other antibiotics of common clinical use in staphylococcal infections, such as vancomycin^{300,302}.

Recently, we evaluated biofilm inhibition and induction in *S. aureus* and *S. epidermidis* strains using 10 conventional antibiotics and suggested that impedance-based real-time cell analysis (RTCA) could facilitate determination of antibiotic sensitivity when bacteria grow in biofilms, resulting in faster and more accurate assays and therefore more efficient antibiotic therapy¹⁹⁶. The aim of the current study was to describe the effectiveness of dalbavancin to prevent *in vitro* biofilm formation of staphylococcal strains (both sensitive and methicillin-resistant isolates) and compare its effect with other antibiotics that are frequently used in clinical practice against indwelling device-related infections. Our biofilm growth measurements were performed by impedance-based cell analysis and confirmed by more classical tests such as crystal violet (CV) staining and counting of colony forming units (CFUs). In addition, the effect of two biofilm disaggregating molecules, NAC and ficin, was tested in combination with the

antibiotic to evaluate potential synergy of a combined therapy to treat staphylococcal biofilm infections.

MATERIALS AND METHODS

Bacterial strains and growth conditions

Supplementary table I-S1 lists bacterial strains used for this study. Staphylococcal strains were grown on tryptic soy agar (TSA) plates and tryptic soy broth (TSB) at 37°C at 120 rpm. *S. epidermidis* strain 43040 was isolated at Microbiology Department of the University of Elche (Spain), MRSA strains were isolated at the Microbiology Department of the Alicante General Hospital (Spain) from a catheter tip in patients diagnosed with indwelling device-related bacteremia. *S. aureus* CETC 240 (*S. aureus* ssp. *aureus* Rosenbach 1884) is a biofilm positive strain isolated by FDA, which is methicillin susceptible, and a reference strain recommended to test antibiotic resistance.

RTCA-based biofilm analysis

Real-time biofilm analysis was performed using xCELLigence RTCA SP equipment (ACEA Biosciences) according to the manufacturer's instructions. For biofilm formation assays, bacterial strains were grown overnight in TSB and diluted with filter-sterilized TSB supplemented with 0.25% of D-glucose (TSB-glu). The experiments were performed as previously described by Ferrer et al.¹⁹⁷. Impedance data were registered at 10-min time intervals for 20h, and they were transformed into cell index (CI) values, which accurately correlate with biofilm mass^{196,197}.

To evaluate antimicrobial efficiency on bacterial biofilms five antibiotics with different mechanisms of action were tested: linezolid (Accordpharma), vancomycin (Pfizer), cloxacillin (Normon), rifampicin (Mavi) and dalbavancin (Angelini). One hundred microliters of each antibiotic diluted in TSB-glu (two-fold dilutions to final concentrations from 32 to 0.0625 mg/L) were used as background for impedance measurements. Further, 100 µl of bacterial cell suspension (OD₆₀₀ = 0.175) were added, reaching a final optical density of 0.0875. This optical density corresponds to 10⁷-10⁸ cells, depending on the strain. The lowest antibiotic concentration

to inhibit bacterial growth with a CI value ≤ 0.05 was considered as the minimum biofilm inhibitory concentration (MBIC)^{1,196}.

To test the antibiotic effect on already-formed bacterial biofilms the experiments were performed as previously described¹⁹⁶. Briefly, 100 μ l of cell suspension ($OD_{600} = 0.153$) was used as background. Then 75 μ l of TSB-glu were added to each well, reaching a final $OD_{600} = 0.0875$, and biofilms were grown for 6h (*S. aureus* Sa240), 7h (*S. aureus* MRSA4) or 9h (*S. epidermidis* 43040), corresponding to the exponential phase of biofilm growth of each strain at which time antibiotics were added (25 μ l of each dilution, reaching final concentrations from 32 mg/L to 0.0625 mg/L for each tested antibiotic). After the addition of antibiotics, CI was monitored for a further 20h. Two replicates of each antibiotic concentration sample and two negative controls were included in each experiment.

Antibiofilm compounds assay

For RTCA experiments, ficin (Sigma) at concentrations of 10, 100 and 1000 mg/L and NAC (Sandoz) at final concentrations of 0.5, 1, 2, 4 and 8 g/L were used alone and in combination with dalbavancin (0.5, 4 and 32 mg/L). In short, ficin and NAC were diluted in TSB-glu to the corresponding concentrations and 100 μ l of each dilution were used as background when anti-biofilm substances were added at the beginning of the experiment. After the background was measured, 100 μ l of cell suspensions ($OD_{600} = 0.175$) were added into corresponding wells and biofilm formation was monitored for 20h.

When NAC and ficin were added at the exponential biofilm growth phase 100 μ l of corresponding cell suspensions were used as background as described above. After that, 75 μ l of TSB-glu were added, reaching a final $OD_{600} = 0.0875$. When bacterial biofilm growth reached exponential growth phase 25 μ l of different concentrations tested for NAC of ficin and their combinations with dalbavancin were added into the corresponding wells. After the addition of biofilm detaching compounds, biofilm growth was registered for 20h more. Two replicates of each condition and their respective controls were tested in each experiment.

The effect of NAC and ficin on planktonic bacterial growth was also measured by the means of an absorbance plate reader Infinite M200 (Tecan, Durham, NC, United States). Briefly,

overnight bacterial cultures were diluted to $OD_{600} = 0.175$ and 100 μ l of each cell suspension was added into corresponding wells of 96-well plates. Then 100 μ l of biofilm-detaching substances were added to the final concentration of 10, 100, 1000 mg/L for ficin, and 0.5, 1, 2, 4, 8, 16 and 32 g/L for NAC. Ninety-six-well plates were incubated at 37°C with orbital shaking at 120 rpm and bacterial planktonic growth dynamics were monitored for 20h. Two replicates of each concentration were included as well as their respective controls.

MIC determination

To determine minimum inhibitory concentrations (MICs) of the tested antibiotics on *S. aureus* and *S. epidermidis* strains on solid media, the *E*-test (bioMerieux) method was used according to manufacturer's instructions, following Baldoni et al.³⁰¹. Broth microdilution assays were performed in accordance with the European Committee on Antimicrobial Susceptibility Testing³⁰³. MBIC (or BIC) was calculated following Bjarnsholt et al.¹ and Ferrer et al.¹⁹⁶

Biofilm quantification

In order to determine dalbavancin and ficin effect alone and in combination on pre-formed MRSA4 biofilms 175 μ l of bacterial suspension ($OD_{600} = 0.0875$) were inoculated in TSB-glu and grown in 96-well flat-bottom Ibidi ibiTreat μ -plates 89626 (Ibidi, Germany). These plates are coated with a thin polymer layer in order to assure better biofilm attachment. After 7h of growth 25 μ l of dalbavancin, ficin, or the combination of these two compounds were added, reaching final concentrations of 32 mg/L and 1,000 mg/L and the biofilms were grown for additional 24h.

After that the supernatant was discarded, bacterial cells were washed with phosphate buffer saline (PBS, pH = 7.4) to remove unadherent cells and bacterial biofilms were stained using 0.1 % CV as previously described³⁰⁴. Biofilm mass was quantified by absorbance plate reader, Infinite M200 (Tecan, Durham, United States) at 610 nm.

Viable count assay

To assess the number of viable unadherent planktonic and biofilm-embedded bacteria, 175 μ l of MRSA4 suspension ($OD_{600} = 0.0875$) was grown for 7h in triplicate in xCELLigence system. After that, 25 μ l of ficin and dalbavancin at the corresponding concentrations were added as described above and the biofilms were cultivated for additional 24h. The supernatant was then collected, and serial dilutions were prepared, using 100 μ l of each dilution for plating onto TSA plates in triplicate.

To evaluate viable cell number in biofilms, biofilms were carefully rinsed using PBS buffer to eliminate non-adherent, resuspended with 200 μ l of PBS and sonicated for 5 minutes in order to disrupt biofilm matrix, and the serial dilutions of each sample were plated on TSA plates in triplicate as described above and incubated in 37°C overnight. After that, CFUs were counted, averaged, and expressed as \log_{10} .

Statistical analysis

To study differences in the biofilm CI values, regression analysis was performed by a linear model using the function `lm` (library `stats`) in the R statistical package³⁰⁵ between 10 and 20h of biofilm formation time. For biofilm inhibition/induction analyses of CFUs and CV staining, the experiments were performed in triplicate with three independent repeats in each experiment. Statistical significance was assessed using Student's t-test, where * $p \leq 0.0$ and *** $p \leq 0.001$.

RESULTS

Dalbavancin effect on staphylococcal biofilm formation

Firstly, we evaluated dalbavancin's effect on staphylococcal biofilm formation by real-time impedance analysis when the antibiotic was added together with the bacterial inoculum. Most of the tested *S. aureus* and *S. epidermidis* had similar biofilm growth dynamics with comparable CI (correspondent to biofilm mass) values. MRSA4 was the strain with the highest biofilm formation capacity (up to 26% higher CI compared to that of MRSA2 at 20h), while the lowest CI values were observed for MRSA1 (**Fig. I-1 and Fig.I-S1**).

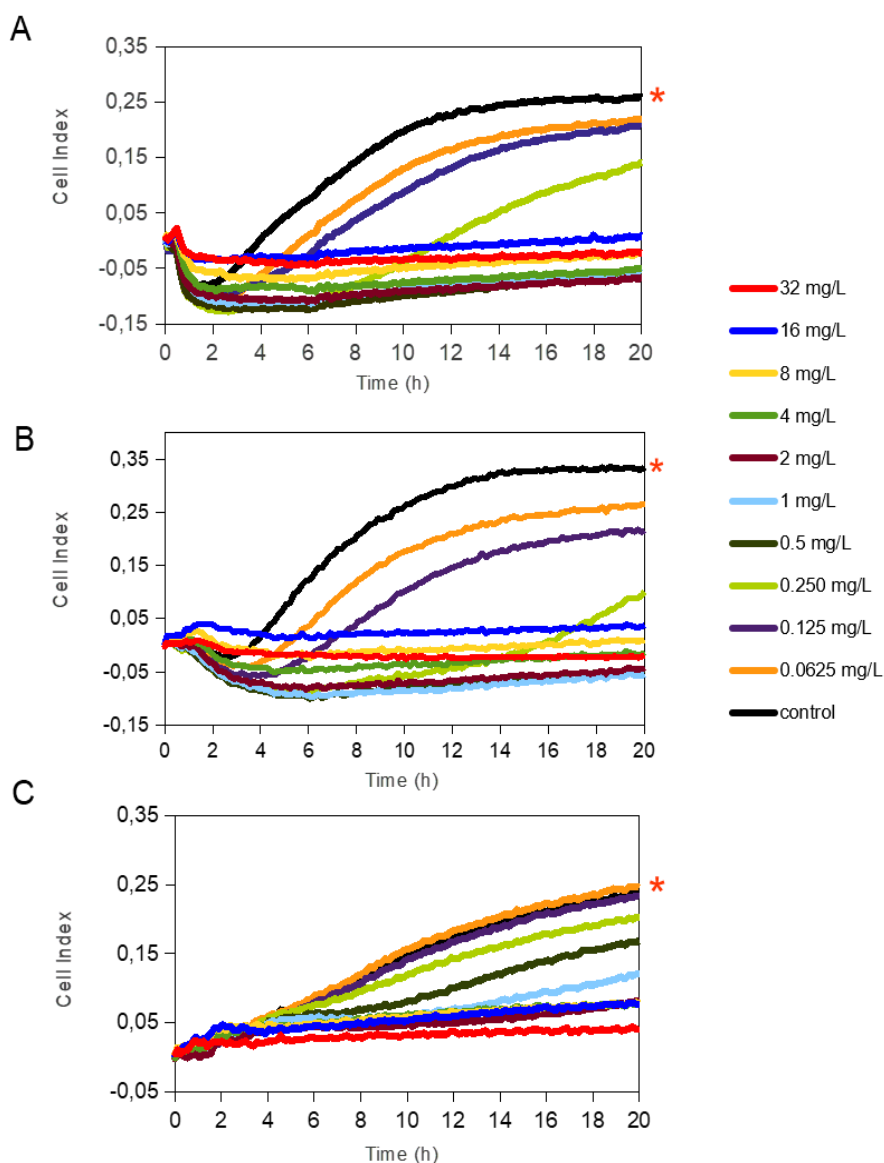


Fig. I-1 Dalbavancin effect on bacterial biofilm formation in *Staphylococcus aureus* Sa240 (A), *S. aureus* MRSA4 (B), and *Staphylococcus epidermidis* 43040 (C) strains. The cell index (CI) values are measured by impedance in an xCELLigence equipment and correlate with total biofilm mass. Red asterisks indicate dalbavancin-free controls. Dalbavancin was added from the beginning of the experiment at the concentrations of 0.0625 mg/L to 32 mg/L as indicated in the legend. Data are the means of two replicates.

The real-time dose response experiments showed that dalbavancin is highly effective antimicrobial and could prevent biofilm formation at low concentrations. The MBICs for the tested *S. aureus* strains were between 0.5 – 1, and 2 mg/L for *S. epidermidis* strain 43040 (**Fig. I-**

1 and Fig.I-S1). Table I-1 shows the values of MBIC and MIC (as measured by *E*-tests) for dalbavancin for *S. epidermidis* and *S. aureus* strains, indicating that MBIC is up to 22 times higher compared to the growth of the same strains on agar plates.

Table I-1 Comparison between dalbavancin MBICs at 20h of growth, as determined by impedance measurements, and MICs measured by standard *E*-test.

STRAIN	MBIC (mg/L)	MIC (mg/L)
<i>S. epidermidis</i> 43040	2	0.094
<i>S. aureus</i> 240	0.5	0.064
MRSA1	1	0.125
MRSA2	0.5	0.094
MRSA3	0.5	0.023
MRSA4	0.5	0.125
MRSA5	0.5	0.125

Dalbavancin effect on biofilm formation compared to other antibiotics

To further evaluate the dalbavancin effect on biofilm formation in *S. aureus* and *S. epidermidis* strains, we compared the effect of dalbavancin on biofilm formation to four antibiotics with different mechanism of action, all of them commonly used in the clinical practice: vancomycin, linezolid, cloxacillin and rifampicin. For these experiments, we selected MRSA4 isolate, which showed the highest CI values compared to other MRSA strains (**Fig.I-S2**), together with methicillin-susceptible *S. aureus* strain 240 and the clinical isolate of *S. epidermidis* 43040. Figures **I-2A-C** show the percentage of biofilm formation inhibition/induction relative to antibiotic-free control for each strain (corresponding to 100% in the graphs). Although antibiotic affect appeared to be strain specific, dalbavancin and rifampicin prevented biofilm formation in a dose-dependent manner, showing higher biofilm inhibition rates than vancomycin, linezolid or cloxacillin. Cloxacillin was only effective against *S. aureus* strain 240 and could partially inhibit biofilm formation at some of the tested concentrations in *S. epidermidis* 43040. However, none of the tested concentrations could eliminate preformed biofilm completely in this strain or in MRSA4. In fact, the exposure of MRSA4 to low

concentrations of cloxacillin (0.06-0.125 mg/L) was not only ineffective but in fact also promoted biofilm formation up to 20% compared to the untreated control (**Fig. I-2B**). Additionally, neither linezolid nor vancomycin appeared to be effective against *S. aureus* and *S. epidermidis* biofilm development at low concentrations, and both tested antibiotics induced biofilm growth at concentrations < 4mg/L in strain MRSA4. It is important to underline that the MBIC for all tested antibiotics is considerably higher than that estimated by the traditional *E*-test method (**Table I-S2**).

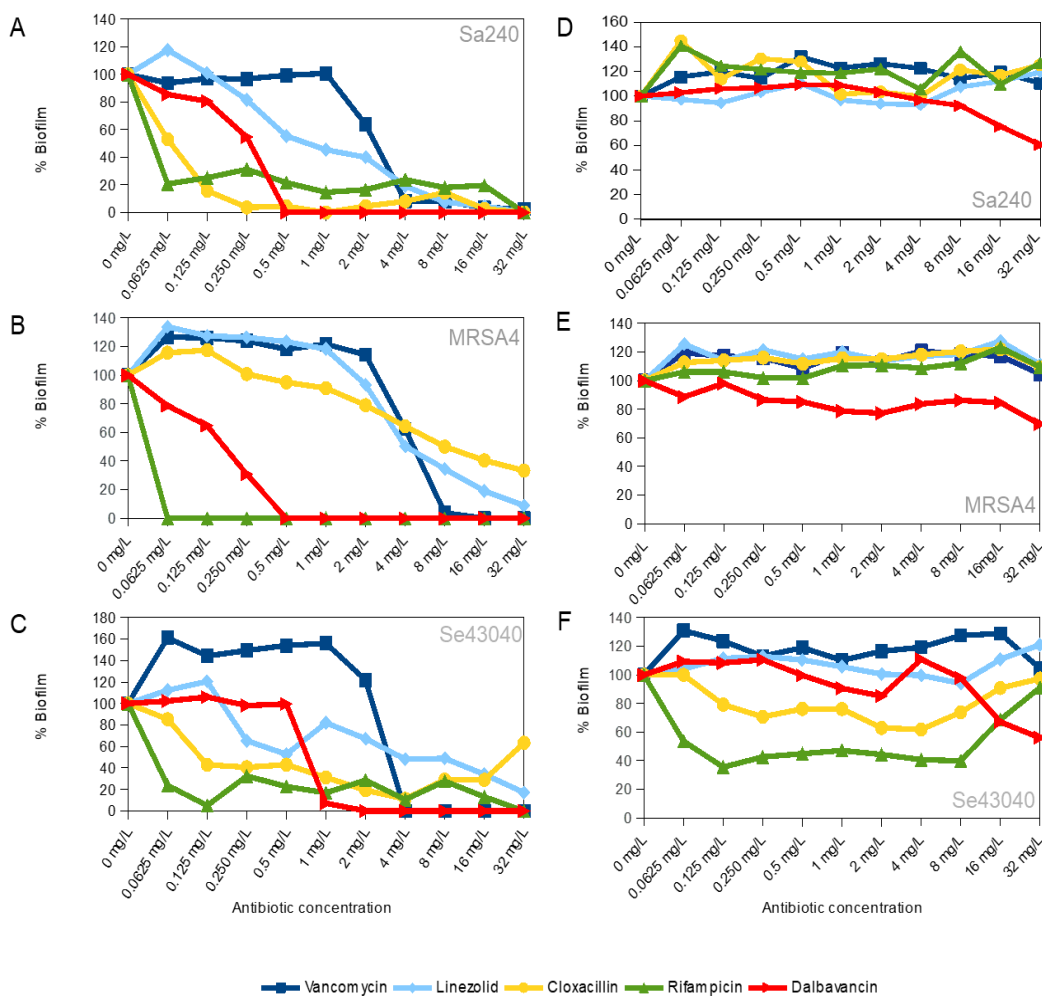


Fig. I-2 Concentration dependent effect of vancomycin, linezolid, cloxacillin, rifampicin and dalbavancin on biofilms in *Staphylococcus aureus* Sa240, *S. aureus* MRSA4 and *S. epidermidis* 43040 strains. (A-C) The antibiotics were added at the beginning of the experiment together with the bacterial inoculum. (D-F) The antibiotics were added when biofilms were already formed at their exponential growth phase. All charts indicate biofilm formation at 20h of growth expressed as the percentage of cell index (CI) compared with the control without antibiotic. Values below

100% indicate biofilm inhibition, whereas values over 100% indicate biofilm induction, in comparison with biofilm mass achieved in the absence of each antibiotic.

Dalbavancin effect on established biofilms

It is known that some antibiotics have a limited to penetrate in established bacterial biofilms³⁰⁶. For this reason, we further tested the effect of dalbavancin on already formed staphylococcal biofilms. In our experimental setting, we considered established biofilms those that which were on exponential biofilm growth phase¹⁹⁷, that is, between 6 and 9h depending on the strain, as previous work has shown that exopolymeric matrix was fully formed by that time^{196,307}. **Figure I-3** shows biofilm growth dynamics when different dalbavancin concentrations were added at the exponential biofilm growth phase. The data indicate that biofilm elimination was never achieved, but high concentrations of this antibiotic (8-32 mg/L) were able to reduce or fully prevent new biofilm formation and its further development in all the tested strains. Moreover, dalbavancin at 32 mg/L concentration was able to decrease the CI values over 40% compared to antibiotic-free controls after 20h of inoculation (**Figs. I-2 D-F**). The potential effect of dalbavancin was evident in the methicillin resistant isolate MRSA4, where all tested concentrations resulted in biofilm growth reduction and partial elimination. Additionally, a strain-dependent effect was observed at low concentrations: whereas a concentration of 0.5 mg/L prevented new biofilm growth in *S. epidermidis* 43040, concentrations lower than 4 mg/L in *S. aureus* 240 turned out to be ineffective (**Figs. I-2 D-F, I-3**).

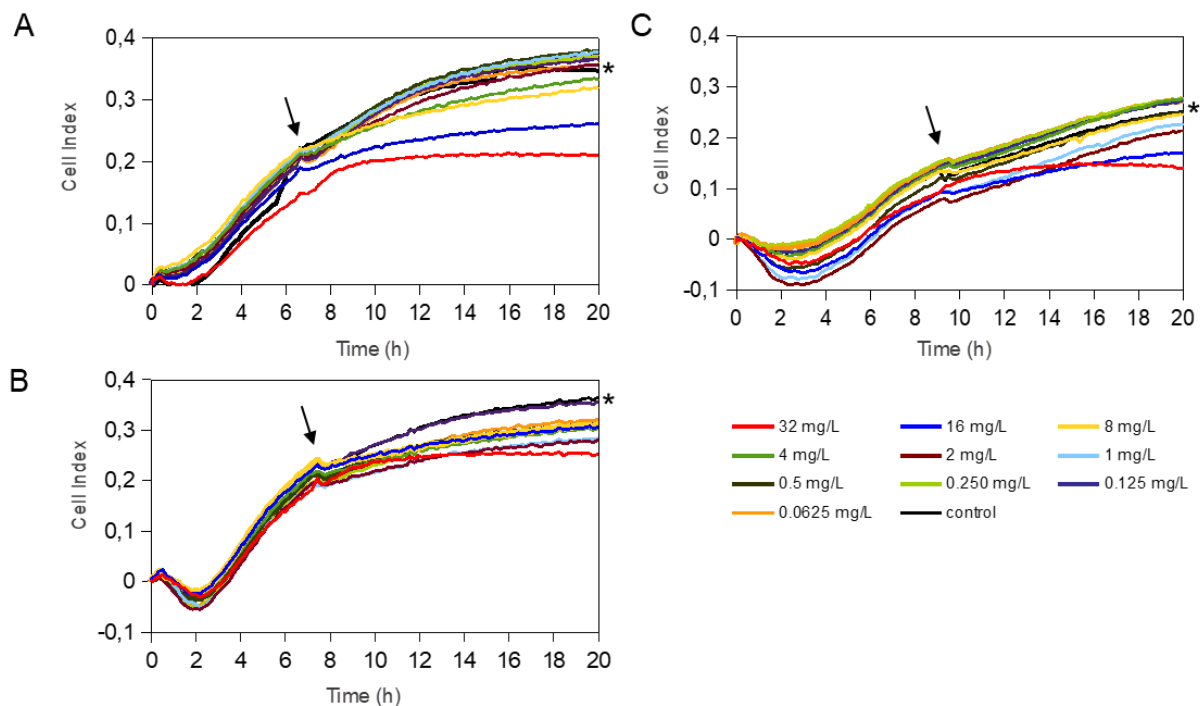


Fig. I-3 Dalbavancin effect on established staphylococcal biofilms in *Staphylococcus aureus* 240 (A), *S. aureus* MRSA 4 (B) and *Staphylococcus epidermidis* 43040 (C) strains. Dalbavancin was added at the exponential growth phase of the biofilm (marked by black arrows) at 6h (*S. aureus* Sa240), 7h (*S. aureus* MRSA4) or 9h (*S. epidermidis* 43040) at the concentrations shown in the legend. Black asterisks indicate antibiotic-free cell control. Data are the means of two replicates.

Dalbavancin effect on established biofilms compared to other antibiotics

To evaluate the potential effect of dalbavancin in a comparative way, we performed dose-response experiments using conventional antibiotics on already pre-formed biofilms (**Figs. I-2 D-F**). In contrast to dalbavancin, exposure of established MRSA4 biofilms to vancomycin, linezolid, cloxacillin and rifampicin had no inhibitory effect at the maximum tested concentration of 32 mg/L. In addition, lower doses of these antibiotics (< 32 mg/L) increased biofilm formation in this strain. The data indicate that dalbavancin was the only effective antimicrobial showing a strong biofilm inhibition capacity for this strain. Dalbavancin also halted new biofilm formation at 8-32 mg/L in *S. aureus* 240, while the other tested antibiotics resulted in increased biofilm growth in at these concentrations. In the case of *S. epidermidis* strain 43040, both rifampicin and cloxacillin were able to decrease biofilm growth at the concentrations ≤ 8 mg/L (**Fig. I-2F**). Surprisingly, higher concentrations of these antibiotics (8-32 mg/L) had a limited effect in *S. epidermidis* 43040. The least effective antibiotic on preformed

biofilm growth inhibition was vancomycin. This antibiotic induced biofilm formation of all tested strains (>30% relative to antibiotic-free controls) at 20h of growth.

Combined effect of biofilm and biofilm-detaching compounds

For this analysis, we selected an emerging therapeutic agent with mucolytic properties, NAC³⁰⁸ and a natural plant protease, ficin, which has recently been described as an enzyme with unique properties to destroy biofilm matrix¹⁹⁴. **Supplementary figure I-S3** summarizes the effect of both anti-biofilm compounds on the biofilm formation of *S. aureus* 240, MRSA4, and *S. epidermidis* 43040 strains, when added at the moment of inoculation. Graphs show that all tested NAC concentrations induced biofilm formation in *S. epidermidis* 43040, while 8 g/L were able to slightly diminish biofilm formation in both Sa240 and MRSA4 strains. On the other hand, ficin (1.000, 100 and 10 mg/L) showed a notable effect on *S. aureus*, inhibiting their formation by 47% in Sa240 and 25% in MRSA4 strains, after 20h of biofilm growth. On the contrary, this compound resulted in induction of *S. epidermidis* 43040 biofilm formation. Thus, the effect of these two compounds is species dependent.

Given that established biofilms are very difficult to eradicate we next tested whether NAC or ficin alone or in combination with dalbavancin could have any effect on preformed staphylococcal biofilms. **Figure I-4** sums up the effect of dalbavancin and biofilm-detaching compounds separately and in combination when they were added at the exponential growth phase. **Figures I-4 A-C** represent CI values taken 10h of biofilm development, while **figures I-4 D-F** represent those taken at 20h. Dalbavancin alone at the concentration of 32 mg/L (represented as D32) greatly diminished new biofilm formation for all the tested strains. NAC, when administered alone on already-formed biofilms, also had an inhibitory effect on all three tested strains (**Fig. I-4**). However, when dalbavancin and NAC were combined, the inhibitory effect was dramatically hampered, and in *S. aureus*, it even led to biofilm induction. This suggests that the combination of NAC and dalbavancin is antagonistic.

Ficin, when administered alone, had a significant effect in both *S. aureus* strains, preventing new biofilm formation up to 52% compared to an untreated control at both 10 and 20h of biofilm growth (**Figs. I-4 A-E**). However, ficin had no inhibitory effect on *S. epidermidis* 43040 biofilms. Interestingly, the combination of ficin with 32 mg/L of dalbavancin on this

strain produced less inhibition than the antibiotic alone (**Fig. I-4F**), suggesting a potential counterproductive effect of both compounds.

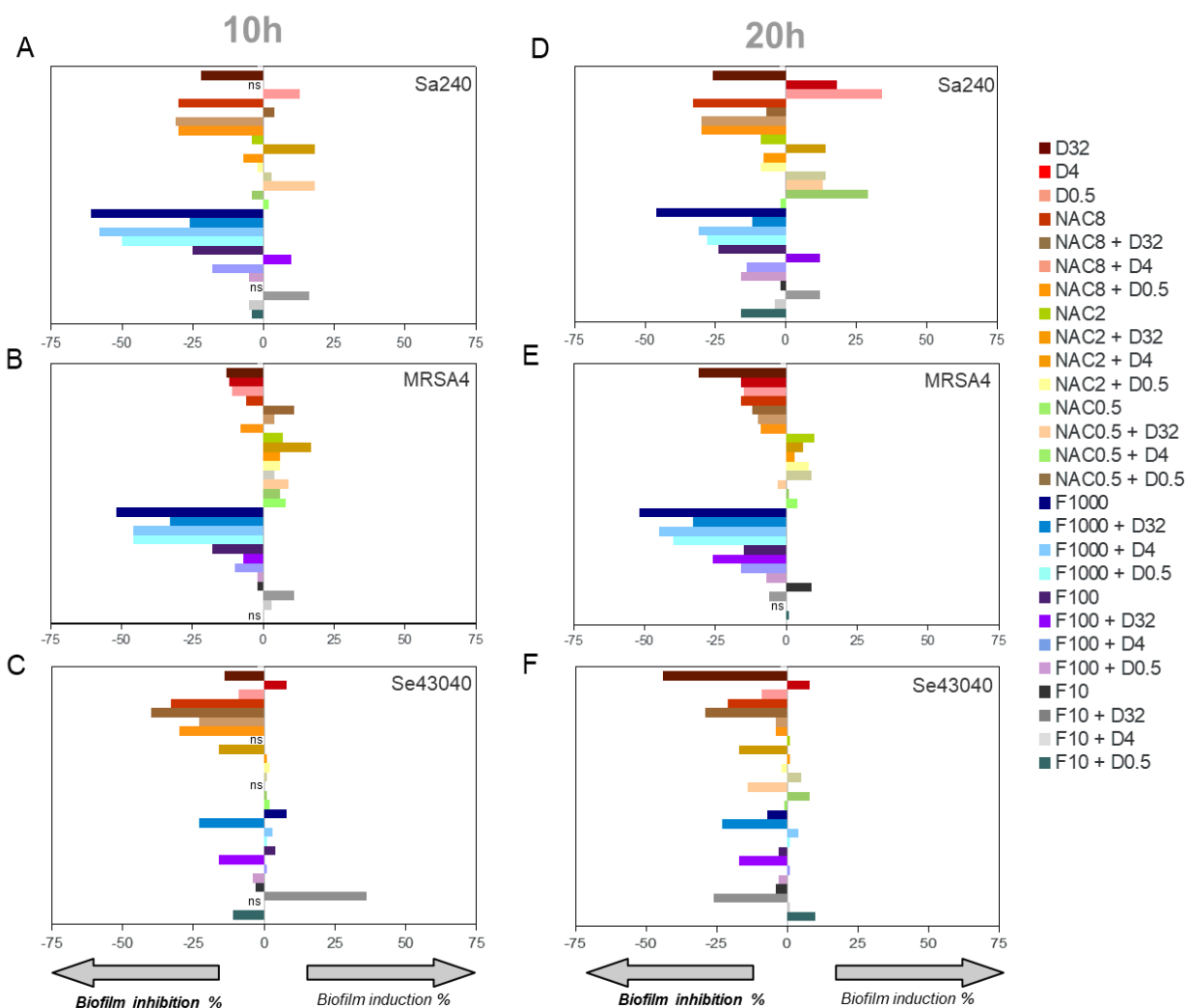


Figure I-4. Effect on the biofilm growth of *Staphylococcus aureus* 240 (**A, D**), MRSA4 (**B, E**) and *S. epidermidis* 43040 (**C, F**), respectively, of the biofilm-detaching compounds ficin –**F**– (1,000, 100, 10 mg/L) and *N*-acetyl-L-cysteine –**NAC**– (8, 2, 0.5 g/L), and the antibiotic dalbavancin –**D**– (32, 4, 0.5 mg/L) alone or in combination. **A-C** graphs correspond to biofilm inhibition or induction values observed at 10h of biofilm formation shown as percentage relative to control, while **D-F** to 20h of biofilm growth, respectively. On the X axis, zero corresponds to biofilm mass of antimicrobial-free cell controls at 10 and 20h of biofilm growth on an xCELLigence 96-well plate.

On the contrary, the combination of 32 mg/L of dalbavancin with 1.000 mg/L of ficin in *S. aureus* MRSA4 led to a significant improvement of biofilm of biofilm inhibition relative to the antibiotic alone ($p < 0.05$) (**Fig. I-5 A**) suggesting a potentiating effect. Although ficin alone produced higher biofilm reduction (**Fig. I-5A**), the detached cells were viable as they were not affected by this molecule (**Fig. I-5B**). This was confirmed by an increase in planktonic cells after ficin administration (**Fig. I-6C**). Thus, when using ficin, an effective antibiotic is needed, in order to inactivate bacterial cells which are detached as a result of enzyme's activity and to prevent further colonization.

Effect of biofilm-detaching compounds on planktonic bacterial growth.

To investigate if NAC and ficin only hold biofilm-detaching properties or also have a direct antimicrobial effect on bacterial cell growth, we further assessed the effect of both compounds on planktonic bacterial growth. After the exposure of *S. aureus* 240, MRSA4 and *S. epidermidis* 43030 to different NAC concentrations (0.5-32 g/L) it was observed that 8 g/L reduced bacterial growth by over 50%, indicating that this compound alone has a strong antimicrobial effect. Bacterial growth was fully eliminated when NAC concentration reached 32 g/L (MIC for all tested strains) (data not shown). On contrary, none of the tested ficin concentrations (1.000, 100, 10 mg/L) affected planktonic bacterial growth, indicating that ficin has proteolytic effect only on biofilm exopolymeric matrix, resulting in an efficient biofilm-embedded cell dispersal (**Fig. I-5B**).

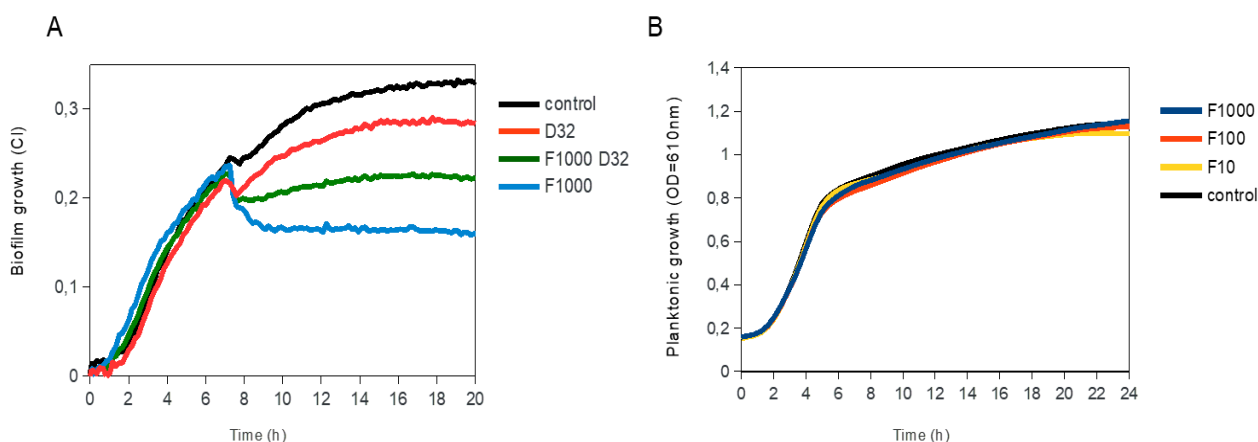


Figure I-5. Biofilm disruption by ficin alone and in combination with dalbavancin. **(A)** Biofilm treatment with ficin [marked as F (1,000, 100 and 10 mg/L)] and dalbavancin [marked as D (32 mg/L)] either alone or in combination (F1000 D32), in methicillin resistant *Staphylococcus aureus* strain MRSA4. Ficin, dalbavancin or both were added on established biofilms after 7h of growth in an xCELLigence equipment. **(B)** Effect of ficin on planktonic bacterial growth, measured as optical density in a 96-well plate. Bacteria were grown in TSB supplemented with 0.25% of glucose at 37°C. Data are the means of three replicates.

Comparison of impedance measurements with classical biofilm quantification methods

To verify that observed changes in CI are comparable to standard methodologies, we performed CV staining and CFUs of MRSA4 biofilms untreated or treated with ficin and dalbavancin alone and their combination. **Figures I-6A-B** represent optical density measurements at 24h of biofilm growth when ficin and dalbavancin were added. The addition of dalbavancin significantly decreased the number of adhered bacterial cells on 96-well plate. Reduced staining in the wells was also observed in cases where ficin was added alone or in combination with dalbavancin, confirming our previous observations of the ability of ficin to detach bacterial cells from biofilms. We also performed viable cell counting both in biofilm and unadherent bacterial cells in supernatants (**Fig. I-6C**). CFU counts showed that the viability of biofilm-embedded cells and planktonic cells was significantly affected by ficin alone. When ficin was added alone, cell viability was not affected and a lower number of bacterial cells were observed in biofilms, together with a higher number of planktonic cells compared to the untreated control. These observations confirm the lack of antimicrobial properties of ficin and its biofilm-disaggregating activity. On the other hand, when ficin was added together with dalbavancin, the viability of both biofilm and unadherent cells decreased almost three orders of magnitude in biofilm cells and two orders of magnitude in unattached cells, showing a potentiating effect and suggesting that ficin increases the susceptibility of biofilms to this antibiotic.

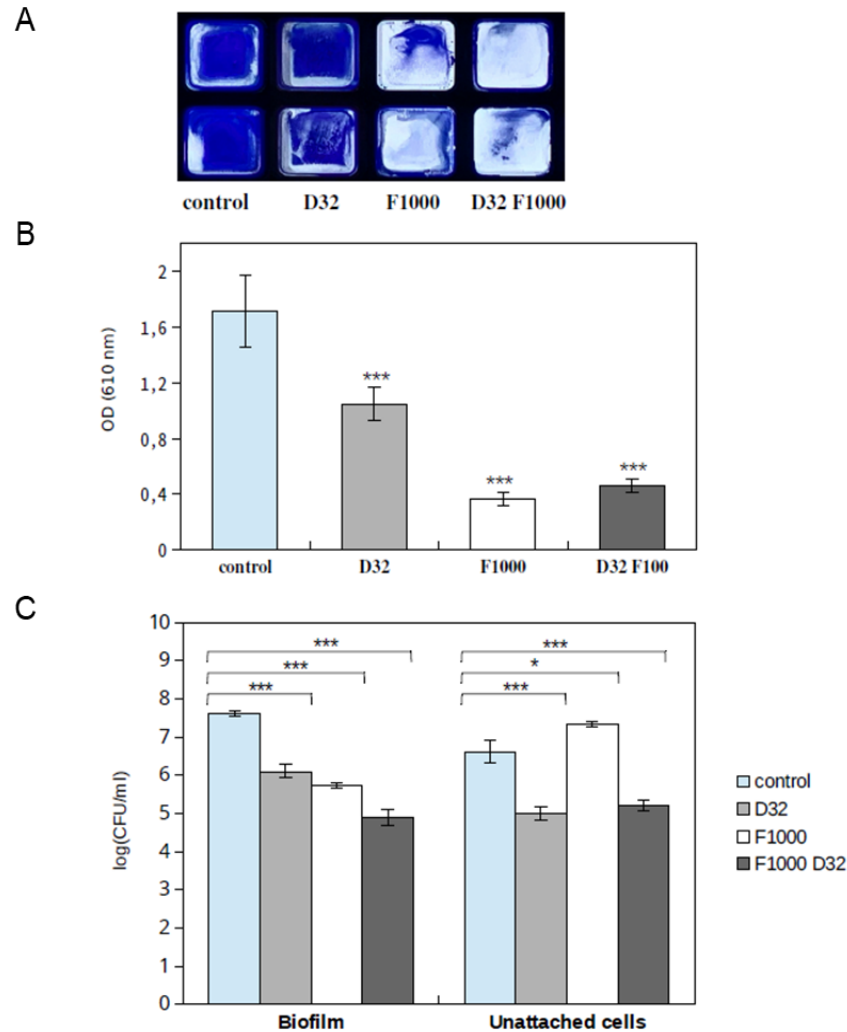


Figure I-6. Effect of 1,000 mg/L of ficin (marked as F1000) and 32 mg/L of dalbavancin (D32) on preformed MRSA4 biofilms as measured by CV staining and viable CFU counting. **(A)** Biofilm quantification by CV in flat-bottom 96-well Ibidi plates performed in duplicate. **(B)** Biofilm formation capacity after different treatments and CV staining (measured as optical density). Data show average values from three biological replicates. **(C)** Bacterial viability of biofilm and planktonic MRSA4 cells after treatment by ficin, dalbavancin and their combination for 24h. Data show the average of log CFUs from three replicates. Statistical significance was assessed by *t*-test, asterisks indicate * $p \leq 0.05$, *** $p \leq 0.001$.

DISCUSSION

Biofilm-forming capacity of staphylococcal strains contributes enormously to the pathogenesis of implant-associated infections, protecting these opportunistic pathogens from

both immune system attack and antibiotic treatment⁶. Dalbavancin has already been described as an antibiotic with a potent *in vitro* bactericidal activity against many gram-positive pathogens including MRSA and MRSE, in planktonic mode of growth²⁹⁵. However, the effect of dalbavancin on bacterial biofilms remains unclear as it has only been tested on a few occasions by using standard methods such as CV staining or MIC determinations^{298,309}. The impedance-based method performed in the current manuscript allows studying of the dynamics of biofilm formation and therefore the extent of biofilm reduction in different time points, obviating the need to select for a specific endpoint¹⁹⁶. In this study we evaluate dalbavancin effect on the pattern and dynamics of *in vitro* biofilm growth in one *S. epidermidis* and six *S. aureus* strains and compare its efficacy to four different conventional antibiotics commonly used in clinical practice (vancomycin, cloxacillin, linezolid, and rifampicin). Our experiments prove that dalbavancin and rifampicin were the best therapeutic agents against *S. aureus* and *S. epidermidis* biofilm formation in a dose-dependent manner when added at the beginning of biofilm growth. Interestingly, the superior efficacy of these two antibiotics is not related to their mechanism of action, as rifampicin inhibits RNA polymerase³¹⁰ and dalbavancin interferes with bacterial cell wall synthesis²⁹⁵. Although rifampicin has been used in clinical practice against staphylococcal biofilm-related infections for almost three decades³¹¹ this antibiotic should be administered carefully because of the danger of rapid emergence of rifampicin-resistant bacteria^{312,313}. Thus, dalbavancin emerges as a promising in the fight against device-related infections, confirming promising results obtained in animal models^{300,301}.

The impedance measurements performed in the current work show that, once biofilm is formed, dalbavancin was the only tested antibiotic which could arrest new biofilm formation and prevent its further development in methicillin resistant isolate MRSA4, and was effective in Sa240 and Se43040 at the concentrations of 8-32 mg/L. The other tested antimicrobials not only lacked an inhibitory effect on already formed-biofilms, but they also caused an induction of biofilm formation (**Figs. I-2 D-F**). Given that some of these antibiotics have been shown to be able to penetrate through thick biofilms, their lack of inhibition could be due to a low metabolic activity of biofilm-embedded cells which is known to decrease their susceptibility to antibiotics^{306,314,315}. Thus, our data suggest that dalbavancin may act on established biofilms more efficiently than linezolid and vancomycin which are among the most common antibiotics clinically administered for biofilm infections caused by *S. aureus* and *S. epidermidis*³¹⁶. This

might be facilitated by its mechanism of action because this antibiotic not only inhibits bacterial cell wall synthesis but also has an ability to bind to bacterial membranes²³⁴.

Given that even dalbavancin showed a limited efficacy to eradicate already-established biofilms, an effort was made to investigate its combined effect together with ficin and NAC, which have been reported to have biofilm-detaching properties. Unexpectedly, *in vitro* interactions between dalbavancin and biofilm-detaching compounds in preformed biofilms showed a dose and species-dependent effect (**Fig. I-4**). For example, the combination of NAC at concentrations of 8, 2 and 0.5 g/L with 32 mg/L of dalbavancin showed a decreased efficiency in inhibiting *S. epidermidis* biofilms compared to dalbavancin alone. This indicates that the combination of biofilm-detaching and antimicrobial compounds should be carefully tested in order to predict its combined effect.

We also observed that NAC had a direct antimicrobial effect on planktonic cells, while ficin did not inhibit bacterial growth at any of the tested concentrations (**Fig. I-5B**). This suggests that ficin is able to detach *S. aureus* biofilms by targeting only the biofilm matrix structure, in contrast to NAC. This should be considered when designing combined treatment strategies. For instance, our data demonstrate that ficin in combination with dalbavancin at final concentrations of 1,000 mg/L and 32 mg/L, respectively, showed an enhanced efficiency in the eradication of established MRSA4 biofilms compared to dalbavancin alone (**Fig. I-5A**). Although ficin alone provided an even greater biofilm reduction, its lack of antimicrobial activity implies that detached biofilm cells without the presence of an appropriate antibiotic could reach the bloodstream and result in serious medical complications. Therefore, we propose the combination of both a biofilm-detaching compound and an efficient antibiotic for maximal efficiency.

Altogether, the observations for the current manuscript show that dalbavancin has a strong activity against staphylococcal biofilms *in vitro*, making this antibiotic a promising agent to combat biofilm-mediated infections. Although its effect on already formed biofilms is limited, ficin appears to intensify its efficacy, and the combination of dalbavancin with this or other disaggregating compounds should be further studied in the future. The differences obtained between agar-grown and biofilm-grown cultures underline that the use of appropriate biofilm susceptibility tests, such as those provided by impedance measurements, may offer a more

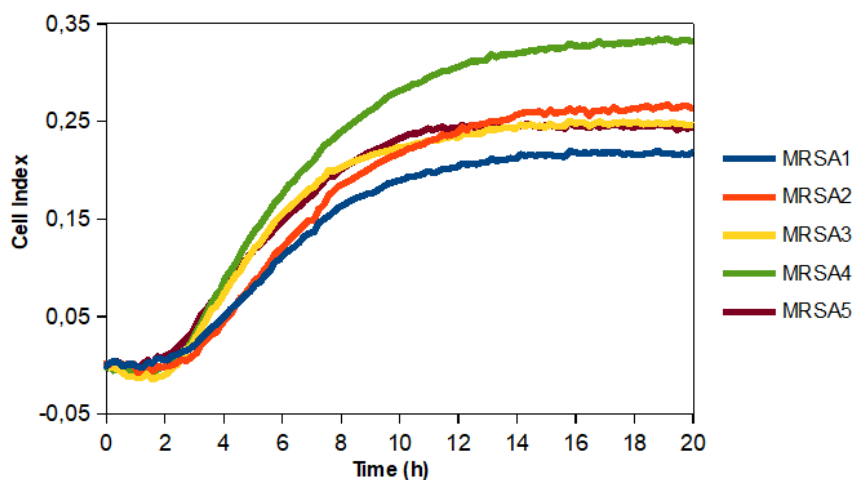
accurate alternative for selection of fast and individualized antibiotic treatment. Whether the use of impedance-based biofilm susceptibility tests allow earlier discharge from the hospital and lower rates of treatment failure should be clinically evaluated in the future.

CHAPTER I SUPPLEMENTARY INFORMATION**Supplementary table I-S1.** Characteristics of bacterial strains used in this study.

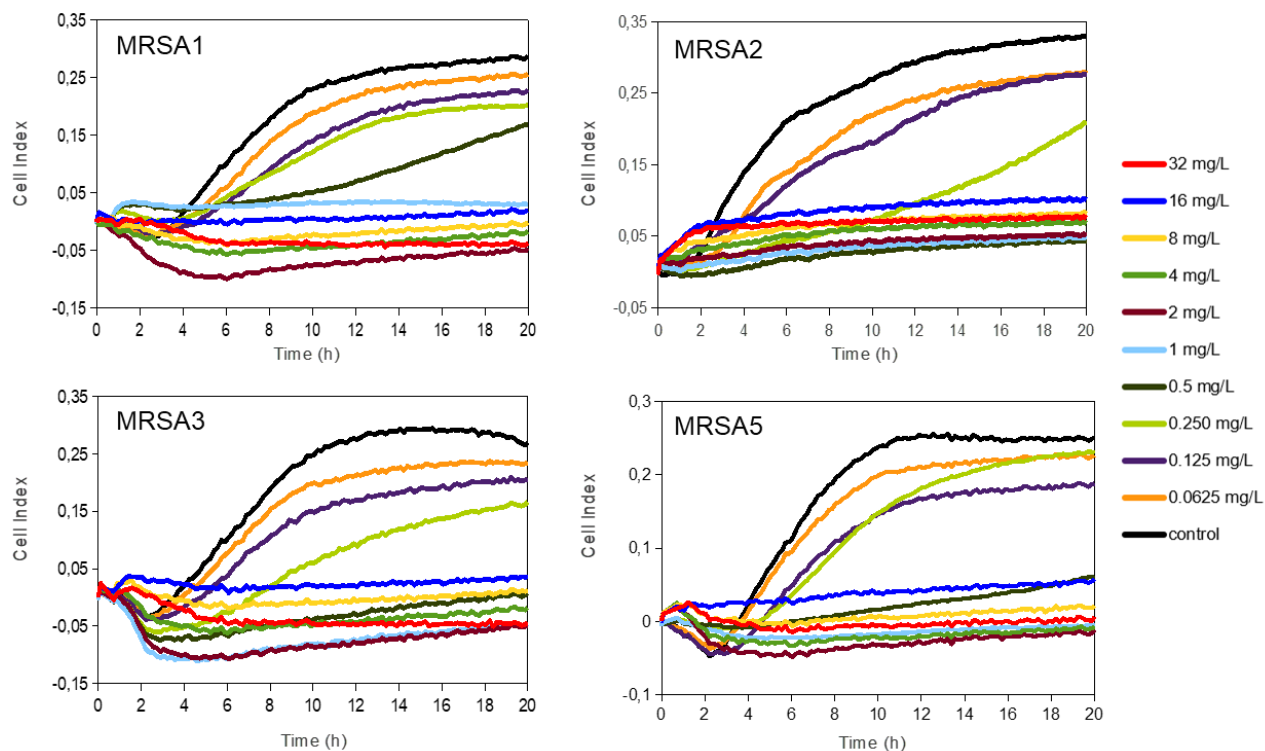
Strain	Species	Relevant properties	Source or reference
43040	<i>S. epidermidis</i>	Clinical isolate from catheter related bacteremia	Ferrer et al., 2017
240	<i>S. aureus</i>	Reference strain for antibiotic test	Human lesion isolated by FDA
MRSA1	<i>S. aureus</i>	Clinical isolate from catheter related bacteremia	This study
MRSA2	<i>S. aureus</i>	Clinical isolate from catheter related bacteremia	This study
MRSA3	<i>S. aureus</i>	Clinical isolate from catheter related bacteremia	This study
MRSA4	<i>S. aureus</i>	Clinical isolate from catheter related bacteremia	This study
MRSA5	<i>S. aureus</i>	Clinical isolate from catheter related bacteremia	This study

Supplementary table I-S2. Minimum inhibitory concentration (MIC) values of vancomycin, linezolid, cloxacillin and rifampicin measured by standard E-test protocols and expressed as mg/L. **S** and **R** in the table indicate if the strain was considered susceptible or resistant according to EUCAST guidelines.

	VANCOMYCIN	LINEZOLID	CLOXACILLIN	RIFAMPICIN
Sa240	0.75 S	0.75 S	0.25 S	0.5 S
MRSA4	1 S	0.5 S	>2 R	0.006 S
Se43030	2S	0.19 S	>32 R	0.5 S

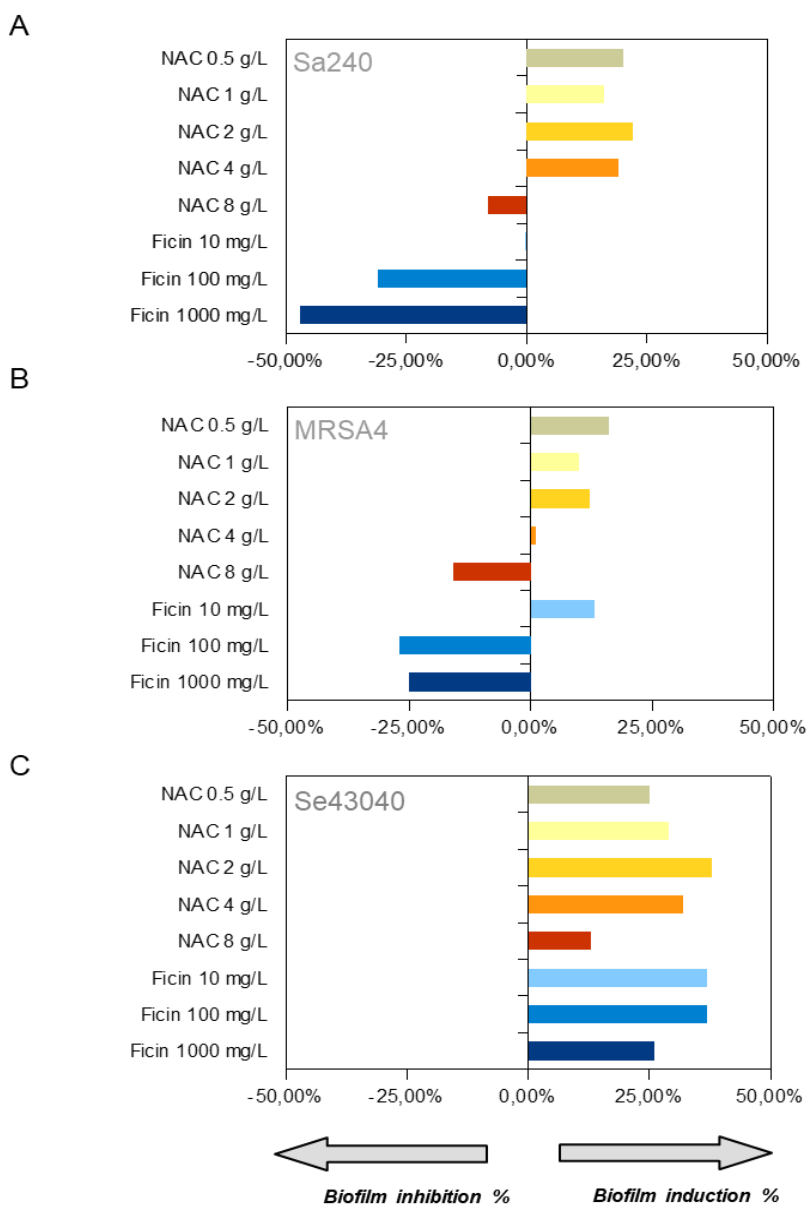


Supplementary figure I-S1. Biofilm growth dynamics of methicillin resistant *Staphylococcus aureus* strains (MRSA). Bacteria were grown on TSB supplemented with 0.25% of glucose at 37°C. The Cell Index values were measured by impedance in xCELLigence equipment and correlate with total biofilm mass. Data are the means of two replicates per strain.



Supplementary Figure I-S2. Dalbavancin effect on bacterial biofilms in methicillin resistant *Staphylococcus aureus* MRSA1, MRSA2, MRSA3 and MRSA5 strains. Dalbavancin was added from the beginning of the experiment at the concentrations indicated in the legend. Bacteria were

grown on TSB supplemented with 0.25% glucose 37°C. Data are the means of two replicates per strain.



Supplementary figure I-S3. Effect of anti-biofilm compounds NAC and ficin on biofilm growth of *Staphylococcus aureus* Sa240 and MRSA4 and *Staphylococcus epidermidis* 43040 strains after 20h of biofilm growth. Biofilm detaching molecules were added at the beginning of the experiments at the concentrations indicated in the Y axis. Each bar represents the percentage of biofilm inhibition/induction compared to untreated control. Biofilm growth was determined by impedance values in xCELLigence equipment. All obtained values were statistically significant (n=5 per treatment, t -test, $p < 0.05$).

CHAPTER II

Real-time monitoring of *Pseudomonas aeruginosa* biofilm growth dynamics and persister cell's eradication

This chapter has been published in *Emerging Microbes & Infections*, October 2021, doi.org/10.1080/22221751.2021.1994355

ABSTRACT

Biofilm formation and appearance of persister cells with low metabolic rates are key factors affecting conventional treatment failure and antibiotic resistance. Using impedance-based measurements, crystal violet staining and traditional culture we have studied the biofilm growth dynamics of 13 *Pseudomonas aeruginosa* strains under the effect of seven conventional antibiotics. Real-time growth quantifications revealed the exposure of established *P. aeruginosa* biofilms to certain concentrations of ciprofloxacin, ceftazidime and tobramycin induced the emergence of persister cells, that showed different morphology and pigmentation as well as increased antibiotic resistance. Whole-genome sequencing of wildtype and persister cells identified several SNPs, a genomic inversion, and a genomic duplication in one of the strains. However, these mutations were not uniquely associated, suggesting that the persister phenotype might be related to metabolic and transcriptional changes. Given that mannitol has been proposed to activate bacterial metabolism, the synergistic combination of mannitol and ciprofloxacin was evaluated on clinical 48h *P. aeruginosa* biofilms. When administered at doses ≥ 320 mg/L, mannitol was capable of preventing persister cell formation by efficiently activating dormant bacteria and making them susceptible to the antibiotic. These results were confirmed by using viable colony counting. As the tested ciprofloxacin-mannitol combination appeared to fully eradicate mature biofilms, we conclude that impedance-based biofilm diagnostics, which permits antibiotic susceptibility testing and the identification of persister cells, is of great potential for the clinical practice and could aid in establishing treatment breakpoints for emerging biofilm-related infections.

INTRODUCTION

Biofilms can be described as bacterial communities immobilized in a self-secreted biopolymeric matrix. This matrix is mainly composed of macromolecules, including DNA, proteins and polysaccharides and has a very selective permeability to nutrients and antimicrobial compounds^{224,317}. Thus, biofilms have already been described to be up to 1,000 times more resistant to antibiotics compared to their planktonic forms and exhibit a large threat to human health²⁴. Although bacterial biofilms have been deeply investigated during the past decades, a mayor limitation is that most of existing methods for biofilm research provide information at a single end point, therefore losing relevant features about the growth and persistence dynamics^{164,168,318}. In addition, classical biofilm mass quantification usually provides high standard deviations, and can result in lack of reproducibility due to manipulation steps. For this reason, methods for continued monitoring of biofilm growth where the biofilm does not need to be labeled or manipulated have been proposed as a powerful alternative to traditional staining procedures^{161,196}.

Pseudomonas aeruginosa is an opportunistic pathogenic bacterium, that causes both acute and chronic infections in severe wounds, urinary tract or in patients undergoing chemotherapy or any other medical condition related to a weakened immune system like cystic fibrosis^{43,226}. The pathogenic success of this bacterium is closely related to quorum sensing systems and the ability to synthesize different metabolites and virulence factors such as pyoverdinin, exotoxin A, phospholipase C and elastase^{76,91,92}. Moreover, *P. aeruginosa* infections are extremely difficult to treat, as this bacterium is extremely resistant to many antimicrobial compounds and can easily survive on abiotic and biotic surfaces such as medical equipment even after disinfection⁹⁵. In addition, biofilm formation capacity contributes enormously to infection development because biofilms protect this bacterium from immune system attack and conventional treatment^{3,35,41,315,319}.

Another impediment to treat *Pseudomonas*-related biofilm infections is the emergence of persister cells, that are characterized as subpopulations exhibiting a non-dividing state, reduced translation, low proton moving force and decreased ATP levels^{227,320,321}. The appearance of these cells can be triggered by conventional antibiotics or environmental stress including special and nutrient constraints within bacterial biofilms^{94,227}. Previous reports have suggested that persister

cells exhibit a different phenotype compared to wildtype (wt) strains, including smaller colony size or changes in pigmentation^{96,289,322}. Given that persisters can enter a non-growing state, tolerate high concentrations of bactericidal antibiotic (for example by activating efflux pumps) and regrow once treatment is ceased, these cells have already been linked to the relapse and recalcitrance of chronic infections^{289,323,324}. Although various strategies to combat persister cells such as utilization of DNA crosslinking agents, use of colistin-based antibiotic combinations or addition of glycolysis intermediates have been suggested, there are still many limitations to study and combat the emergence of persister cells within biofilms^{260,284}.

Thus, the objective of the current work was to study *P. aeruginosa* biofilm formation capacity and growth dynamics, in order to gain insights on persister cell formation and eradication. We tested biofilm formation capacity of 10 clinical isolates, two reference strains and the derivative mutant PaO1 Δ rhl Δ las by real-time impedance measurements and conventional biofilm staining methodology. Further, we described *in vitro* therapeutic efficacy of seven conventional antibiotics on biofilm formation and eradication and development as well as the effect of four of them on biofilm eradication once the biofilm was already formed. Using Real-Time impedance monitoring, we were able to identify and study persister subpopulations within mature *P. aeruginosa* biofilms treated with subinhibitory ciprofloxacin concentrations, and to evaluate the effect of mannitol alone and in combination with ciprofloxacin to eradicate the biofilms. Finally, we assessed genetic and genomic differences between dormant *P. aeruginosa* cells treated with ciprofloxacin and controls, in order to identify potential mutations associated with persistence.

MATERIALS AND METHODS

Bacterial strains and growth conditions

Clinically relevant *P. aeruginosa* strains were isolated at the Microbiology Department of the Alicante General Hospital (Spain). Model strains ATCC27853 and PaO1, and the derivative strain PaO1 Δ rhl Δ las (PaO1 Δ) with the reduced ability to form biofilms, were also used (**Table II-S1**). PaO1 was considered as strong, ATCC27853 moderate and PaO1 Δ weak biofilm-forming strains, respectively. *P. aeruginosa* strains were cultured on Tryptic Soy Agar (TSA), Lysogeny

Broth Agar (LBA) or Brain Heart Infusion (BHI) agar plates and then inoculated in Tryptic Soy Broth (TSB), Lysogeny Broth (LB) or Brain Heart Infusion (BHI) media at 37°C with vigorous orbital shaking (120 rpm).

Real-time biofilm growth assay

Real-time biofilm growth monitoring experiments were performed using xCELLigence RTCA SP equipment (Agilent) according to manufacturer's instructions as previously described^{196,198}.

To determine the most suitable conditions for *P. aeruginosa* biofilm growth in this system BHI, LB and TSB media supplemented with or without 0.5% or 1% of glucose were tested. Firstly, 100 µl of each medium were used for background measurements. After that, overnight cultures of *P. aeruginosa* were diluted with BHI, LB and TSB growth media supplemented with or without 0.5% or 1% of glucose and 100 µl of these bacterial cell suspensions were added into E-plates wells, reaching a final OD₆₀₀=0.15 and 0.3, respectively. Biofilm growth was then measured every 10 min at 37°C for 72h.

To evaluate antibiotic efficacy to inhibit biofilm formation, seven antibiotics commonly used in clinical practice were tested: ceftazidime (CAZ, Normon), ciprofloxacin (CIP, Kern Pharma), colistin (COL, Accord), tobramycin (TOB, Brown), imipenem (IPM, Fresenius Kabi), meropenem (MEM, Kern Pharma) and piperacillin-tazobactam (TZP, Accord). Biofilm formation capacity in presence of the antibiotics was monitored for 72h, in the form of Cell Index (CI) values, which correlate with total biofilm mass^{197,215}.

For treatment of mature biofilms, antibiotics with highest antimicrobial activity in prevention of biofilm formation (TZP, CAZ, CIP and TOB) were tested. In short, 100 µl of bacterial suspension (OD₆₀₀=0.2625) were used for background measurements. After that 75 µl of LB were added (reaching the final OD₆₀₀=0.15) and biofilms were grown for 24 h (PaO1) and 48 h (MF120), respectively, depending on the biofilm growth rate of each strain. At this time, corresponding to highest CIs for both PaO1 and MF120, 25 µl of the corresponding antibiotic were added, reaching final concentrations from 128 to 0.0626 mg/L. Biofilm inhibition/eradication capacity of the antibiotics was the quantified for further 120 h.

Crystal violet staining

Biofilm formation assay in microtiter plates for crystal violet staining was performed as previously described¹⁶⁴. Briefly, overnight cultures of *P. aeruginosa* strains were diluted in LB medium to OD₆₀₀=0.1 and 300 µl of bacterial suspensions were transferred into corresponding wells of 96 well flat-bottom plated 89626 (Ibidi, Germany). Biofilms were grown for 8, 24, 30, 48, 56 and 72h at 37°C. After that, the culture supernatant was discarded, cells were rinsed using Phosphate Buffer Saline (PBS pH=7.4) and attached biomass was stained with 0.1 % crystal violet (CV) for 20 mins. Subsequently, CV was removed, biofilm embedded cells were rinsed with PBS in order to remove unattached cells and residual CV and resuspended with 300 µl of 96.5% v/v EtOH. After that, optical density of released CV was measured by means of absorbance plate reader Infinite M200 (Tecan, Durham NC) at 610 nm.

Effect of mannitol on planktonic *P. aeruginosa* growth

The overnight cultures of *P. aeruginosa* isolates PaO1 and MF120 were diluted in LB medium to OD₆₀₀=0.1 and 100 µl of these suspensions were added into corresponding wells of 96-well microplates (Thermo Fisher Scientific). After that 100 µl of mannitol were added into the corresponding wells reaching final concentrations of 3200, 320, 64, 32, 16, 8, 4, 2, 1, 0.5, 0.25, 0.125 and 0.0625 mg/L/ Thereafter, microplates were incubated at 37°C with orbital shaking at 120 rpm and the effect of mannitol on planktonic bacterial growth was evaluated for 24h by the means of an absorbance plate reader Infinite M200 (Tekan, Durham NC).

MIC determination

The minimum inhibitory concentrations (MICs) of CIP, CAZ, COL, TOB, IMI, MEM and TZP were assessed using the CSLI broth microdilution method as previously described³⁰³. UMIC microdilution test for CST (Biocentric, Bucker) and E-test (Biomerieux) for the rest antibiotics were used. MBICs (minimum biofilm inhibitory concentrations) were calculated for PaO1 and for the clinical isolates with the strongest biofilm formation capacity (i.e. MF120 and MF124), considering the time points where antibiotic-free cell control reached the highest CIs (24 h for PaO1, 48 h for MF120 and 72 h for MF124, respectively), following Ferrer et al¹⁹⁶.

Identification of persisters and regrowth assay

To confirm the presence of bacterial persistent cells and not CIP mutants, *P. aeruginosa* MF120 biofilms were cultivated in the xCELLigence system for 48 h as described above. After that, CIP was added reaching a final concentration of 0.25 mg/L. At 140 h of growth, the experiment was stopped, and the biofilms exposed to CIP were plated on LBA plates containing 0.25 mg/L of CIP, in order to maintain the persister phenotype, while MF120 control cells were plated on LBA plates without additional antibiotics.

Besides the changes in growth the ability of white persister cells (MF120 treated with CIP) to revert greenish wt phenotype was investigated by two independent observers. Five persister colonies and five controls without antibiotic were selected and resuspended in 200 µl of LB media containing mannitol (3200 mg/L) and LB alone and grown at 37°C for 120 h to observe the switch from persister population into actively growing cells.

Effect of mannitol alone and in combination with ciprofloxacin on *P. aeruginosa* persisters

To describe the effect of mannitol on *P. aeruginosa* biofilm formation, mannitol was serially diluted in LB medium reaching final concentrations 3200-0.0625 mg/L. One hundred microliters of each dilution in triplicate were used for background measurements. After that, 100 µl of PaO1 and MF120 bacterial suspensions were added into the corresponding E-plate wells reaching final bacterial cell optical density of $OD_{600}=0.15$ and continuous biofilm growth was observed for 72 h in xCELLigence equipment.

The ability of mannitol to potentiate the effect of CIP and/or prevent persister bacteria formation within *P. aeruginosa* MF120 biofilms was then investigated using mannitol concentrations of 3200, 320, 64, 32, and 16 mg/L. Firstly, mannitol was added together with bacterial inoculum ($OD_{600}=0.15$). After 48 h of biofilm growth, 25 µl of CIP were added (final concentration: 0.25 mg/L), and biofilm growth was observed for additional 140 h. Similar experiments were performed adding 25 µl of mixed suspensions of mannitol and CIP on mature MF120 biofilms at 48 h. Biofilm growth after addition of both compounds was quantified for 140 h.

Colony forming unit (CFU) counting

To assess the number of viable cells after biofilm treatment with mannitol, CIP or their combination, *P. aeruginosa* biofilms were collected at 140h of growth in RTCA system and sonicated for 5 min in order to eliminate bacterial aggregates and disrupt extracellular biofilm matrix. After sonication, serial dilutions were prepared, plated in triplicates on LB plates and incubated at 37°C overnight. CFUs then were counted, averaged, and expressed as log₁₀ CFUs. Each experiment included three technical replicates and was repeated three times (biological replicates). Statistical significance was assessed using Student's *t*-test, where *p*-value 0.05 was considered as significant.

Whole-genome sequencing and bioinformatic analysis

DNA from individual colonies grown in the presence of CIP (0.25 mg/L), mannitol (3200 mg/L) or their combination (exhibiting non-identical phenotypes) was extracted using MagNA Pure LC DNA Isolation Kit III for Bacteria and Fungi (Roche diagnostics) following manufacturer's instructions. For each colony type, two colonies from the same agar plate were selected as replicates. After that, Illumina libraries were constructed at the Sequencing Platform in FISABIO (Valencia, Spain) and the genomes were sequenced with NextSeq technology (Illumina) using the 500/550 High Output 75 cycles Kit (single-ends 75 bp reads).

Resultant sequenced reads (75 bp long) were trimmed for low quality reads (<20) and length (<50) using prinseq³²⁵. SPAdes³²⁶ was used for genome assembly and ORFs were detected using prodigal³²⁷ and annotated using hmmsearch³²⁸. For genomic mutations, the software flex2 (<https://github.com/asierzaragoza/flex2>) was used to visually detect genomic insertions, duplications, and inversions. Single nucleotide polymorphisms (SNPs) were detected using the software snippy and snippy-core through the Galaxy server (<https://github.com/tseemann/snippy>). The assembled contigs and the original reads have been deposited in SRA database under the accession number PRJNA753320.

Statistical analysis

Biofilm inhibition/induction after treatment with different antibiotics were considered to be significantly different from controls using linear models from the `lm` library in the R Statistical Package version 1.0.1.7 with p -value < 0.05 (<https://cran.r-project.org/web/packages/glmulti>) (accessed in January, 2021). Student's t -tests were performed to reveal statistical differences between treatments after CFUs counts. p -values < 0.05 were considered significant.

RESULTS

Influence of culture conditions on *P. aeruginosa* biofilms

Biofilm assembly can be influenced by many different factors including culturing conditions and initial inoculum size^{196,198}. We investigated the effect of initial optical density and culture growth medium on bacteria attachment and biofilm formation on E-plate surfaces. **Figure II-S2** shows biofilm formation dynamics of model strain PaO1 and clinical isolates MF117, MF118 and MF124 when grown in TSB growth media using initial OD₆₀₀ of 0.15 and 0.3. Results showed that only slight differences in total biofilm mass (CIs) for all tested strains. In addition, we tested how biofilm growth dynamics might be influenced by several growth media: LB, TSB and BHI. Since CIs reached with BHI media with or without additional glucose were very low (between 0.01 and 0.1) for most tested strains compared to other culture media, this growth medium was considered as not suitable (data not shown). On contrary, both TSB and LB permitted *P. aeruginosa* to form robust biofilms overtime, reaching high biofilm mass (CI values up to 10 times higher when compared to those observed using BHI medium) (**Fig. II-S1**). The use of TSB medium (with or without additional sugars) resulted in biofilm growth delay for all tested strains, except clinical isolate MF123 (**Fig. II-S1 AB**). For example, strain PaO1 reached the maximum CI in LB medium at 24 h, while similar CI was observed only at 55 h in TSB-0.5%-glucose. A similar trend in biofilm growth delay was observed when LB medium was supplemented with 0.5% of glucose (**Fig. II-S1 D**). Given its highest biofilm formation capacity, LB without additional glucose was chosen for *P. aeruginosa* biofilm growth in the xCELLigence system.

Comparison of impedance-based measurements to CV staining

Culturing plates materials have an impact on the adhesion capacity of *P. aeruginosa* and estimates of biofilm mass are also influenced by the quantification methods used³²⁹. **Figure II-1** A represents biofilm growth dynamics of different *P. aeruginosa* strains when grown in 96-well E-plates, as measured by impedance during 72 h; panel B corresponds to the quantification of released CV measured as OD₆₁₀ at 8, 24, 36, 48, 56 and 72 h, while panel C depicts *P. aeruginosa* biofilm biomass staining with CV at 36 h of growth for each tested strain. The results indicate that most tested strains had a similar biofilm formation and growth dynamics in both xCELLigence and Ibidi plates, suggesting that these methodologies are comparable. For example, strains PAO1, MF120 and MF124 were the strongest biofilm formers in both settings. However, as it can be seen in panel B, some of these isolates were able to adhere and form biofilms faster and stronger in Ibidi plates.

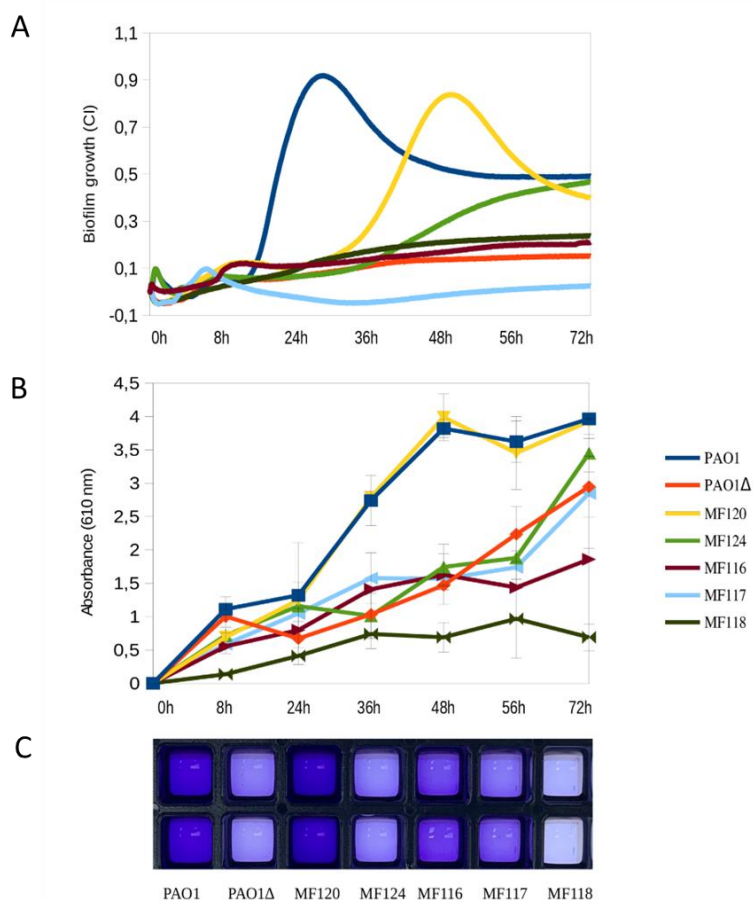


Figure II-1. Biofilm formation capacity of seven *P. aeruginosa* strains as quantified by impedance-based measurements in xCELLigence (**A**) and by Crystal Violet (CV) staining (**B**, **C**). Panel **B** represents the absorbance of released CV at 0, 8, 24, 36, 48, 56 and 72 h, where higher absorbance indicates larger biofilm growth. Panel **C** depicts biofilm formation in ibiTreat 96-well plates at 36 h, where more intense color reflects larger biofilm mass. Bacterial strains used in the experiment are indicated in the legend and include a mutant of PaO1 strain with impaired biofilm formation. Data are the means of three biological replicates.

Effect of conventional antibiotics on biofilm formation

For further analysis we chose *P. aeruginosa* strains that exhibited the highest biofilm formation capacity as measured by impedance (PaO1, MF120 and MF124) and evaluated the effect in real time of seven conventional antibiotics commonly used in clinical practice (ciprofloxacin (CIP), tobramycin (TOB), ceftazidime (CAZ), colistin (CST), piperacillin tazobactam (TZP), imipenem (IMP) and meropenem (MEM)).

Figure II-2 summarizes the effectiveness of antibiotics on biofilm formation in PaO1 and MF120 strains, while **figure II-S3** depicts the effect of these antibiotics on MF124. CIP showed a high efficiency and suppressed biofilm formation of all tested strains in a dose-dependent manner. However, the exposure of PaO1 and MF120 biofilms to 0.0625 mg/L of this antibiotic resulted in biofilm growth induction and changes in biofilm growth dynamics (**Fig. II-2**). TOB and TZP also inhibited biofilm formation when added at high concentrations. In addition, lower concentrations were not able to inhibit biofilm formation for any of the tested strains, although most of them resulted in biofilm growth delay or decreased biomass. Although none of tested concentrations of CAZ could fully inhibit biofilm formation in any of the tested strains, the inhibitory capacity of this antibiotic was concentration-dependent, and most concentrations of CAZ resulted in biofilm growth delay. Neither CST nor IMP or MEM could completely inhibit or delay biofilm growth in PaO1 and MF120. In contrast, the exposure of MF124 biofilms to 32 mg/L of CST resulted in complete biofilm growth inhibition, while lower concentrations of CST showed a dose-dependent effect (**Fig. II-S3**). These results indicate that each biofilm-forming strain should be analyzed individually, taking into account more than one end-point in order to assure the best clinical outcome.

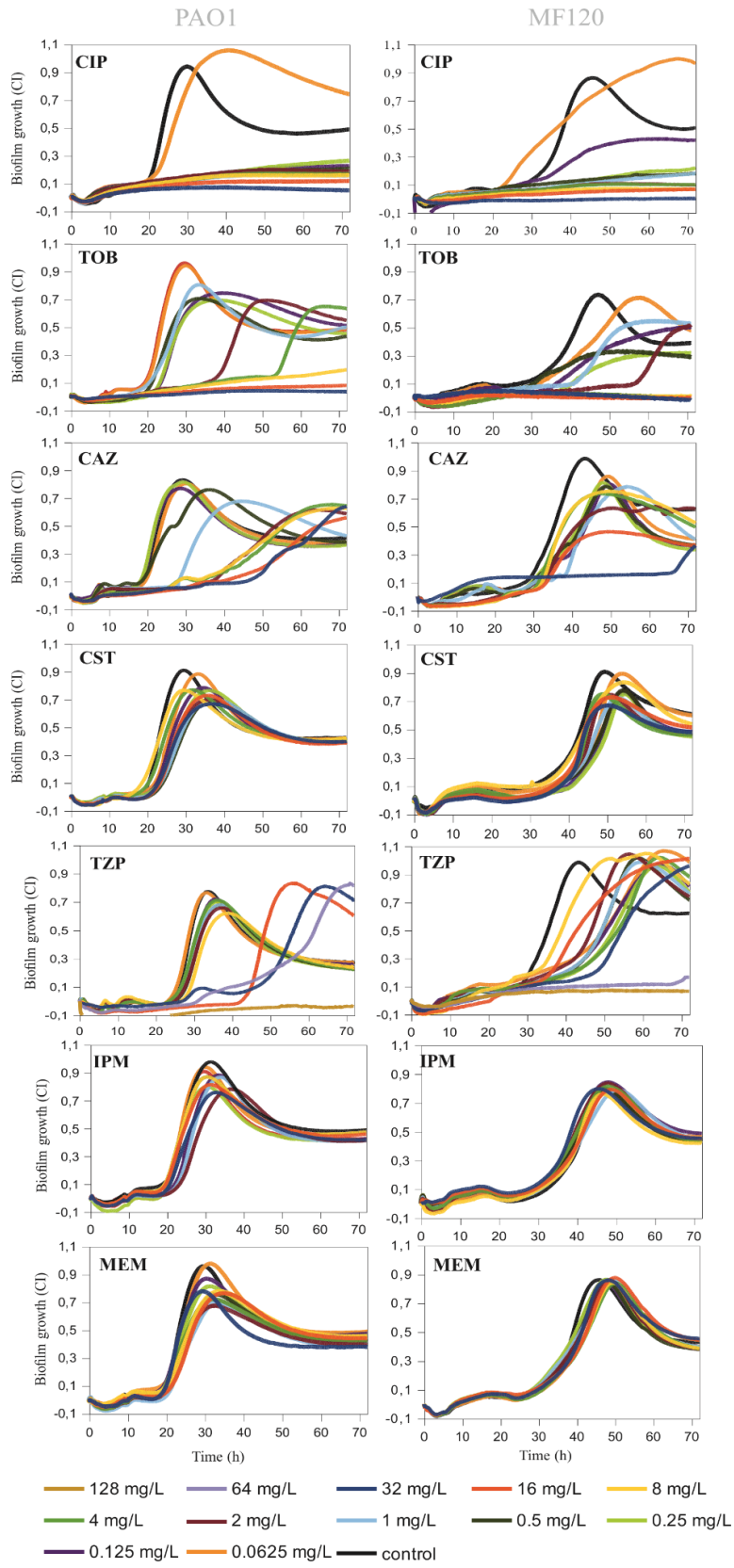


Figure II-2. Effect of ciprofloxacin (CIP), tobramycin (TOB), ceftazidime (CAZ), colistin (CST), piperacillin-tazobactam (TZP), imipenem (IPM) and meropenem (MEM) on *P. aeruginosa* PaO1 and MF120 biofilm formation. Graphs show estimates of total biofilm mass as measured at 37°C using impedance-based measurements. Black lines indicate untreated controls. Each line represents the mean of three biological replicates. All antibiotics were added at the beginning of the experiment together with bacterial inoculum from 0.0625 to 32 mg/L for all antibiotics except TZP (0.0625 to 128 mg/L). SDs are not shown for clarity.

Finally, **Table II-1** shows antibiotic susceptibilities of planktonic broth cultures (MIC) compared to the same isolates when they were grown in biofilms (MBIC). MBICs were up to 32 times higher compared to traditional MICs obtained by E-test and microdilution (**Table II-1** and **Table II-S2**).

Table II-1. Minimum inhibitory concentration (MIC) vs minimum biofilm inhibitory concentration (MBIC) values for ciprofloxacin (CIP), tobramycin (TOB), ceftazidime (CAZ), colistin (CST), piperacillin-tazobactam (TZP), imipenem (IPM) and meropenem (MEM) in different *P. aeruginosa* strains.

Minimum Inhibitory Concentration/Minimum Biofilm Inhibitory Concentration							
Strain	CIP	TOB	CAZ	CST	TZP	IPM	MEM
PAO1	0.094S/0.125	1.5S/2	1S/2	1S/>32	3S/16	1.5S/>32	0.38S/>32
MF120	0.125S/0.250	<=2S/4	2S/16	1S/>32	<=8S/32	<=1S/>32	<=1S/>32
MF124	0.19S /2	1S/8	2S/>32	1S/32	8S/32	2S/>32	0.75S/>32

Notes: MICs were measured by standard protocols (UMIC microdilution test for CST and E-tests for rest of antibiotics) and expressed as (mg/L), while MBIC were calculated according to impedance-based measurements in xCELLigence system. **S** and **R** in the table indicate if a strain is considered susceptible or resistant according to EUCAST guidelines³⁰³. MBICs were assessed by the evaluation of normalized biofilm growth curves using impedance measures (Cell Index measurements) at 24 h for PaO1, 48 h for MF120 and 72 h for MF124, respectively following¹⁹⁶.

Capability of antibiotics to eradicate pre-formed biofilms

Preformed biofilms are notoriously difficult to eradicate, as antibiotics must cross the biofilm matrix to reach biofilm-embedded bacteria². Thus, to obtain further insights on biofilm eradication dynamics, we chose antibiotics that showed the highest efficacy when added at the

beginning of biofilm growth (TZP, CAZ, CIP and TOB) and tested their ability to eradicate *P. aeruginosa* PaO1 and MF120 biofilms at 24 and 48 h, respectively. Impedance-based measurements showed that the tested concentrations of TZP (128-0.0625 mg/L) could not disrupt biofilms of the examined strains (**Fig. II-3**). CAZ, which has a similar mechanism of action to TZP and inhibits bacterial cell wall synthesis, had no biofilm inhibitory effect on MF120 biofilms, but was able to disrupt PaO1 biofilms when added at the highest dose tested (32 mg/L). However, the increase in CI at 90 h suggests that this antibiotic is not able to kill all biofilm-embedded bacteria, which could consequently result in relapsed biofilm infection (**Fig. II-3**). On the other hand, when mature *P. aeruginosa* were exposed to CIP, high concentrations of this antibiotic suppressed new biofilm accumulation and completely eradicated pre-formed biofilm in both PaO1 and MF120 strains. On the contrary, low concentrations of this antibiotic (0.0625 mg/L in PaO1 and 0.125-0.0625 mg/L) were ineffective.

In addition, we observed that certain concentrations of CIP (0.125 mg/L in PaO1 and 0.25 mg/L in MF120) although initially seemed effective, resulted in a sudden increase in CIs at approximately 80 and 100 h, respectively. This second peak of growth observed after treatment with these CIP concentrations suggested the emergence of a dormant cell fraction within PaO1 and MF120 biofilms (**Fig. II-3**) which was later investigated in more detail.

Comparably to CIP, TOB completely eradicated mature MF120 biofilm when added at relatively high concentrations (32-4 mg/L), suggesting that TOB can penetrate through the exopolysaccharide matrix and efficiently kill biofilm-embedded bacterial cells. On the other hand, TOB was not efficient on mature PaO1 biofilm, given that none of the tested concentrations could disrupt the biofilm, indicating a strain-dependent effect. In addition, similarly to CIP, TOB at 1 and 2 mg/L resulted in the rise of a second biofilm peak at 90 and 120 h, respectively, suggesting that both antibiotics can only kill a part of bacterial cells embedded in the biofilms and induce the emergence of dormant cells within *P. aeruginosa* biofilms.

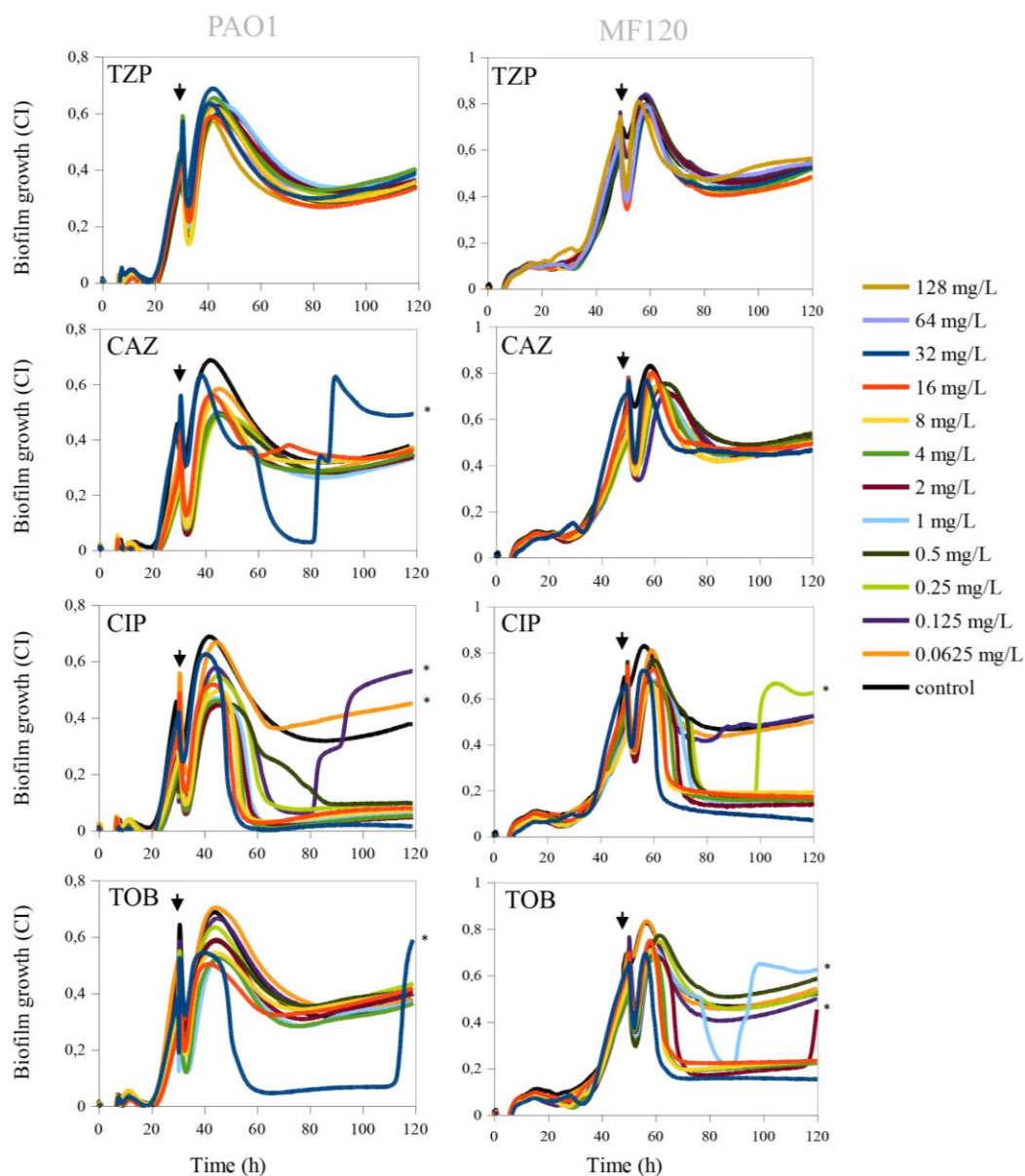


Figure II-3. Effect of piperacillin-tazobactam (TZP), ceftazidime (CAZ), ciprofloxacin (CIP) and tobramycin (TOB) on mature biofilms of PaO1 (24 h after inoculation) and MF120 (48 h) strains. After the addition of antibiotics, biofilm growth was observed for an additional 100 h. Black lines represent antibiotic-free controls while black arrows indicate the time when antibiotics were added. Each line represents the mean of three replicates. The emergence of dormant cells, which appeared after the biofilm eradication using different antibiotics is marked by black asterisks.

Mannitol effect on planktonic and biofilm growth

A range concentrations of mannitol were tested to characterize its effect on both planktonic and adherent *P. aeruginosa* growth. Absorbance measurements showed that the tested concentrations did not affect PaO1 or MF120 planktonic growth (data not shown), indicating that this compound does not have antimicrobial activity. Given that many compounds without antimicrobial effects have been linked to biofilm disassembly^{65,162,330} we have also tested if mannitol had an effect on biofilm disaggregation. Impedance measurements showed that the tested concentrations did not affect biofilm mass compared to the untreated control (**Fig. II-4 A**). This suggests that mannitol alone is not a biofilm dispersal agent. Thus, considering that mannitol has been shown to be involved in the switching of persister and tolerant phenotypes to metabolically active cells³³¹, we further evaluated how the combination of mannitol and CIP could affect biofilm formation and maturation of pre-formed MF120 biofilms in real-time.

Mannitol enhances the effect of ciprofloxacin

The addition of mannitol alone at the beginning of biofilm growth (3200 mg/L) did not result in any changes in total biofilm mass compared to the untreated control (**Fig. II-4 A**). However, when mannitol pre-treatment (3200 mg/L) was combined with a CIP concentration that favored the appearance of dormant cells (0.250 mg/L) added on a 48h biofilm, the biofilm was completely eradicated. Given that lower mannitol concentrations were not efficient and resulted in the appearance of the second biofilm peak, we conclude that mannitol may be metabolized overtime. For this reason, we have tested, whether mannitol could potentiate CIP effect more efficiently when added together with the antibiotic at 48 h. **Figure II-4 B** shows that the addition of 3200 mg/L and 320 mg/L of mannitol in combination with CIP at 48 h resulted in a complete disruption of mature MF120 biofilms. However, the combination of CIP with lower mannitol concentrations was not sufficient to revert all persister cells into actively growing bacteria. Nevertheless, a concentration-dependent effect was observed, with a delay in the second growth peak at mannitol concentrations of 16, 32 and 64 mg/L. These results were confirmed by colony counts (**Fig. II-4 C**), where CIP alone reduced cell viability 2.5 orders of magnitude, whereas 3200 mg/L of mannitol combined with CIP completely killed all bacteria

embedded in the biofilm matrix while 320 mg/L resulted in almost seven orders of magnitude reduction in the viable cell number (p -value < 0.0001).

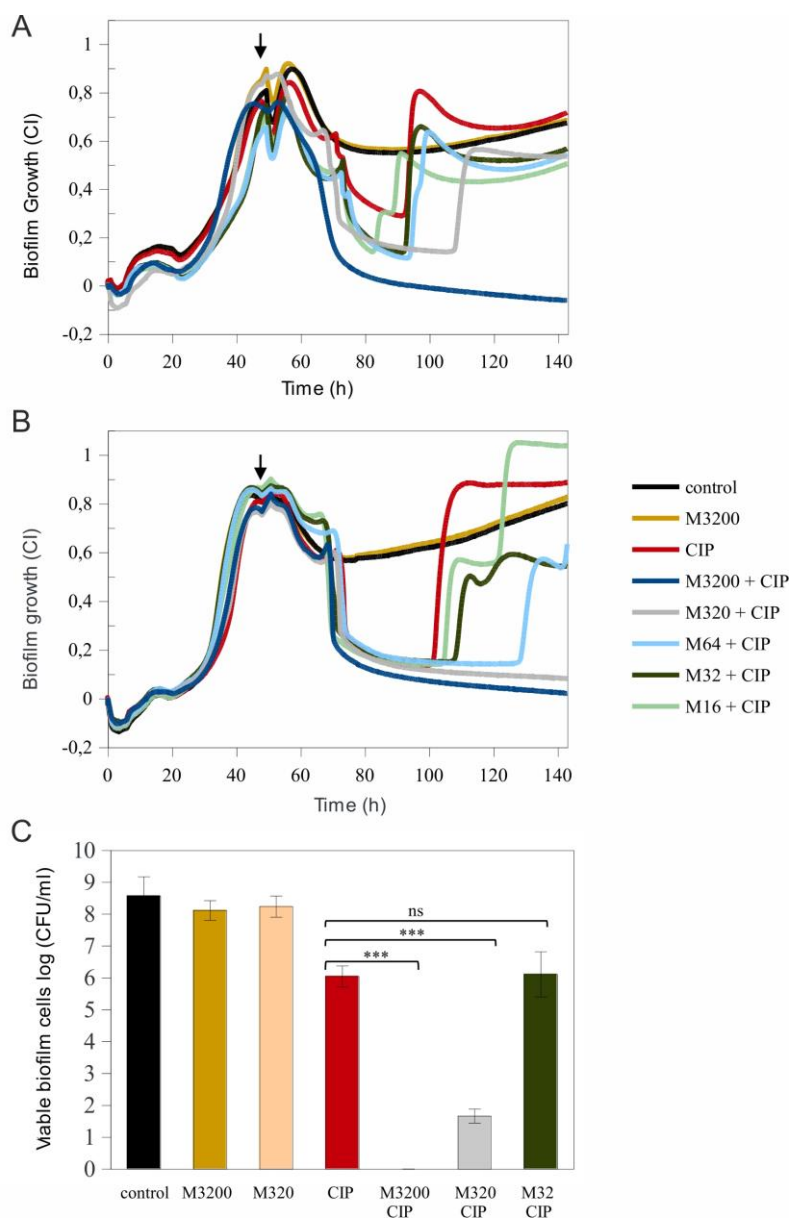


Figure II-4. Mannitol effect alone and in combination with ciprofloxacin in the eradication of persistent *P. aeruginosa* MF120 cells. **(A)** Biofilm growth when mannitol was added at the beginning of the experiment and ciprofloxacin added at 48h (vertical arrow). Panel **(B)** corresponds to a second experiment where both mannitol and CIP were added together at 48 h (vertical arrow), reaching final concentrations of 3200-16 mg/L for mannitol and 0.25 mg/L for CIP. Panel **(C)** represents bacterial cell viability after treatment with different combinations of mannitol and CIP. Data show the average of log CFUs counts from three biological replicates. Statistical significance was assessed by t -test at 140 h; asterisks indicate $p \leq 0.001$, ns – not significant. M – mannitol; CIP – ciprofloxacin (0.25 mg/L).

Identification of persister subpopulation

Bacterial cells grown with CIP after the second peak were cultured on LBA plates with CIP in order to maintain persister phenotype. Persister cells had a different colony morphology, were less mucoid and were not able to produce pyocyanin (white colonies). In addition, they were opaquer, compared to the greenish untreated control colonies plated on LBA plates without additional antibiotics (**Fig. II-5 A**).

It is known that persisters revert to normal wt phenotype once antibiotic presence is ceased²⁴⁷. Thus, we further determined the reversibility of this phenotype after CIP removal. Persisters and untreated controls were reinoculated into fresh growth media supplemented with mannitol (3200 mg/L) and without mannitol (LB alone) and bacterial growth and color changes were observed. After 72 h of growth, persister cells had a phenotype similar to that of untreated controls in media which contained mannitol but not in LB alone, concluding that persisters were reverted into actively growing cells. In addition, persister cells that were inoculated in LB media without mannitol restored pyocyanin production at 96h (**Fig. II-5 B**), concluding that mannitol accelerated the reversal of persisters to the wt phenotype. We have also assessed MICs for persister cells subcultures in LB agar plates with CIP and found that the resistance to this antibiotic increased at least 10 times. Persister cells also had increased resistance to IMI and MEM (**Table II-S3**). Finally, we reinoculated persisters to fresh LB media supplemented with mannitol and LB media supplemented with CIP. MICs performed at 96h of inoculation showed that persister cells grown in a presence of mannitol became more susceptible to most of the tested antibiotics while in LB alone they showed increased resistance to CIP and IMI. This indicates that, in addition, to phenotypic changes (**Fig. II-5**), persisters grown in the absence of antibiotic also revert their resistance profile. On the contrary, persisters reinoculated in LB media supplemented with CIP maintained the white phenotype and showed increased resistance to all tested antibiotics (**Table II-S3**).

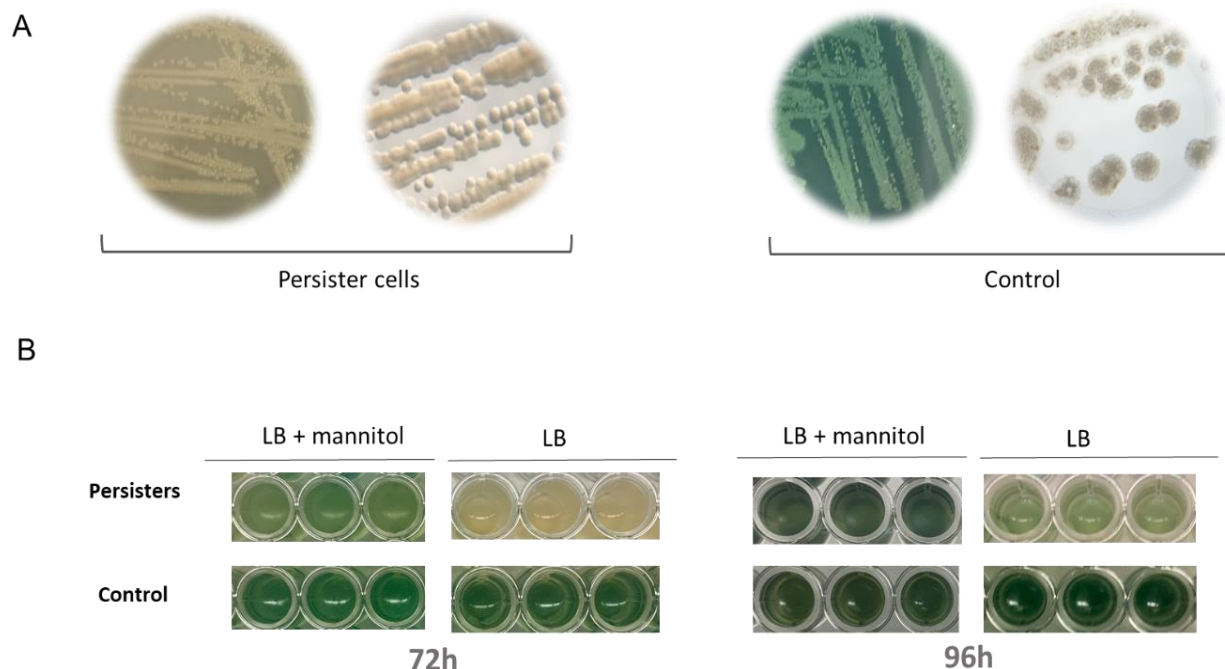


Figure II-5. Persister regrowth assay. **(A)** Phenotypic differences between persister cells (treated with ciprofloxacin [CIP] 0.25 mg/L) and control cells. Clear differences in pigment coloration are observed. In order to maintain persisters phenotype, MF120 cells treated with CIP were subcultured in LBA plates supplemented with CIP, while controls were continuously cultured in LBA plates without antibiotics. **(B)** Persister regrowth and reversion into actively growing cells in fresh LB supplemented with mannitol (3200 mg/L) or LB alone at 72 and 96 h, respectively. Three biological replicates and negative controls for each condition were included in the experiment. Pigment reversion phenotypes are observed with time in persister cells, and the reversion is accelerated in the presence of mannitol. The genomes of control and persister cells were fully sequenced and the observed mutations are described in **Table II-2**.

Genetic changes associated with persister phenotype

We extracted DNA from colonies grown in the presence of CIP (0.25 mg/L), mannitol (3200 mg/L) or their combination that represented non-identical phenotypes and sequenced their genomes in order to test if phenotypic differences are caused by genetic mutations (SNPs, insertions, deletions, or inversions). For each colony type we selected two colonies from the same agar plate as replicates. In particular, the colonies had the following phenotypes: CIP were small and white (isolates 7, 8), and (isolates 9 and 10) big white; mannitol (isolates 13, 14) were green, and their combination (isolates 11, 12) were small white. In addition, these phenotypes were compared to green (isolates 3, 4) and white (5, 6) colonies of untreated controls and to the

wt strain (1, 2) (**Table II-S2**). In total, we sequenced 14 genomes for which we obtained a mean coverage of 109x. An average of 66 ± 11 per isolate were assembled.

We detected a duplication in one of the colonies isolated from plate with CIP (isolate 7). The duplicated region was 43.6 Kbp and included 42 ORFs (**Table II-S2; Fig. II-6**). Among these, the annotation revealed the presence of two genes involved in pilus assembly (*fimV* and *pilE*) and nine genes coding for general secretion pathways (type II secretion system). Interestingly, this secretion pathway is related with membrane transport during biofilm formation.

In addition, we studied single-nucleotide polymorphisms (SNPs) in the different variants using the wt strain genome as reference. In the colonies grown with CIP, we detected an insertion (C \rightarrow CA) in *tdh* gene (L-threonine 3-dehydrogenase) in the bigger colony and missense substitution (A \rightarrow G) in a gene coding for a hypothetical protein.

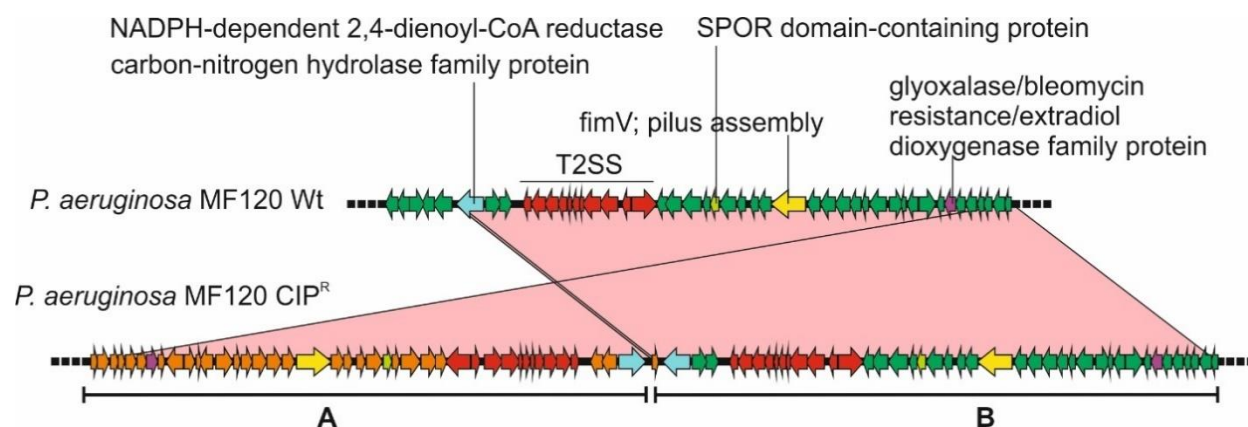


Figure II-6. Genomic duplication in the *P. aeruginosa* CIP^R variant. The wild type strain (wt) and the persister colony from CIP-treated plate were sequenced and compared (using blastn). A region spanning 42 genes was found duplicated and inverted in CIP^R variant. This is marked as **A** whereas the original sequence is shown as **B**. Relevant genes are colored differently and their names indicated. The sequence identity of the original alignment was 100% for all genes. T2SS, type 2 secretion system.

Additionally, we found a mutation (T → C) in the promoter region of a hypothetical protein. The rest of detected SNPs are shown in **Table II-2**. Thus, we did not detect any polymorphisms that could be uniquely and consistently associated with persister colonies.

Table II-2. Single Nucleotide Polymorphisms (SNPs) detected in *P. aeruginosa* control and persister variants.

Contig	Position	Type	Wild type	mutant	Sample variant	Region	EFFECT	gene
contig-03	97212	complex	CGTT	AACG	6	Promotor		Promotor (Dihydrolipoyllysine-residue acetyltransferase component of pyruvate dehydrogenase complex)
contig-04	204656	snp ¹	T	G	6	CDS ⁴	missense_variant c.1255A>C p.Met419Leu	Gamma-glutamylputrescine synthetase PuuA
contig-04	204666	snp	T	G	6	CDS	missense_variant c.1245A>C p.Glu415Asp	Gamma-glutamylputrescine synthetase PuuA
contig-04	204675	snp	C	T	6	CDS	synonymous_variant c.1236G>A p.Glu412Glu	Gamma-glutamylputrescine synthetase PuuA
contig-04	204719	snp	T	A	2,3,4,6,8,9,10,11,12	CDS	missense_variant c.1192A>T p.Met398Leu	Gamma-glutamylputrescine synthetase PuuA
contig-05	326236	snp	T	C	2,3,4,6,8,9,10,12,13,14	Promotor		hypothetical protein
contig-11	220551	snp	G	C	5	CDS	missense_variant c.727C>G p.Arg243Gly	hypothetical protein
contig-11	220546	del ²	ACGCCGC CCCC	A	6	CDS	frameshift_variant c.722_731delGGGGCGCG p.Gly241fs	hypothetical protein
contig-13	6466	snp	G	A	11,12	CDS	synonymous_variant c.1698C>T p.Asn566Asn	hypothetical protein
contig-24	6439	complex	AGGAG	GGGA A	6	CDS	synonymous_variant c.252_256delCTCTinsTTCCC p.87	hypothetical protein
contig-24	6457	complex	GG	AGA	6	CDS	frameshift_variant&missense_variant c.237_238delCCinsTCT p.Arg80fs	hypothetical protein
contig-24	6466	snp	G	A	6	CDS	stop_gained c.229C>T p.Arg77*	hypothetical protein
contig-24	6470	ins ³	G	GGC	6	CDS	frameshift_variant c.224_225insGC p.Asp75fs	hypothetical protein
contig-30	53663	ins	C	CA	8	CDS	frameshift_variant c.716dupA p.Leu240fs	L-threonine 3-dehydrogenase
contig-44	1027	snp	A	G	3,9,10,11,12	CDS	missense_variant c.124A>G p.Met42Val	hypothetical protein

DISCUSSION

Bacteria growing in biofilms are highly associated with increased resistance to conventional antibiotics, resulting in treatment failure⁶. Our data show the importance of evaluating biofilm formation capacity for each strain individually, as the functional characteristics of biofilms change substantially depending on the isolate. In addition, we show that growing conditions like initial inoculum concentration and above all culture media have a dramatic effect on the resulting biofilm phenotype, with some strains even failing to form biofilms at all depending on the medium. This emphasizes the need for standardizing growth conditions and reducing the manipulation of biofilms in order to obtain consistent and reliable measures of biofilm growth and resistance^{161,198}. The data presented in the current study show a large potential of impedance measures to study biofilm growth dynamics, for example by evaluating antibiotic resistance of individual strains and by identifying the emergence of persister cells. The results were confirmed by the counting of viable *P. aeruginosa* cells, as well as by biofilm mass quantification after crystal violet staining. Hence, Real-Time measurements of biofilm growth are reliable and could therefore be useful in providing faster assays of antibiotic susceptibility compared to more traditional end-point measures.

In the current study, the exposure of *P. aeruginosa* biofilms to conventional drugs showed that antibiotics which target bacterial cell wall synthesis such as CAZ, IMP, MEM OR TZP were not able to completely prevent biofilm formation or disrupt mature pseudomonal biofilms (**Figs. II-3 and II-4**). Given that none of the tested CST concentrations were able to halt the development of *P. aeruginosa* biofilms completely, we hypothesize that this antibiotic is not able to penetrate into deep biofilm layers or might alter the production of exopolysaccharide matrix compounds as observed elsewhere^{320,332}. The largest anti-biofilm effect (in both prevention and eradication) was observed with CIP (an inhibitor of DNA gyrase) and TOB (inhibitor of protein synthesis). Our data show that certain concentrations of both CIP and TOB resulted in dormant cell populations within mature *P. aeruginosa* biofilms, in agreement with the results recently described by Soares et al. We investigated whether the use of mannitol alone or in combination with CIP could help to eradicate mature biofilms in the clinical strain MF120, following the work of Barraud and colleagues, that detected an increase in TOB efficiency up to three orders of magnitude by altering bacterial metabolic activity³³³. Our results indicate that

mannitol alone has neither antimicrobial nor biofilm dispersal properties, but this compound was able to enhance the efficiency of subinhibitory CIP concentrations. Specifically, mannitol at 3200 mg/L in combination with CIP (0.25 mg/L) completely killed all bacterial cells embedded in mature clinical MF120 biofilms, while 320 mg/L of mannitol combined with CIP resulted in five orders of magnitude decrease in viable cell counts compared to that of CIP alone (dose-dependent quinolone potentiation) (**Fig. II-4 C**). We therefore suggest the possible adjuvant use of mannitol to successfully disrupt and kill antibiotic-resistant *P. aeruginosa* biofilms. Our results also show that mannitol can revert persister cells in actively growing cells faster than LB alone (**Fig. II-5**), in agreement with the proposed mechanism for this compound in bacterial metabolism^{333,334}.

There are several genes whose activity has been linked to the persistent phenotype of *P. aeruginosa*^{286,331}. However, the whole-genome sequence analysis of different phenotypical variants did not show mutations in any of these genes. Some phenotypical variants showed two genomic mutations compared to the wt strain and future studies should demonstrate if any of these changes are responsible for any of the morphological or behavioral changes of persisters. For example, a genomic inversion has been shown in *S. aureus* to induce a phenotypic change towards small colony variants associated with persistent infections³³⁵. However, both the genomic inversion and the identified single nucleotide substitutions were not common to all persisters (**Table II-2**). This suggests that, although some of these mutations could contribute to the persister phenotype, the main origin for the switch from wt to an antibiotic tolerant persister cell, is probably a transcriptomic change^{104,336}. Thus, future work should focus on studying transcriptional changes associated with persister populations, in order to identify potential drug targets.

We conclude that impedance-based technology could therefore help to prognose the response of a given strain to an antibiotic as well as to select the best treatment strategy for each patient individually. In the case of persister cell eradication, we show that a compound with the ability to restore bacterial metabolic activity, as it is the case with mannitol for *P. aeruginosa* biofilms, produced a dramatic improvement of the antibiotic efficacy in our system. We hope that the current study stimulates further work to test this kind of combined treatments *in vivo*.

CHAPTER II SUPPLEMENTARY INFORMATION**Supplementary table II-S1.** Bacterial strains used in this study.

Strain	Description/Use	Reference
PAO1	Laboratory strain; wt	Pseudomonas Genetic Stock Center
PAO1 $\Delta rhl \Delta las$	Laboratory strain; <i>lasI-rhlI</i> double mutant of <i>PAO1</i>	337
ATCC27853	Model strain to test antibiotic susceptibilities	338
MF116	Isolate from rectal swab	This study
MF117	Isolate from urinary tract infection	This study
MF118	Isolate from wound exudate	This study
MF119	Isolate from ulcer exudate	This study
MF120	Isolate from urinary tract infection	This study
MF121	Isolate from ulcer exudate	This study
MF122	Isolate from wound exudate	This study
MF123	Isolate from bronchial aspirate	This study
MF124	Isolate from blood culture	This study

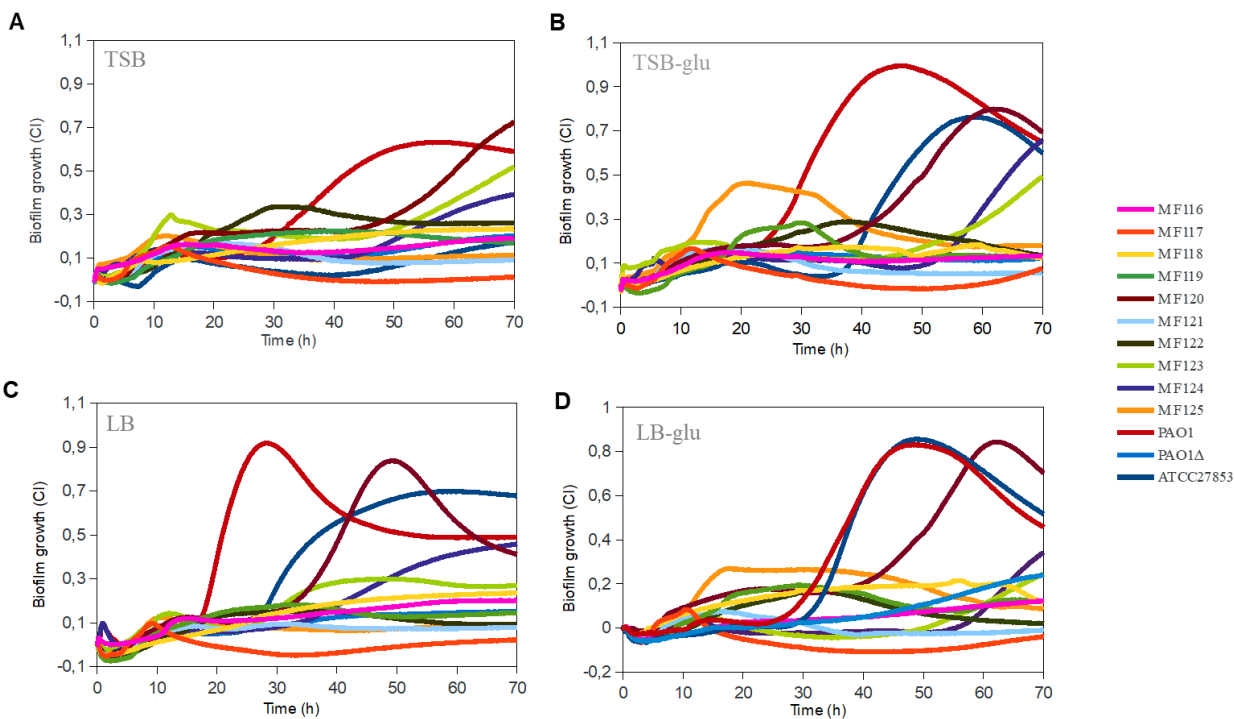
Supplementary table II-S2. Minimum inhibitory concentration (MIC) values of ciprofloxacin (CIP), tobramycin (TOB), ceftazidime (CAZ), colistin (CST), piperacillin-tazobactam (TZP), imipenem (IPM), and meropenem (MEM) in different *P. aeruginosa* strains as measured by standard protocols and expressed as mg/L. **S** and **R** in the table indicate if the strain is considered susceptible or resistant according to EUCAST guidelines.

Minimum Inhibitory Concentration							
Strain	CIP	TOB	CAZ	CST	TZP	IPM	MEM
PAO1	0.094 S	1.5 S	1 S	1 S	3 S	1.5 S	0.38 S
PAO1 $\Delta rhl \Delta las$	0.094 S	2 S	1 S	0.5 S	4 S	2 S	0.38 S
ATCC27853	0.125 S	1 S	1 S	1 S	4 S	3 S	0.25 S
MF116	2 R	>8 R	16 R	1 S	>64 R	>16 R	>32 R
MF117	≤ 0.5 S	≤ 2 S	8 S	8 R	≤ 8 S	≤ 2 S	≤ 1 S
MF118	>2 R	4 S	16 R	1 S	>4 R	32 R	16 R
MF119	>2 R	>8 R	>16 R	≥ 2 S	>64 R	>8 R	≤ 1 S
MF120	0.125 S	≤ 2 S	2 S	1 S	≤ 8 S	≤ 1 S	≤ 1 S
MF121	>2 R	>8 R	4 S	1 S	≤ 8 S	4 S	≤ 1 S
MF122	≤ 0.5 S	≤ 2 S	2 S	≤ 2 S	≤ 8 S	≤ 1 S	≤ 1 S

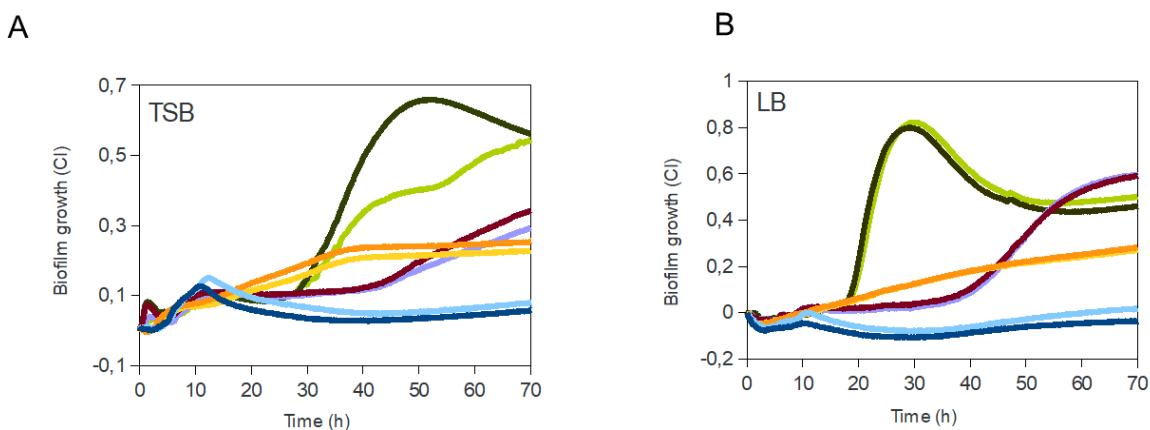
MF123	≤0.5S	≤2S	≤1 S	≤2 S	≤ S	≤1S	≤1 S
MF124	0.19S	1S	2 S	1 S	8 S	2 S	0.75 S

Supplementary table II-S3. Minimum inhibitory concentration (MIC) values of ciprofloxacin (CIP), tobramycin (TOB), ceftazidime (CAZ), colistin (CST), piperacillin-tazobactam (TZP), imipenem (IPM), and meropenem (MEM) for *P. aeruginosa* MF120 persister cells grown in the presence of ciprofloxacin (final concentration 0.25 mg/L) vs MICs of persister cells re-inoculated in fresh LB medium, LB medium supplemented with mannitol (3.200 mg/L) or CIP (0.25 mg/L) for 96h. MICs were measured by standard E-test protocols. S and R in the table indicate if the strain is considered susceptible or resistant according to EUCAST guidelines. Data from two replicates for each treatment are shown.

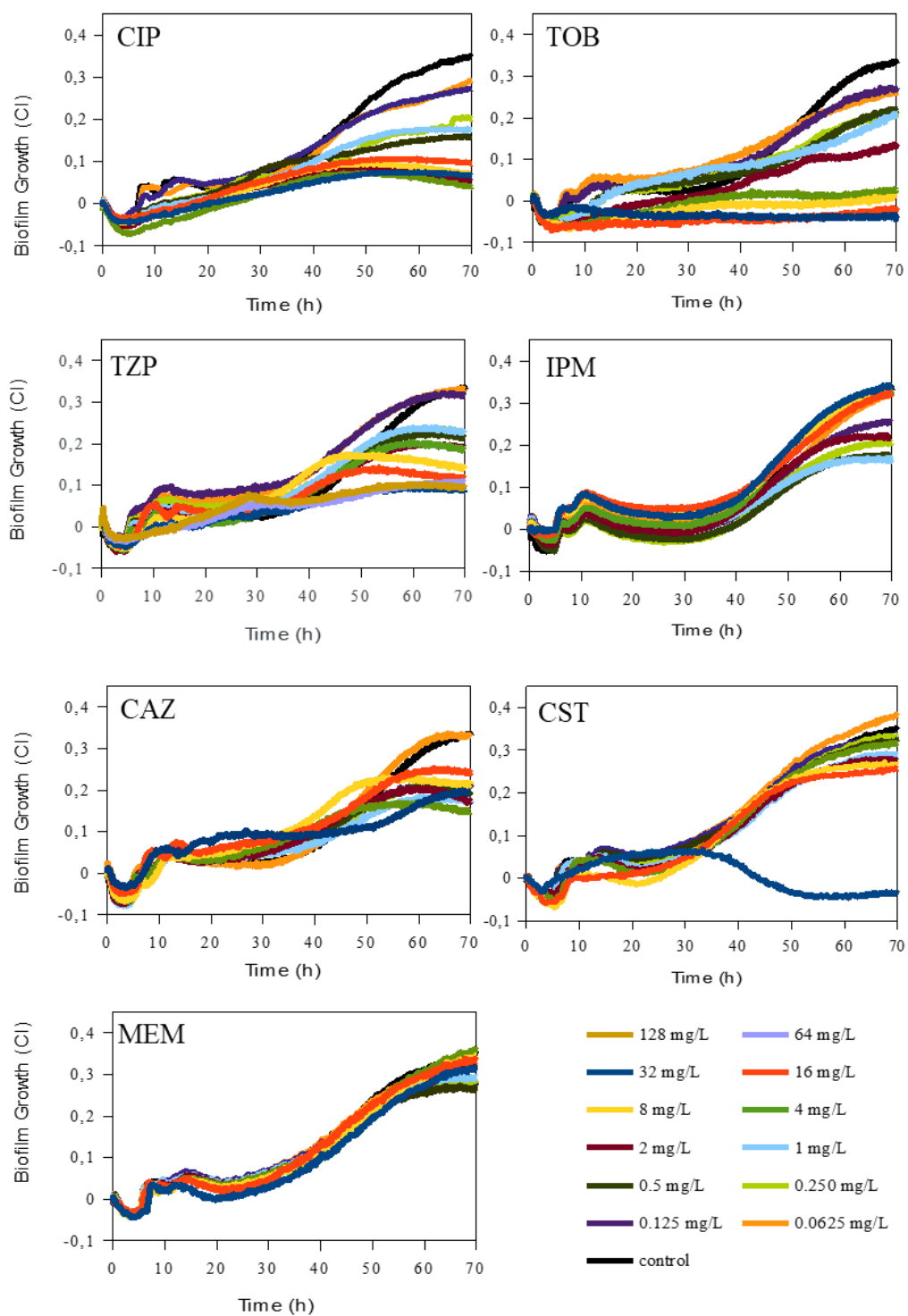
Minimum Inhibitory Concentration							
Strain	CIP	TOB	CAZ	CST	TZP	IPM	MEM
Control	0.19 (S)	1.5 (S)	1 (S)	1 (S)	6 (S)\	2 (S)	0.38 (S)
	0.19 (S)	1.5 (S)	1.5 (S)	2 (S)	6 (S)	1.5 (S)	0.25 (S)
Persisters	2 (R)	0.5 (S)	0.75 (S)	0.75 (S)	3 (S)	> 32 (R)	0.5 (S)
	3 (R)	0.75 (S)	0.75 (S)	0.75 (S)	4 (S)	> 32 (R)	0.75 (S)
Persisters reinoculated in LB	3 (R)	1.5 (S)	1 (S)	1 (S)	6 (S)	>32 (R)	0.5 (S)
	2 (R)	1.5 (S)	1.5 (S)	1 (S)	6 (S)	8 (S)	0.25 (S)
Persisters reinoculaed in LB + mannitol (revertant)	0.25 (S)	1.5 (S)	1.5 (S)	1 (S)	8 (S)	1.5 (S)	0.38 (S)
	0.19 (S)	1.5 (S)	1.5 (S)	1 (S)	8 (S)	2 (S)	0.25 (S)
Persisters reinoculated to LB + CIP	3 (R)	1 (S)	1.5 (S)	1 (S)	3 (S)	> 32 (R)	1 (S)
	3 (R)	0.75 (S)	48 (R)	1 (S)	256 (R)	> 32 (R)	4 (S)



Supplementary figure II-S1. The effect of culture medium composition on *P. aeruginosa* biofilm formation: **A** - TSB with no additional sugars; **B** - TSB + 0.5% of glucose; **C** - LB with no additional sugars; **D** - LB + 0.5% of glucose. Cell Index (CI) was measured using xCELLigence equipment for 72h and correlates with total biofilm mass. Data are the means of 3 biological replicates. SDs are not shown for clarity.



Supplementary figure II-S2. The effect of initial bacterial cell optical density on *P. aeruginosa* biofilm formation in the real-time cell analysis xCELLigence system. Biofilm growth was measured using TSB and LB culture media without additional sugars every 10 minutes for 70h using initial OD of 0.15 and 0.3, respectively. Data are means of three biological replicates. SDs are not shown for clarity.



Supplementary figure II-S3. Effect of ciprofloxacin (CIP), tobramycin (TOB), ceftazidime (CAZ), colistin (CST), piperacillin-tazobactam (TZP), imipenem (IPM) and meropenem (MEM)

on *P. aeruginosa* MF124 biofilm formation. Graphs show estimates of total biofilm mass as quantified by impedance-based measurements. Black lines indicate untreated controls. Each line represents the mean of two replicates. All antibiotics were added at the beginning of the experiment together with bacterial inoculum, with concentrations ranging from 0.625 mg/L to 32 mg/L for all antibiotics except TPZ (0.625 mg/L to 128 mg/L). Biofilm growth was registered every 10 mins for 70h. SDs are not shown for clarity.

CHAPTER III

Real-time monitoring of biofilm growth identifies andrographolide as a potent antifungal compound eradicating *Candida* biofilms**ABSTRACT**

Candida species cause life-threatening infections with high morbidity and mortality rates and their resistance to conventional therapy is closely linked to biofilm formation. Thus, the development of new approaches to study *Candida* biofilms and the identification of novel therapeutic strategies could yield improved clinical outcomes. In the current study, we have set up an impedance-based *in vitro* system to study *Candida* spp. biofilms in real-time and to evaluate their sensitivity to two conventional antifungal groups used in clinical practice - azoles and echinocandins. Both fluconazole and voriconazole were unable to inhibit biofilm formation in most strains tested, while echinocandins showed biofilm inhibitory capacity at relatively low concentrations (starting from 0.625 mg/L). However, assays performed on 24h *Candida albicans* and *C. glabrata* biofilms revealed that micafungin and caspofungin failed to eradicate mature biofilms at all tested concentrations, evidencing that once formed, *Candida* spp. biofilms are extremely difficult to eliminate using currently available antifungals. We then evaluated the antifungal and anti-biofilm effect of andrographolide, a natural compound isolated from the plant *Andrographis paniculata* with known antibiofilm activity on gram-positive and gram-negative bacteria. Optical density measures, impedance evaluation, CFU counts, and electron microscopy data showed that andrographolide strongly inhibits planktonic *Candida* spp. growth and halt *Candida* spp. biofilm formation in a dose-dependent manner in all tested strains. Moreover, andrographolide was capable of eliminating mature biofilms and viable cell numbers by up to 99.9% in the *C. albicans* and *C. glabrata* strains tested, suggesting its potential as a new approach to treat multi-resistant *Candida* spp. biofilm-related infections.

INTRODUCTION

Candida species (*C. albicans*, *C. krusei*, *C. parasilopsis*, *C. glabrata*, and others) are the most common opportunistic fungal pathogens colonizing skin, oral cavity, gastrointestinal, respiratory and urinary tracts in humans^{105,339,340}. The adaptation capacity and colonization of these pathogens are linked to their growth on different surfaces, where they are encased in a self-produced biopolymeric matrix forming biofilms. This increases their resistance to first-line antifungal agents more than 1,000 times compared to planktonic growth of the same strains^{27,121,125}. In addition, *Candida* spp. show high resistance to disinfectants and antiseptics repeatedly used in hospitals, being able to survive and persist in healthcare facilities^{109,341}. For this reason, biofilm-related antifungal resistance contributes enormously to implantable medical device-related infections and healthcare-associated outbreaks^{112,114,115}.

The *in vitro* activity of antifungals is a key parameter for the good evolution of patients. Currently, amphotericin B, 5-fluorocytosine, azoles, and echinocandins are the four groups of drugs that can be used in the treatment of invasive candidiasis, but the last two families are the most effective and the best tolerated, which is why they are the most used in clinical practice^{114,342,343}. While fungistatic azoles inhibit ergosterol synthesis, leading to cell membrane damage, fungicidal echinocandins interfere with fungal cell wall biosynthesis^{118,344}. Recent studies have demonstrated that the resistance to these antifungal agents is highly associated with biofilm formation and the metabolic state of *Candida* spp. cells embedded in biofilms^{33,117,119}. In addition, it has been observed that biofilm-grown *Candida* spp. can upregulate efflux pumps to survive high concentrations of drugs³⁴⁵⁻³⁴⁷, and the use of high dosages of conventional antifungals can lead to both multi-resistance and severe health complications such as arrhythmias, renal failure, and kidney damage among others^{118,125}. Recent studies also underline the high rate of strains resistant to antifungals in patients with COVID³⁴⁸. Therefore, there is a need to investigate novel, effective and rapid approaches to treat fungal biofilm-related infections^{33,125}. This could be reached using already known antifungal combinations and/or searching for novel natural or synthetic compounds that attribute anti-biofilm properties alone or in combination with conventional antifungals. For example, various polyphenols, including flavonoids, terpenoids and others, have been shown to interfere with *Candida* ssp. biofilm

formation and proliferation *in vitro*³⁴⁹. However, most of these compounds cannot eradicate mature biofilms^{33,349}.

Andrographolide is a natural compound isolated from *Andrographis paniculata* plant, commonly used in oriental medicine³⁵⁰. This compound was proposed as effective in treating fever, influenza, and other life-threatening diseases, including dysentery, malaria, various forms of cancer and respiratory infections^{351–353}. Andrographolide was shown to have *in vitro* inhibitory effect against staphylococcal biofilms, including both *Staphylococcus epidermidis* and methicillin-resistant *S. aureus*, suppressing quorum sensing (QS) systems³⁵³. Similar effect on the inhibition of different genes involved in elastase and pyocyanin synthesis was also observed in *Pseudomonas aeruginosa*^{354–356}. However, the antifungal effect of this compound against fungal biofilms remains elusive.

Standard protocols to study fungal biofilms and evaluate antifungal sensitivity are based on end-point measures where biofilm growth is quantified by crystal violet staining¹⁶⁹. However, these methods have limited reproducibility due to human manipulation, are influenced by the point at which biofilm growth is stopped and lack information about biofilm growth dynamics^{164,169}. This has been solved in bacterial biofilms using real-time measurements derived from time-lapse confocal microscopy or electric impedance measurements^{357,358}. The latter is based on the fact that bacteria growing attached to electrodes impede an electrical flow, and this impedance has been shown to be proportional to biofilm mass and to correlate well with other classical measures^{196,198}. In the current manuscript, we first set up an impedance-based method to monitor fungal biofilm formation in real-time. We have also evaluated the efficacy of commonly used azole and echinocandin antifungals groups (fluconazole and voriconazole; and micafungin and caspofungin, respectively) in the prevention of *Candida* spp. biofilm formation, as well as the echinocandins effect on pre-formed, mature 24h biofilms. Finally, we assessed the antifungal properties of andrographolide on planktonic *Candida* spp. growth and on their biofilm formation and eradication, both alone and in combination with micafungin. Obtained results were confirmed using viable cell counting and scanning electron microscopy, in order to establish the efficacy of the different compounds and their joined potential as treatment for *Candida* spp. biofilms-associated infections.

MATERIALS AND METHODS

Strains and growth conditions

Fungal strains used in the current manuscript are listed in **Table III-S1**. The strains were isolated from vaginal exudates at the Microbiology Department of Alicante General Hospital (Alicante, Spain) and cultivated on YPDA (Yeast Peptone Dextrose Agar) plates. For biofilm assays, *Candida* spp. strains were grown in YPD (Yeast Peptone Dextrose), YNB (Yeast Nitrogenase Base) or RPMI1640 with 165 mM MOPS liquid media alone or supplemented with 2% of glucose when needed, at 30°C at 120 rpm overnight.

In vitro real-time yeast biofilm growth monitoring

Real-time *Candida* spp. biofilm growth analysis was performed in 96-well E-plates using an xCELLigence SP equipment (Agilent) according to the manufacturer's instructions¹⁹⁷. To set up the system for yeasts, three different growth media were tested: YPD (Yeast Peptone Dextrose), YNB (Yeast Nitrogenase Base), and RPMI1640 with 165 mM MOPS, glucose-free or supplemented with 2% of glucose. Briefly, 100 μ L of growth media (with or without additional glucose) were added into the E-plates wells in triplicate for background measurements. Subsequently, overnight *Candida* spp. cultures were diluted in fresh growth media and 100 μ L were added into corresponding wells reaching a final optical density of $OD_{600} = 0.1$ (approximately 1×10^5 cells/mL, depending on the strain). Appropriate negative controls (growth media minus fungal inoculum) were included in each experiment in triplicate. The plates were introduced into the device and incubated at 37°C and fungal biofilm growth was measured for 72h by cell impedance measurements which were registered every 10 minutes. The biofilm growth was expressed as Cellular Index (CI), which directly correlates to total fungal biofilm mass, and CI data were normalized by subtracting corresponding negative control values^{133,198,215,358}.

Biofilm quantification with Crystal Violet staining

To quantify the biofilm formation capacity of different *C. albicans* and *C. glabrata* isolates in microtiter plates, 24h and 48h biofilms were stained using Crystal Violet (CV) as previously described³⁵⁹. Briefly, each strain was grown overnight in YPD broth as described above. Overnight cultures were diluted to $OD_{600} = 0.1$ and 300 μ l of fungal suspensions were inoculated into 96-well flat-bottom Ibidi Treat plates 89626 (Ibidi, Germany) for 24h and 48h, respectively. After that, the culture supernatant was discarded, biofilms were gently washed using Phosphate Buffer Saline (PBS pH = 7.4) and attached biomass was stained for 30 mins using 0.4% CV. Subsequently, CV was removed, biofilms were washed with PBS to remove residual CV and resuspended using 30% acetic acid. After that, the absorbance of the released CV was measured by an absorbance plate reader Infinite M200 (Tekan, Durham NC) at 610 nm. Each strain was tested for biofilm production in triplicates and the assay was repeated three times (biological replicates).

Antifungal susceptibility assay in *Candida* spp. biofilms

In order to evaluate the effect of conventional antifungals on the prevention of *Candida* spp. biofilm formation (minimal biofilm inhibitory concentrations - MBICs), different antifungals: azoles – fluconazole (TEVA) and voriconazole (TEVA) – and echinocandins – caspofungin (Sandoz) and micafungin (Astelas), were tested. Shortly, 100 μ l of each antifungal diluted in YPD media without additional glucose (two-fold serial dilutions to final concentrations from 128 mg/L to 0.0625 mg/L) were used for background measurements^{196,358}. Next, 100 μ l of fungal suspensions were added into the corresponding wells in E-plates, reaching a final concentration of $OD_{600} = 0.1$. After that, biofilm was grown at 37°C for 48h registering impedance values every 10 minutes.

For the study of established biofilm eradication, 100 μ l of fungal suspensions ($OD_{600} = 0.233$) were used for background measurements. Afterwards, 75 μ l of YPD medium were added into the corresponding wells and biofilm growth was monitored for 24h^{198,358}. Next, 25 μ l of antifungals were added, reaching final concentrations from 128 to 0.0625 mg/L (two-fold serial

dilutions) for each tested antifungal. Biofilm growth was measured for an additional 48h. Each experiment included two replicates of each condition and two negative controls.

MIC and MBIC determination

Minimum Inhibitory Concentrations (MICs) of fluconazole, voriconazole, micafungin and caspofungin was evaluated using an E-test assay (bioMérieux) according to the Clinical and Laboratory Standards Institute (CLSI)³⁶⁰. Given that EUCAST breakpoints have been not yet established for caspofungin, strains susceptible to micafungin were also considered susceptible to caspofungin as suggested by European Committee on Antimicrobial Susceptibility testing³⁶⁰.

Minimum Biofilm Inhibitory Concentrations (MBICs) were determined using impedance-based graphs where CI threshold values ≤ 0.15 at 48h of biofilm growth were considered as inhibitory.

Andrographolide effect on planktonic *Candida* spp. growth

To describe andrographolide effect on planktonic growth, *Candida* spp. overnight cultures were adjusted to $OD_{600} = 0.2$ and 100 μ L of these suspensions were transferred into 96 well-plates (ThermoFisher Scientific). After that, 100 μ L of andrographolide compound were added into the corresponding wells reaching final concentrations from 5 g/L to 20 mg/L (serial two-fold dilutions). Subsequently, the plates were incubated at 37°C with orbital and linear shaking at 120 rpm and fungal cell growth was monitored for 24h every 30 minutes with an absorbance plate reader Infinite M200 (Tekan, Durham NC).

Andrographolide effect alone and in combination with micafungin on *Candida* spp. biofilms

To assess andrographolide effect on biofilm formation, andrographolide was serially diluted in YPD broth (two-fold dilutions to concentrations ranging from 5 g/L to 165 mg/L) and 100 μ L of these suspensions were used for background measurements in the xCELLigence system. Then, overnight cultures of *Candida* spp. strains were diluted using fresh YPD broth and 100 μ L of these suspensions added to the corresponding E-plate wells, reaching a final $OD_{600} =$

0.1. After that, biofilm growth was monitored for 24h in real-time. Each experiment included two replicates of each condition and two negative controls for each andrographolide concentration.

To evaluate whether andrographolide alone or in a combination with micafungin, could eradicate mature *Candida* spp. biofilms, the biofilms were growth and monitored in the impedance system for 24h as described above. Later, 25 μ L of andrographolide, micafungin or their combination were added on the biofilms to the corresponding E-plate wells reaching final concentrations of 5 and 2.5 g/L for andrographolide and 128 mg/L for micafungin, respectively, and biofilm growth was quantified in real-time for additional 24h.

Viable cell counting

Established 24h biofilms of *Candida* spp. treated with micafungin (128 mg/L), andrographolide (5 g/L and 2.5 g/L) or their combination as described above, were collected using 100 μ L of PBS and suspensions were sonicated for 2 mins in order to eliminate cell aggregates and released fungal cells embedded in the biofilm matrix. After sonication, serial dilutions were prepared and 100 μ L of each condition suspension were plated in triplicate on YPD agar plates and incubated at 37°C for approximately 48h. Colony-forming units (CFUs) were then counted, averaged, and expressed as log₁₀ CFUs/ml. Each experiment included three technical replicates and was repeated three times.

Scanning electron microscopy

To assess the effect on the biofilm spatial structure after treatment with micafungin and andrographolide alone or their combination, scanning electron microscopy was used. Biofilms of *C. albicans* strain 86 and *C. glabrata* 96 were grown for 24h in the xCELLigence system and then treated with micafungin, andrographolide or their combination. After additional 24h, supernatants were discarded, and biofilms were gently washed using PBS to eliminate unattached cells. Prior to observations, samples were fixed using Karnovsky's fixative for 8h (4°C), rinsed with PBS three times, dehydrated using gradual ethanol series (30%-50%-70%) twice and dried using critical point drying with CO₂. Biofilm samples were observed with a

Hitachi S-4800 high-resolution electron microscope (Electron Microscopy Service, University of Valencia Spain), applying an accelerating voltage range of 10 kV and a magnification of x 1K.

Statistical analysis

Differences in biofilm CI values before and after treatment were evaluated by regression analysis using a linear model (<https://cran.r-project.org/web/packages/glmulti>) function `lm`, library `stats`, accessed in April 2022) in the R statistical package at 24h of biofilm growth. Viable cell counting experiments (CFUs counts) were performed in triplicate with three independent replicates in each experiment. Statistical significance was assessed using Student's t-test, where a $p\text{-value} < 0.05$ was considered significant.

RESULTS

Influence of culture conditions on *Candida spp.* biofilm formation

To evaluate the capacity of *Candida spp.* to attach on 96 well E-plate surfaces and to form biofilms, three different growth media (YPD, YNB and RPMI1640) alone or supplemented with 2% of glucose were used. Real-time measurements showed that the most suitable medium for biofilm growth of both *C. albicans* and *C. glabrata* strains was YPD (**Fig. III-S1**), and therefore this culture medium was selected for future experiments. In general, all tested strains showed the ability to form robust biofilms in both YPD and YNB medium, reaching at least two times higher CI values compared to those in RPMI1640 alone or with additional glucose. When YPD and YNB media were supplemented with glucose, the biofilm growth of most of the tested strains was not affected, suggesting that glucose might not be a crucial factor in the robust biofilm formation of these strains. Besides, the presence of additional glucose in YPD media decreased the biofilm formation capacity of laboratory strains CA86, CA94 and CG96, as a delay in biofilm growth and a decrease in final CI values were observed.

In contrast, the weakest biofilm formation capacity of all tested strains was observed in RPMI1460 medium. In this case, the effect of glucose addition was strain dependent, causing a biofilm growth delay (CA95), or growth acceleration (CA86), and even no effect compared to when they were grown in RPMI1460 alone.

We have also tested the most suitable initial optical density on *Candida* spp. biofilm growth in the impedance system and results showed that although higher optical density did have an influence on biofilm formation time, final CI values were similar in all tested cases (**Fig. III-S2**).

Comparison of CV staining and impedance-based measurements

We evaluated whether impedance-based measurements are comparable with the classical end point method of fungal biofilm staining with CV. **Figure III-1** shows the biofilm formation dynamics of both *C. albicans* and *C. glabrata* isolates when grown in real time in the xCELLigence system using YPD growth media (panel A), while panel B represents biofilm biomass stained with CV at both 24h and 48h of biofilm growth of these strains, respectively. In accordance with impedance-based measurements, *C. albicans* isolates exhibited a very strong biofilm formation capacity, reaching high CI values at approximately 15 hours of growth, while *C. glabrata* isolate (CG96) showed a lower capability to produce biofilm. Similar biofilm formation capacity results were observed for all tested strains between impedance and CV staining methods at both 24h and 48h of biofilm growth.

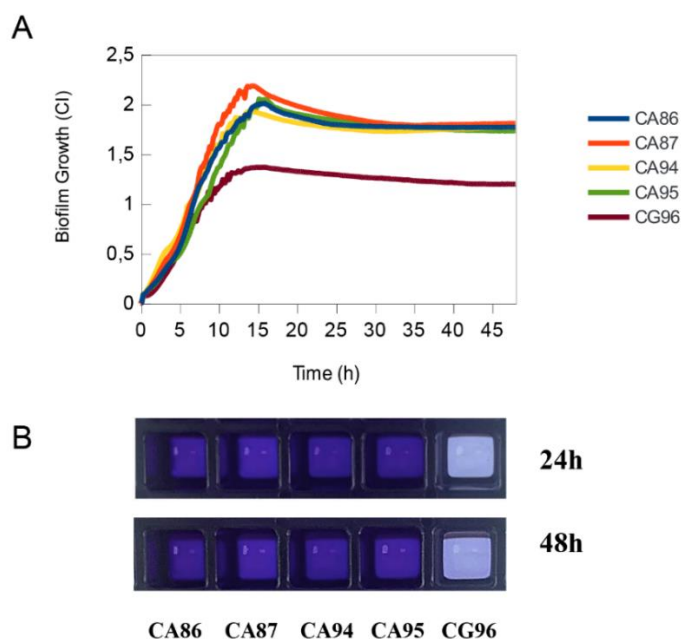


Figure III-1. A - Biofilm formation capacity of *Candida albicans* (CA) and *C. glabrata* (CG) isolates when grown in YPD medium quantified in real-time using impedance measurements during 48h of biofilm growth. Data are means of triplicates. SDs are not shown for clarity. **B** - Quantification of biofilm biomass by classical CV staining in Ibidi 96-well plates at 24h and 48h of biofilm growth.

Impact of conventional antifungals on *Candida* spp. biofilm formation

To evaluate the efficacy of conventional antifungals in preventing *Candida* spp. biofilm formation, four first-line antifungals – fluconazole, voriconazole, micafungin, and caspofungin - were added together with fungal inoculum, and biofilm formation was monitored for 48 hours in real time. Both tested antifungal groups showed a clear concentration- and species-dependent effect (**Figs. III-2 and III-3**). Within the azole group (**Fig. III-2**), both fluconazole and voriconazole provoked strain-dependent changes in biofilm growth dynamics. They showed only a slight biofilm inhibitory effect in the model strain CA86 and in the clinical isolate CA95, although none of the tested concentrations could halt biofilm formation completely. In addition, low concentrations of fluconazole (0.0625 - 1 mg/L) resulted in biofilm growth induction in both CA86 and CA95 strains reaching final CIs values higher than those observed in untreated controls (**Fig. III-2**). In contrast, in strain CA94, the highest tested concentration of these antifungals was able to inhibit biofilm formation to a great extent. Regarding *C. glabrata* strain CG96, voriconazole showed a delay in biofilm growth in a concentration-dependent manner. However, although concentrations of 128 and 64 mg/L were efficient in preventing biofilm formation, subinhibitory concentrations produced an increase in the amount of biofilm formed (0.0625-4 mg/mL) ($p\text{-value} < 0.05$). By contrast, no concentration of fluconazole tested was able to inhibit the biofilm formation of the *C. glabrata* strain. In fact, high concentrations (128-4 mg/L) of this antifungal resulted in biofilm biomass induction (**Fig. III-2**). Contrary to azoles, both caspofungin and micafungin, which interfere with fungal cell wall biosynthesis (**Fig. III-3**), fully prevented biofilm formation of almost all tested strains. Even at low concentrations both antifungals were able to prevent biofilm formation. For instance, the lowest concentrations (0.125 mg/L and 0.0625 mg/L) of micafungin inhibited biofilm formation up to 82% in strain CA86, 77% in both CA94 and CA95, and up to 69% in strain CG96 at 48h of biofilm growth ($p\text{-values} < 0.001$). This inhibition degree was even stronger in the case of caspofungin, suggesting that this antifungal could be more efficient in preventing biofilm-related fungal infections.

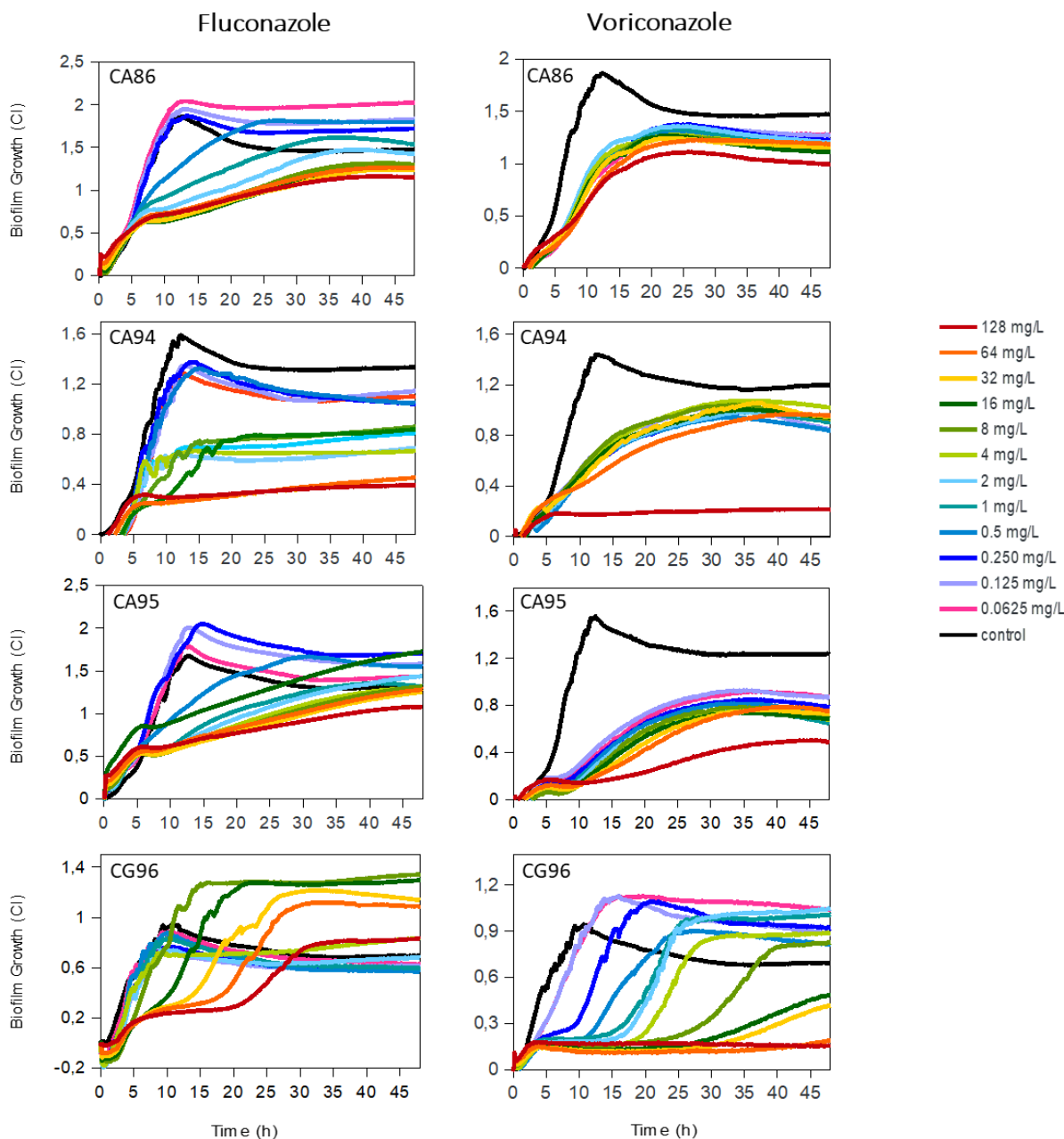


Figure III-2. The effect of fluconazole and voriconazole on *Candida albicans* (CA) and *C. glabrata* (CG) biofilm formation. Both antifungals were added at the beginning of biofilm formation together with the fungal inoculum at concentrations ranging from 128 to 0.0625 mg/L. Biofilm growth was monitored in real-time for 48h at 37°C in triplicates using impedance-based measurements. Black lines represent untreated controls. SDs are not shown for clarity.

In contrast to these results, the standard E-test showed that minimum inhibitory concentrations (MICs) for some antifungals were at least 100 times lower compared to the minimum biofilm inhibitory concentrations (MBICs) obtained by impedance measurements

(Table III-S2). In addition, both MICs and MBICs values were higher for azoles when compared to echinocandins, suggesting limited antifungal properties of azoles against the tested strains (Table III-S2).

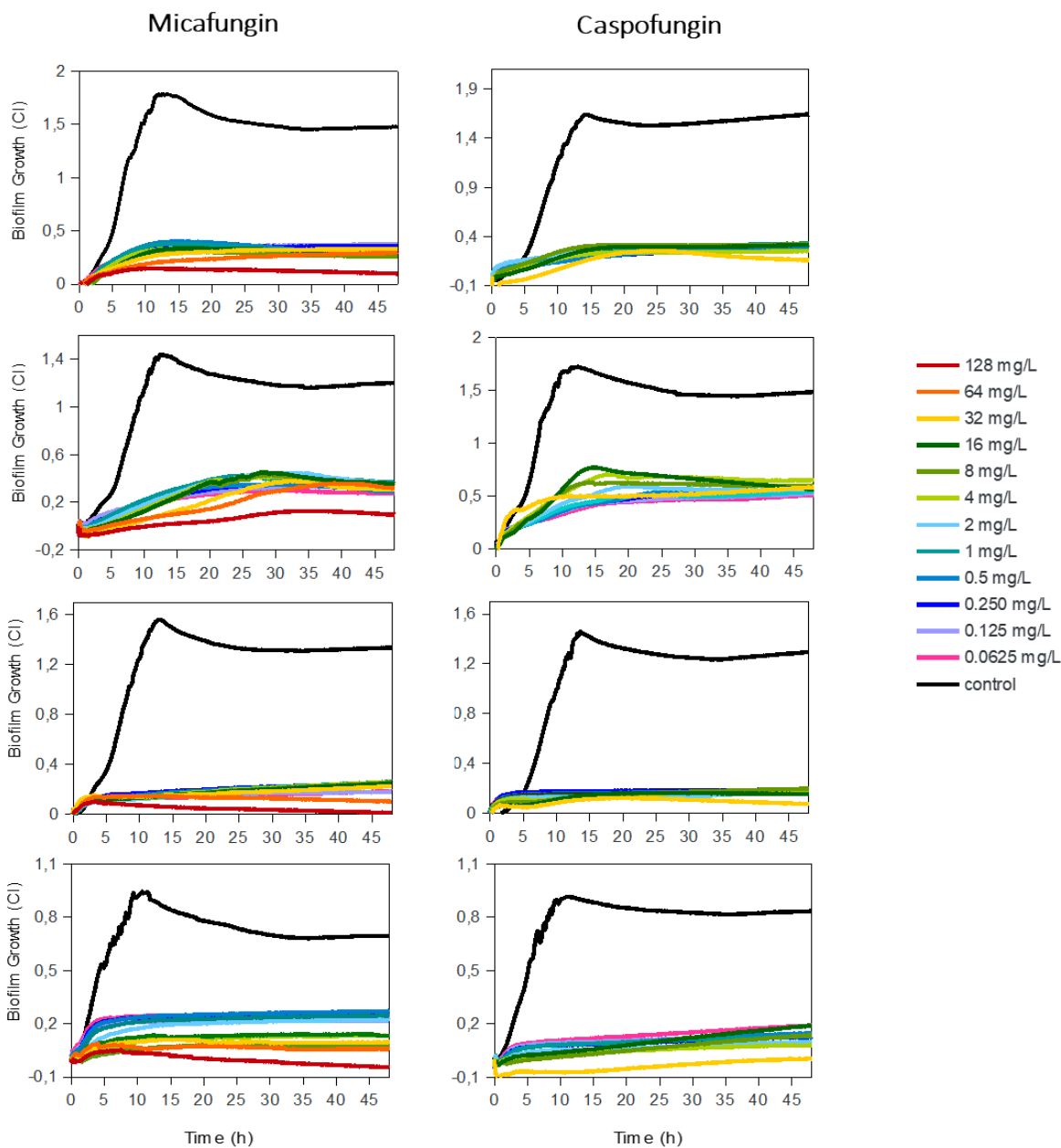


Figure III-3. The effect of micafungin and caspofungin on *Candida albicans* (CA) and *C. glabrata* (CG) biofilm formation. Both antifungals were added at the beginning of biofilm formation together with the fungal inoculum at concentrations ranging from 128 to 0.0625 mg/L. Biofilm growth was monitored in real-time for 48h at 37°C in triplicates using impedance-based measurements. Black lines represent untreated controls. SDs are not shown for clarity.

Mature biofilm disruption by echinocandins

In contrast to azole group antifungals, echinocandins showed a strong capacity to inhibit *Candida spp.* biofilm formation when added together with the fungal inoculum. For this reason, we further investigated whether micafungin and caspofungin were able to disaggregate or eliminate mature *Candida spp.* biofilms. Dose-response experiments in real-time performed on 24h biofilms of *C. albicans* and *C. glabrata* strains showed that both micafungin and caspofungin did not eradicate mature biofilms, and in most cases even resulted in an induction of new biofilm accumulation up to 30% (p -value < 0.001) when compared to untreated controls, confirming that established biofilms are extremely difficult to eradicate (**Fig. III-4**).

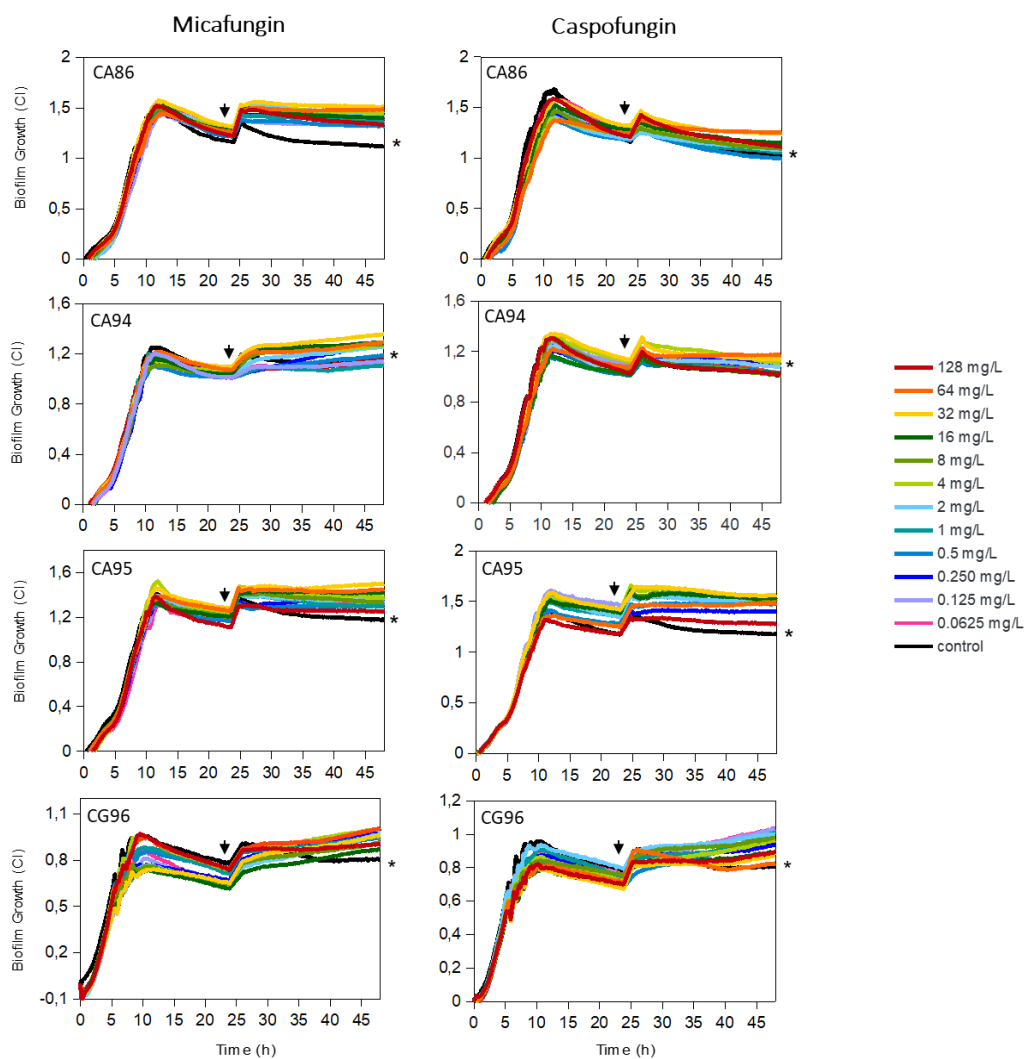


Figure III-4. The effect of micafungin and caspofungin on mature 24h *Candida albicans* (CA) and *C. glabrata* (CG) biofilms. Both antifungals were added on the established biofilm at 24h of growth (indicated by black arrows) at concentrations ranging from 128 to 0.0625 mg/L. After the addition of antifungals, biofilm growth was monitored for an additional 24h period. Black lines represent untreated controls and are marked by asterisks. Data are means of three replicates. SDs are not shown for clarity.

Andrographolide effect on *Candida* spp. planktonic and biofilm growth

As previous experiments showed that established *Candida* spp. biofilms were extremely resistant to tested conventional antifungals, we wanted to investigate whether andrographolide, with demonstrated activity against biofilms of gram-positive and gram-negative bacterial species, could also have an effect against *Candida* spp. Results in **Fig. III-S3** show that 2.5 g/L and 5 g/L of andrographolide were able to completely suppress planktonic growth of all tested *C. albicans* and *C. glabrata* strains, while lower concentrations (1.25 g/L – 315 mg/L) resulted in concentration-dependent growth inhibition or delay.

Given that andrographolide showed antifungal properties on planktonic growth in all tested *Candida* strains, we further evaluated the potential capacity of this compound to prevent *Candida* biofilm formation. Impedance-based measurements showed that concentrations equal to 5 g/L of andrographolide (2x MIC value) completely inhibited biofilm formation in all tested strains, while lower andrographolide concentrations showed a concentration-dependent effect in *Candida* spp. biofilm inhibition (**Fig. III-5**).

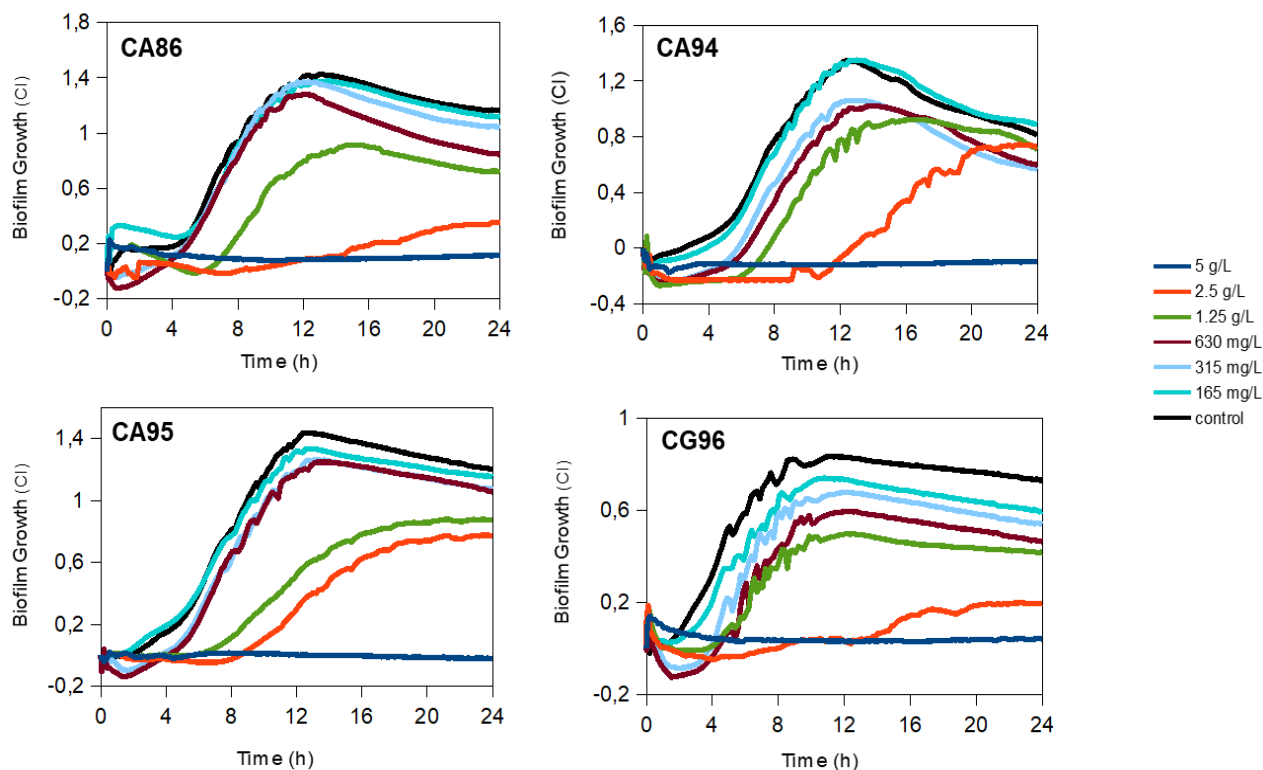


Figure III-5. Effect of andrographolide on biofilm formation in real-time of *Candida albicans* (CA) and *C. glabrata* (CA) strains. Andrographolide was added together with fungal cells at concentrations ranging from 5 g/L to 0.165 g/L. Biofilm growth was registered every 10 minutes for 24h at 37°C. Black line indicates the untreated control. Each line is the mean of two replicates. SDs are not shown for clarity.

The next approach was to evaluate the ability of the natural compound to eliminate *Candida* mature biofilms. Similarly, when andrographolide was added on 24h biofilms at the concentrations of 2.5 g/L and 5 g/L, it provoked a notable decrease in CI values in both *C. albicans* strains (up to more than 60% in biofilm reduction, p -value<0.001) and up to 100% in *C. glabrata*, suggesting that this compound besides the biofilm prevention properties is also capable to interfere with mature biofilm architecture and detach yeast cells embedded in 24h-old biofilms (**Fig. III-6**).

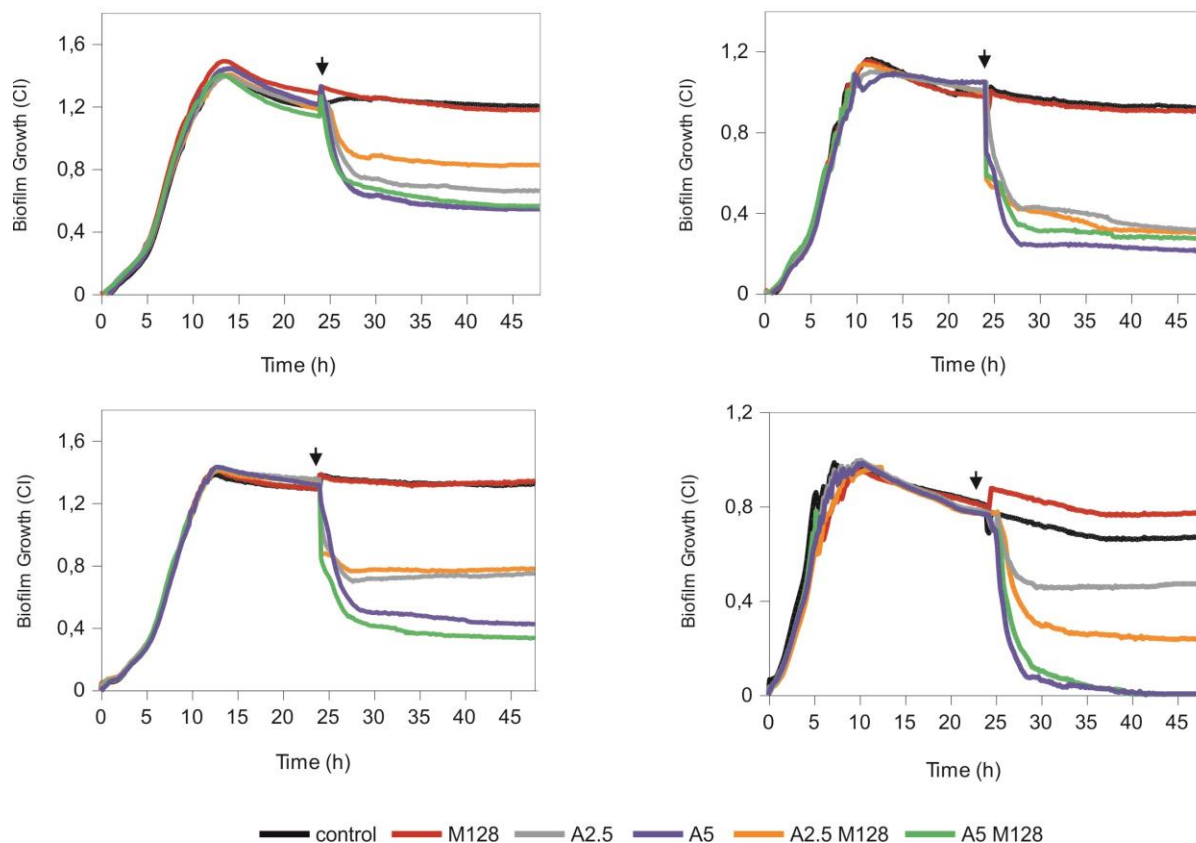


Figure III-6. *Candida albicans* (CA) and *C. glabrata* (CG) biofilm eradication using either andrographolide or micafungin alone and their combination. Both compounds were added on mature 24h old biofilms (indicated by black arrows) and the biofilms were grown for an additional 24h. Black lines represent untreated controls. SDs are not shown for clarity. **M128** - micafungin 128 mg/L; **A2.5** - andrographolide 2.5 g/L; **A5** - andrographolide 5 g/L; **A2.5M128** - andrographolide 2.5 g/L + micafungin 128 mg/L; **A5M128** - andrographolide 5 g/L + micafungin 128 mg/L.

In order to assess whether andrographolide, besides the ability to detach established biofilms, also had fungicidal properties, we performed viable cell counts of the biofilms treated with andrographolide at 24h of biofilm growth. The results showed a similar trend which was observed using impedance-based measures (**Figure III-7**). Andrographolide was able both to eradicate fungal biofilms and kill biofilm-embedded fungal cells up to 99.9 % of *C. albicans* cells (three orders of magnitude) when administered at 5 g/L, suggesting the potential of this compound against fungal biofilm-related infections (**Fig. III-7**). It is important to highlight that in *C. glabrata* isolate CG96, andrographolide provoked almost immediate and larger biofilm detachment as detected by the impedance system, while showing a lower effect on cell viability

compared to all tested *C. albicans* isolates. This may suggest that biofilm architecture is different in *C. glabrata* (Figs. III-6 and III-7).

Further experiments were undertaken to evaluate the possible synergistic effect between andrographolide and micafungin on established biofilms. The combination of micafungin (final concentration of 128 mg/L) with 5 g/L of andrographolide did not show any synergy either in detaching capacity (assessed by impedance) or in fungicidal properties (measured by colony counting). In fact, micafungin combination with andrographolide (both 2.5 g/L and 5 g/L, respectively) showed a mild antagonistic effect as indicated by biofilm viability counts (Fig. III-7).

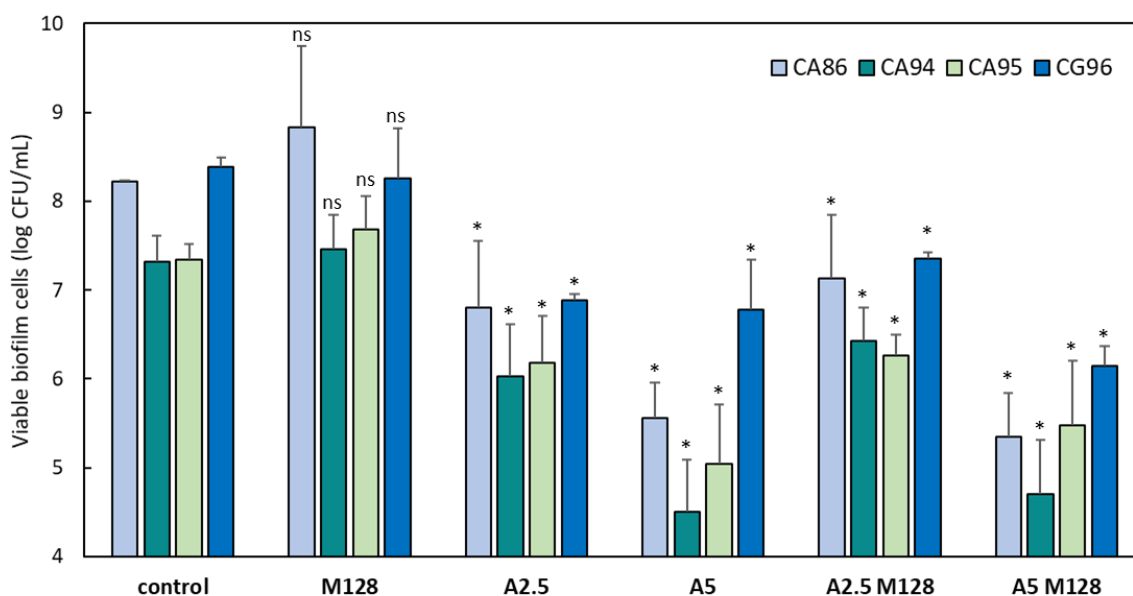


Figure III-7. Andrographolide effect alone and in combination with micafungin on mature *Candida spp.* biofilm viability. Both compounds were added at 24h of biofilm growth and viable cell counting was performed after an additional 24h. Data show the average of log CFUs counts from three independent biological replicates. **p*-value < 0.05, ns – not significant. CA - *C. albicans*; CG - *C. glabrata*; M128 - micafungin 128 mg/L; A2.5 - andrographolide 2.5 g/L; A5 - andrographolide 5 g/L; A2.5M128 - andrographolide 2.5 g/L + micafungin 128 mg/L; A5M128 - andrographolide 5 g/L + micafungin 128 mg/L.

In addition, micafungin resulted in a nonsignificant decrease in viable cell number, when compared to untreated controls. Similar results were obtained using SEM microscopy of 24h biofilms where andrographolide alone resulted in almost complete biofilm eradication in both of

the tested strains, validating results obtained by impedance measurements. On the contrary, micafungin alone did not affect biofilm architecture in *C. albicans* nor in *C. glabrata* established biofilms (**Fig. III-8B** and **Fig. III-S4B**). Thus, the effect observed in the combined treatment of micafungin with andrographolide is due exclusively to the latter, which resulted in almost complete biofilm removal in both species (**Fig. III-8** and **Fig. III-S4**).

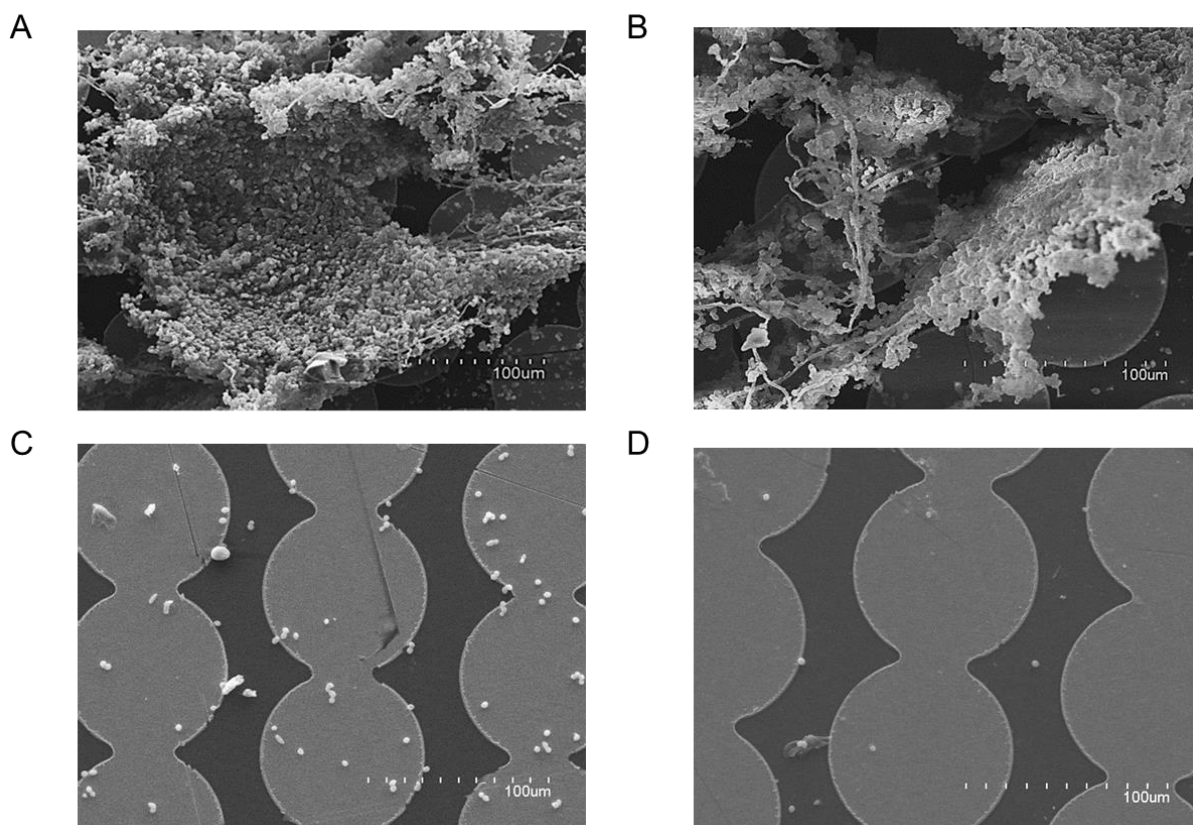


Figure III-8. Scanning electron microscopy (SEM) micrographs of 24h *Candida albicans* strain 86 biofilms treated with andrographolide, micafungin or their combination. Both compounds were added at 24h of biofilm growth and biofilms were grown for additional 24h. **A** – untreated control; **B** – biofilms treated with 128 mg/L of micafungin; **C** – biofilms treated with 5 g/L of andrographolide; **D** – biofilms treated with both andrographolide (5 g/L) and micafungin (128 mg/L). Scale bar: 100 μm .

DISCUSSION

Candida spp. cause different life-threatening infections with a high mortality rate^{112,361}. Moreover, their ability to adopt a biofilm growth form allows *Candida* spp. strains to withstand conventional treatment and immune system attack^{114,349}. For this reason, conventional

antifungals usually fail to eradicate the infection and tend to only suppress it, despite high dosages and long-term treatments^{120,121}. Although numerous *in vitro* studies, including microfluidics and time-lapse microscopy have been undertaken^{115,362} to study fungal biofilm development, none of them describe *Candida* spp. biofilm growth dynamics and eradication patterns using impedance measurements. In the current manuscript, we evaluated the ability of *Candida* spp. to attach and form biofilms on electrodes-coated plates and assessed in real-time the influence of nutritional conditions such as growth media composition and additional glucose on the capacity of different *Candida* spp. strains to produce biofilms. In contrast to standard biofilm testing methods, this methodology permits to evaluate biofilm growth continuously (showing each phase of their growth), without previous labeling or manipulation^{164,358}.

Results from our study indicate that all of the tested *Candida* spp. isolates were able to form robust biofilms in YPD and YNB media rich in dextrose and suggest that RMPI1460 medium might favor planktonic, but not a biofilm mode of growth, as observed CIs values were up to ten times lower in some of the tested strains when compared to YPD growth medium¹¹¹. Moreover, the results indicate that glucose addition to the media delayed *C. albicans* biofilm formation, while *C. glabrata* biofilm growth was not affected, suggesting that *C. glabrata* strains might have some mechanisms to facilitate biofilm formation regardless of glucose levels. Our results also highlight the importance of standardizing experimental protocols for biofilm growth, such as the time of biofilm mass measurement, to accurately describe each isolate's capacity to form biofilms.

In addition, in this study we have also used the impedance system for dose-response experiments to test biofilm susceptibility to commonly used antifungals. Impedance measurements showed that azole group antifungals (fluconazole and voriconazole) were not able to fully prevent biofilm formation but resulted in biofilm growth delay. Moreover, both fluconazole and voriconazole provoked changes in biofilm growth dynamics in all tested strains, suggesting that these antifungals might interfere with some components in the EPS biofilm matrix and provoke changes in biofilm architecture. Similar findings have been reported by other authors who demonstrated that azole group antifungals can result in phenotypical changes in biofilm development and structure^{363–365}. Contrary to azole group antifungals, echinocandins (micafungin and caspofungin) showed a strong biofilm formation inhibitory effect when added

together with the fungal inoculum, as has been described elsewhere^{115,342,344}. However, both micafungin and caspofungin lacked a biofilm eradication effect when added on 24h biofilms, and at some concentrations even induced biofilm formation (**Figs. III-2 and III-4**). These findings are similar to those described by Kaneko and colleagues, who found that although micafungin was capable to suppress biofilm formation and development, fluconazole resulted in only partial biofilm inhibition, and they both failed to eradicate established fungal biofilms¹¹⁵. Thus, this emphasizes the need for new potent strategies to combat established fungal biofilms¹⁰⁹. For this reason, an effort was undertaken to study the effect of the novel compound andrographolide, a natural component from the plant *Andrographis paniculate*, which was shown to have anti-inflammatory, anti-viral and antimicrobial properties against different bacteria^{350,351,353,356,366}. Andrographolide not only showed the capacity to inhibit planktonic *Candida* spp. growth but also resulted in biofilm inhibition when added at concentrations equal to or higher than 2.5 g/L in all tested strains, suggesting that this compound could be used as a promising tool to prevent fungal biofilms formation and accumulation (**Figs. III-5 and III-S3**). This antibiofilm capacity against *C. albicans* and *C. glabrata* has not been shown before, and our data indicate that andrographolide was also effective against mature fungal biofilms, where the addition of this compound resulted in almost complete biofilm detachment (**Fig. III-6**). Additionally, andrographolide reduced cell viability by up to 99.9% in *C. albicans*. Although andrographolide showed strong biofilm detachment capacity in *C. glabrata* strain 96 as measured by impedance, cell viability of this strain was decreased less when compared to *C. albicans*. These results suggest that *C. glabrata* biofilms might have different biofilm architecture and composition when compared to those of *C. albicans*. Additionally, SEM's images confirmed the effect of andrographolide on mature *Candida* spp. biofilm detachment and eradication. For instance, these results indicate that andrographolide shows considerably higher efficacy on mature biofilms than both caspofungin and micafungin. On the other hand, we have also demonstrated that andrographolide and micafungin did not show a significant synergistic effect. In conclusion, obtained results strongly indicate the anti-biofilm properties (prevention and eradication) of andrographolide against *Candida* spp. (**Figs. III-7, III-8 and III-S4**).

Overall, the data presented in the current manuscript underline the importance of testing new natural compounds with biocidal or detaching properties in order to obtain improved clinical outcomes from fungal biofilm-associated infections than those obtained with existing

conventional therapies^{114,120,125}. Our study demonstrates a potent effect of andrographolide against *C. albicans* and *C. glabrata* fungal biofilm formation and eradication. Thus, we suggest that future studies should evaluate the *in vivo* effect of andrographolide to treat fungal infections.

CHAPTER III SUPPLEMENTARY INFORMATION**Supplementary table III-S1.** Fungal strains used in this study.

Strain	Description	Reference
<i>Candida albicans</i> 86	Laboratory strain ATCC14053	367
<i>Candida albicans</i> 87	Clinical isolate from vaginal exudate	This study
<i>Candida albicans</i> 94	Clinical isolate from vaginal exudate	This study
<i>Candida albicans</i> 95	Clinical isolate from vaginal exudate	This study
<i>Candida glabrata</i> 96	Clinical isolate from vaginal exudate	This study

Supplementary table III-S2. Minimum Inhibitory Concentration (MIC) vs. Minimum Biofilm Inhibitory concentration (MBIC) values for fluconazole, voriconazole, micafungin and caspofungin in different *Candida albicans* (CA) and *C. glabrata* (CG) strains. MICs were measured by standard E-test protocol, while MBICs were established according to impedance-based measurements in xCELLigence system, and both were expressed as (mg/L). **S** and **R** in the table indicate if a strain is considered susceptible or resistant according to EUCAST guidelines.

		MIC / MBIC			
Strain		CA86	CA94	CA95	CG96
Antifungal	Fluconazole	>256 (R) / >128	>256 (R) / >128	>256 (R) / >128	>256 (R) / >128
	Voriconazole	>32 (R) / >128	>32 (R) / >128	>32 (R) / >128	0.5 (S) / 64
	Micafungin	0.012 (S) / 128	0.032 (R) / 128	0.032 (R) / 64	0.016 (S) / 2
	Caspofungin	0.19 (R) >32	0.064 (R) / >32	0.064 (R) / 32	0.023 (S) / 4

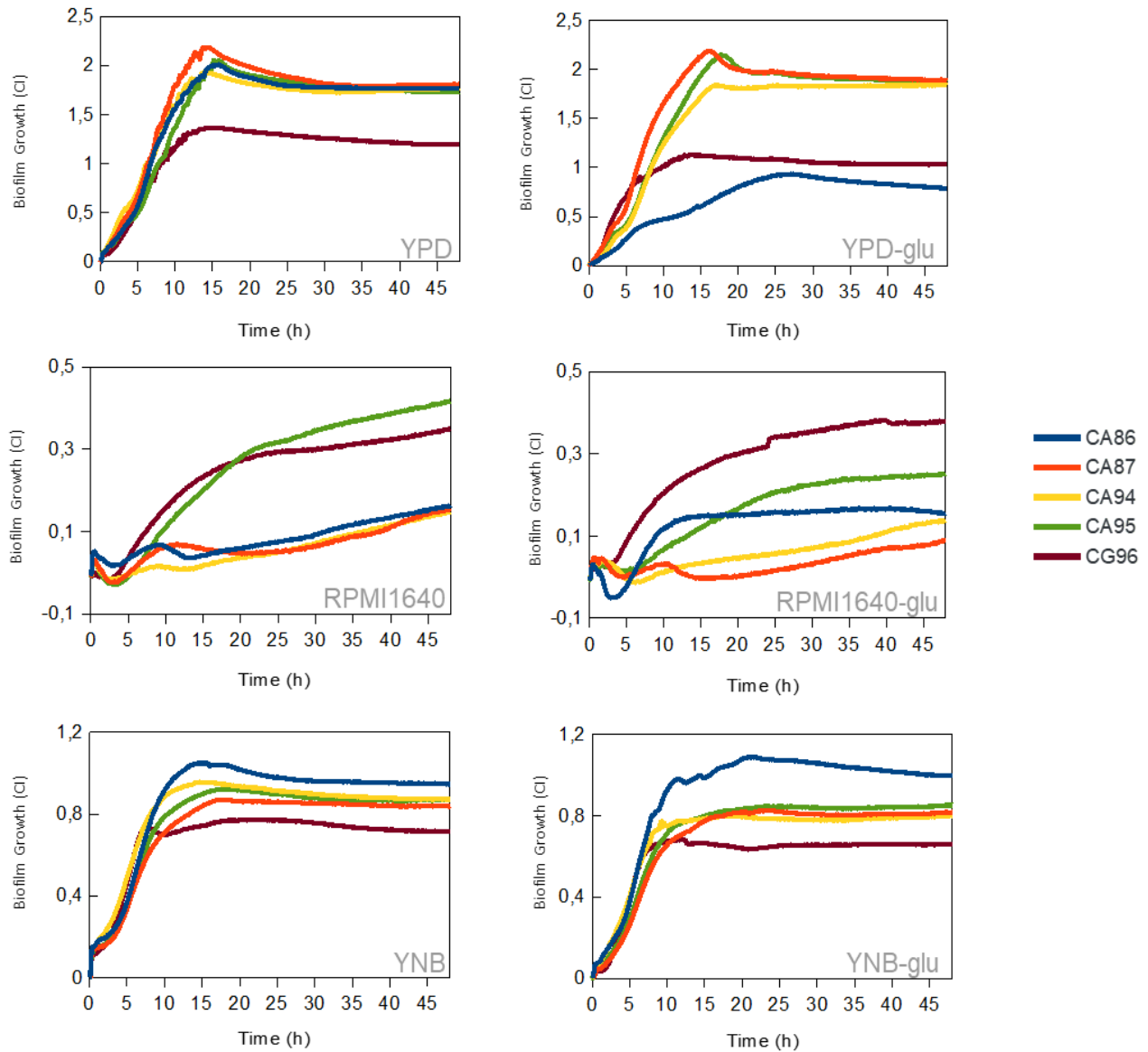


Figure III-S1. *Candida albicans* (CA) and *C. glabrata* (CG) biofilm formation capacity as revealed by impedance measurements in an xCELLigence system with different culture media: YPD, RPMI1640 and YNB alone or supplemented with 2% of glucose, respectively. Biofilm growth was measured every 10 minutes at 37°C for 48h.

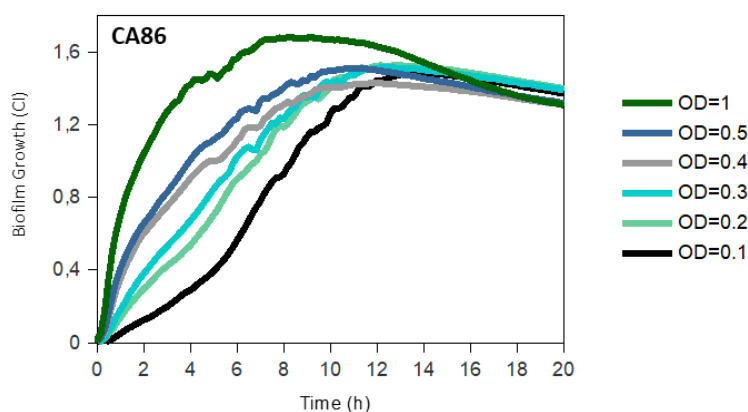


Figure III-S2. The effect of initial fungal cell optical density on biofilm formation in real-time as measured by impedance in *C. albicans* strain 86. Biofilm growth was measured using YPD culture medium without additional sugars every 10 minutes for 20h using initial OD_{600} of 1, 0.5, 0.4, 0.3, 0.2 and 0.1, respectively. Data are means of two biological replicates. SDs are not shown for clarity.

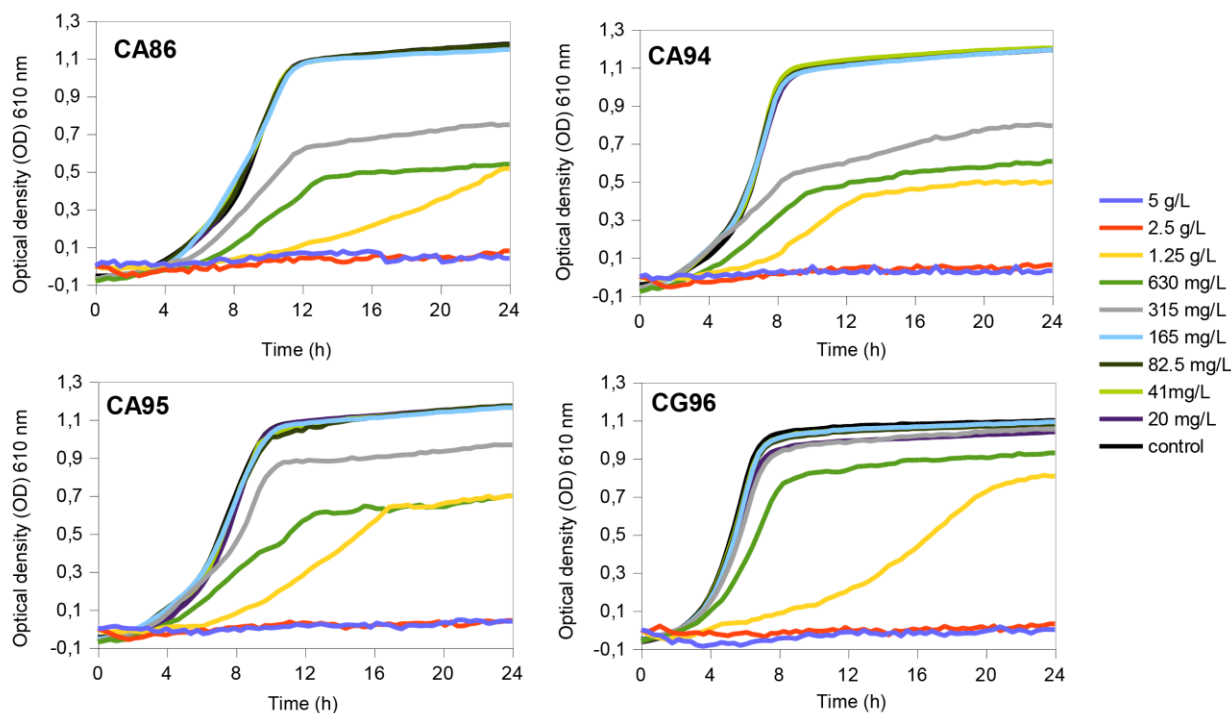


Figure III-S3. Andrographolide effect on planktonic growth of *Candida albicans* (CA) and *C. glabrata* (CG) strains. Andrographolide was added together with fungal inoculum at the concentrations ranging from 5 g/L to 0.02 g/L. Planktonic growth was measured as optical density (OD_{600}) for 24h. Three replicates of each condition were included in each experiment.

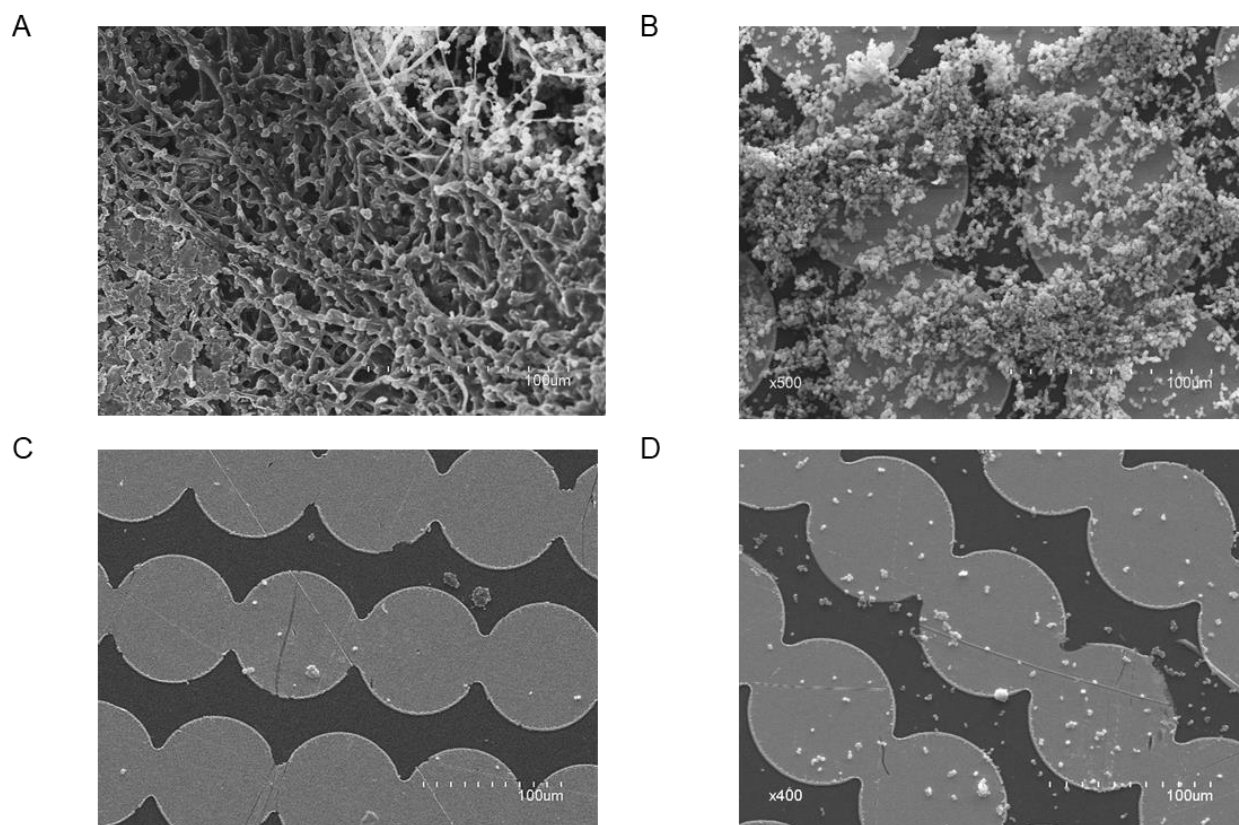


Figure III-S4. Scanning electron microscopy (SEM) micrograms of 24h *Candida glabrata* 96 biofilms treated with andrographolide and micafungin. Both compounds were added at 24h of biofilm growth and biofilms were grown for additional 24h. **A** – untreated control; **B** – biofilms treated with 128 mg/L of micafungin; **C** – biofilms treated with 5 g/L of andrographolide; **D** – biofilms treated with both andrographolide (5 g/L) and micafungin (128 mg/L). Scale bar: 100 µm.

CHAPTER IV

Personalized antibiotic selection in periodontal treatment improves clinical and microbiological outputs**ABSTRACT**

Antibiotic treatment in periodontal patients is typically selected empirically or using qPCR or DNA hybridization methods. These molecular approaches are directed toward establishing the levels of different periodontal pathogens in samples from periodontal pockets to infer the antibiotic treatment with potential best efficacy. However, current methods are costly and do not consider the antibiotic susceptibility of the whole subgingival biofilm. In the current manuscript, we have developed a method to culture subgingival samples *ex vivo* in a fast, label-free impedance-based system where biofilm growth is monitored in real-time under exposure to different antibiotics, producing results in less than 4 hours. To test its efficacy, we have performed a double-blind, randomized clinical trial where patients with chronic periodontitis were treated with an antibiotic either selected by the hybridization method (n=32) or by the one with the best effect in the *ex vivo* growth system (n=32). The antibiotic selection was different in both methods in more than 80% of the cases. Clinical parameters such as periodontal pocket depth, clinical attachment level, and bleeding upon probing improved in both groups. However, dental plaque was significantly reduced only in the group where antibiotics were selected according to the *ex vivo* growth. In addition, 16S rRNA gene sequencing showed a larger reduction in periodontal pathogens and a larger increase in health-associated bacteria after treatment also in the *ex vivo* growth group. We hypothesize that the disagreements with DNA-based molecular methods stem from the polymicrobial nature of periodontal disease giving rise to multiple interactions and unpredictable antibiotic susceptibility, as well as from intra-species variability in antibiotic susceptibility. Thus, the results of clinical and microbiological parameters, together with the reduced cost and low analysis time, support the use of the impedance system for improved individualized antibiotic selection.

INTRODUCTION

Biofilms are defined as bacterial communities composed of single or various bacterial species attached to each other on biotic/abiotic surfaces and encased in a self-secreted extracellular polymeric substance (EPS)^{112,368}. For instance, oral biofilms such as dental plaque are composed of several hundred species firmly attached to the teeth above (supragingival dental plaque) or below the gum line (subgingival dental plaque)^{130,131,369}. Oral biofilms are strongly associated with the occurrence and the progression of oral diseases such as dental caries, gingivitis, periodontitis and halitosis^{127,146}. Gingivitis is a reversible inflammatory lesion resulting from interactions between the subgingival dental plaque and the host's immune-inflammatory response, which remains contained within the gingiva and does not extend to the periodontal attachment. Contrarily, periodontitis is a chronic multifactorial inflammatory disease associated with dysbiotic subgingival biofilms and characterized by progressive destruction of the tooth-supporting apparatus, which can eventually lead to its exfoliation^{143,370,371}. In addition, there exist many different factors that contribute enormously to the occurrence and development of this disease, including mechanical disruption of gums, tobacco smoking, pathogen infection, deficient oral hygiene and the failure of immune homeostasis^{141,372}.

Despite the significant advances in the treatment of periodontal diseases, this pathology continues to increase, being the sixth-most common prevalent condition in the world. In fact, lack of adequate treatment and proper personal hygiene have been suggested as the potential causes of the aggravation of the disease¹⁴⁴. Although subgingival dental plaque elimination by radicular scraping reduces inflammation, the effect is usually transient, and inflammation returns with time, especially in high-risk individuals. For this reason, the combination of mechanical treatment and systemic antibiotics or antiseptics is commonly used, although the specific cases where this is recommended vary among countries^{143,373,374}. In order to choose an effective antibiotic therapy in each particular case, different PCR and DNA probe hybridization techniques based on the quantification of periodontal bacteria have been developed. Private laboratories usually use Socransky's complex-based (purple, red, orange, yellow, and green) detection and quantification of periodontal pathogens, including *Aggregatibacter actinomycetemcomitans*, *Porphyromonas gingivalis*, *Tannerella forsythia* and *Treptononema*

denticola among others^{375,376}. However, these techniques are expensive and only consider the presence of specific bacterial species rather than the antibiotic effect on the whole biofilm (where some bacterial strains can be susceptible and others resistant to a given antibiotic)¹⁴⁷. Moreover, these molecular genetic techniques overlook the interaction between different communities and the presence of EPS which can protect biofilm-embedded bacteria^{49,132,377}. All these difficulties can lead to treatment failure and consequently to other serious health complications, including bacteremia, pre-mature birth, cardiovascular diseases, or autoimmune diseases, among others^{17,378}. Therefore, there is a need to develop new, faster, inexpensive, and more reliable methodologies able to predict the best individualized antibiotic treatment for patients with periodontal disease.

In the current manuscript, we used Real-Time Cell Analysis (RTCA) to evaluate the *in vitro* antibiotic effect on periodontal biofilm growth dynamics of 64 patients with severe periodontal disease. This method consists of growing fresh periodontal samples in a microcosm model where biofilm growth is monitored in real time using impedance-based measurements^{197,215}. After that, in order to assess the efficacy of antibiotic use based on this method, a clinical trial was performed where half of the patients were treated with the antibiotic selected by this growth-based system, while the other half were treated with the antibiotic suggested by a standard methodology (hybridization-based antibiotic selection). One and two months after the antibiotic treatment, we compared the disease evolution by evaluation of clinical parameters (including periodontal pocket depth, clinical attachment loss, bleeding on probing and presence of plaque) and changes in subgingival plaque microbiological composition using 16S rRNA gene Illumina sequencing.

MATERIALS AND METHODS

Sample collection, transportation, and storage

To select the most suitable transport media and optimal storage time for periodontal biofilm samples, subgingival plaque from 5 individuals was collected by introducing 10 sterile paper-points (size 20) into the deepest subgingival pockets (≥ 6 mm) for 30-60 seconds and placed into 2 mL of three different transport media (**RTF**: Reduced Transport Fluid, **VMG III**:

Viability Medium Goteborg without agar or agarose and **VMG III-Agar**: Viability Medium Goteborg with agar and agarose) that were prepared following Dahlen *et al.*³⁷⁹. Samples were then immediately transported from the dental clinic to the laboratory and stored at room temperature for 24 and 48 h to determine the optimal conditions for their storage and recovery, based on bacterial composition similarity between the sample and the biofilm grown (**Fig. IV-S1**).

Study design and patients' selection

To evaluate the use of the RTCA system in antibiotic selection for the individualized treatment of patients with periodontal disease, and to compare the *in vivo* effect of those antibiotics to the current antibiotic selection techniques, a randomized, double blind, parallel group clinical study was designed. The study protocol was reviewed and approved by the Ethics Committee of the University of Valencia (Spain) (H1547805836517). The study was conducted from September 2019 to May 2022.

Required sample size was calculated by a power estimation based on the differences in clinical attachment level (CAL) of 1 mm between the groups with variation in the population of 0.5, a confidence level of 80% and a power of 95%, which suggested a sample size of 20 individuals per group. Due to the length of the study and the multiple visits, a high dropout rate (>15%) was expected. Therefore, a final sample size of over 60 volunteers fulfilling the inclusion/exclusion criteria was estimated.

Inclusion criteria included: adults between 40 and 70 years old, non-smokers or smokers of less than 10 cigarettes a day, with stage III and IV grade A-B periodontitis, presence of at least 20 teeth in the mouth, including at least one molar per quadrant and good general health. Exclusion criteria included: smokers of more than 10 cigarettes a day, patients who have been treated with periodontal therapy in the last 12 months, patients who have been taking antibiotics in the last three months or who routinely used antiseptics in the previous month, patients who due to their systemic condition take antibiotics, pregnant or lactating woman, patients who take medication that might alter the immune system or bone metabolism, patients who are allergic to the antibiotics used in the study and people with diabetes with more than 7% glycosylated

hemoglobin. After signing the informed consent form, clinical periodontal indexes such as bleeding on probing (BOP), probing depth (PD), clinical attachment level (CAL) and plaque presence (PLAQUE) were evaluated as previously described^{145,380,381}. Following visits to the dental clinic are indicated in the flow diagram of the study design (**Fig. IV-S2**)

After the evaluation of clinical parameters, the subgingival plaque samples of 64 volunteers were collected into VMG III transport media, as described above, for both biofilm growth monitoring in real-time (Real-Time culture; RT-Culture) using the xCELLigence impedance monitoring system (Agilent Technologies) and for bacterial composition determination before treatment. In parallel, subgingival plaque samples from the same volunteers were collected into sterile tubes using micro-IDent® plus11 kit (Hain Lifescience GmbH, Germany) and following the instructions provided by a private laboratory (Echevarne Laboratory, Barcelona, Spain) and sent immediately for PCR and specific probe hybridization-based quantification of 11 of the most common periodontal pathogenic species (*Aggregatibacter actinomycetemcomitans*, *Porphyromonas gingivalis*, *Tannerella forsythia*, *Treponema denticola*, *Prevotella intermedia*, *Peptostreptococcus micros*, *Fusobacterium nucleatum/periodonticum*, *Campylobacter rectus*, *Eubacterium nodatum*, *Eikenelia corrodens* and *Capnocytophaga gingivalis/ochracea/sputigena*) and the corresponding levels of five bacterial complexes based on Socransky's classification^{382,383}. Patients were then randomly assigned to one of the two treatment groups: half of the patients (32 volunteers) were treated with the antibiotic selected by the *in vitro* culturing system using impedance-based results, while the other half were treated with the antibiotic selected by the hybridization methodology (32 volunteers).

After four and eight weeks of systemic antibiotic treatment, the patient's oral health was re-evaluated, including all clinical parameters described above (**Fig. IV-S2**). In addition, new subgingival plaque samples were collected in VMG III transport media, as previously indicated, for the evaluation of the total bacterial composition after antibiotic treatment in both study groups (**Fig IV-1**). After the treatment, clinical and microbiological parameters were analyzed and compared between methodologies. Three patients of the RT-Culture group were not analyzed, as one of took another antibiotic prescribed by another professional because of additional infection, and two failed to attend their 2-month reevaluation visit to the dental clinic

because of COVID. Similarly, six patients from the hybridization group did not participate in all needed dental clinic visits, and five had incomplete or wrong antibiotic dosing (**Fig. IV-S3**).

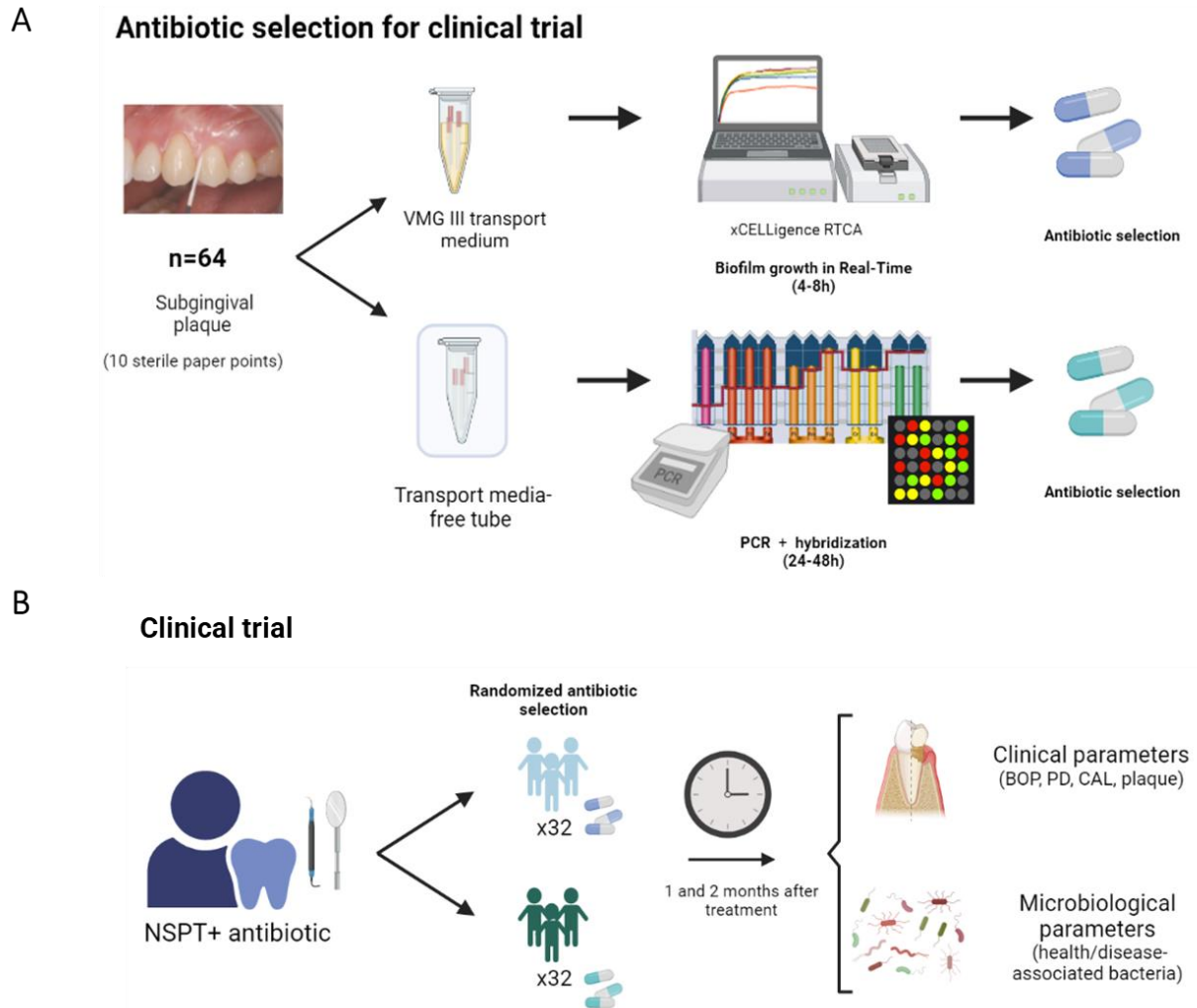


Figure IV-1. Diagram of the clinical study protocol: subgingival plaque samples from 64 individuals with severe periodontal disease were collected in VMGIII transport media and grown in an impedance system for monitoring periodontal biofilm growth in real time in the presence of antibiotics (Real-Time Culture). Derived biofilms were collected at 8h of growth for DNA extraction and 16S rRNA gene sequencing. In parallel, subgingival plaque samples from these 64 patients were used for standard hybridization-based periodontal pathogen quantification and associated antibiotic recommendations by the German Society of Periodontology³⁸⁴ (**A**). For the clinical trial, half of the patients were randomly treated with the antibiotic suggested by the RT-Culture system and the other half with the antibiotic prescribed based on the hybridization of periodontal pathogens. One and two months after antibiotic treatment, the improvement in

clinical and microbiological parameters was evaluated for both study groups to assess disease progression (**B**).

Randomization and blinding

A randomized, double-blind clinical trial was carried out where patients and dentists were unaware of which methodology was used to select the antibiotic as part of the periodontal therapy. In detail, after consent form approval, dental clinic staff responsible for the prescription of the periodontal antibiotic treatment assigned each patient a code, which was previously generated randomly by another research team member. Depending on the method of treatment selection, this code consisted of a patient number and a letter A or B. Thus, 32 patients were randomly assigned to one method treatment group, while the other 32 were assigned to the other group.

Real-Time biofilm growth monitoring

To select the most suitable transport media for periodontal biofilm samples, the subgingival plaque samples were collected in 2 mL of three different transport media, as indicated above, and homogenized by vortexing for 60 sec. Paper points were discarded, samples were vortexed again for 30 sec and split into three equal aliquots for biofilm growth in real-time either fresh or after 24 and 48h ($t=0$, $t=24$, and $t=48$) of storage at room temperature. At each time point, the aliquots were centrifuged at 10,000 rpm for 3 minutes, supernatants were discarded, and bacterial pellets were resuspended with 400 μL of BHI supplemented with vitamin K₁ (VitK₁) and hemin-menadione (reaching final concentrations of 0.2 mM and 0.5 mM, respectively). Two hundred microliters of the samples were used to monitor biofilm growth in the xCELLigence impedance monitoring system and the other 200 μL of the suspensions were centrifuged, and the pellets stored at -20°C for DNA extraction and subsequent 16S rRNA gene sequencing.

For biofilm growth evaluation of periodontal plaque samples that were stored at room temperature for 0, 24 and 48h ($t=0$, $t=24$, and $t=48\text{h}$), the xCELLigence RTCA system was used as previously described^{198,358}. Briefly, 100 μL of BHI supplemented with VitK₁ and hemin-

menadione were used for background measurements. Further, 100 μ L of the subgingival plaque suspensions of the different time points were added into E-plate wells in duplicate. Then, an overlay of sterile mineral oil was gently added to the top of each well to favor anaerobic conditions. BHI supplemented with VitK₁ and hemin-menadione without bacterial inoculum was included in each experiment as a negative control. After that, E-plates were incubated in the RTCA system at 37°C, and periodontal biofilm growth was monitored for 8h and 24h, respectively. To analyze the bacterial composition of the formed periodontal biofilms at the bottom of the wells, supernatants were discarded, and biofilms were gently washed with PBS (phosphate buffer saline, pH=7.0) to eliminate unattached bacterial cells. The adhered biofilm was collected using 200 μ L of PBS, centrifuged, and the pellet stored at -20°C for further analysis. The same procedure was repeated with the periodontal samples stored at room temperature for 24h and 48h (t=24h and t=48h, respectively) in the different transport media.

Evaluation of periodontal biofilm susceptibility to antibiotics by real-time monitoring of biofilm growth

To identify the best individual treatment for each patient with severe periodontal disease, three systemic antibiotics commonly used in dental practice, namely amoxicillin, metronidazole and azithromycin (SIGMA), and the combination of amoxicillin and metronidazole, were tested, by evaluating their effect on biofilm formation of the subgingival plaque samples. Similarly to the experiments described above, the subgingival plaque was collected into 2 mL of VMG III transport media and vortexed for 60 seconds. After that, paper-points were discarded, and samples were centrifuged at 10.000 rpm for 3 minutes. Hereafter, the pellet was resuspended with 2 mL of fresh BHI medium supplemented with VitK₁ and hemin-menadione^{133,385}. All samples were divided into two equal aliquots. A pellet of 1 mL of each sample was used for DNA extraction and 16S rRNA gene sequencing, while the other 1 mL was used for biofilm growth in the RTCA system in the presence of different antibiotics.

To grow periodontal biofilms in the presence of conventional antibiotics in the RTCA system, 100 μ L of each antibiotic diluted in BHI medium supplemented with VitK₁ and hemin-menadione reaching final concentrations of 8 mg/L for amoxicillin, 16 mg/L for metronidazole

and 0.4 mg/L for azithromycin, respectively, were used for background measurements. These concentrations correspond to the maximum crevicular gingival fluid concentrations reached after oral administration of each antibiotic^{148,386-388}. Then, 100 µL of homogenized periodontal samples were added into the wells, followed by a drop of mineral oil. Then, E-plates were incubated in the RTCA system at 37°C to monitor biofilm growth in real-time. After 8h of growth, supernatants were discarded, and bacterial cells attached to the E-plate surface were gently washed and collected using 200 µL of PBS. Obtained pellets were stored at -20°C for further analysis. Two replicates of each condition and negative controls were included in each experiment. Biofilm growth dynamics graphs were plotted using the normalized average of the replicates.

DNA extraction, 16S rRNA gene sequencing and bioinformatic analyses

Genomic DNA from samples of the subgingival dental plaque collected before (initial inocula, t0) and 1 and 2 months after antibiotic treatment (t1 and t2, respectively), and the corresponding biofilms grown in xCELLigence impedance system for eight hours (alone and in combination with antibiotics) was isolated using MagNA Pure LC DNA Isolation Kit III for Bacteria and Fungi (Roche Diagnostics) according to manufacturer's instructions. The 16S rRNA gene V3-V5 regions were amplified as previously described³⁸⁹. The 16S rRNA gene Metagenomic Sequencing Library Preparation Illumina protocol (Part #15044223 Rev. A) was used to prepare an Illumina amplicon library. The amplicons were sequenced using 2x300 bp paired-end sequencing on an Illumina MiSeq Sequencer following the manufacturer's instructions (Illumina, San Diego, California, USA) at the Sequencing Service in FISABIO Institute (Valencia, Spain).

The obtained reads were analyzed as previously described using dada2 v1.16³⁹⁰. Briefly, forward and reverse primers were removed, reads were quality-filtered by end-trimming and by a maximum number of expected errors. After that, reads were dereplicated, paired reads were merged, chimeras and host reads were removed, and the high-quality remaining reads were annotated using SILVA database v138.1³⁹¹.

R programming language was used to compare statistically the proportion of bacteria between groups³⁹². Analysis of compositions of microbiomes with bias correction (ANCOM-BC³⁹³) was used to normalize and compare the abundance of bacterial taxa. Multivariate analyses, including principal component analyses (PCA) and canonical correspondence analysis (CCA) were performed using *vegan* library³⁹⁴. PCA loadings were represented using red arrows when indicated and computed as the correlation of the original variables with the first two principal components, whereas coordinates of observations or 'scores' were computed as the projection of the original observations on the first two principal components.

Based on the results from previous microbial-based studies, we grouped bacterial species considered periodontal pathogens into “disease-associated”, whereas those that are known to be more abundant in healthy individuals were computed as “health-associated”, following Perez-Chaparro et al³⁹⁵. The list of bacteria included in these two groups is enumerated in **Supplementary table IV-1**.

Reads have been deposited at the SRA database (accession number: PRJNA892459).

RESULTS

Evaluation of different transport media and growth conditions for periodontal samples

In order to select the most suitable transport media for periodontal biofilm samples from deep periodontal pockets, subgingival biofilms from five volunteers were collected in three different transport media (RTF, VMG III and VMG III Agar) and stored at room temperature for 0h, 24h and 48h. A flowchart of the protocol is represented in **Supplementary Figure IV-1**. **Supplementary figure IV-4A** shows periodontal biofilm growth in real time after the preservation in RTF, VMG III and VMG III-Agar transport media assessed by impedance measurements. The best recovery and biofilm growth were observed in RTF and VMG III media at 0h. However, in contrast to VMG III, sample storage in RTF media for 24h and 48h resulted in biofilm growth delay and lower total biofilm mass accumulation compared to these parameters at 0h. Similarly, subgingival plaque storage in VMG III-Agar reduced its capacity to form biofilms, reaching lower CI values compared to those of VMG III alone in all tested time points. In addition, 16S rRNA gene sequencing was used to compare the initial microbial composition

of the inoculum (t=0) to that after 24 and 48h of storage in VMG III transport media. 16S rRNA gene sequencing data revealed that VMGIII preserved periodontal bacteria diversity for at least 24h (**Fig. IV-S4B**). Moreover, a similar bacterial composition was observed after 48h of storage, suggesting that VMG III media could be appropriate for periodontal biofilm transportation. In addition, sequencing data indicated that grown biofilms derived from periodontal samples should be collected at 8h (not 24h) in order to preserve representative periodontal microbiota and avoid the overgrowth of *Streptococcus* genera (data not shown).

We also performed principal component analysis (PCA) comparing the microbial composition of 24 periodontal samples collected in VMGIII transport media (initial inoculum) to derived biofilms grown in the impedance system collected after 8h (**Fig. IV-S4C**). Importantly, periodontal biofilms grown in the xCELLigence system contained a bacterial composition similar to the initial inocula. Although the increase in *Streptococcus* genera was observed in some cases, the biofilms grown *in vitro* contained representative periodontal microbiota, including common periodontal pathogens such as *Tannerella*, *Treponema*, *Filifactor*, *Fusobacterium*, *Treponema*, among others, as previously described¹³³.

The effect of conventional antibiotics on periodontal biofilm formation in Real-Time

Once the most suitable conditions for periodontal biofilm transportation and growth were established, we grew subgingival biofilms of 64 patients with periodontal disease *in vitro* in the presence of systemic antibiotics commonly used in clinical practice. **Figure IV-2** illustrates the effect of the tested antibiotics on biofilm formation in six different susceptibility cases. As it can be observed in the figure, periodontal biofilms showed a sample-dependent effect. For example, amoxicillin showed a strong biofilm inhibition capacity in case **E** and a moderate inhibitory effect in cases **A** and **B**, while in other samples, the effect of this antibiotic had no inhibitory effect or even induced biofilm growth compared to the antibiotic-free cell control (case **F**). Although metronidazole favored biofilm formation in most of the cases (for example, **Fig. IV-2 ACDF**), this antibiotic also showed the highest biofilm inhibition capacity in cases **B** and **E**. Given that there is compelling evidence that conjunctive antibiotic therapy usually results in better clinical outcomes³⁹⁶, we also evaluated the effect of a combination of both antibiotics (amoxicillin and metronidazole added together) on subgingival biofilm formation. As shown in

figure IV-2, this combination was selected as the most efficient treatment strategy in case **C**, where periodontal biofilm development was inhibited by almost 50% compared to the untreated control. However, similarly to metronidazole alone, this combination induced biofilm formation in other cases. Finally, azithromycin, which is effective against many anaerobes including red-complex periodontopathogens, resulted in biofilm inhibition in case **D**, where other tested antibiotics resulted in biofilm growth induction. However, we have also noted some cases (2/64 of tested cases) where none of the tested antibiotics could halt biofilm formation (**Fig. IV-2F**), suggesting that it might be necessary to test more antibiotics or their combinations in order to select an effective treatment for these patients. Finally, the data show that impedance-based antibiotic selection was consistent between four and eight hours, supporting that suitable antibiotics can normally be chosen in less than four hours (see, for example, **Fig. IV-2E**).

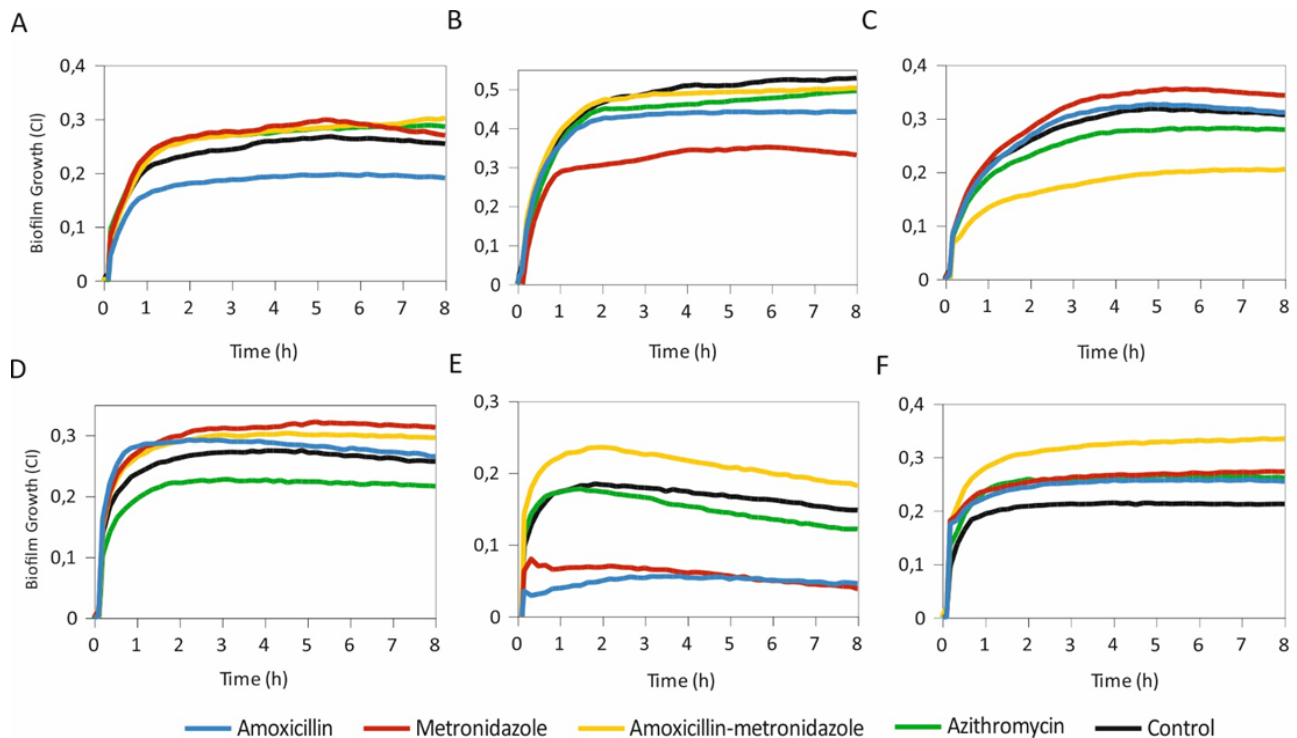


Figure IV-2 Biofilm growth derived from subgingival plaque samples grown in real time in an impedance-based monitoring system in the presence/absence of amoxicillin, metronidazole, their combination and azithromycin. Antibiotics were added at the beginning of the experiment, along with fresh subgingival plaque samples. Black lines represent antibiotic-free controls. Biofilm growth was registered every 10 minutes for 8 h; SDs are not shown for clarity. Each panel represents a different patient and are representative of cases where one of the antibiotic treatments was effective in reducing biofilm mass compared to the rest (panels **A-D**), where the

amoxicillin+metronidazole combination worked worse than each antibiotic alone (panel E) or where all antibiotics were ineffective and induced further biofilm growth (panel F).

Antibiotic selection

After determining the most effective antibiotic treatment *in vitro* for each patient with both methodologies (RT-Culture by impedance measurements and hybridization), patients were divided in two groups: 32 patients were given the systemic antibiotic treatment selected by standard hybridization method, and the other 32 patients the antibiotic suggested by the impedance biofilm growth system (**Fig. IV-2**). Figure **IV-S5** shows the percentage of cases where each antibiotic was suggested in the two methodologies. The most common antibiotic therapy recommended by the impedance system was azithromycin (41.3% of the cases), while the hybridization method mainly suggested metronidazole (60.4% of cases). In addition, the impedance method recommended amoxicillin in 31.7%, metronidazole in 14.3% and their combination in 12.7% of the cases. In contrast to these results, the hybridization method selected amoxicillin in 15.1% of the cases, amoxicillin and metronidazole combination in 13.2% and azithromycin in 11.3% of the cases. Interestingly, both methodologies suggested the same antibiotic only in 18.9% of the cases.

Clinical parameters before and after antibiotic therapy

In order to assess the clinical improvement observed in each group after antibiotic treatment, clinical parameters (periodontal pocket depth - PD, clinical attachment level - CAL, bleeding on probing - BOP and plaque presence (PLAQUE)) were evaluated at 2 months after the patients received antibiotic therapy (after treatment, AT) and compared these values to baseline (before treatment, BT). **Fig. IV-3A** shows the percentage of improvement of the clinical parameters after treatment with antibiotics selected by standard Hybridization and by culturing the subgingival sample in the impedance system (RT-Culture). All clinical parameters measured improved similarly in both groups, and was highest in BOP, which reached over a $50 \pm 34\%$ SD reduction in the PCR hybridization group and over $60 \pm 19\%$ SD reduction in the RT-Culture group. Similarly, plaque presence was reduced considerably in both treatment groups. However, this reduction was significantly higher in the patients who received the antibiotic selected using

the impedance-based system in comparison to the hybridization-based methodology. **Fig. IV-S6A** shows the comparison between evaluated clinical parameters before and after treatment (BT and AT, respectively) for each study group. BOP, PD and CAL were significantly lower after antimicrobial therapy in both-hybridization and RT-Culture groups, while plaque levels were significantly reduced only in the group treated with the antibiotics suggested by the RT-Culture system (p -value=0.0001).

Besides evaluating whether clinical outcomes depending on the methodology, we also assessed the effect of each antibiotic on the improvement of the clinical parameters (PD, CAL, BOP and PLAQUE). **Fig. IV-3B** indicates that all antibiotics reduced all clinical parameters after 2 months of treatment. However, we detected differences in clinical parameters values before and after the treatment depending on the antibiotic used (**Fig. IV-S6B**). For instance, amoxicillin, metronidazole, and azithromycin resulted in a significant decrease in PD (p -value < 0.005), which is a fundamental feature of periodontal disease. Similarly, these antibiotics also resulted in significantly decreased CAL and BOP. On the contrary, only amoxicillin and azithromycin showed a statistically significant decrease in the presence of dental plaque after treatment. Interestingly, no statistically significant decrease was observed in any of the evaluated clinical parameters when the patients were treated with the amoxicillin and metronidazole combination, which is among the most common antimicrobial therapies used to treat periodontitis.

Changes in microbial composition depending on antibiotic selection methodology and antibiotic treatment

In order to evaluate the effect of antibiotic treatment and the differences in the antibiotic selection methodology on the subgingival plaque microbiota composition, we sequenced the V3-V5 region of the 16S rRNA gene. On average, 112,000 reads/sample were sequenced, from which 47,600 reads/sample were annotated at the species level. Using the minimum number of reads annotated to the species level in a sample (22,900 reads), rarefaction analyses were performed, and the curves flattened after 20,000 sequences, showing that bacterial diversity was fully covered.

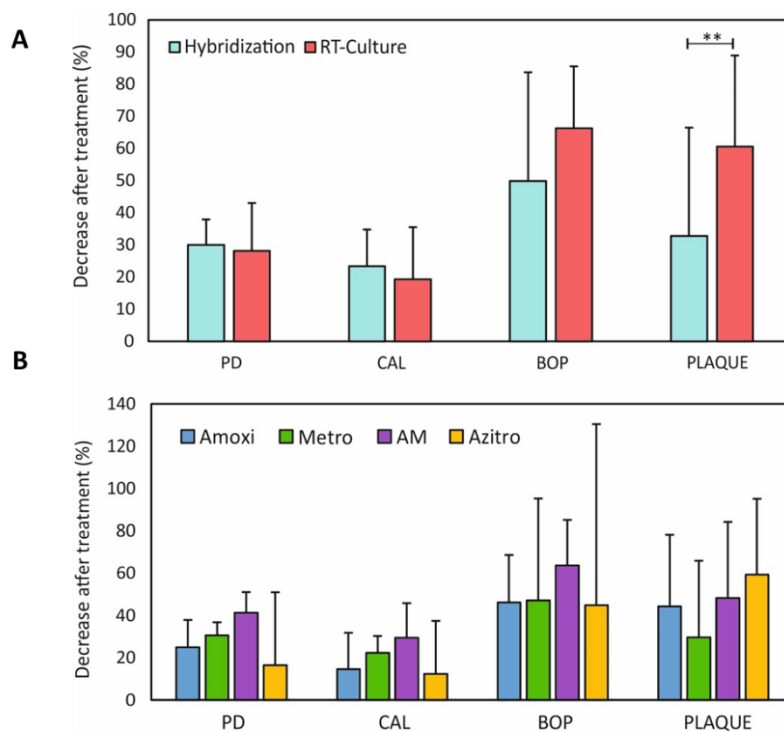


Figure IV-3. A - Improvement of clinical parameters 2 months after periodontal treatment with antimicrobial therapy suggested by standard hybridization methodology and RT- culture. **B**- Comparison of clinical parameters improvement 2 months after periodontal treatment among the different systemic antibiotics. Data are represented as a percentage of decrease (improvement) in different clinical parameters. **PD** - pocket depth; **CAL**- clinical attachment loss; **BOP** - bleeding on probing; **PLAQUE** – plaque presence; **Amoxi** - amoxicillin; **Metro** - metronidazole; **AM** - amoxicillin and metronidazole; **Azitro** – azithromycin. ** p -value < 0.01

Chao1 richness index analysis showed that there were no significant differences in the estimated number of bacterial species between both groups before treatment (BT_hybridization vs. BT_RT-Culture) nor after treatment (AT-hybridization vs. AT-RT-Culture). On the other hand, a statistically significant reduction in the number of bacterial species after treatment was observed in the group treated with the antibiotic selected by the impedance system (**Fig. IV-4A**). The CCA plot indicated similarities between the samples before treatment and showed that there were significant differences in the bacterial composition between both groups after antimicrobial therapy (ADONIS p -value=0.001) (**Fig. IV-4B**). In addition, the relative abundance of red complex pathogens (*P. gingivalis*, *T. forsythia* and *T. denticola*) after treatment was decreased significantly in both treatment groups (adjusted p -value<0.001) (**Fig. IV-S7A**). Interestingly, when this decrease was compared between both antibiotic selection methodologies, *P. gingivalis* had a significantly higher decrease in the group where the antibiotic treatment was prescribed

based on the RT-Culture method compared to hybridization (**Fig. IV-4C**) (p -value<0.05). Moreover, 16S rRNA gene sequencing data indicated that periodontal pathogens such as *F. nucleatum*, *Fretibacterium feline*, *Filifactor alocis* and other disease-associated bacteria decreased after the antibiotic treatment independently on the method used (**Figs. IV-4D, IV-S7B and IV-S8A, Tables IV-S2 and IV-S3**). In addition, health-associated bacteria, including *Veillonela*, *Neisseria*, *Rothia*, *Streptococcus* and other genera increased after treatment in both groups (adjusted p -value<0.001) (**Figs. IV-4D, IV-S7B, IV-S8A, Tables IV-S2 and S3**).

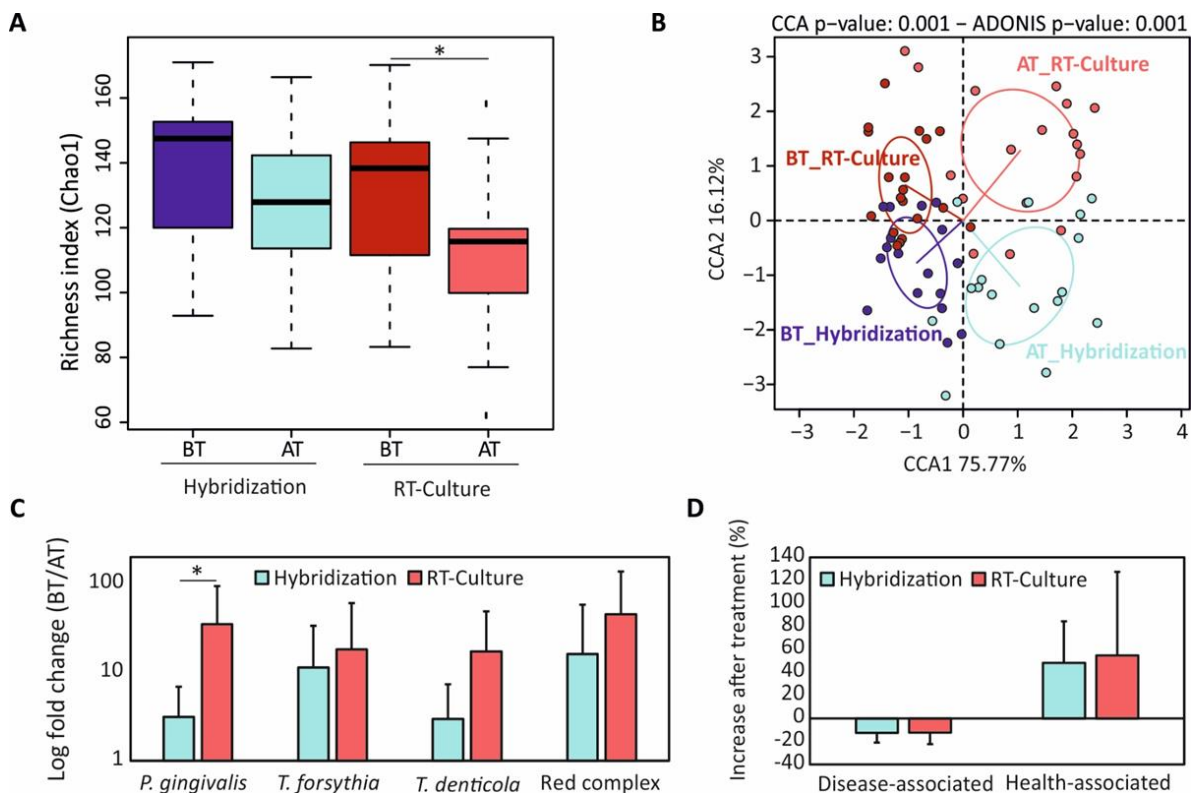


Figure IV-4. Comparison of microbial composition under different antibiotic selection methodologies. **A** - Alpha-diversity analysis (bacterial richness Chao1 index) comparison between the two antibiotic selection methods before and two months after treatment. **B** - Canonical correspondence analyses showing the differences in microbial composition among groups and timepoints. **C** - Changes in relative abundance of “red complex” periodontal pathogens and their members after treatment (expressed as fold change: before treatment/after treatment) for the two antibiotic selection methods. **D**- Percentage of increase or decrease in periodontal disease-associated and health-associated bacteria two months after periodontal treatment. **BT** - before treatment; **AT** - after treatment; **Amoxi** - amoxicillin; **Metro** - metronidazole; **AM** - amoxicillin and metronidazole; **Azitro** - azithromycin. * p -value < 0.05.

Further, we compared whether bacterial richness and composition depended on the antibiotic used. The Chao1 index showed a notable decrease in bacterial richness after treatment with all antibiotics or their combination. However, this decrease was not statistically significant, except in the case of azithromycin ($p\text{-value} < 0.001$) (**Fig. IV-5A**). In addition, when we compared the Chao1 index after the treatment among the different antibiotics, a significant decrease in bacterial richness was found in the group treated with azithromycin when compared to amoxicillin. (**Fig IV-5A**). Bacterial composition was also significantly affected by antibiotic treatment (**Fig IV-5B**). All tested antibiotics except the amoxicillin metronidazole combination significantly reduced the abundance of red complex members (adjusted $p\text{-value} < 0.05$) (**Fig. IV-S9A**). Interestingly, when the reduction of these bacteria was compared between antibiotics, important differences were found. For instance, the combination of amoxicillin and metronidazole decreased *P. gingivalis* levels significantly more than when these two antibiotics were used separately (**Fig. IV-5C**). In addition, *T. forsythia* was significantly more decreased after azithromycin treatment compared to amoxicillin. Similarly, *T. denticola* was significantly more reduced when azithromycin was used in comparison to metronidazole or to the amoxicillin – metronidazole combination (**Fig. IV-5C**). Finally, when these three bacteria were combined into the so-called “red complex”, azithromycin significantly enhanced its reduction in comparison to amoxicillin or metronidazole (adjusted $p\text{-value} < 0.005$) (**Fig. IV-5C**). In addition, it is important to mention that none of the antibiotics used in the study were able to completely eradicate *Fusobacterium* and *Leptotrichia* species, suggesting the need to test other antibiotics or their combinations (**Fig. IV-S8B, Tables IV-S4-7**). On the other hand, both the amoxicillin – metronidazole combination and azithromycin were very efficient not only against red complex pathogens but also against other pathogenic bacteria such as *Fillifactor* or *Alloprevotella* spp (**Fig. IV-S8B, Tables IV-S4-7**). In contrast to periodontal disease-related pathogens, health-associated bacteria were observed to increase after treatment with all tested antibiotics (**Fig IV-5D, Fig. IV-S8B, Fig. IV-S9B**).

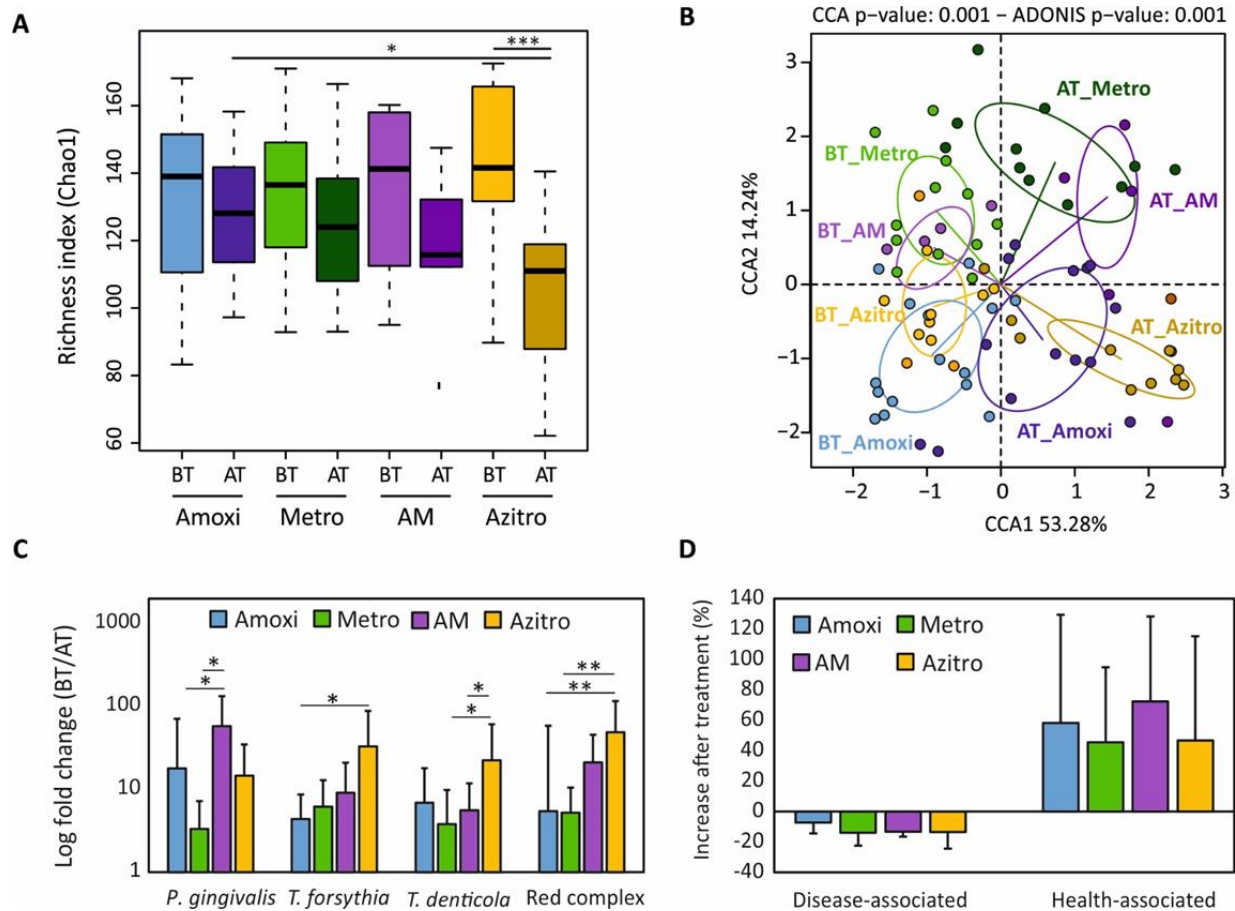


Figure IV-5. Effect of different systemic antibiotic treatments on microbial composition *in vivo*. **A** - Alpha-diversity (bacterial richness Chao1 index) analysis for different antibiotic treatment groups. **B** - Canonical Correspondence Analysis (CCA) of microbial community composition of different treatment groups. **C** - Changes in abundance of periodontal “red complex” cluster and their members after periodontal treatment and systemic antibiotic use (expressed as fold change: before treatment/after treatment). **D**- Percentage of increase in disease-associated and health-associated bacteria two months after periodontal treatment for each antibiotic treatment group. **BT** -before treatment; **AT** - two months after treatment; **Amoxi** - amoxicillin; **Metro** - metronidazole; **AM** - amoxicillin and metronidazole; **Azitro** - azithromycin. **p*-value<0.05; ** adjusted *p*-value<0.001.

Clinical and microbiological outcomes one and two months after antibiotic treatment

Given that the effect of periodontal therapy is usually transient and periodontal pathogens and inflammation tend to return over time, we also evaluated the effect of antibiotic therapy prescribed by both RT-Culture and hybridization methodologies one and two months after treatment (AT1M and AT2M, respectively). Clinical evaluation showed that all clinical

parameters significantly improved after one month of treatment (BT vs AT1M) in both methodologies (**Fig. IV-S10**). No significant differences were observed when these parameters were compared between both methodologies. However, PD and CAL were reduced by up to 30% in both groups, while the improvement observed in BOP and plaque parameters was higher in the group treated with antibiotics selected with the RT-Culture system, reaching up to almost 80% reduction (**Fig. IV-S10**). Further, the results showed that there were no statistically significant differences between the bacterial diversity before and after treatment with antibiotics prescribed by the standard hybridization method at both time points (**Fig. IV-6A**). On the contrary, sequencing data in the RT-Culture group showed that bacterial diversity was significantly lower (an indication of improvement in bacterial dysbiosis) already at one month of treatment. In addition, even though bacterial diversity slightly increased after two months, the diversity values remained significantly lower compared to the baseline. The CCA plot in **figure IV-6B** shows the clustering of samples before and 1 and 2 months after treatment and suggests that microbial composition varied to a greater extent after one month of antibiotic therapy and returned closer to the initial state after 2 months of treatment in both groups. In addition, red complex pathogens also decreased in both treatment groups one month after treatment (**Fig. IV-6C**). Interestingly, a significant reduction in *P. gingivalis* was found only in the RT-Culture group after two months of treatment (p -value=0.02) (**Fig. IV-4C**). In general, most periodontal pathogens such as *Fusobacterium*, *Porphyromonas* and others were less abundant after one month of treatment when compared to two months (**Fig. IV-S11**). However, when the decrease of disease-associated microbes was compared between RT-Culture and hybridization groups after one month of treatment, a significantly higher reduction was found in the RT-Culture group (p -value=0.02) (**Fig. IV-6D**). In addition, health-associated bacteria increased after one month of treatment in both treatment groups (**Fig. IV-6D** and **Fig. IV-S12**). Nevertheless, the abundance of health-associated bacteria was significantly higher one month after antibiotic treatment only in the group treated with the RT-Culture methodology (**Fig. IV-S12**).

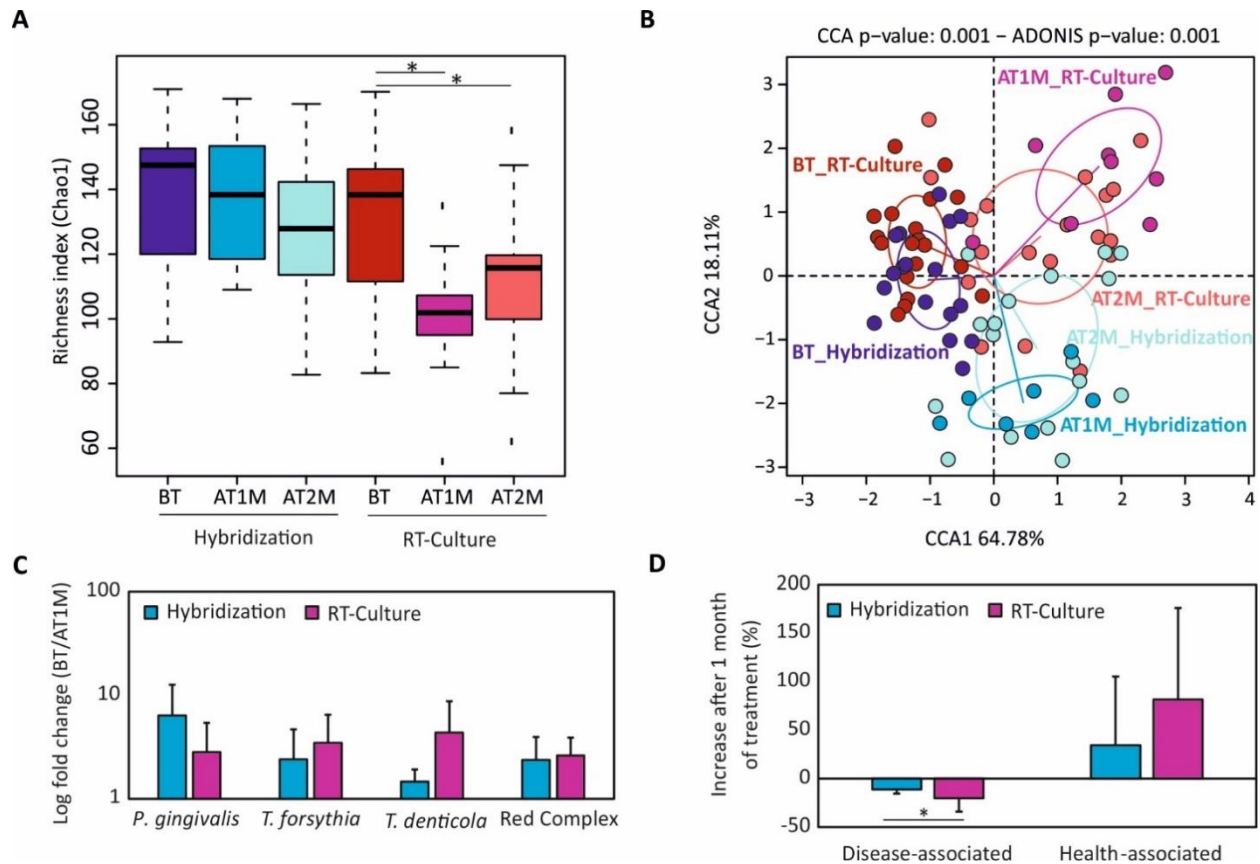


Figure IV-6. Microbial composition of subgingival plaque samples before and one (AT1) or two months (AT2) after antibiotic treatment. **A** - Alpha-diversity analysis (bacterial richness Chao1 index) one and two months after antibiotic treatment depending on the antibiotic selection method. **B** - Canonical correspondence analyses showing the differences in microbial composition among treatment groups and timepoints. **C** - Changes in abundance of the periodontal “red complex” cluster and their members one month after treatment (expressed as log fold change: before treatment/after treatment). **D** - Percentage of disease-associated and health-associated bacteria increase or decrease one month after periodontal treatment, for both antibiotic selection methodologies. **BT** - Before treatment; **AT** - After treatment. **p*-value < 0.05.

DISCUSSION

Periodontitis is an inflammatory disease that occurs due to prolonged inflammation of the gingiva, accumulation of opportunistic pathogens within subgingival dental plaque, their interaction with the host and the dysbiosis of microbiota embedded in dental biofilms^{132,151,397}. It has been established that conventional treatment, such as radicular scraping, alone or in combination with antimicrobial therapy, usually reduces bacterial counts without entirely

eliminating the pathogenic community, and many disease-associated species return with time. The guidelines for antibiotic use as part of periodontal therapy vary among countries, and previous studies have reported that conventional antibiotics have different effects on periodontitis progression^{142,147,177}, emphasizing the need to choose an individualized therapy with the most appropriate antibiotic for each patient, which could result in better clinical outcomes. When used, the choice of an antibiotic is normally made empirically, but several molecular techniques exist to select a personalized antibiotic therapy for periodontal patients. These techniques are based on DNA extraction from subgingival samples followed by quantification of periodontal bacteria by either qPCR or DNA hybridization with species-specific probes^{398,399}. Based on the levels of periodontal pathogens, an antibiotic treatment protocol has been proposed³⁸⁴. However, these techniques have several limitations, such as the heterogeneity in antibiotic susceptibility among strains from the same species⁴⁰⁰, and they do not consider the potential effect of the EPS matrix on antibiotic resistance^{147,150}, or the complex interactions between different bacterial species within biofilms, which could derive in an antibiotic susceptibility pattern which is difficult to predict from bacterial composition^{199,373}. An alternative to molecular methods is the culture of periodontal samples in agar plates in the presence of different antibiotics, in order to establish the overall antibiotic susceptibility of the bacterial community⁴⁰¹ but there are currently no standardized protocols to culture periodontal samples in biofilms and its efficacy compared to qPCR or molecular probes methodologies needs to be evaluated.

In the current manuscript, we have developed a fast method for culturing fresh periodontal samples with minimal sample processing that allows biofilm growth quantification in real time through impedance measurements. Given that the periodontal disease-associated biofilm is composed of several hundred species and that bacterial composition highly varies among individuals¹⁷⁸, we have tested three different transport media to select the best conditions for periodontal biofilm transportation. The evaluation of RTF, VMG III and VMG III with agar and agarose transport media for these samples showed that VMGIII without additional agar or agarose preserved initial bacterial composition and viability to form biofilms for up to 48h. This suggests that periodontal pocket samples could be collected, transferred from the dental clinics and stored in this media at room temperature until further laboratory analysis. In addition,

periodontal biofilms grown *in vitro* in the xCELLigence impedance system and collected at 8h showed representative bacterial composition similar to the initial inoculum. It should be noted that under these conditions, *Streptococcus* showed an overgrowth compared to the initial inoculum, possibly due to the sugar concentration of the medium used, suggesting that BHI without sugar, artificial saliva or another medium⁴⁰² should be used as an alternative for unbiased periodontal biofilm cultivation in future studies.

Once the protocol for culturing periodontal samples was optimized, we performed a clinical trial to evaluate the use of this biofilm *ex vivo* monitoring system for the selection of individualized antibiotic therapy when compared to standard antibiotic selection methodology using hybridization probes. Our impedance-based measurements showed a remarkable variability in antibiotic susceptibility patterns for different patients with periodontal disease, and the antibiotic with best efficacy in reducing biofilm growth could not be predicted from the corresponding bacterial composition. Interestingly, the results in the current manuscript also highlight that amoxicillin and metronidazole combination often resulted in biofilm growth induction (**Fig IV-6B**) when compared to monotherapy in agreement with recent studies showing that antibiotic combinations often result in reduced antimicrobial efficacy⁴⁰³. It must be underlined that antibiotic selection by the culturing method agreed with the hybridization method in less than 20% of the cases, indicating that it is very difficult to predict how a whole subgingival biofilm is going to react to a given antibiotic based on the levels of some bacterial species in the sample. In addition, impedance measures were capable of identifying two (2/64) patients for which the periodontal biofilms did not respond to any tested treatment, as all evaluated antibiotics induced biofilm growth, suggesting that other antibiotics or their combinations should be tested.

Half of the patients were prescribed the antibiotic selected by one of the two methods, and we compared the clinical and microbiological outcomes after one and two months in both study groups. The results showed that clinical parameters such as PD, CAL and BOP were improved in both groups after treatment independently of the antibiotic selection method and/or the antibiotic used, and the improvement in BOP was larger in the RT-Culture group (**Figs. IV-3A and IV-S6A**). However, a significant plaque reduction was only observed in the group treated with antibiotics selected by the impedance system (**Figs. IV-3A and IV-S6A**).

Considering that the amount of plaque is an important factor for the development of the disease, the higher decrease in plaque accumulation in these individuals could represent a significant benefit for periodontal health. Interestingly, the improvement in clinical parameters did not vary between antibiotics (**Fig. IV-3B**), indicating that there was no antibiotic with overall superior performance. This suggests that antibiotic selection should be personalized for optimal effect.

Regarding microbiological parameters, 16S rRNA gene sequencing data showed that bacterial richness was significantly decreased only after the use of antibiotics selected by the real-time Culture system. This is a relevant feature as periodontitis is associated to higher numbers of bacterial species compared to the healthy condition^{142,175}, probably derived from impairment of the immune system and from increased nutrient availability⁴⁰⁴. The results of our study also indicated that periodontal therapies applied to the tested population decreased periodontal pathogenic taxa such as *Tannerella*, *Treponema*, *Fusobacterium*, or *Filifactor* in both tested groups although the improvement was larger in the RT-Culture methodology (**Figs. IV-4C and IV-S8A**). *P. gingivalis*, which is considered a keystone periodontal pathogen, was significantly reduced in the group treated with antibiotics suggested by RT-Culture compared with the standard method (**Fig. IV-4C**). In addition, an increase in health-associated taxa, including *Rothia*, *Neisseria*, *Veillonella* and others, was observed in both treatment groups. but was only significant at one month in the RT-culture group (**Fig. IV-S12, Tables IV-S2-9**). Additionally, a significant reduction in disease-associated bacteria was observed only in RT-Culture group after one month of treatment (**Fig. IV-6D**).

In addition, our results also indicate that antibiotics' adjunctive influence on the subgingival microbiota depends on the antibiotic (**Figs. IV-5 and IV-S9**). For instance, although all antibiotics inhibited red-complex pathogens the highest inhibition was observed by azithromycin ($p\text{-value} < 0.01$). Moreover, azithromycin was the only antibiotic which significantly decreased bacterial richness after treatment (**Fig IV-5A**). Similar findings were also described by other authors who suggested that the use of azithromycin as adjunctive therapy together with radicular scrapping results in improved microbiological outcomes⁴⁰⁵⁻⁴⁰⁷. Furthermore, the comparison of clinical parameters and microbiological data indicates that most of the patients showed better outcomes one month after antibiotic therapy compared to two months (**Figs. IV-6, IV-S10-S12**). This can be related to the ability of periodontal pathogens to

persist inside periodontal pockets and regrow, causing inflammation once the treatment is ceased. Similar findings were observed in another study, which investigated the effect of mechanical treatment of subgingival plaque at several timepoints¹⁴⁶. Another study by Bizzaro et al., also found that an antibiotic effect was seen on periodontal microbiota three, but not six months after treatment, suggesting that it is extremely difficult to eradicate periodontal pathogens from deep periodontal pockets¹⁷⁷.

Although many studies have been performed to investigate the critical factors in the occurrence and development of periodontitis and its treatment, to our knowledge, this is the first study which compares personalized antibiotic selection methods evaluating both clinical and microbiological outcomes. Multiple studies have shown that antibiotic use can improve the outcome of periodontal treatment^{148,373}. However, the clinical conditions under which antibiotics should be prescribed in periodontal patients are controversial and vary among countries^{148,399} and are beyond the scope of the current manuscript. In the cases where antibiotics are used, our data indicate that the use of impedance-based measurements of periodontal biofilms is a reliable antibiotic selection tool. The *in vivo* results indicate that patients treated with an antibiotic selected by this culture method showed equivalent and in many cases better clinical and microbiological outcomes when compared to a standard antibiotic selection methodology performed by hybridization technology. In addition, we show that this methodology is more selective, faster (allows the identification of best individual treatment in less than 4h) and cheaper when compared to standard antibiotic selection tools. Thus, we conclude that the Real-Time evaluation of periodontal biofilm growth could improve antibiotic treatment within a personalized dentistry framework. Moreover, the ability of impedance measurements to identify the antibiotics that result in biofilm growth induction might help to assess possible clinical outcomes, or even the relationship between infection, inflammation, and shift of oral microbiota causing the disease, as ineffective treatment results in the regrow of periodontal pathogens leading to the aggravation of the disease. We believe that the use of personalized antibiotic selection in dentistry could not only contribute to a more rationale use of antimicrobials and reduce overall costs of healthcare but might also increase patients' willingness to treatment and favor the establishment of health-associated microorganisms in subgingival dental plaque^{142,153}.

CHAPTER IV SUPPLEMENTARY INFORMATION

Supplementary table IV-1. Health-associated and disease-associated bacterial species in periodontitis. Red-complex-associated periodontal pathogens are marked by asterisks.

Health-associated species	Disease-associated species
<i>Actinomyces naeslundii</i>	<i>Fusobacterium nucleatum</i>
<i>Actinomyces odontolyticus</i>	<i>Porphyromonas gingivalis</i> *
<i>Actinomyces oris</i>	<i>Tannerella forsythia</i> *
<i>Corynebacterium durum</i>	<i>Filifactor alocis</i>
<i>Corynebacterium matruchotii</i>	<i>Porphyromonas endodontalis</i>
<i>Rothia dentocariosa</i>	<i>Parvimonas micra</i>
<i>Rothia mucilaginosa</i>	TM7x NA
<i>Capnocytophaga sputigena</i>	<i>Selenomonas</i> NA
<i>Selenomonas noxia</i>	<i>Campylobacter gracilis</i>
<i>Veillonella atypica</i>	<i>Selenomonas sputigena</i>
<i>Veillonella dispar</i>	<i>Desulfobulbus</i> NA
<i>Veillonella parvula</i>	<i>Treponema denticola</i> *
<i>Eikenella corrodens</i>	<i>Fretibacterium fastidiosum</i>
<i>Neisseria mucosa</i>	<i>Alloprevotella tannerae</i>
<i>Neisseria subflava</i>	[<i>Eubacterium</i>] <i>brachy</i> group <i>brachy</i>
<i>Aggregatibacter segnis</i>	<i>Treponema medium</i>
<i>Haemophilus parainfluenzae</i>	[<i>Eubacterium</i>] <i>nodatum</i> group NA
	<i>Selenomonas artemidis</i>
	<i>Prevotella nigrescens</i>
	<i>Treponema vincentii</i>
	<i>Fusobacterium periodonticum</i>
	<i>Peptostreptococcus stomatis</i>
	<i>Prevotella intermedia</i>
	<i>Mogibacterium timidum</i>
	<i>Aggregatibacter actinomycetemcomitans</i>
	<i>Anaeroglobus geminatus</i>
	<i>Campylobacter showae</i>
	<i>Dialister pneumosintes</i>
	[<i>Eubacterium</i>] <i>saphenum</i> group <i>saphenum</i>
	<i>Prevotella denticola</i>
	<i>Treponema lecithinolyticum</i>

Supplementary table IV-2. List of species differentially abundant after 2 months of antibiotic treatment (AT2M) when hybridization method was used as the antibiotic selection treatment. **BT** - before treatment.

Feature	ANCOMBC.pval	ANCOMBC.adj.pval.fdr	BT	AT2M	log2FC
<i>Treponema NA</i>	8.07E-12	1.20E-10	5.71	1.60	1.84
<i>Porphyromonas gingivalis</i>	8.72E-09	7.48E-08	5.44	1.76	1.63
<i>Streptococcus NA</i>	2.04E-15	5.78E-14	4.09	10.01	-1.29
<i>Porphyromonas endodontalis</i>	7.93E-08	6.07E-07	3.84	2.63	0.55
<i>Tannerella forsythia</i>	8.57E-18	3.46E-16	3.52	0.86	2.04
<i>Filifactor alocis</i>	9.78E-14	1.98E-12	3.50	0.81	2.10
<i>Parvimonas micra</i>	1.34E-03	4.84E-03	1.99	0.81	1.30
<i>Prevotella NA</i>	1.88E-04	8.88E-04	1.95	1.45	0.43
<i>F0058 NA</i>	7.84E-14	1.71E-12	1.94	0.76	1.36
<i>Treponema denticola</i>	1.79E-09	1.75E-08	1.86	1.06	0.81
<i>Prevotella intermedia</i>	1.19E-08	9.92E-08	1.73	0.90	0.95
<i>Desulfobulbus NA</i>	9.68E-26	1.37E-23	1.71	0.16	3.46
<i>Leptotrichia NA</i>	1.48E-02	3.81E-02	1.69	2.21	-0.39
<i>Alloprevotella tannerae</i>	4.56E-03	1.42E-02	1.62	2.38	-0.56
<i>Fretibacterium NA</i>	1.43E-13	2.70E-12	1.53	0.51	1.59
<i>Fretibacterium feline</i>	3.72E-33	1.05E-30	1.21	0.13	3.25
<i>Selenomonas sputigena</i>	1.16E-03	4.37E-03	1.20	1.04	0.21
<i>Veillonella NA</i>	2.32E-09	2.19E-08	1.10	3.37	-1.62
<i>Porphyromonas NA</i>	7.17E-03	2.05E-02	1.05	0.19	2.48
<i>W5053 NA</i>	3.43E-06	2.11E-05	0.92	0.11	3.00
<i>Anaerovoracaceae NA</i>	1.81E-25	1.71E-23	0.87	0.14	2.63
<i>[Eubacterium] brachy group brachy</i>	3.79E-06	2.28E-05	0.87	0.12	2.91
<i>Fretibacterium fastidiosum</i>	3.08E-15	7.93E-14	0.86	0.29	1.58
<i>Prevotella pleuritidis</i>	7.25E-09	6.41E-08	0.86	0.22	1.98
<i>Lentimicrobium NA</i>	1.03E-06	6.76E-06	0.69	0.66	0.07
<i>Treponema socranskii</i>	3.72E-03	1.18E-02	0.68	0.54	0.33
<i>Saccharimonadales NA</i>	1.74E-05	9.84E-05	0.68	0.21	1.67
<i>[Eubacterium] saphenum group saphenum</i>	1.46E-11	1.96E-10	0.64	0.05	3.64
<i>Prevotella oris</i>	2.88E-05	1.51E-04	0.63	2.54	-2.02
<i>Campylobacter gracilis</i>	2.14E-05	1.16E-04	0.62	1.26	-1.02
<i>Treponema maltophilum</i>	7.12E-05	3.54E-04	0.54	0.26	1.08
<i>[Eubacterium] nodatum group NA</i>	4.96E-10	5.20E-09	0.54	0.16	1.73
<i>Defluviitaleaceae UCG-011 NA</i>	8.22E-11	9.69E-10	0.43	0.11	2.00
<i>Rikenellaceae RC9 gut group NA</i>	1.22E-07	9.12E-07	0.39	0.41	-0.07
<i>Leptotrichia wadei</i>	3.58E-03	1.15E-02	0.38	1.12	-1.55
<i>Actinomyces NA</i>	1.21E-06	7.79E-06	0.38	1.55	-2.02
<i>Johnsonella NA</i>	8.33E-04	3.47E-03	0.37	0.20	0.93

<i>Prevotella nigrescens</i>	2.16E-03	7.36E-03	0.34	1.39	-2.01
<i>Capnocytophaga NA</i>	1.05E-03	4.12E-03	0.34	0.92	-1.42
<i>Oceanivirga NA</i>	4.81E-04	2.13E-03	0.33	0.00	12.24
<i>Flexilinea NA</i>	5.97E-22	3.38E-20	0.32	0.06	2.47
<i>Leptotrichia buccalis</i>	5.94E-10	6.01E-09	0.29	0.08	1.77
<i>Leptotrichia hofstadii</i>	3.75E-05	1.89E-04	0.28	0.05	2.51
<i>Mycoplasma NA</i>	4.67E-14	1.10E-12	0.24	0.05	2.16
<i>Peptostreptococcus stomatis</i>	3.11E-04	1.40E-03	0.23	0.20	0.16
<i>Phocaeicola abscessus</i>	3.80E-09	3.47E-08	0.23	0.08	1.52
<i>Moryella NA</i>	3.06E-13	5.41E-12	0.23	0.01	4.20
<i>Haemophilus NA</i>	2.14E-05	1.16E-04	0.22	1.18	-2.41
<i>Capnocytophaga leadbetteri</i>	2.39E-02	5.59E-02	0.22	0.69	-1.66
<i>Capnocytophaga ochracea</i>	2.29E-02	5.44E-02	0.21	0.57	-1.44
<i>Prevotella fusca</i>	1.19E-02	3.16E-02	0.21	0.03	2.67
<i>Parvimonas NA</i>	8.48E-06	4.90E-05	0.19	0.04	2.18
<i>Prevotella dentalis</i>	5.46E-16	1.93E-14	0.19	0.04	2.34
<i>Granulicatella NA</i>	4.95E-07	3.42E-06	0.19	0.66	-1.81
<i>Butyrivibrio NA</i>	2.08E-03	7.19E-03	0.18	0.16	0.22
<i>Solobacterium moorei</i>	2.47E-02	5.68E-02	0.18	0.20	-0.15
<i>Peptoanaerobacter stomatis</i>	9.93E-04	3.96E-03	0.16	0.10	0.76
Family XIII UCG-001 NA	2.30E-18	1.09E-16	0.15	0.05	1.67
<i>Acholeplasma NA</i>	2.09E-04	9.69E-04	0.13	0.01	3.95
<i>Bulleidia extracta</i>	3.03E-03	9.86E-03	0.13	0.03	2.03
<i>Catonella NA</i>	2.72E-05	1.45E-04	0.13	0.02	2.92
<i>Prevotella melaninogenica</i>	7.68E-03	2.15E-02	0.12	0.33	-1.41
<i>Prevotella conceptionensis</i>	1.79E-02	4.37E-02	0.11	0.20	-0.83
<i>Absconditabacteriales (SRI) NA</i>	1.06E-04	5.16E-04	0.11	0.04	1.44
<i>Rothia dentocariosa</i>	1.94E-07	1.41E-06	0.11	1.10	-3.30
<i>Leptotrichia hongkongensis</i>	3.92E-11	5.05E-10	0.09	0.90	-3.31
<i>Lautropia mirabilis</i>	8.55E-23	6.05E-21	0.08	0.70	-3.10
<i>Capnocytophaga gingivalis</i>	2.33E-08	1.83E-07	0.08	0.57	-2.83
<i>Clostridia vadinBB60 group NA</i>	2.31E-08	1.83E-07	0.08	0.09	-0.18
<i>Prevotella oulorum</i>	5.80E-11	7.14E-10	0.07	0.43	-2.57
<i>Prevotella loescheii</i>	1.21E-03	4.49E-03	0.07	0.43	-2.60
<i>Prevotella maculosa</i>	1.68E-02	4.22E-02	0.07	0.20	-1.53
<i>Eikenella corrodens</i>	3.01E-05	1.55E-04	0.07	0.23	-1.80
<i>Stomatobaculum longum</i>	2.09E-02	5.04E-02	0.06	0.18	-1.56
<i>Olsenella NA</i>	6.34E-03	1.89E-02	0.06	0.03	1.19
<i>Pseudoramibacter alactolyticus</i>	1.84E-10	2.08E-09	0.06	0.01	2.63
<i>Cardiobacterium hominis</i>	1.26E-02	3.30E-02	0.06	0.54	-3.26
<i>Capnocytophaga sputigena</i>	5.23E-06	3.08E-05	0.06	0.59	-3.41
Family XI NA	6.90E-03	2.01E-02	0.05	0.00	9.60
<i>Erysipelotrichaceae UCG-006 NA</i>	2.83E-07	2.00E-06	0.05	0.01	1.67

<i>Bacteroides heparinolyticus</i>	9.88E-03	2.69E-02	0.05	0.01	1.70
<i>Shuttleworthia satelles</i>	1.71E-02	4.26E-02	0.04	0.03	0.47
<i>Prevotella saccharolytica</i>	1.11E-03	4.32E-03	0.04	0.15	-1.80
<i>Prevotella salivae</i>	1.35E-03	4.84E-03	0.04	0.20	-2.24
<i>Mogibacterium timidum</i>	1.10E-11	1.56E-10	0.04	0.01	2.66
<i>Treponema parvum</i>	7.03E-04	2.97E-03	0.04	0.02	0.96
<i>Gemella sanguinis</i>	1.79E-02	4.37E-02	0.04	0.08	-1.02
<i>Prevotella enoeca</i>	1.63E-02	4.13E-02	0.04	0.02	0.71
<i>Desulfovibrio NA</i>	1.04E-02	2.81E-02	0.04	0.01	2.56
<i>Kingella oralis</i>	1.53E-15	4.82E-14	0.04	1.15	-5.00
<i>Haemophilus parainfluenzae</i>	8.74E-04	3.59E-03	0.03	0.25	-2.92
<i>Rothia NA</i>	3.65E-10	3.97E-09	0.03	0.23	-2.92
<i>Bergeyella NA</i>	1.86E-12	3.10E-11	0.03	0.18	-2.60
<i>Comamonas NA</i>	1.39E-02	3.62E-02	0.03	0.00	4.40
<i>Eggerthia catenaformis</i>	5.23E-04	2.28E-03	0.03	0.00	2.52
<i>Olsenella uli</i>	1.14E-03	4.36E-03	0.03	0.01	2.23
<i>Actinomyces cardiffensis</i>	9.48E-03	2.60E-02	0.03	0.00	8.67
<i>Izemoplasmatales NA</i>	5.34E-04	2.29E-03	0.03	0.02	0.56
<i>Pyramidobacter piscolens</i>	1.73E-03	6.05E-03	0.02	0.00	3.90
<i>Actinomyces naeslundii</i>	7.78E-12	1.20E-10	0.02	0.31	-3.76
<i>Atopobium parvulum</i>	1.62E-02	4.12E-02	0.02	0.19	-3.17
<i>Campylobacter showae</i>	6.69E-03	1.97E-02	0.02	0.09	-2.14
<i>Actinomyces israelii</i>	7.15E-03	2.05E-02	0.02	0.00	8.01
<i>Brachymonas NA</i>	2.19E-03	7.36E-03	0.02	0.00	2.15
<i>DNF00809 NA</i>	1.74E-04	8.34E-04	0.01	0.00	7.76
<i>Abiotrophia defectiva</i>	1.61E-03	5.69E-03	0.01	0.07	-2.36
<i>Prevotellaceae UCG-004 NA</i>	5.26E-03	1.60E-02	0.01	0.00	1.45
<i>Propionivibrio NA</i>	2.79E-06	1.75E-05	0.01	0.00	1.95
<i>Rhodospirillales NA</i>	7.50E-03	2.12E-02	0.01	0.00	4.55
<i>Actinomyces oricola</i>	5.37E-03	1.62E-02	0.00	0.00	3.94
<i>Granulicatella elegans</i>	5.03E-03	1.55E-02	0.00	0.03	-2.81
<i>Corynebacterium NA</i>	2.18E-02	5.22E-02	0.00	0.01	-0.60
<i>[Eubacterium] brachy group NA</i>	2.65E-03	8.82E-03	0.00	0.00	2.87
<i>Pseudopropionibacterium propionicum</i>	9.50E-07	6.40E-06	0.00	0.06	-4.45
<i>Porphyromonadaceae NA</i>	2.86E-03	9.42E-03	0.00	0.00	3.31
<i>Ammipila NA</i>	9.26E-03	2.57E-02	0.00	0.00	4.77
<i>Actinomyces odontolyticus</i>	2.40E-04	1.09E-03	0.00	0.02	-3.84
<i>[Eubacterium] coprostanoligenes group NA</i>	2.36E-02	5.56E-02	0.00	0.00	4.41
<i>Treponema pectinovorum</i>	4.45E-03	1.40E-02	0.00	0.01	-2.12
<i>Lactobacillales NA</i>	2.46E-02	5.68E-02	0.00	0.01	-3.82
<i>Actinomyces oris</i>	1.31E-03	4.81E-03	0.00	0.04	-9.30
<i>Streptococcus gordonii</i>	9.53E-04	3.85E-03	0.00	0.01	-7.63
<i>Prevotella oris</i>	1.20E-02	3.16E-02	0.00	0.00	-3.66

Supplementary table IV-3. List of bacterial species that were differentially abundant after 2 months of antibiotic treatment (AT2M) when RT-Culture were used as an antibiotic selection method. **BT** – before treatment.

Feature	ANCOMBC.pval	ANCOMBC.adj.pval.fdr	BT	AT2M	log2FC
<i>Porphyromonas gingivalis</i>	6.46E-15	1.49E-13	12.98	3.18	2.03
<i>Fusobacterium nucleatum</i>	5.61E-03	1.58E-02	11.93	9.92	0.27
<i>Treponema NA</i>	9.51E-17	2.93E-15	4.47	1.18	1.92
<i>Tannerella forsythia</i>	3.27E-11	4.76E-10	4.19	1.44	1.54
<i>Filifactor alocis</i>	8.09E-13	1.32E-11	4.09	1.12	1.87
<i>Streptococcus NA</i>	5.35E-09	5.70E-08	4.08	10.01	-1.29
<i>Porphyromonas endodontalis</i>	1.45E-05	8.05E-05	3.33	1.99	0.74
<i>Treponema denticola</i>	6.36E-10	8.80E-09	3.14	1.20	1.39
<i>Prevotella intermedia</i>	3.87E-05	1.88E-04	2.21	1.05	1.07
<i>Prevotella NA</i>	5.46E-05	2.48E-04	1.73	0.96	0.86
<i>Dialister invisus</i>	4.44E-04	1.64E-03	1.46	0.75	0.97
<i>F0058 NA</i>	7.67E-08	6.07E-07	1.43	0.59	1.28
<i>Fretibacterium NA</i>	1.21E-22	8.95E-21	1.42	0.19	2.90
<i>Campylobacter NA</i>	1.23E-02	3.09E-02	1.39	1.27	0.13
<i>Desulfobulbus NA</i>	1.93E-24	2.99E-22	1.36	0.25	2.45
<i>Fretibacterium feline</i>	1.57E-20	8.69E-19	1.22	0.37	1.73
<i>Saccharimonadaceae NA</i>	7.19E-08	5.86E-07	1.15	0.90	0.35
<i>W5053 NA</i>	3.18E-08	2.76E-07	1.13	0.36	1.63
<i>Alloprevotella tannerae</i>	6.08E-03	1.68E-02	0.96	1.17	-0.28
<i>Neisseria NA</i>	3.45E-04	1.33E-03	0.86	2.03	-1.23
<i>Fretibacterium fastidiosum</i>	3.82E-13	7.05E-12	0.79	0.28	1.49
<i>Lentimicrobium NA</i>	7.58E-13	1.31E-11	0.77	0.15	2.32
<i>Defluviitaleaceae UCG-011 NA</i>	1.97E-20	9.08E-19	0.77	0.12	2.64
<i>Treponema socranskii</i>	6.18E-08	5.19E-07	0.70	0.35	0.99
<i>Oceanivirga NA</i>	4.07E-04	1.52E-03	0.70	0.38	0.89
<i>Anaerovoracaceae NA</i>	1.08E-13	2.30E-12	0.69	0.16	2.06
<i>Veillonella NA</i>	4.28E-09	4.75E-08	0.67	2.89	-2.10
<i>Treponema maltophilum</i>	9.30E-09	9.20E-08	0.64	0.28	1.20
<i>Porphyromonas NA</i>	1.19E-05	7.01E-05	0.63	0.36	0.82
<i>Prevotella pleuritidis</i>	1.01E-04	4.31E-04	0.47	0.38	0.31
<i>Rikenellaceae RC9 gut group NA</i>	1.29E-22	8.95E-21	0.44	0.09	2.32
<i>Veillonella parvula</i>	7.22E-07	4.88E-06	0.43	1.88	-2.14
<i>[Eubacterium] nodatum group NA</i>	1.79E-07	1.34E-06	0.42	0.16	1.38
<i>Saccharimonadales NA</i>	9.27E-10	1.22E-08	0.42	0.15	1.49
<i>Capnocytophaga NA</i>	9.62E-05	4.16E-04	0.36	1.29	-1.84
<i>Flexilinea NA</i>	1.20E-19	4.73E-18	0.35	0.07	2.38
<i>Mycoplasma NA</i>	1.51E-15	4.19E-14	0.33	0.07	2.34
<i>[Eubacterium] brachy group brachy</i>	9.44E-03	2.51E-02	0.32	0.71	-1.14
<i>Actinomyces NA</i>	1.19E-04	4.91E-04	0.30	0.80	-1.43
<i>[Eubacterium] saphenum group saphenum</i>	1.33E-08	1.19E-07	0.27	0.09	1.53
<i>Porphyromonas pasteri</i>	1.05E-02	2.74E-02	0.25	0.58	-1.19
<i>Johnsonella NA</i>	1.29E-03	4.39E-03	0.24	0.18	0.44
<i>Peptococcus NA</i>	1.70E-15	4.29E-14	0.22	0.03	2.74
<i>Parvimonas NA</i>	4.22E-03	1.26E-02	0.22	0.04	2.51
<i>Anaeroglobus geminatus</i>	3.47E-07	2.53E-06	0.21	0.09	1.28
<i>Moryella NA</i>	1.71E-17	5.93E-16	0.21	0.05	2.00

<i>Leptotrichia buccalis</i>	1.18E-09	1.49E-08	0.20	0.13	0.63
<i>Granulicatella NA</i>	5.12E-07	3.64E-06	0.19	0.99	-2.38
<i>Prevotella dentalis</i>	3.97E-05	1.90E-04	0.18	0.07	1.36
<i>Haemophilus NA</i>	9.33E-06	5.62E-05	0.18	0.77	-2.11
<i>Peptostreptococcus stomatis</i>	4.64E-03	1.35E-02	0.17	0.14	0.26
<i>Catonella NA</i>	1.14E-03	3.94E-03	0.16	0.18	-0.11
<i>Phocaeicola abscessus</i>	3.16E-09	3.65E-08	0.16	0.02	2.65
<i>Prevotella conceptionensis</i>	1.39E-04	5.67E-04	0.15	0.02	2.59
<i>Butyrivibrio NA</i>	6.79E-07	4.70E-06	0.14	0.01	4.06
<i>Oribacterium NA</i>	2.86E-03	8.89E-03	0.14	0.55	-1.96
<i>Lachnospiraceae NA</i>	4.78E-03	1.37E-02	0.13	0.04	1.77
<i>Family XIII UCG-001 NA</i>	2.32E-13	4.58E-12	0.12	0.05	1.36
<i>Lautropia mirabilis</i>	2.16E-24	2.99E-22	0.10	0.99	-3.27
<i>Alloprevotella rava</i>	2.09E-04	8.25E-04	0.09	0.06	0.67
<i>Clostridia UCG-014 NA</i>	2.73E-03	8.59E-03	0.09	0.09	0.03
<i>Abiotrophia defectiva</i>	3.53E-03	1.06E-02	0.08	0.13	-0.67
<i>Candidatus Pacebacteria NA</i>	9.98E-03	2.63E-02	0.08	0.00	4.16
<i>Prevotella melaninogenica</i>	3.53E-04	1.34E-03	0.07	0.37	-2.30
<i>Acholeplasma NA</i>	1.06E-02	2.74E-02	0.07	0.05	0.48
<i>Clostridia vadinBB60 group NA</i>	8.88E-08	6.83E-07	0.07	0.02	1.98
<i>Campylobacter concisus</i>	2.30E-05	1.18E-04	0.06	0.13	-1.01
<i>Prevotella baroniae</i>	2.03E-04	8.15E-04	0.06	0.05	0.31
<i>Prevotella oulorum</i>	1.12E-02	2.86E-02	0.06	0.40	-2.75
<i>Kingella oralis</i>	2.50E-06	1.54E-05	0.06	0.35	-2.59
<i>Megasphaera micronuciformis</i>	2.73E-03	8.59E-03	0.06	0.21	-1.86
<i>Pseudoramibacter alactolyticus</i>	8.05E-05	3.60E-04	0.06	0.02	1.61
<i>Treponema medium</i>	1.10E-06	7.24E-06	0.06	0.00	9.86
<i>Prevotella micans</i>	5.96E-03	1.67E-02	0.05	0.20	-1.86
<i>Treponema parvum</i>	2.35E-05	1.18E-04	0.05	0.02	1.24
<i>Izemoplasmatales NA</i>	2.33E-05	1.18E-04	0.05	0.01	2.14
<i>Prevotella fusca</i>	1.15E-04	4.81E-04	0.05	0.00	4.56
<i>Wolinella succinogenes</i>	3.40E-03	1.04E-02	0.05	0.00	9.77
<i>Capnocytophaga sputigena</i>	8.27E-05	3.64E-04	0.05	0.19	-1.89
<i>Prevotella loescheii</i>	7.28E-09	7.47E-08	0.05	0.89	-4.12
<i>Prevotella veroralis</i>	2.92E-03	9.00E-03	0.05	0.21	-2.08
<i>Absconditabacteriales (SRI) NA</i>	2.28E-12	3.52E-11	0.05	0.02	1.67
<i>Capnocytophaga gingivalis</i>	9.89E-09	9.45E-08	0.04	0.31	-2.92
<i>Rothia NA</i>	4.95E-05	2.32E-04	0.04	0.27	-2.91
<i>Anaeroglobus NA</i>	6.72E-03	1.84E-02	0.03	0.01	2.07
<i>Mogibacterium timidum</i>	9.27E-04	3.29E-03	0.03	0.01	1.18
<i>Family XI NA</i>	2.45E-03	7.97E-03	0.03	0.01	2.52
<i>Bergeyella NA</i>	6.09E-04	2.19E-03	0.03	0.09	-1.65
<i>Rothia mucilaginosa</i>	3.76E-05	1.86E-04	0.03	0.34	-3.55
<i>Selenomonas artemidis</i>	1.73E-06	1.09E-05	0.03	0.32	-3.51
<i>Prevotella pallens</i>	1.95E-02	4.77E-02	0.02	0.09	-2.05
<i>Erysipelotrichaceae UCG-006 NA</i>	9.12E-03	2.45E-02	0.02	0.01	1.27
<i>Atopobium parvulum</i>	1.74E-05	9.29E-05	0.02	0.20	-3.26
<i>Pyramidobacter piscolens</i>	2.23E-09	2.68E-08	0.02	0.00	4.81
<i>Prevotella salivae</i>	1.28E-08	1.18E-07	0.02	0.12	-2.55
<i>Gracilibacteria JGI 0000069-P22 NA</i>	1.31E-03	4.43E-03	0.02	0.00	1.85
<i>Gemella sanguinis</i>	1.35E-06	8.72E-06	0.02	0.14	-3.11
<i>Eggerthia cateniformis</i>	2.02E-02	4.88E-02	0.02	0.01	0.84
<i>Dialister NA</i>	4.55E-04	1.66E-03	0.01	0.00	4.98
<i>Gracilibacteria NA</i>	1.03E-03	3.61E-03	0.01	0.00	7.80
<i>Streptococcus gordonii</i>	2.33E-03	7.68E-03	0.01	0.05	-2.14
<i>Bifidobacterium dentium</i>	1.67E-02	4.17E-02	0.01	0.01	1.05

<i>DNF00809 NA</i>	1.18E-02	3.00E-02	0.01	0.00	4.32
<i>Veillonella tobetsuensis</i>	1.30E-05	7.32E-05	0.01	0.17	-4.11
<i>Leptotrichia goodfellowii</i>	2.66E-03	8.55E-03	0.01	0.29	-5.41
<i>[Eubacterium] saphenum group NA</i>	7.15E-03	1.94E-02	0.01	0.00	0.47
<i>Veillonella dispar</i>	4.63E-03	1.35E-02	0.00	0.10	-4.51
<i>Actinomyces gerencseriae</i>	2.52E-04	9.85E-04	0.00	0.09	-4.38
<i>Oribacterium sinus</i>	1.51E-03	5.04E-03	0.00	0.03	-2.79
<i>Pseudopropionibacterium propionicum</i>	1.66E-05	8.99E-05	0.00	0.02	-4.85
<i>Corynebacterium durum</i>	4.69E-03	1.35E-02	0.00	0.03	-6.07
<i>Haemophilus parainfluenzae</i>	1.24E-05	7.13E-05	0.00	0.18	-11.54
<i>Actinobacillus pleuropneumoniae</i>	1.96E-02	4.77E-02	0.00	0.03	-8.72
<i>Prevotella nanceiensis</i>	5.17E-05	2.39E-04	0.00	0.02	-8.60
<i>Streptococcus parasanguinis</i>	1.75E-02	4.32E-02	0.00	0.01	-6.84

Supplementary table IV-4. List of bacterial species found differentially abundant after 2 months of amoxicillin treatment (AT2M_Amoxi). BT – before treatment.

Feature	ANCOMBC.pval	ANCOMBC.adj.pval.fdr	BT.Amoxi	AT2M.Amoxi	log2FC
<i>Treponema NA</i>	3.64E-24	9.64E-22	5.20	1.74	1.58
<i>Lautropia mirabilis</i>	3.32E-23	4.40E-21	0.05	0.61	-3.74
<i>Filifactor alocis</i>	4.12E-15	3.64E-13	3.32	1.14	1.54
<i>Rikenellaceae RC9 gut group NA</i>	6.52E-14	4.32E-12	0.47	0.13	1.91
<i>Tannerella forsythia</i>	2.15E-13	1.14E-11	4.33	2.04	1.08
<i>Fretibacterium feline</i>	7.13E-12	2.84E-10	1.31	0.51	1.36
<i>Mycoplasma NA</i>	7.51E-12	2.84E-10	0.21	0.09	1.22
<i>Moryella NA</i>	5.44E-11	1.80E-09	0.26	0.06	2.06
<i>Desulfobulbus NA</i>	1.19E-10	3.49E-09	1.29	0.39	1.73
<i>Lentimicrobium NA</i>	1.82E-10	4.81E-09	0.80	0.18	2.13
<i>Fretibacterium NA</i>	1.20E-09	2.90E-08	1.44	0.37	1.95
<i>Capnocytophaga gingivalis</i>	1.36E-09	3.00E-08	0.06	0.35	-2.65
<i>Defluviitaleaceae UCG-011 NA</i>	1.98E-09	4.03E-08	0.87	0.23	1.93
<i>Kingella oralis</i>	2.18E-09	4.13E-08	0.04	0.26	-2.90
<i>Flexilinea NA</i>	5.06E-09	8.94E-08	0.45	0.11	2.04
<i>Anaerovoracaceae NA</i>	5.67E-09	9.40E-08	0.72	0.23	1.65
<i>Peptococcus NA</i>	1.15E-08	1.80E-07	0.19	0.06	1.70
<i>Fretibacterium fastidiosum</i>	1.41E-08	2.08E-07	0.90	0.33	1.44
<i>Leptotrichia buccalis</i>	1.74E-08	2.42E-07	0.50	0.19	1.41
<i>F0058 NA</i>	2.22E-08	2.94E-07	1.94	0.97	0.99
<i>Prevotella oulorum</i>	3.07E-08	3.88E-07	0.07	0.36	-2.35
<i>Prevotella salivae</i>	3.75E-08	4.52E-07	0.03	0.28	-3.04
<i>Prevotella pleuritidis</i>	6.60E-08	7.61E-07	0.89	0.47	0.91
<i>Treponema medium</i>	1.20E-07	1.32E-06	0.06	0.00	3.52
<i>Eikenella corrodens</i>	1.24E-07	1.32E-06	0.08	0.23	-1.58
<i>Selenomonas artemidis</i>	1.92E-07	1.96E-06	0.06	0.33	-2.35
<i>Streptococcus NA</i>	2.52E-07	2.47E-06	4.75	9.18	-0.95
<i>Butyrivibrio NA</i>	7.11E-07	6.73E-06	0.07	0.01	3.36
<i>Bergeyella NA</i>	8.95E-07	8.18E-06	0.03	0.10	-1.71
<i>Treponema parvum</i>	1.00E-06	8.87E-06	0.06	0.03	1.23

<i>Capnocytophaga sputigena</i>	2.53E-06	2.16E-05	0.05	0.30	-2.64
<i>Porphyromonas NA</i>	3.41E-06	2.82E-05	1.12	0.48	1.23
<i>[Eubacterium] saphenum group saphenum</i>	4.99E-06	4.00E-05	0.26	0.13	1.01
<i>Family XIII UCG-001 NA</i>	7.07E-06	5.51E-05	0.12	0.08	0.66
<i>Phocaeicola abscessus</i>	7.54E-06	5.71E-05	0.12	0.03	2.16
<i>Rothia NA</i>	1.19E-05	8.76E-05	0.02	0.25	-3.35
<i>Actinomyces odontolyticus</i>	1.33E-05	9.53E-05	0.00	0.01	-7.29
<i>Atopobium parvulum</i>	1.56E-05	1.09E-04	0.06	0.18	-1.73
<i>Porphyromonas gingivalis</i>	2.34E-05	1.54E-04	10.11	5.10	0.99
<i>Saccharimonadales NA</i>	2.39E-05	1.54E-04	0.30	0.16	0.97
<i>Treponema maltophilum</i>	2.39E-05	1.54E-04	0.46	0.28	0.72
<i>Haemophilus NA</i>	2.48E-05	1.56E-04	0.15	0.71	-2.28
<i>Actinomyces NA</i>	2.92E-05	1.80E-04	0.28	0.86	-1.61
<i>W5053 NA</i>	3.58E-05	2.16E-04	1.45	0.47	1.61
<i>Acholeplasma NA</i>	4.86E-05	2.86E-04	0.15	0.02	2.92
<i>Oribacterium asaccharolyticum</i>	5.13E-05	2.96E-04	0.00	0.04	-8.70
<i>Treponema denticola</i>	8.47E-05	4.78E-04	2.34	1.44	0.70
<i>Oceanivirga NA</i>	9.93E-05	5.48E-04	0.88	0.51	0.77
<i>Bacteroides NA</i>	1.05E-04	5.70E-04	0.01	0.00	2.82
<i>Anaeroglobus geminatus</i>	1.12E-04	5.88E-04	0.13	0.07	0.78
<i>Actinomyces naeslundii</i>	1.13E-04	5.88E-04	0.01	0.12	-3.85
<i>Peptoanaerobacter stomatis</i>	1.27E-04	6.48E-04	0.09	0.12	-0.30
<i>Campylobacter gracilis</i>	1.42E-04	7.10E-04	0.44	1.01	-1.19
<i>Bacteria NA</i>	2.00E-04	9.80E-04	0.00	0.00	3.45
<i>Bacteroidales NA</i>	2.57E-04	1.24E-03	0.03	0.02	0.14
<i>Leptotrichia hongkongensis</i>	3.33E-04	1.58E-03	0.05	0.29	-2.49
<i>Clostridia UCG-014 NA</i>	4.78E-04	2.22E-03	0.11	0.10	0.11
<i>Gracilibacteria NA</i>	5.00E-04	2.28E-03	0.02	0.00	7.70
<i>Gemella sanguinis</i>	5.64E-04	2.53E-03	0.02	0.07	-1.99
<i>Prevotella oris</i>	6.55E-04	2.89E-03	0.47	2.22	-2.25
<i>Eggerthia cateniformis</i>	7.57E-04	3.29E-03	0.01	0.00	6.96
<i>Pseudomonas NA</i>	9.08E-04	3.88E-03	0.00	0.01	-7.22
<i>Rothia mucilaginosa</i>	9.54E-04	4.01E-03	0.06	0.15	-1.40
<i>Fusobacterium simiae</i>	9.90E-04	4.10E-03	0.11	0.05	1.06
<i>Oribacterium NA</i>	1.05E-03	4.26E-03	0.13	0.38	-1.49
<i>Family XI NA</i>	1.21E-03	4.87E-03	0.20	0.00	11.12
<i>Wolinella succinogenes</i>	1.57E-03	6.13E-03	0.01	0.00	6.95
<i>Haemophilus parainfluenzae</i>	1.57E-03	6.13E-03	0.01	0.06	-2.62
<i>Granulicatella NA</i>	1.61E-03	6.14E-03	0.23	0.66	-1.55
<i>Prevotella fusca</i>	1.62E-03	6.14E-03	0.12	0.02	2.62
<i>[Eubacterium] nodatum group NA</i>	1.88E-03	7.00E-03	0.26	0.22	0.24
<i>F0332 NA</i>	2.05E-03	7.55E-03	0.03	0.01	1.93
<i>DNF00809 NA</i>	2.46E-03	8.93E-03	0.02	0.00	4.10
<i>Lactobacillales NA</i>	2.50E-03	8.94E-03	0.00	0.01	-3.88
<i>Bacteroidia NA</i>	2.59E-03	9.13E-03	0.00	0.00	2.77
<i>Absconditabacteriales (SR1) NA</i>	2.96E-03	1.03E-02	0.06	0.02	1.37
<i>Stomatobaculum longum</i>	3.07E-03	1.06E-02	0.05	0.11	-1.29
<i>Johnsonella ignava</i>	3.14E-03	1.07E-02	0.04	0.16	-2.17
<i>[Eubacterium] brachy group NA</i>	3.22E-03	1.08E-02	0.00	0.00	4.73

<i>Prevotella NA</i>	3.38E-03	1.12E-02	0.78	0.77	0.03
<i>Treponema socranskii</i>	4.62E-03	1.51E-02	0.72	0.50	0.51
<i>Clostridia vadinBB60 group NA</i>	5.67E-03	1.83E-02	0.06	0.03	0.88
<i>Candidatus Pacebacteria NA</i>	5.89E-03	1.88E-02	0.16	0.00	6.23
<i>Prevotella melaninogenica</i>	6.60E-03	2.08E-02	0.10	0.15	-0.64
<i>Prevotella loescheii</i>	7.26E-03	2.26E-02	0.09	0.44	-2.26
<i>Leptotrichia hofstadii</i>	7.61E-03	2.32E-02	0.28	0.11	1.40
<i>Rhodospirillales NA</i>	7.62E-03	2.32E-02	0.01	0.00	7.20
<i>Dialister NA</i>	8.61E-03	2.59E-02	0.01	0.00	4.19
<i>Catonella NA</i>	9.24E-03	2.74E-02	0.15	0.20	-0.39
<i>Leptotrichia NA</i>	9.30E-03	2.74E-02	1.48	2.14	-0.53
<i>Prevotella NA</i>	1.02E-02	2.96E-02	1.71	1.41	0.28
<i>Actinomyces oricola</i>	1.13E-02	3.26E-02	0.00	0.00	5.34
<i>Odoribacter denticanis</i>	1.14E-02	3.26E-02	0.36	0.01	4.75
<i>[Eubacterium] saphenum group NA</i>	1.48E-02	4.17E-02	0.01	0.01	0.63
<i>Prevotella conceptionensis</i>	1.63E-02	4.54E-02	0.14	0.02	2.53
<i>Leptotrichia massiliensis</i>	1.70E-02	4.68E-02	0.01	0.14	-4.31
<i>Pseudopropionibacterium propionicum</i>	1.73E-02	4.72E-02	0.00	0.01	-2.15
<i>Bacteroidales F082 NA</i>	1.80E-02	4.87E-02	0.03	0.02	0.96
<i>Prevotella micans</i>	1.84E-02	4.93E-02	0.05	0.09	-0.88
<i>Izomoplasmatales NA</i>	1.86E-02	4.93E-02	0.03	0.03	-0.17

Supplementary table IV-5. List of bacterial species found differentially abundant after 2 months of metronidazole (AT2M_Metro) treatment. **BT** – before treatment

Feature	ANCOMBC.pval	ANCOMBC.adj.pval.fdr	BT.Metro	AT2M.Metro	log2FC
<i>Desulfobulbus NA</i>	1.20E-31	3.10E-29	2.10	0.13	3.99
<i>Fretibacterium feline</i>	3.15E-18	4.06E-16	1.74	0.29	2.58
<i>Family XIII UCG-001 NA</i>	6.24E-18	5.37E-16	0.18	0.05	1.92
<i>Anaerovoracaceae NA</i>	3.91E-16	2.52E-14	0.89	0.15	2.60
<i>Prevotella dentalis</i>	1.11E-14	5.72E-13	0.32	0.06	2.41
<i>Prevotella oris</i>	3.20E-13	1.37E-11	0.63	2.36	-1.91
<i>Mogibacterium timidum</i>	3.97E-12	1.46E-10	0.06	0.01	2.91
<i>Eikenella corrodens</i>	6.39E-12	2.06E-10	0.04	0.29	-2.68
<i>Flexilinea NA</i>	3.39E-11	9.72E-10	0.35	0.07	2.37
<i>[Eubacterium] nodatum group NA</i>	8.38E-11	2.16E-09	0.71	0.18	1.99
<i>Tannerella forsythia</i>	2.55E-10	5.97E-09	3.61	0.94	1.95
<i>Fretibacterium fastidiosum</i>	3.24E-10	6.96E-09	0.86	0.30	1.54
<i>Lautropia mirabilis</i>	9.26E-10	1.84E-08	0.10	0.86	-3.08
<i>Moryella NA</i>	3.04E-09	5.61E-08	0.26	0.02	3.92
<i>Paludibacteraceae F0058 NA</i>	4.14E-09	7.13E-08	1.71	0.51	1.75
<i>Erysipelotrichaceae UCG-006 NA</i>	5.93E-09	9.57E-08	0.06	0.02	1.73
<i>Rothia dentocariosa</i>	6.57E-09	9.97E-08	0.14	1.39	-3.34
<i>[Eubacterium] saphenum group saphenum</i>	1.15E-08	1.65E-07	0.71	0.02	4.95
<i>Leptotrichia buccalis</i>	2.07E-08	2.81E-07	0.19	0.02	3.21
<i>Fretibacterium NA</i>	4.09E-08	5.28E-07	1.07	0.47	1.20

<i>Filifactor alocis</i>	8.87E-08	1.09E-06	3.66	0.99	1.89
<i>Defluviitaleaceae UCG-011 NA</i>	1.31E-07	1.51E-06	0.37	0.05	2.77
<i>Leptotrichia hongkongensis</i>	1.34E-07	1.51E-06	0.14	1.10	-2.97
<i>Bergeyella NA</i>	1.70E-07	1.83E-06	0.03	0.20	-2.74
<i>Treponema denticola</i>	2.68E-07	2.77E-06	1.86	0.89	1.06
<i>Kingella oralis</i>	4.24E-07	4.21E-06	0.05	0.85	-4.08
<i>Streptococcus NA</i>	4.46E-07	4.26E-06	4.31	9.61	-1.16
<i>[Eubacterium] brachy group brachy</i>	1.21E-06	1.12E-05	1.08	0.15	2.83
<i>Porphyromonas endodontalis</i>	1.82E-06	1.62E-05	4.44	3.39	0.39
<i>Pseudoramibacter alactolyticus</i>	7.20E-06	6.19E-05	0.12	0.01	2.96
<i>Campylobacter gracilis</i>	1.66E-05	1.36E-04	0.47	1.12	-1.25
<i>Peptostreptococcus stomatis</i>	1.68E-05	1.36E-04	0.26	0.16	0.75
<i>Mycoplasma NA</i>	1.81E-05	1.42E-04	0.23	0.04	2.40
<i>Phocaeicola abscessus</i>	2.59E-05	1.97E-04	0.24	0.08	1.55
<i>Treponema NA</i>	3.20E-05	2.36E-04	4.85	1.39	1.81
<i>Prevotella saccharolytica</i>	4.52E-05	3.24E-04	0.03	0.07	-1.12
<i>Prevotella intermedia</i>	4.66E-05	3.25E-04	1.24	1.05	0.24
<i>Pseudopropionibacterium propionicum</i>	5.27E-05	3.58E-04	0.00	0.09	-9.78
<i>Catonella NA</i>	8.34E-05	5.52E-04	0.18	0.05	1.91
<i>Rothia NA</i>	1.18E-04	7.59E-04	0.02	0.25	-3.34
<i>Capnocytophaga gingivalis</i>	1.30E-04	8.19E-04	0.05	0.54	-3.57
<i>Porphyromonas gingivalis</i>	1.71E-04	1.05E-03	5.13	2.04	1.33
<i>Parvimonas NA</i>	2.35E-04	1.41E-03	0.21	0.04	2.32
<i>DNF00809 NA</i>	3.99E-04	2.34E-03	0.03	0.00	8.06
<i>Actinomyces naeslundii</i>	4.20E-04	2.41E-03	0.04	0.32	-3.08
<i>Prevotella veroralis</i>	4.41E-04	2.47E-03	0.19	0.03	2.82
<i>Propionivibrio NA</i>	4.80E-04	2.63E-03	0.01	0.00	1.84
<i>Veillonella NA</i>	5.02E-04	2.70E-03	0.80	2.42	-1.59
<i>Capnocytophaga sputigena</i>	5.17E-04	2.72E-03	0.05	0.80	-3.99
<i>Prevotella nigrescens</i>	6.02E-04	3.11E-03	0.39	1.57	-1.99
<i>Prevotella pleuritidis</i>	6.19E-04	3.13E-03	0.58	0.14	2.01
<i>Izempiasmatales NA</i>	7.51E-04	3.73E-03	0.02	0.00	5.78
<i>Treponema pectinovorum</i>	8.88E-04	4.32E-03	0.00	0.01	-5.86
<i>Saccharimonadales NA</i>	9.05E-04	4.32E-03	1.10	0.19	2.57
<i>Leptotrichia hofstadii</i>	1.40E-03	6.59E-03	0.10	0.01	3.53
<i>W5053 NA</i>	1.59E-03	7.31E-03	0.94	0.15	2.61
<i>Comamonas NA</i>	1.64E-03	7.42E-03	0.04	0.00	8.73
<i>Treponema maltophilum</i>	1.83E-03	8.14E-03	0.53	0.25	1.07
<i>Streptococcus gordonii</i>	1.93E-03	8.43E-03	0.00	0.02	-7.34
<i>Corynebacterium durum</i>	1.96E-03	8.43E-03	0.00	0.04	-8.83
<i>Actinomyces oricola</i>	2.09E-03	8.86E-03	0.01	0.00	3.47
<i>Centipeda NA</i>	2.18E-03	9.05E-03	0.56	1.17	-1.06
<i>Olsenella NA</i>	2.47E-03	1.01E-02	0.08	0.03	1.64
<i>Aggregatibacter NA</i>	2.67E-03	1.06E-02	0.10	0.07	0.63
<i>Clostridia vadinBB60 group NA</i>	2.67E-03	1.06E-02	0.09	0.11	-0.32
<i>Absconditabacteriales (SRI) NA</i>	2.87E-03	1.12E-02	0.12	0.05	1.34
<i>Prevotella oulorum</i>	3.40E-03	1.31E-02	0.07	0.35	-2.34
<i>Gemella morbillorum</i>	3.49E-03	1.33E-02	0.50	0.89	-0.82
<i>Parvimonas micra</i>	3.58E-03	1.33E-02	2.52	0.69	1.86

<i>Campylobacter showae</i>	3.60E-03	1.33E-02	0.02	0.11	-2.79
<i>Olsenella uli</i>	6.86E-03	2.49E-02	0.03	0.01	2.31
<i>Actinomyces gerencseriae</i>	7.00E-03	2.51E-02	0.00	0.01	-6.93
<i>Prevotellaceae UCG-004 NA</i>	7.27E-03	2.57E-02	0.01	0.00	1.54
<i>Lentimicrobium NA</i>	7.80E-03	2.72E-02	0.55	1.02	-0.90
<i>Capnocytophaga leadbetteri</i>	7.99E-03	2.75E-02	0.21	0.83	-2.01
<i>Rikenellaceae RC9 gut group NA</i>	8.35E-03	2.84E-02	0.38	0.58	-0.61
<i>Actinomyces NA</i>	8.59E-03	2.88E-02	0.48	1.39	-1.55
<i>Pyramidobacter piscolens</i>	8.82E-03	2.92E-02	0.03	0.00	3.58
<i>Actinomyces odontolyticus</i>	8.95E-03	2.92E-02	0.00	0.02	-7.67
<i>Brachymonas NA</i>	9.74E-03	3.14E-02	0.02	0.00	1.95
<i>Prevotella enoeca</i>	1.11E-02	3.55E-02	0.05	0.01	2.20
<i>Rothia mucilaginosa</i>	1.25E-02	3.94E-02	0.29	0.09	1.64
<i>Capnocytophaga NA</i>	1.34E-02	4.17E-02	0.31	0.64	-1.04
<i>[Eubacterium] brachy group NA</i>	1.40E-02	4.29E-02	0.01	0.00	3.29
<i>Dialister invisus</i>	1.48E-02	4.49E-02	1.52	1.10	0.47
<i>Prevotella micans</i>	1.67E-02	4.96E-02	0.04	0.04	0.20
<i>Atopobium NA</i>	1.68E-02	4.96E-02	0.46	0.23	1.02
<i>Acholeplasma NA</i>	1.69E-02	4.96E-02	0.06	0.01	2.80

Supplementary table IV-6. List of bacterial species found differentially abundant after 2 amoxicillin and metronidazole (AT2M_AM) treatment. **BT** – before treatment.

Feature	ANCOMBC.pval	ANCOMBC.adjpvval.fdr	BT.AM	AT2M.AM	log2FC
<i>Olsenella NA</i>	2.88E-30	7.09E-28	0.04	0.00	4.02
<i>Bifidobacterium dentium</i>	8.30E-20	6.81E-18	0.00	0.00	1.78
<i>Veillonellales-Selenomonadales NA</i>	8.30E-20	6.81E-18	0.00	0.00	1.78
<i>Lautropia mirabilis</i>	1.11E-18	6.85E-17	0.04	0.28	-2.73
<i>Capnocytophaga gingivalis</i>	4.02E-15	1.98E-13	0.02	0.20	-3.18
<i>Family XIII UCG-001 NA</i>	1.41E-13	5.79E-12	0.17	0.02	3.30
<i>Capnocytophaga leadbetteri</i>	3.15E-13	1.11E-11	0.13	1.25	-3.30
<i>Johnsonella ignava</i>	8.97E-12	2.76E-10	0.04	0.00	6.64
<i>Leptotrichia buccalis</i>	3.00E-11	8.21E-10	0.27	0.00	9.36
<i>Veillonella NA</i>	6.96E-11	1.71E-09	0.40	2.11	-2.41
<i>Flexilinea NA</i>	1.48E-10	3.30E-09	0.33	0.02	4.19
<i>Saccharimonadales NA</i>	7.93E-10	1.63E-08	0.87	0.15	2.54
<i>Filifactor alocis</i>	6.98E-09	1.27E-07	5.10	0.87	2.55
<i>Rothia NA</i>	7.20E-09	1.27E-07	0.00	0.25	-9.27
<i>Atopobium parvulum</i>	8.69E-09	1.43E-07	0.00	0.42	-10.00
<i>Clostridia vadinBB60 group NA</i>	3.38E-08	5.20E-07	0.06	0.01	2.10
<i>Fretibacterium feline</i>	3.83E-08	5.54E-07	0.48	0.01	6.08
<i>Mogibacterium timidum</i>	6.22E-08	8.50E-07	0.07	0.00	4.94
<i>Kingella oralis</i>	8.20E-08	1.06E-06	0.02	0.51	-4.69
<i>Porphyromonas NA</i>	9.69E-08	1.19E-06	0.93	0.08	3.62
<i>Porphyromonas gingivalis</i>	1.53E-07	1.78E-06	14.76	1.31	3.49

<i>Rikenellaceae RC9 gut group NA</i>	1.59E-07	1.78E-06	0.40	0.08	2.36
<i>Campylobacter gracilis</i>	2.69E-07	2.88E-06	0.43	1.16	-1.45
<i>Bergeyella cardium</i>	4.63E-07	4.75E-06	0.02	0.01	1.43
<i>Granulicatella NA</i>	1.20E-06	1.18E-05	0.14	1.63	-3.54
<i>Family XI NA</i>	1.46E-06	1.38E-05	0.05	0.02	1.26
<i>Erysipelotrichaceae UCG-006 NA</i>	2.07E-06	1.89E-05	0.03	0.01	1.02
<i>Fretibacterium NA</i>	4.30E-06	3.78E-05	1.57	0.21	2.93
<i>Capnocytophaga NA</i>	8.08E-06	6.58E-05	0.23	1.55	-2.75
<i>Prevotella oris</i>	8.14E-06	6.58E-05	0.65	2.84	-2.12
<i>Pyramidobacter piscolens</i>	8.29E-06	6.58E-05	0.02	0.00	3.01
<i>Mycoplasma NA</i>	1.42E-05	1.09E-04	0.38	0.04	3.19
<i>Veillonella parvula</i>	1.54E-05	1.15E-04	0.30	1.37	-2.19
<i>Prevotella NA</i>	2.00E-05	1.44E-04	1.90	1.20	0.67
<i>Defluviitaleaceae UCG-011 NA</i>	3.24E-05	2.28E-04	0.29	0.04	2.80
<i>Desulfobulbus NA</i>	6.46E-05	4.37E-04	1.02	0.13	2.99
<i>Gemella sanguinis</i>	6.57E-05	4.37E-04	0.01	0.07	-3.20
<i>Abiotrophia defectiva</i>	7.37E-05	4.66E-04	0.04	0.17	-2.19
<i>Actinomyces NA</i>	7.39E-05	4.66E-04	0.22	0.66	-1.58
<i>Prevotella loescheii</i>	1.05E-04	6.46E-04	0.05	1.28	-4.75
<i>Anaerovoracaceae NA</i>	1.53E-04	9.20E-04	0.95	0.08	3.55
<i>Aggregatibacter aphrophilus</i>	1.60E-04	9.35E-04	0.11	0.00	8.03
<i>Prevotella salivae</i>	1.75E-04	1.00E-03	0.01	0.16	-4.34
<i>Prevotella dentalis</i>	2.16E-04	1.21E-03	0.09	0.05	0.70
<i>Alloprevotella rava</i>	2.84E-04	1.53E-03	0.19	0.04	2.31
<i>Shuttleworthia satelles</i>	2.86E-04	1.53E-03	0.02	0.00	2.08
<i>Prevotella intermedia</i>	3.21E-04	1.66E-03	2.80	0.21	3.74
<i>Prevotellaceae UCG-004 NA</i>	3.23E-04	1.66E-03	0.01	0.00	3.79
<i>Bulleidia extracta</i>	3.58E-04	1.78E-03	0.13	0.01	4.06
<i>Olsenella uli</i>	3.62E-04	1.78E-03	0.02	0.00	5.73
<i>Aggregatibacter actinomycetemcomitans</i>	4.01E-04	1.94E-03	0.01	0.00	3.85
<i>Stomatobaculum longum</i>	4.54E-04	2.15E-03	0.07	1.00	-3.76
<i>Peptococcus NA</i>	5.36E-04	2.49E-03	0.36	0.04	3.24
<i>Veillonella tobetsuensis</i>	6.30E-04	2.82E-03	0.05	0.10	-0.98
<i>Anaeroglobus NA</i>	6.31E-04	2.82E-03	0.06	0.00	7.17
<i>Fretibacterium fastidiosum</i>	9.26E-04	4.07E-03	0.55	0.34	0.70
<i>Lachnoanaerobaculum NA</i>	9.51E-04	4.10E-03	0.17	0.56	-1.74
<i>Prevotella pleuritidis</i>	1.45E-03	6.16E-03	0.17	0.01	4.34
<i>[Eubacterium] saphenum group saphenum</i>	1.50E-03	6.26E-03	0.17	0.02	3.30
<i>Eikenella NA</i>	2.11E-03	8.67E-03	0.08	0.17	-1.04
<i>Sphaerochaeta NA</i>	2.92E-03	1.17E-02	0.01	0.01	0.12
<i>Absconditabacteriales (SRI) NA</i>	2.96E-03	1.17E-02	0.06	0.05	0.39
<i>[Eubacterium] nodatum group NA</i>	3.14E-03	1.23E-02	0.85	0.15	2.49
<i>Neisseria NA</i>	3.83E-03	1.47E-02	0.73	0.94	-0.36
<i>Treponema NA</i>	4.02E-03	1.51E-02	3.55	1.52	1.22
<i>Tannerella forsythia</i>	4.04E-03	1.51E-02	4.43	0.92	2.26
<i>Pseudopropionibacterium propionicum</i>	4.23E-03	1.55E-02	0.00	0.01	-5.23

<i>Mogibacterium NA</i>	4.67E-03	1.69E-02	0.00	0.00	-3.36
<i>Porphyromonas endodontalis</i>	4.95E-03	1.76E-02	3.16	1.74	0.86
<i>Slackia exigua</i>	6.19E-03	2.15E-02	0.01	0.00	2.78
<i>Moryella NA</i>	6.21E-03	2.15E-02	0.07	0.02	1.90
<i>Catonella morbi</i>	6.72E-03	2.30E-02	0.36	0.28	0.36
<i>Corynebacterium durum</i>	7.48E-03	2.49E-02	0.00	0.07	-7.47
<i>[Eubacterium] brachy group brachy</i>	7.50E-03	2.49E-02	0.28	0.09	1.59
<i>Haemophilus parainfluenzae</i>	7.76E-03	2.54E-02	0.00	0.08	-7.54
<i>Cardiobacterium valvarum</i>	7.89E-03	2.55E-02	0.04	0.04	0.06
<i>Actinomyces naeslundii</i>	8.89E-03	2.80E-02	0.00	0.03	-6.24
<i>Prevotella saccharolytica</i>	8.89E-03	2.80E-02	0.02	0.18	-3.24
<i>Leptotrichia hongkongensis</i>	9.13E-03	2.84E-02	0.06	0.44	-2.83
<i>Eikenella corrodens</i>	1.11E-02	3.41E-02	0.02	0.12	-2.84
<i>Peptostreptococcus stomatis</i>	1.12E-02	3.41E-02	0.38	0.21	0.90
<i>Treponema denticola</i>	1.22E-02	3.65E-02	3.41	1.49	1.19
<i>Bacteroides heparinolyticus</i>	1.28E-02	3.80E-02	0.03	0.00	6.42
<i>Prevotella enoeca</i>	1.37E-02	4.02E-02	0.02	0.00	2.02
<i>Treponema socranskii</i>	1.48E-02	4.29E-02	0.61	0.51	0.25
<i>Prevotella NA</i>	1.51E-02	4.31E-02	1.04	1.65	-0.66
<i>Phocaicola abscessus</i>	1.60E-02	4.53E-02	0.23	0.11	1.09
<i>Campylobacter NA</i>	1.70E-02	4.75E-02	0.98	0.93	0.08

Supplementary table IV-7. List of bacterial species found differentially abundant after 2 months of azithromycin treatment (**AT2M.Azitra**). **BT** – before treatment.

Feature	ANCOMBC.pval	ANCOMBC.adj.pval.fdr	BT.Azitra	AT2M.Azitra	log2FC
<i>Porphyromonas gingivalis</i>	2.62E-20	7.26E-19	9.11	0.74	3.62
<i>Treponema NA</i>	3.39E-13	4.68E-12	5.05	1.00	2.33
<i>Porphyromonas endodontalis</i>	1.06E-04	4.12E-04	4.34	2.68	0.70
<i>Streptococcus NA</i>	3.98E-15	6.61E-14	4.21	10.55	-1.32
<i>Filifactor alocis</i>	2.81E-15	5.00E-14	3.98	0.84	2.24
<i>Tannerella forsythia</i>	7.54E-26	3.13E-24	3.41	0.23	3.91
<i>Treponema denticola</i>	6.00E-13	7.86E-12	2.89	0.64	2.17
<i>Prevotella intermedia</i>	9.85E-06	4.89E-05	2.47	1.26	0.97
<i>Paludibacteraceae F0058 NA</i>	5.37E-06	2.79E-05	2.00	0.65	1.62
<i>Fretibacterium NA</i>	3.07E-17	6.38E-16	1.46	0.13	3.45
<i>Saccharimonadaceae NA</i>	1.66E-11	2.06E-10	1.43	0.25	2.52
<i>Campylobacter NA</i>	1.75E-03	4.83E-03	1.41	0.54	1.40
<i>Fretibacterium feline</i>	2.42E-37	1.51E-35	1.37	0.04	5.07
<i>Desulfobulbus NA</i>	3.18E-181	7.91E-179	1.31	0.00	10.35
<i>Lentimicrobium NA</i>	5.89E-54	7.33E-52	1.23	0.02	6.09
<i>Dialister invisus</i>	6.12E-03	1.51E-02	1.13	0.60	0.91
<i>Veillonella NA</i>	2.41E-08	2.00E-07	1.02	4.78	-2.23

<i>Porphyromonas NA</i>	5.40E-03	1.36E-02	0.96	0.44	1.14
<i>Fretibacterium fastidiosum</i>	5.89E-19	1.33E-17	0.87	0.11	2.96
<i>Selenomonas sputigena</i>	1.39E-02	2.95E-02	0.86	0.38	1.17
<i>Neisseria NA</i>	2.50E-04	8.40E-04	0.78	2.55	-1.71
<i>Family XI W5053 NA</i>	2.72E-08	2.12E-07	0.76	0.01	6.15
<i>Defluviitaleaceae UCG-011 NA</i>	1.11E-24	3.95E-23	0.71	0.04	4.08
<i>Treponema maltophilum</i>	1.21E-05	5.78E-05	0.67	0.23	1.55
<i>Prevotella pleuritidis</i>	2.38E-02	4.73E-02	0.66	0.31	1.11
<i>Centipeda NA</i>	2.18E-02	4.46E-02	0.65	0.77	-0.24
<i>Veillonella parvula</i>	3.02E-14	4.42E-13	0.65	2.85	-2.12
<i>Anaerovoracaceae NA</i>	2.23E-20	6.94E-19	0.59	0.06	3.26
<i>Treponema socranskii</i>	3.68E-11	4.16E-10	0.59	0.18	1.73
<i>Oceanivirga NA</i>	3.19E-03	8.37E-03	0.50	0.00	12.52
<i>Saccharimonadales NA</i>	3.33E-07	2.30E-06	0.49	0.21	1.21
<i>Capnocytophaga NA</i>	3.15E-11	3.74E-10	0.46	1.80	-1.98
<i>Rikenellaceae RC9 gut group NA</i>	9.99E-20	2.49E-18	0.43	0.06	2.86
<i>Mycoplasma NA</i>	7.72E-17	1.48E-15	0.38	0.11	1.82
<i>[Eubacterium] saphenum group saphenum</i>	1.87E-10	2.03E-09	0.37	0.04	3.12
<i>[Eubacterium] nodatum group NA</i>	1.46E-09	1.40E-08	0.36	0.07	2.39
<i>Prevotella nigrescens</i>	1.46E-02	3.08E-02	0.32	0.83	-1.38
<i>Aggregatibacter NA</i>	1.11E-02	2.45E-02	0.29	0.15	0.91
<i>Tannerella NA</i>	1.26E-04	4.55E-04	0.28	0.81	-1.51
<i>Actinomyces NA</i>	5.10E-07	3.34E-06	0.28	1.05	-1.90
<i>Johnsonella NA</i>	6.28E-03	1.51E-02	0.24	0.21	0.23
<i>Granulicatella NA</i>	8.74E-06	4.44E-05	0.24	0.98	-2.04
<i>Leptotrichia buccalis</i>	6.68E-05	2.68E-04	0.22	0.09	1.28
<i>Flexilinea NA</i>	5.32E-45	4.42E-43	0.21	0.01	4.36
<i>Aggregatibacter aphrophilus</i>	1.64E-02	3.41E-02	0.18	0.29	-0.63
<i>Haemophilus NA</i>	2.55E-08	2.05E-07	0.18	1.69	-3.26
<i>Peptostreptococcus stomatis</i>	6.09E-04	1.85E-03	0.17	0.09	0.92
<i>Leptotrichia hofstadii</i>	8.53E-03	1.95E-02	0.17	0.07	1.20
<i>Moryella NA</i>	1.81E-33	9.02E-32	0.16	0.01	4.73
<i>Catonella NA</i>	9.89E-03	2.22E-02	0.16	0.07	1.20
<i>Phocaeicola abscessus</i>	1.18E-14	1.84E-13	0.15	0.01	4.24
<i>Lachnospiraceae NA</i>	3.51E-04	1.13E-03	0.14	0.00	5.97
<i>Selenomonas noxia</i>	4.11E-04	1.28E-03	0.14	0.08	0.81
<i>Clostridia UCG-014 NA</i>	1.45E-09	1.40E-08	0.13	0.02	2.48
<i>Peptococcus NA</i>	1.52E-06	8.23E-06	0.12	0.04	1.64
<i>Lautropia mirabilis</i>	1.54E-08	1.32E-07	0.12	0.98	-3.00
<i>Prevotella dentalis</i>	1.25E-04	4.55E-04	0.12	0.05	1.21
<i>Oribacterium NA</i>	7.56E-03	1.79E-02	0.11	0.70	-2.73
<i>Family XIII UCG-001 NA</i>	9.96E-10	1.03E-08	0.10	0.03	1.99
<i>Butyrivibrio NA</i>	5.78E-04	1.78E-03	0.10	0.01	3.18
<i>Capnocytophaga gingivalis</i>	1.49E-04	5.22E-04	0.10	0.42	-2.07

<i>Alloprevotella rava</i>	6.32E-03	1.51E-02	0.10	0.09	0.12
<i>Rothia dentocariosa</i>	8.39E-03	1.94E-02	0.09	1.00	-3.43
<i>Gemella NA</i>	2.76E-03	7.31E-03	0.09	0.32	-1.81
<i>Leptotrichia massiliensis</i>	1.12E-02	2.45E-02	0.09	0.00	10.02
<i>Prevotella oulorum</i>	8.28E-03	1.93E-02	0.09	0.54	-2.63
<i>Prevotella melaninogenica</i>	4.10E-04	1.28E-03	0.08	0.60	-2.84
<i>Megasphaera micronuciformis</i>	6.81E-04	2.02E-03	0.08	0.18	-1.17
<i>Prevotella veroralis</i>	1.79E-06	9.47E-06	0.07	0.84	-3.52
<i>Selenomonas artemidis</i>	4.40E-03	1.14E-02	0.07	0.28	-1.98
<i>Streptococcus gordonii</i>	2.09E-03	5.65E-03	0.07	0.05	0.58
<i>Kingella oralis</i>	1.18E-06	6.85E-06	0.07	1.02	-3.85
<i>Veillonella atypica</i>	6.29E-03	1.51E-02	0.07	0.11	-0.68
<i>Prevotella maculosa</i>	6.81E-07	4.24E-06	0.07	0.34	-2.34
<i>Clostridia vadinBB60 group NA</i>	9.39E-08	7.09E-07	0.07	0.01	3.04
<i>Rothia NA</i>	1.13E-02	2.45E-02	0.06	0.26	-2.00
<i>Treponema medium</i>	6.30E-03	1.51E-02	0.06	0.00	9.55
<i>Absconditabacteriales (SRI) NA</i>	1.20E-08	1.07E-07	0.06	0.00	9.44
<i>Rothia mucilaginosa</i>	5.23E-07	3.34E-06	0.06	0.26	-2.17
<i>Capnocytophaga sputigena</i>	5.93E-05	2.42E-04	0.05	0.10	-0.93
<i>Dialister pneumosintes</i>	2.73E-05	1.19E-04	0.05	0.06	-0.08
<i>Prevotella loescheii</i>	6.33E-04	1.90E-03	0.05	0.92	-4.15
<i>Veillonella tobetsuensis</i>	2.41E-02	4.76E-02	0.04	0.24	-2.71
<i>Treponema parvum</i>	1.09E-04	4.12E-04	0.04	0.01	1.35
<i>Campylobacter concisus</i>	1.47E-06	8.16E-06	0.04	0.19	-2.40
<i>Bacteroidales NA</i>	1.34E-06	7.58E-06	0.03	0.00	4.41
<i>Actinomyces pacaensis</i>	8.22E-03	1.93E-02	0.03	0.00	8.52
<i>Bergeyella NA</i>	1.08E-04	4.12E-04	0.03	0.09	-1.48
<i>Izomoplasmatales NA</i>	2.60E-05	1.16E-04	0.03	0.00	8.51
<i>Erysipelotrichaceae UCG-006 NA</i>	1.45E-03	4.10E-03	0.03	0.01	2.26
<i>Gemella sanguinis</i>	6.26E-09	5.78E-08	0.03	0.25	-3.27
<i>Atopobium parvulum</i>	3.55E-04	1.13E-03	0.02	0.14	-2.69
<i>Abiotrophia defectiva</i>	3.02E-04	1.00E-03	0.02	0.13	-2.58
<i>Brachymonas NA</i>	2.24E-02	4.54E-02	0.02	0.00	7.84
<i>Pseudoramibacter alactolyticus</i>	1.55E-07	1.10E-06	0.02	0.00	2.18
<i>Propionivibrio NA</i>	2.36E-02	4.73E-02	0.02	0.00	4.14
<i>Pyramidobacter piscolens</i>	2.06E-03	5.65E-03	0.02	0.00	7.66
<i>Prevotella pallens</i>	1.01E-04	3.99E-04	0.02	0.05	-1.65
<i>Actinobacillus NA</i>	1.49E-02	3.13E-02	0.01	0.04	-1.38
<i>Leptotrichia goodfellowii</i>	7.80E-04	2.26E-03	0.01	0.41	-4.87
<i>Prevotella salivae</i>	5.04E-07	3.34E-06	0.01	0.20	-4.07
<i>Campylobacter showae</i>	7.44E-07	4.41E-06	0.01	0.05	-1.99
<i>Veillonella dispar</i>	1.00E-05	4.89E-05	0.01	0.16	-3.80
<i>Capnocytophaga haemolytica</i>	2.43E-04	8.30E-04	0.01	0.12	-3.42
<i>Streptococcus sanguinis</i>	4.67E-03	1.20E-02	0.01	0.16	-4.30

<i>Veillonella rogosae</i>	1.73E-02	3.55E-02	0.01	0.08	-3.37
<i>Actinomyces gerencseriae</i>	7.33E-07	4.41E-06	0.01	0.14	-4.27
<i>Pseudopropionibacterium propionicum</i>	1.33E-04	4.74E-04	0.01	0.03	-2.29
<i>Prevotellaceae NA</i>	1.37E-02	2.94E-02	0.01	0.01	-1.02
<i>Streptococcus massiliensis</i>	4.29E-05	1.81E-04	0.00	0.02	-1.79
<i>Oribacterium sinus</i>	1.17E-03	3.36E-03	0.00	0.04	-3.59
<i>Streptococcus mutans</i>	1.64E-03	4.59E-03	0.00	0.09	-5.18
<i>Haemophilus parainfluenzae</i>	1.51E-04	5.23E-04	0.00	0.30	-6.99
<i>Filifactor NA</i>	9.22E-03	2.09E-02	0.00	0.00	-1.49
<i>Peptoniphilus lacrimalis</i>	5.21E-05	2.16E-04	0.00	0.00	-1.28
<i>Bacteroidia NA</i>	1.00E-02	2.23E-02	0.00	0.00	1.00
<i>Lautropia NA</i>	2.58E-05	1.16E-04	0.00	0.00	-1.89
<i>Conservatibacter NA</i>	2.36E-03	6.33E-03	0.00	0.00	-0.88
<i>Prevotella nanceiensis</i>	1.52E-07	1.10E-06	0.00	0.04	-7.36
<i>Staphylococcus NA</i>	5.23E-03	1.33E-02	0.00	1.63	-14.22
<i>Prevotella histicola</i>	7.33E-04	2.15E-03	0.00	0.11	-10.27
<i>Actinobacillus pleuropneumoniae</i>	1.12E-04	4.18E-04	0.00	0.04	-8.88
<i>Haemophilus sputorum</i>	3.09E-04	1.01E-03	0.00	0.04	-8.71
<i>Streptococcus parasanguinis</i>	1.28E-05	6.00E-05	0.00	0.01	-7.07
<i>Gemella parahaemolysans</i>	3.04E-05	1.31E-04	0.00	0.01	-6.38
<i>Micrococcales NA</i>	1.66E-05	7.64E-05	0.00	0.00	-3.80

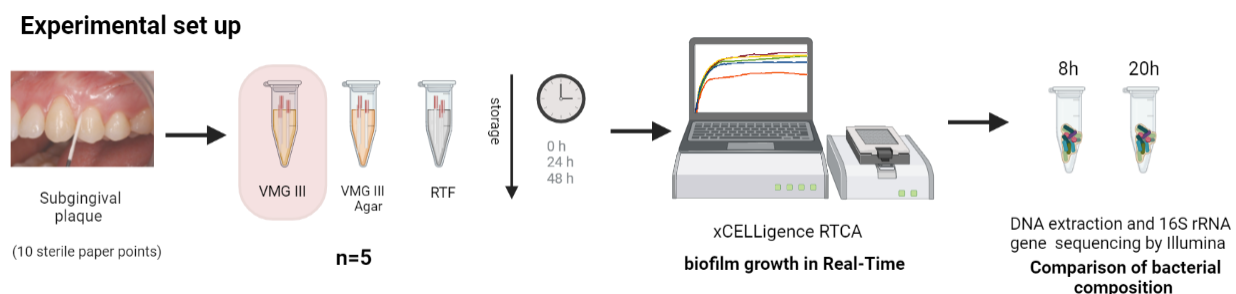


Figure IV-S1. Workflow of experimental set up to evaluate transport media selection and growing conditions. Subgingival plaque samples (n=5) were collected and placed into RTF, VMGIII and VMG III Agar transport media using 10 sterile paper points and stored at room temperature for 0, 24 and 48h. After that, periodontal biofilms were grown in the impedance xCELLigence system, which measures biofilm growth in real-time. Formed biofilms were collected at 8h and 20h for DNA extraction and 16S rRNA gene Illumina sequencing to compare biofilm bacterial composition to the initial subgingival sample inoculum.

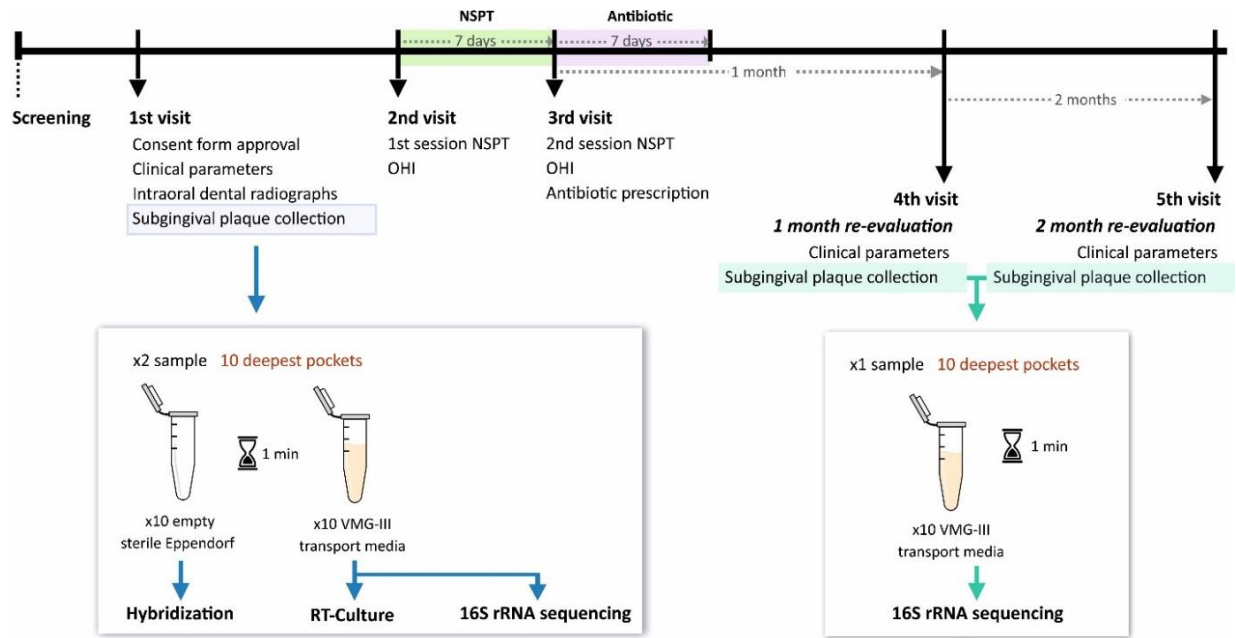


Figure IV-S2. Flow diagram of the clinical study design. Patients were referred to the University Dental Clinic and evaluated for eligibility criteria. On the first visit, personal data and clinical parameters (probing depth, clinical attachment level, bleeding on probing, and presence of plaque) were recorded, and a complete periapical radiographic series was performed. Subgingival plaque samples were collected with paper points and split in two: One into an empty Eppendorf tube for the quantification of periodontal pathogens by hybridization method; and the other was put in VMG-III transport medium and taken to the lab for evaluation of biofilm growth dynamics in the presence of different antibiotics, followed by determination of the bacterial composition using 16S rRNA gene sequencing. On the second and third visits, non-surgical periodontal treatment (NSPT) was performed, and oral hygiene instructions (OHI) provided. On the third visit, the antibiotic indicated by one of the methodologies was prescribed randomly among patients. At one and two months (fourth and fifth visits), clinical parameters were reevaluated, and subgingival plaque samples were collected for 16S rRNA sequencing to assess the bacterial composition after treatment.

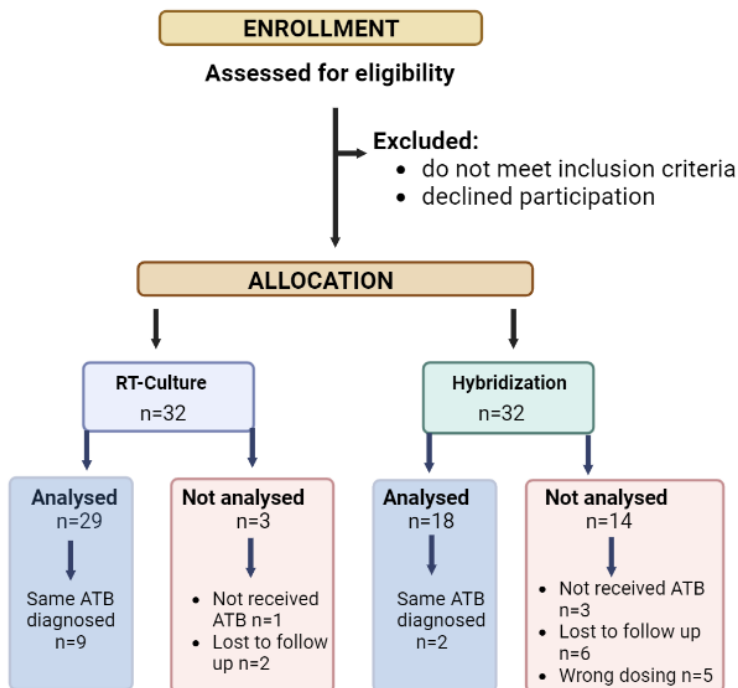


Figure IV-S3. Flow diagram of patient selection. Sixty-four patients who met inclusion criteria and agreed to participate in the study were allocated into two groups for antibiotic selection: RT-culture (n=32) and standard, commercially available hybridization (n=32). After the periodontal and antibiotic treatment, clinical and biological parameters were analyzed. Nine patients of the RT-culture group and two patients of the hybridization group were excluded from the statistical analysis when methodologies were compared because both approaches suggested the same antibiotic. In addition, one patient of the RT-culture group was not analysed, as the patient took a different antibiotic prescribed by another professional because of an additional infection and another two failed to attend their 2-month reevaluation visit to the dental clinic because of COVID. Similarly, six patients from the PCR-hybridization group did not attend all needed dental clinic visits, three did not receive antibiotics and five had incomplete antibiotic dosing.

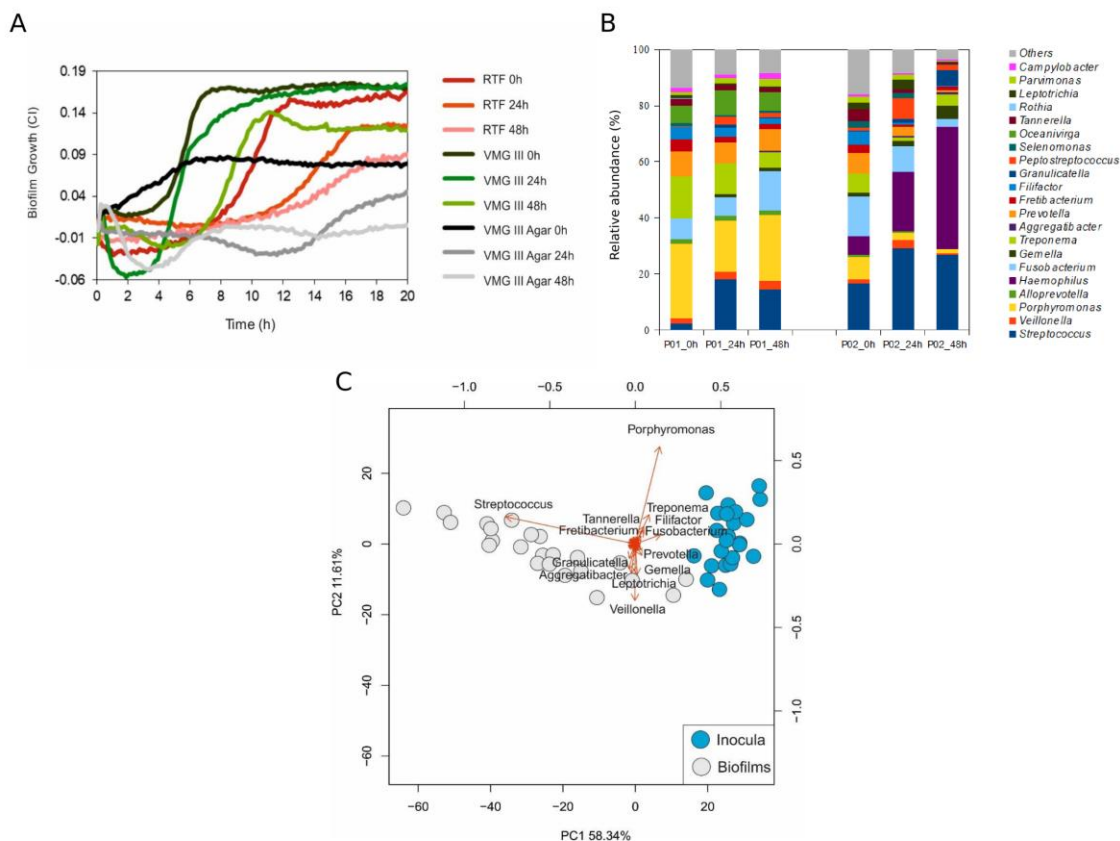


Figure IV-S4. A – *In vitro* periodontal biofilm growth in real-time as measured by impedance after preservation of the subgingival plaque in RTF, VMGIII and VMG III-Agar transport media. Samples of periodontal pockets were stored at room temperature for 0h, 24h and 48h. Then, subgingival samples biofilms were grown in the impedance-based monitoring xCELLigence system in real time. Biofilm growth was expressed as Cellular Index (CI), which correlates to total biofilm mass. Data are means of three replicates. SDs are not shown for clarity. **B** – Bacterial composition in subgingival plaque samples collected from two different periodontal patients after storage in VMGIII transport media for 0, 24 and 48h. **C** – Principal component analysis of subgingival plaque bacterial composition (“inocula”, blue circles) collected in VMGIII growth media and the derived biofilms grown in the impedance xCELLigence system for 8h (“biofilms”, white circles). The red arrows represent correlations of specific bacteria with the principal components (PC1 and PC2).

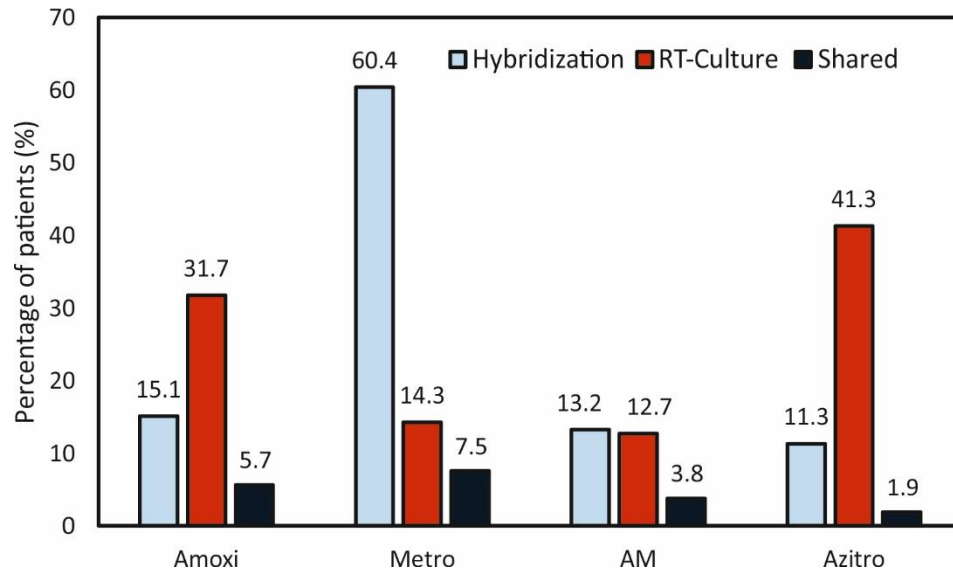


Figure IV-S5. Percentage of cases where each systemic antibiotic was prescribed by standard hybridization of periodontal pathogens and RT-culture methodologies. Amoxi – amoxicillin, Metro – metronidazole, AM – amoxicillin and metronidazole and Azitro – azithromycin. Black bars indicate cases when both methodologies suggested the use of the same conventional therapy (Shared).

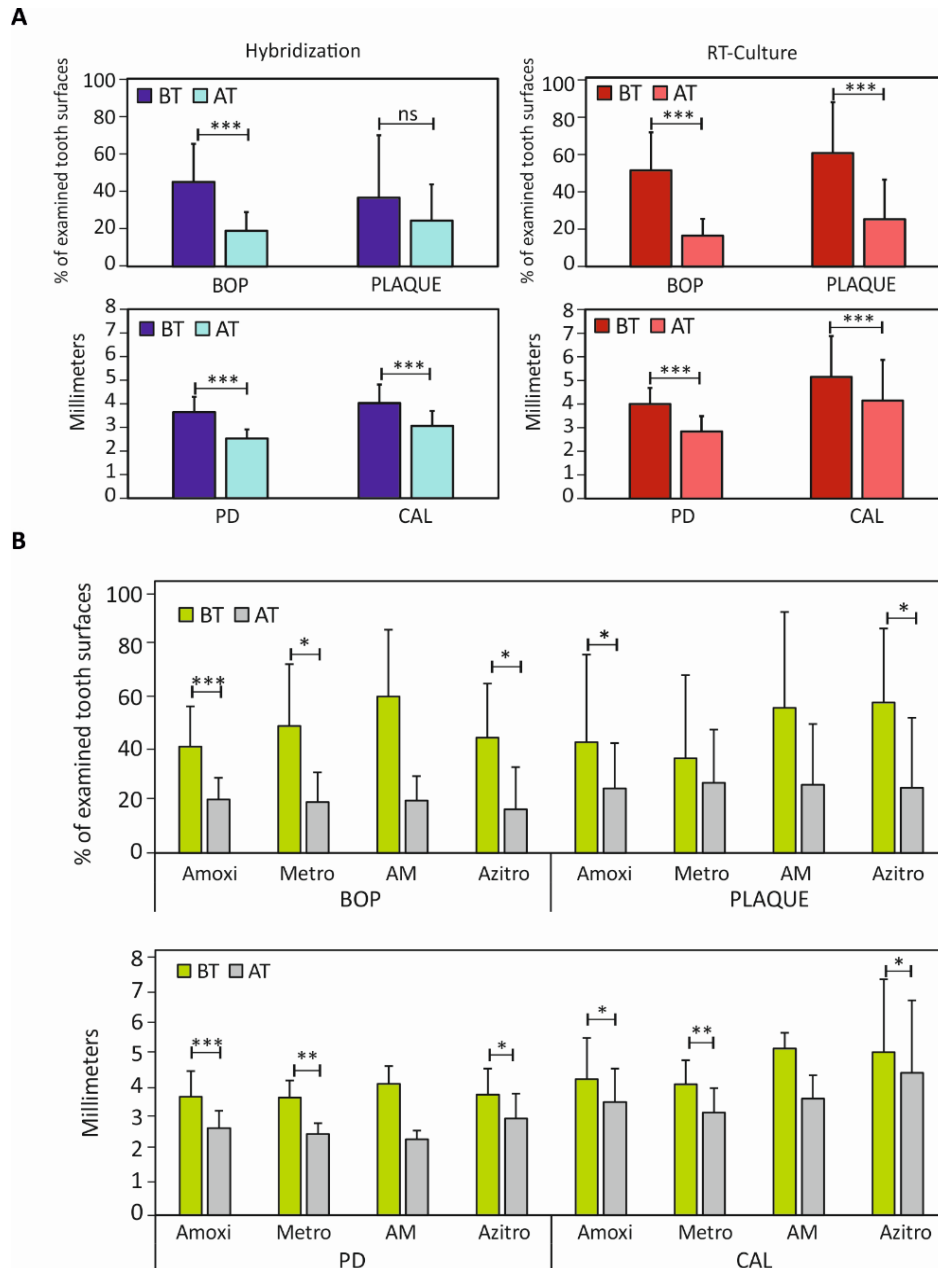


Figure IV-S6. A- Comparison of clinical parameters before and after 2 months of treatment. The percentage of examined tooth surfaces (top) and millimeters of pocket depth (bottom) before and after treatment in patients that used the antibiotic determined by **hybridization** or **impedance (RT-culture)**, and **B-** comparison in clinical parameters in the same patients, grouped by the antibiotic used. **PD** - pocket depth; **CAL**- clinical attachment loss; **BOP** - bleeding on probing; **PLAQUE** – plaque presence; **BT** - before treatment; **AT** - after treatment; **Amoxi**-amoxicillin; **Metro**-metronidazole; **AM**-amoxicillin and metronidazole; **Azitro** - azithromycin. * *p*-value < 0.05, ** *p*-value < 0.01, *** *p*-value < 0.005; **ns** - not significant.

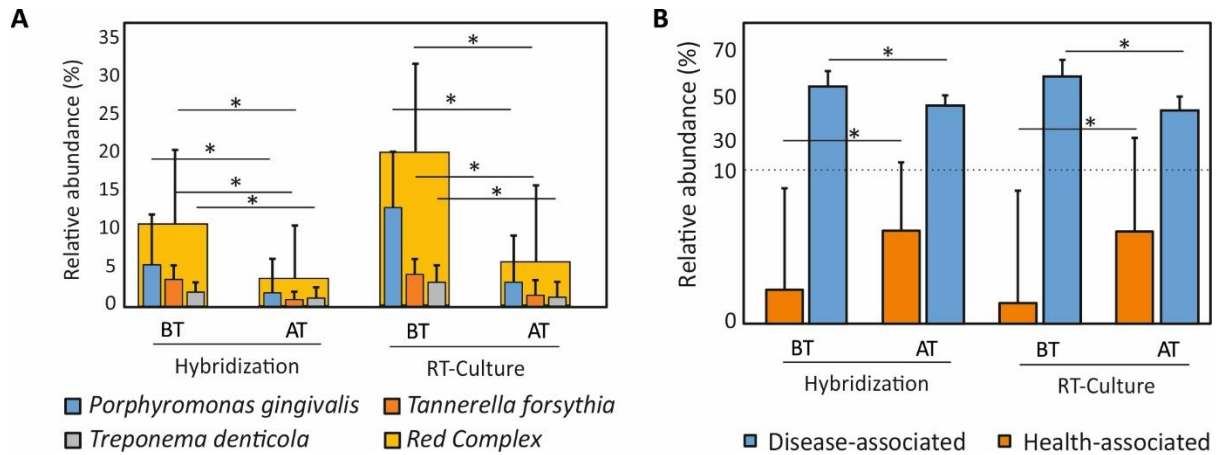


Figure IV-S7. A - Relative abundance of red complex pathogens (%) before and two months after antibiotic treatment in the groups receiving antibiotics selected by standard hybridization and RT-culture methodologies. **B**- Relative abundance of disease and health-associated bacteria before and after two months after antibiotic treatment. **BT** – before treatment; **AT** - after treatment; * *p.value* < 0.05.

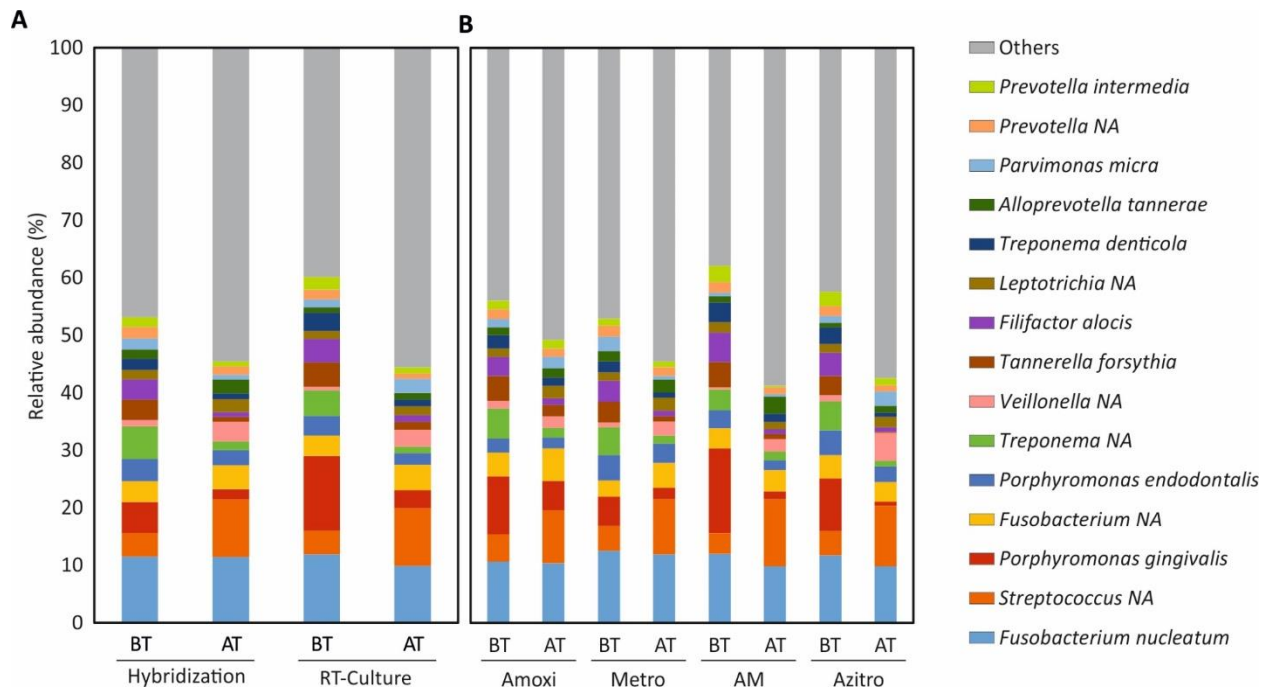


Figure VI-S8. Bacterial species mean abundance (%) in each group studied. **A** – Hybridization vs. RT-Culture system. **B**- Patients grouped by the antibiotic used, regardless of the antibiotic

selection methodology. **BT** - before treatment; **AT** – two months after treatment; **Amoxi**-amoxicillin; **Metro**-metronidazole; **AM**-amoxicillin and metronidazole; **Azitra**-azithromycin.

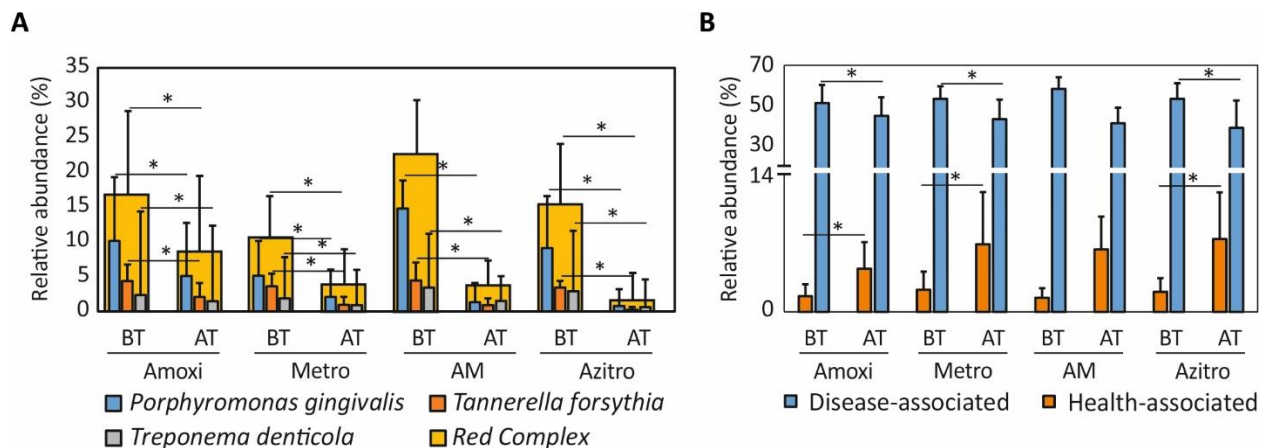


Fig. IV-S9. A- Relative abundance (%) of red-complex pathogens two months after periodontal treatment, compared by the prescribed antibiotic group. **B** – Relative abundance (%) of disease-associated and health-associated bacteria two months after treatment. **BT** -before treatment; **AT** - after treatment; **Amoxi** - amoxicillin; **Metro** - metronidazole; **AM** - amoxicillin and metronidazole; **Azitra** - azithromycin. * $p.value < 0.05$.

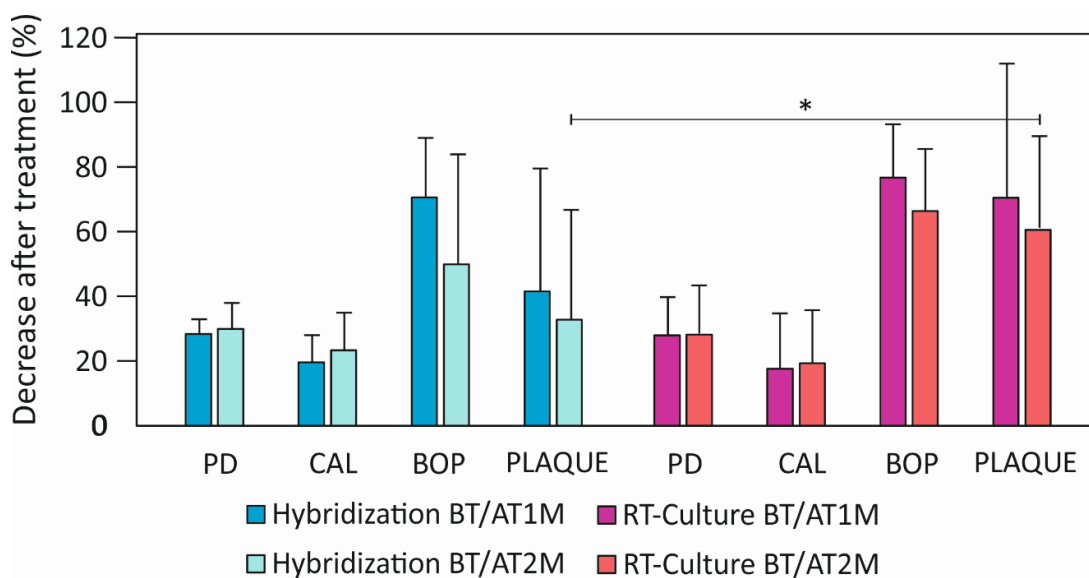


Fig. IV-S10. Comparison of clinical parameters improvement (as a percentage of decrease) one and two months after antibiotic treatment according to the antimicrobial therapy (suggested by standard hybridization methodology or RT-culture). **PD** - pocket depth; **CAL**- clinical attachment loss; **BOP** - bleeding on probing; **PLAQUE** –plaque presence. **p.value* < 0.05.

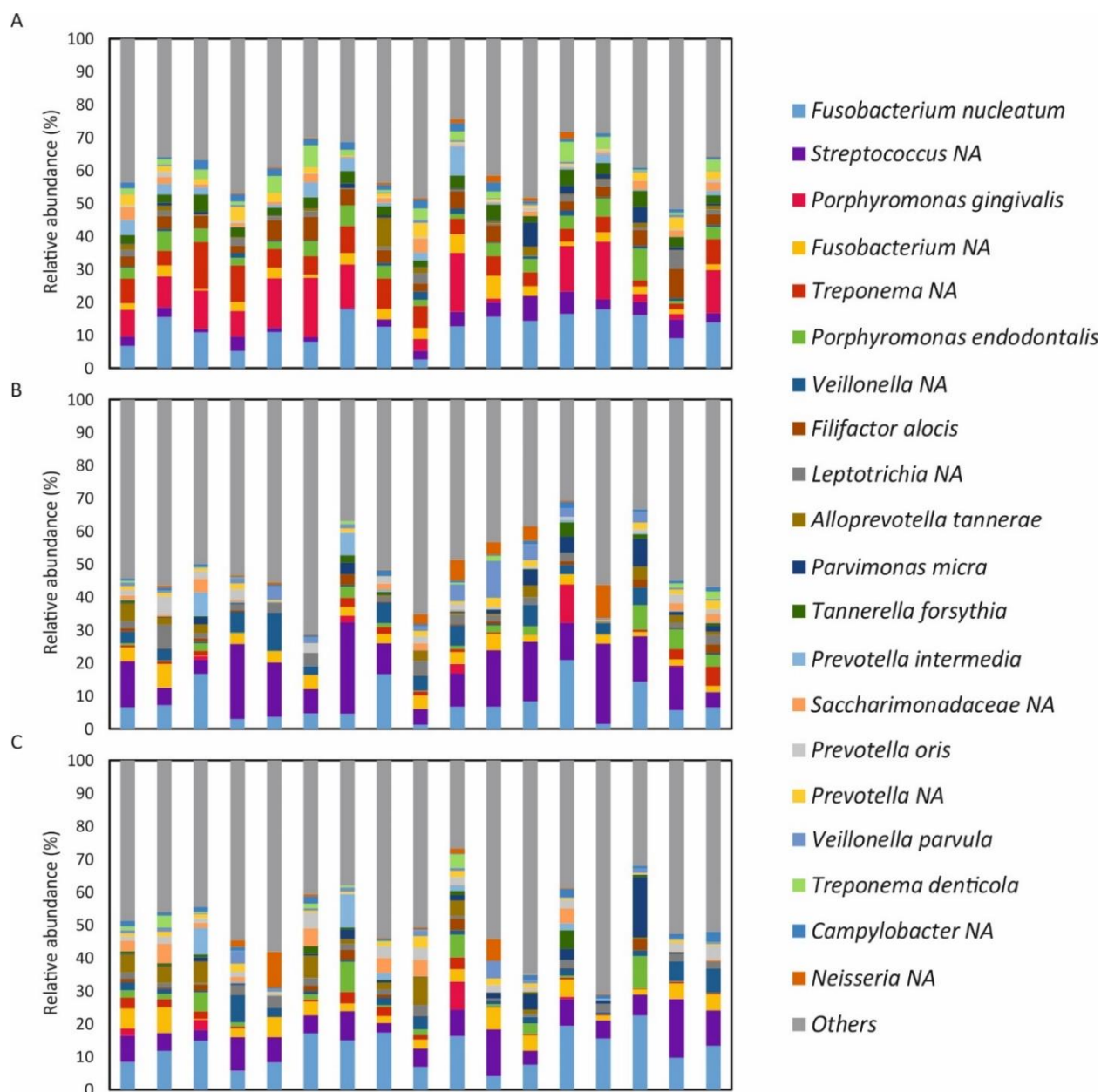


Fig. IV-S11. Bacterial species mean abundance (%) in subgingival dental plaque from individuals before treatment (A), after one (B) and after two months (C) of periodontal treatment

in combination with antibiotics. Each column represents a different patient. Only patients for which samples were available at all three timepoints are included.

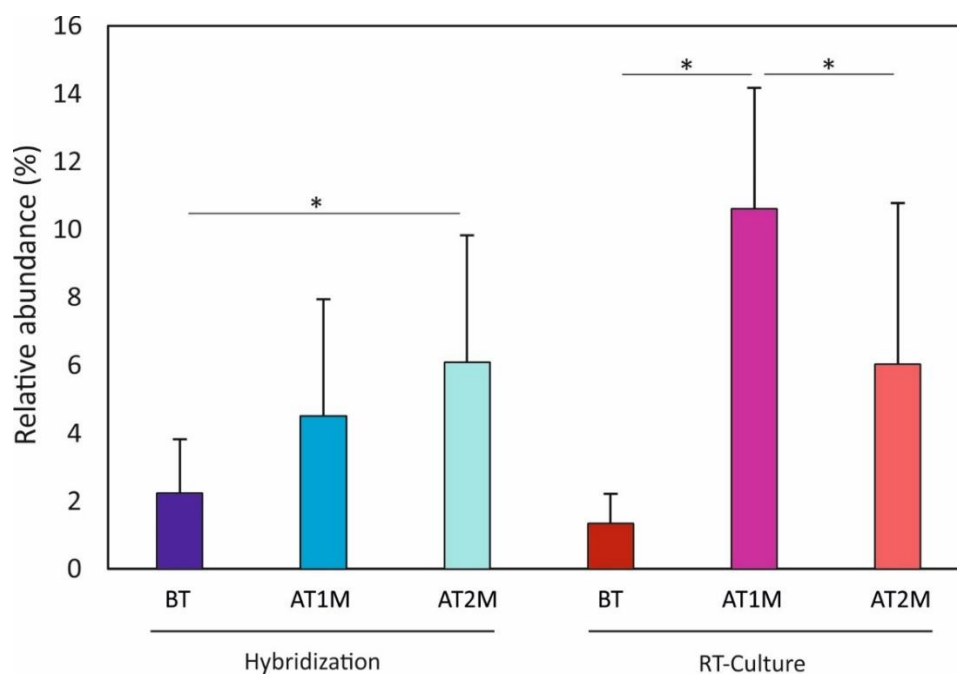


Fig. IV-S12. Health-associated species mean abundance (%) in individuals before periodontal treatment (BT) and after 1 (AT1M) or 2 (AT2M) months of treatment, for the two groups of treatment (selected by conventional hybridization and RT-Culture, respectively). **p-value* < 0.05.

CHAPTER V

Self-propelled nanoparticles for bacterial biofilm eradication

This chapter has been accepted for its publication in the journal of Chemistry of Materials. *IN PRESS*. DOI: 10.1021/acs.chemmater.3c00587

ABSTRACT

Recalcitrance to conventional treatment of different bacteria is closely related to their capacity to adhere to surfaces, secrete a self-produced extracellular matrix and form biofilms. Additionally, biofilm formation is a key factor in multidrug resistance, suggesting the need for new biofilm treatment strategies. Thus, here we report the application of a novel self-propelled Janus nanodevice that consists of a H₂O₂ inducible platinum nanomotor, mesoporous silica nanoparticles loaded with vancomycin and the plant protease ficin that acts as a nanodrill breaking down the biofilm matrix. We show that the exposure of both pre-formed and mature *Staphylococcus aureus* biofilms to these self-propelled nanoparticles results in efficient biofilm detachment and killing. In detail, real-time impedance measurements show that while treatment of pre-formed biofilms with vancomycin alone results in failure, the addition of self-propelled nanoparticles leads to biofilm biomass reduction to up to 82%, highlighting a robust biofilm disassembly capacity. Moreover, viable cell counts indicated that 96% of bacterial cells in the pre-formed biofilms were killed after the application of nanoparticles. Scanning electron microscopy confirmed the efficiency of self-propelled nanoparticles against mature 24h biofilms, as biofilm treated with H₂O₂ activated nanoparticles resulted in almost complete biofilm elimination. These results show an extraordinary capacity of novel nanoparticles against biofilms, especially when compared to vancomycin, ficin or other components alone. Our data indicate a synergistic effect between these compounds when added in the form of nanoparticles and highlight the ability of this nanodevice to eliminate and kill biofilm-embedded bacteria. Thus, we propose the use of self-propelled platinum nanoparticles as a novel tool for biofilm-associated infection treatment.

INTRODUCTION

Biofilms can be described as bacterial aggregates encased in self-produced extracellular substances, that consist of different macromolecules, including proteins, polysaccharides, extracellular DNA and others^{198,408}. Bacterial biofilms are commonly adhered to indwelling medical devices and play a key role in chronic and persistent infections, particularly in immunocompromised patients^{263,409}. Moreover, biofilms are known to be up to 1,000 times more resistant to antibiotic treatment and immune system components when compared to their planktonic forms^{1,26}. Their increased recalcitrance to conventional treatment is often linked to limited antibiotic penetration into deep biofilm layers, activation of efflux pumps and changes in cell metabolic activity^{19,25,27,248}. Thus, biofilm treatment with conventional therapy often results in multidrug resistance and treatment failure highlighting the need to investigate new strategies against biofilm-associated infections^{30,63,159}.

Nanomaterials recently emerged as a potential approach in biomedicine, including clinical diagnostics and infection treatment, as they can be used as drug carriers to infection sites^{259–261}. Additionally, different nanoparticles have been shown to be effective in inhibiting different gram-positive and gram-negative bacteria, spores and viruses^{258,264,274} and some of them were proposed as approaches for intravenous catheter coating or treatment of chronic sinusitis^{265–267}. However, although various metal nanoparticles with antimicrobial properties such as ZnO, MnO, CuO among others have been shown to inhibit the biofilm formation of various bacterial pathogens by several recent studies, disarming pre-formed or mature biofilms is considerably more challenging^{240,258,261,264}. For example, no significant differences were found when the biofilm disruption effect of gentamicin-carrying gold nanoparticles was compared to gentamycin alone in the study performed by Mu and colleagues²⁷². On the other hand, in another study, topical ferumoxytol nanoparticles have been shown to be effective in disrupting *Streptococcus mutans* biofilms both *in vitro* and *in vivo*. However, they were not able to completely kill all bacterial cells embedded within biofilms, as small separate cell clusters were detected after biofilm treatment²⁷³. Therefore, established biofilm disassembly and eradication can only be achieved using nanoparticles that could reach the biofilm backbone, penetrate inner biofilm layers, uniquely interact with the biofilm-embedded bacteria and successfully release the cargo^{268–271}.

Staphylococcus aureus (*S. aureus*) is a leading cause of nosocomial and chronic infections associated with indwelling medical devices and soft tissues, with high morbidity and mortality rates^{15,88}. Although various strategies against *S. aureus* biofilm prevention and eradication, such as the combination of conventional antibiotics with antibiofilm compounds such as DNases and/or proteases, were proposed, they still fail to eliminate biofilms completely^{65,194,410}. For this reason, in the current study, we have tested a novel H₂O₂ inducible platinum nanodevice, which consists of a platinum nanomotor and mesoporous silica nanoparticles loaded with a conventional antibiotic (vancomycin) and capped with the plant protease ficin on pre-formed and mature *S. aureus* biofilms (**Figure V-1**). The rationale of these components lies on conferring movement, matrix breakdown capacity and controlled antibiotic release. Ficin is a protease derived from the Ficus plant, that has been shown to degrade biofilm structural proteins and is expected to work as a “molecular drill” that would facilitate the movement of the nanodevice and the release of the antimicrobial drug to the lower surfaces. Movement is achieved by the chemical degradation of H₂O₂ by platinum, which generates an oxygen gradient that would self-propel the particles when H₂O₂ is available. Finally, a silene-based “molecular gate” keeps the antibiotic inside the porous silica nanoparticle and only releases the cargo under acidic pH, which is a typical chemical feature of biofilms. Given that the cargo release of these novel nanoparticles is sensitive to pH and will uniquely interact with bacterial cells embedded in biofilms, we use impedance measures, viable cell counts and different microscopic techniques to assess their efficiency on established biofilms. Additionally, the synergistic interaction between the self-propelled movement, biofilm matrix breakdown and cell killing using vancomycin is tested by using different combinations of these components in order to validate the use of self-propelled nanoparticles for biofilm-associated infection treatment *in vitro*.

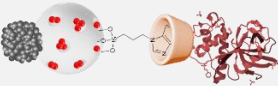
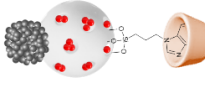
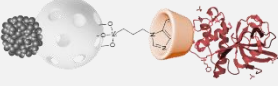
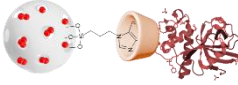
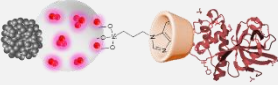
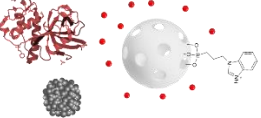
MATERIALS AND METHODS

Synthesis of self-propelled nanoparticles and cargo release experiments

Synthesis of novel nanodevice, consisting of propelling element (platinum nanodendrites), mesoporous silica nanoparticles loaded with vancomycin and anchored with protease ficin (β -cyclodextrin-modified ficin) were synthesized in the Department of Chemistry

of the Polytechnic University of Valencia by Ramón Martínez-Máñez laboratory. In addition to complete nanoparticles, controls lacking different parts of the complete device were also synthesized. The different nanoparticles constructions used in this study are listed in **Table V-I**.

Table V-I. Nanoparticles used in this study. **NMs** – nanomaterials (mesoporous silica nanoparticles) with platinum nanodendrites (H_2O_2 inducible nanomotor), **F** – protease ficin (molecular drill), **bCD**- β -cyclodextrins (molecular gate), **Pt** – platinum (nanomotor), **V** – vancomycin, **V-Rh B** - rhodamine B-functionalized vancomycin.

Nanomaterial	Description	Description
NM_{VF}		FINAL DEVICE: NMs loaded with vancomycin and capped with F-bCD
NM_V		NMs loaded with vancomycin and capped with bCD without ficin
NM_F		Empty NMs capped with F-bCD
MSN_{VF}		MSNs loaded with vancomycin and capped with F-bCD, without PtNDs
NM_{V-RHF}		NMs loaded with V-Rh B and capped with F-bCD *
NA		Non assembled nanodevice: free vancomycin, ficin, bCD, MSN and Pt

* - used for monitoring of cargo release dynamics only

Cargo release experiments performed with the colored dye rhodamine at Ramón Martínez-Mañez laboratory indicated that nanoparticles released loaded cargo under acidic conditions within 1 hour. Furthermore, after nanoparticle construction, 1 mg of nanoparticles contained 23 $\mu\text{g/mL}$ of vancomycin and 25 $\mu\text{g/mL}$ of ficin.

Bacterial strains and growth conditions

Experiments were performed using *S. aureus* strain Sa240 (*S. aureus ssp. aureus* Rosenbach 1884). The strain was subcultured on TSA (Tryptic Soy Agar) plates and grown TSB (Tryptic Soy Broth) (Scharlab) overnight at 37 °C with vigorous shaking at 120 rpm.

Real-time biofilm eradication

To evaluate the effect of different nanoparticles on 6 h pre-formed *S. aureus* biofilms, xCELLigence Real-Time Analyzer was used in accordance with the manufacturer's instructions. The pre-formed biofilm eradication experiments were performed as previously described^{198,215,358}. The biofilm growth was expressed as Cellular Index (CI), which corresponds to total biofilm mass. Briefly, *S. aureus* 240 strain was grown overnight in TSB medium. One hundred microliters of TSB-glu (TSB supplemented with 0.25% of D-glucose) were used for background measurements (in triplicate for each condition). After that, 75 μl of Sa240 bacterial suspension diluted in TSB-glu to $\text{OD}_{600} = 0.153$ were added into corresponding E-plate wells, reaching a final concentration of $\text{OD}_{600} = 0.0875$. This OD corresponds to approximately 10^7 cells.

Subsequently, E-plates were incubated in the xCELLigence system at 37°C, and the biofilm growth was measured for 6h with CIs values registered every 10 min. After 6 h of biofilm growth, the experiment was stopped, and different treatments were added into the corresponding wells of 96- well E-plates. Following the treatments, biofilm growth was monitored for an additional 24 h. Appropriate negative controls were included in each experiment in triplicate. CIs values (total biofilm mass) were obtained by subtracting their respective negative controls.

H₂O₂ effect on planktonic and biofilm growth

To assess the H₂O₂ effect on planktonic Sa240 growth, 100 µL (OD₆₀₀ = 0.175) of bacterial suspensions were added into corresponding 96-well standard plates in triplicate for each condition. After that, 100 µL of H₂O₂ diluted in TSB supplemented with 0.25% filter-sterilized D-glucose (TSB-glu) were added, reaching final H₂O₂ concentrations of 0.35%, 0.30%, 0.25%, 0.20%, 0.15% and 0.1% (v/v). Continuous Sa240 growth was then monitored by means of absorbance (Tecan, Durham, NC, United States) at 610 nm for 24 h at 37°C.

To assess the effect of H₂O₂ on pre-formed biofilms, impedance measurements in the xCELLigence system were used. Briefly, 100 µL of TSB-glu were used for background measurements. Then, the overnight culture of *S. aureus* 240 was diluted to OD₆₀₀ = 0.153, and 75 µL of bacterial suspensions were added into corresponding wells in 96 well E-plates, reaching final OD₆₀₀ = 0.0875. Subsequently, biofilm growth was registered every 10 mins for 6h. After that, 25 µL of H₂O₂ were added into corresponding wells, reaching final concentrations of 0.35%, 0.30%, 0.25%, 0.20%, 0.15% and 0.1% (v/v), respectively, and biofilm growth was monitored for additional 24h.

Viable colony count assay

To assess the number of viable unattached planktonic bacteria after *S. aureus* Sa240 biofilm treatments, the supernatant was collected, and serial 10-fold dilutions were prepared. After that, 100 µl of each dilution were plated on TSA plates. Three biological replicates were plated for each condition. To assess viable cell number in bacterial biofilms, the biofilms were rigorously rinsed using PBS pH 7.4 to eliminate non-adherent cells. Afterwards, the biofilms were collected using 200 µl of PBS and sonicated for 5 min to disrupt the biofilm matrix and release biofilm-embedded bacterial cells. Disrupted biofilms then were serial-diluted and plated in triplicate as described above. TSA plates were incubated at 37°C overnight. After that, viable colonies (CFUs) were counted, averaged, and expressed as log₁₀ CFUs mL⁻¹.

Biofilm visualization by confocal microscopy

To show how nanoparticles interact with the biofilm EPS, Alexa Fluor 488 fluorescent conjugate which binds to N-acetyl neuraminic acid and to polysaccharide adhesins involved in biofilm formation was used. Briefly, *S. aureus* 240 overnight cultures were diluted to $OD_{600} = 0.0875$, and 175 μL of bacterial suspension were added into corresponding wells of IBIDI 80827 $\mu\text{-Slide}$ 8-well plates. After, 25 μL of Alexa Fluor 488, fluorescent conjugate, were added according to manufacturer's instructions. After that, biofilms were grown at 37°C for 6h as described above. Subsequently, the supernatants were removed, and the biofilm was washed with PBS several times. After that, 1 mg mL^{-1} NM_{VF} , 0.15% H_2O_2 NM_{VF} and 0.15% H_2O_2 were added into corresponding wells, and Sa240 biofilms were grown for an additional 24h.

To quantify live cells within bacterial biofilms after treatment with 1 mg mL^{-1} NM_{VF} , 0.15% H_2O_2 NM_{VF} and 0.15% H_2O_2 , SYTO9 fluorescent dye that binds to microbial DNA (FilmTracer™ *LIVE/DEAD Biofilm Viability Kit*) was employed. Biofilms were grown as described above. After that, treatments were added into corresponding wells, and Sa240 biofilms were grown for an additional 24h. Subsequently, the supernatant was discarded, biofilms were carefully rinsed with PBS to eliminate unattached cells and stained with 200 μL of SYTO9 solution (working solution 3 μL of SYTO9 in 2 mL of sterile water) for 20 min in the dark. After biofilm staining, the dye excess was removed by gently washing using PBS. After that, CLSM image acquisition was carried out. To acquire the signals, a 679 nm excitation laser and 702 nm emission filters were used for Alexa Fluor 680-dextran conjugate, and a 488 nm laser and 505-550 emission filter were used for SYTO9.

Scanning electron microscopy

To evaluate biofilm spatial structure after the treatments, scanning electron microscopy (SEM) was used. *S. aureus* 240 overnight culture was adjusted to $OD_{600} = 0.0875$, and the biofilms were grown on separate gold electrodes for 24h. After that, biofilms were treated with self-propelled nanoparticles in the presence and absence of H_2O_2 , vancomycin and ficin combination, and vancomycin alone for 6h. Then supernatants were discarded, and biofilms were gently washed with PBS to eliminate non-adherent cells. Prior to observations, biofilm samples

were fixed with Karnovsky's fixative for 4h, rinsed with PBS three times and dehydrated using gradual ethanol series (30%-50%-70%) twice. Then, the samples were dried using critical point drying with CO₂. Subsequently, the samples were observed at Electron Microscopy Service (Valencia University, Spain) using Hitachi S-4800, applying an accelerating voltage range of 0.5 kV and a magnification range of x2.50k.

Statistical analysis

In order to study the differences between CIs, regression analysis was assessed by a linear model at 24h of biofilm growth, using the lm library in the R Statistical Package version 1.0.7.1.⁴¹¹ Statistical differences in viable cell number were assessed using Student's t-test. The data were presented as mean \pm SDs from triplicates of three independent experiments for each condition (n=9). For comparisons between means in CLSM analysis, ordinary one-way ANOVA and Dunnett's multiple comparison test were employed (n=3). P-values < 0.05 were considered as significant.

RESULTS

Effect of H₂O₂ on planktonic and biofilm growth

Given that one of the components of the novel nanoparticles is the H₂O₂ inducible nanomotor, which would allow nanoparticles to move and disrupt biofilm architecture, we first tested whether H₂O₂ alone affects planktonic or biofilm growth of *S. aureus* 240 strain. Absorbance measurements showed that when peroxide was added together with bacterial inoculum, none of the tested concentrations ranging from 0.10 to 35 % could inhibit or delay planktonic *S. aureus* Sa240 growth when compared to the untreated control (**Fig. V-2A**). On the contrary, impedance measurements in real-time revealed that the exposure of 6h *S. aureus* Sa240 biofilms to 0.35% of H₂O₂ resulted in biofilm detachment. At the same time, other concentrations did not affect further biofilm growth and development (**Fig. V-2B**). Thus, we selected a concentration of 0.15% of H₂O₂ for self-propelled nanodevice activation and tested whether this concentration had any effect on cell viability in both biofilm and supernatant. Viable cell counts showed that 0.15% of H₂O₂ had no effect on cell viability in residual biofilm or supernatant when

compared to untreated control (**Fig. V-2C**) and therefore can be used for motion activation without causing biofilm disassembly or resulting in its killing.

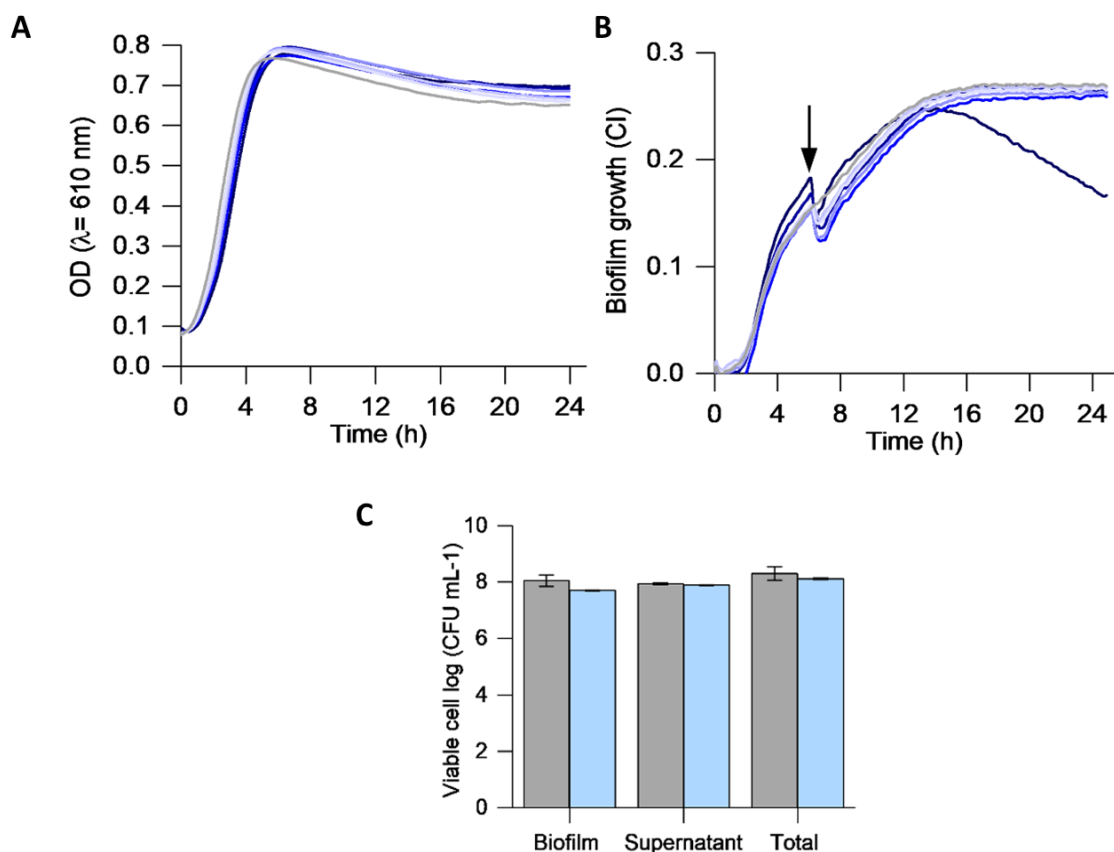


Figure V-2. **A** -Effect of different H₂O₂ concentrations: 0 (grey), 0.10, 0.15, 0.20, 0.25, 0.30 and 0.35% (from light blue to dark blue) on planktonic *S. aureus* growth, measured as optical density (OD) in the presence of H₂O₂ for 24 h. **B** - Effect of H₂O₂ on *S. aureus* Sa240 biofilm, as measured by means of CI impedance values. The concentrations ranging from 0 to 0.35% of H₂O₂ were added at 7h of biofilm growth (indicated by a black arrow). **C** - Bacterial cell viability of biofilm and supernatant after the addition of selected 0.15% of H₂O₂ (blue bars), expressed as log (CFU mL⁻¹) ± SE. (n=3). Grey bars indicate untreated control.

Anti-biofilm and antimicrobial capacity of self-propelled nanoparticles on pre-formed *S. aureus* biofilms

In order to evaluate the effect of self-propelled mesoporous nanoparticles on pre-formed *S. aureus* biofilms, impedance measurements in real time in combination with viable cell counts were used (**Fig. V-3B** and **Fig. V-S1A**). Pre-formed 6h *S. aureus* biofilms were treated with 1

mg/mL (contains 23 $\mu\text{g/mL}$ of vancomycin and 25 $\mu\text{g/mL}$ of ficin) of complete nanoparticles (**NM_{vF}**) in the presence or absence of H_2O_2 (activated and not activated, respectively), free vancomycin (**V**) (final concentration 23 $\mu\text{g/mL}$), free ficin (final concentration 25 $\mu\text{g/mL}$) (**F**), or with a combination of both compounds (**VF**). Impedance measurements showed that free vancomycin reduced total biofilm mass by only 4% at 24h of biofilm growth. On the contrary, the combination of vancomycin and ficin reduced biofilm mass up to 34%, suggesting a possible synergy between these two compounds. As expected, non-activated **NM_{vF}** reduced biofilm biomass by up to 33%, almost identically to when free VF combination was administered on pre-formed *S. aureus* 240 biofilm. Finally, pre-formed biofilm treatment with the activated, H_2O_2 -fueled **NM_{vF}** resulted in 82% biofilm mass reduction in only one hour of treatment and up to 72% at 24 h compared to the untreated control (**Fig. V-3B**).

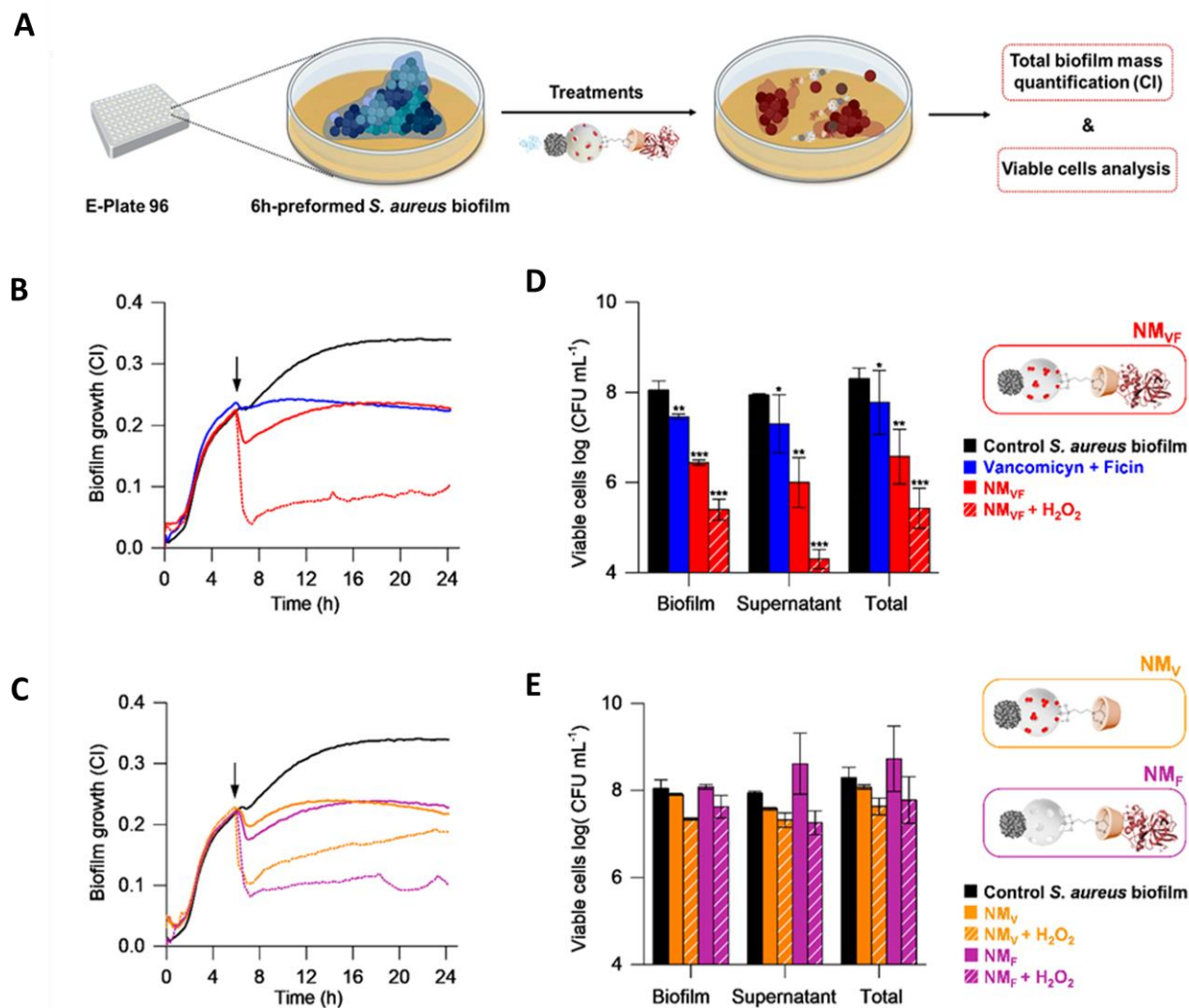


Figure V-3. Anti-biofilm capacity of self-propelled nanoparticles NM_{VF} on pre-formed 6h *S. aureus* biofilms. **A** - Schematic representation of the experimental procedures used to evaluate the effect of NM_{VF} and control nanodevices on pre-formed *S. aureus* biofilm growth. **B** - Biofilm growth, as quantified by impedance measurements after treatment with free VF (blue), non-fueled NM_{VF} (red), and NM_{VF} in the presence of 0.15% H₂O₂ (red striped), (data presented as means, n=3). **C** - Biofilm growth, as quantified by impedance measurements after treatment with control nanodevices, NM_V (orange) and NM_F (purple), in the absence and presence of 0.15% H₂O₂ (striped), (data presented as means, n=3). **D** and **E** - Bacterial cell viability in biofilms and supernatants after the same treatments, expressed as log (CFU mL⁻¹) ± standard error of the mean (SE). Statistically different CFUs counts were assessed at 24 h or growth. T-Test values * p<0.05, ** p<0.01, ***p<0.001.

Additionally, the effect of incomplete nanomotors, **NM_v** (nanoparticles loaded with vancomycin but without ficin) or **NM_f** (nanoparticles without vancomycin, capped with ficin), on biofilm disruption was evaluated. Real time pre-formed biofilm eradication assays showed that both control nanodevices (**NM_v** or **NM_f**) were able to reduce preformed biofilms to a similar degree when compared to free **VF** treatment. In addition, when both nanodevices were activated with 0.15% H₂O₂, biofilm biomass was reduced up to 44% for **NM_v** and 68% for **NM_f**, respectively (**Fig. V-3C**).

After the efficacy of the complete nanodevice and its respective controls to detach pre-formed biofilms was assessed, we further evaluated their antimicrobial capacity. The number of viable bacteria was determined in the remaining biofilm and in the supernatant (**Fig. V-3D**). Both free V and VF treatments showed a low capacity (<1 log decrease) to reduce cell viability in the supernatant, and this effect was even weaker for bacteria embedded in the residual biofilms (**Figs. V-3D and V-S1B**). In contrast to these results, total cell viability was reduced by almost two orders of magnitude when biofilms were treated with **NM_{vf}** in the absence of H₂O₂. On the other hand, the activation of movement by the propelling element in **NM_{vf}** led to the efficient killing of biofilm-embedded and free-floating bacterial cells, reaching over 3-logs reduction in viable cells when compared to untreated controls. Likewise, the biocidal effect of incomplete nanomotors, **NM_f** or **NM_v**, was evaluated on both biofilms and supernatants. Similarly to the effect with free ficin, **NM_f** in the presence or absence of H₂O₂ did not produce a reduction in cell viability, neither in the biofilm nor in the supernatant (**Fig. V-3E**). This suggests that ficin alone has a strong biofilm detachment capacity but does not confer bactericidal activity. Similar results were observed for **NM_v**, suggesting that while this antibiotic is capable of killing detached bacterial cells, it cannot penetrate deep biofilm layers. Finally, we also tested the effect of the control **MSN_{vf}** (complete nanodevice, without H₂O₂-inducible nanomotor) and the unassembled nanodevice, where all elements were added planktonically (**NA**) on bacterial cell viability. Results shown in **Fig. V-S2** indicate that neither **MSN_{vf}** nor **NA** showed a significant decrease in cell viability.

Effect of the self-propelled nanoparticles on biofilm matrix

To visualize the effect of NM_{VF} on biofilms, the EPS of pre-formed 6 h *S. aureus* biofilms were labeled using an Alexa Fluor 647-dextran conjugate and treated with 0.15% H_2O_2 , 1 mg/mL of NM_{VF} or 1 mg/mL and NM_{VF} + 0.15% H_2O_2 . A significant reduction in the area covered by the EPS matrix (labeled in red) is observed after the application of H_2O_2 -fueled NM_{VF} , whereas the non-fueled NM_{VF} or 0.15% H_2O_2 did not show any significant effect (Fig. V-4A). Additionally, biofilm 3D reconstruction using ImageJ software indicated the ability of activated self-propelled nanoparticles to destroy biofilm matrix when compared to untreated control (Fig. V-4B). When the effect of activated nanodevice (NM_{VF}) was compared to untreated control, it resulted in the reduction of EPS surface area by up to 66% (Fig. V-4C), confirming previous results obtained using real time impedance measurements.

Besides the assessment of biofilm matrix changes after treatment with activated and non-activated nanodevices NM_{VF} , the percentage of viable bacterial cells within *S. aureus* biofilms were quantified by CLSM. In this case, pre-formed *S. aureus* biofilms were incubated with 0.15% H_2O_2 , 1 mg/mL NM_{VF} or 1 mg/mL NM_{VF} + 0.15% H_2O_2 for 24 h and then stained using SYTO9 green. CLSM images showed a drastic decrease in live cells when biofilms were treated with NM_{VF} in the presence and absence of H_2O_2 (Fig. V-4D). Notably, H_2O_2 -fueled NM_{VF} produced a 96% decrease in viable cells compared to the untreated control, whereas H_2O_2 alone did not significantly affect cell viability in the biofilm (Fig. V-4E).

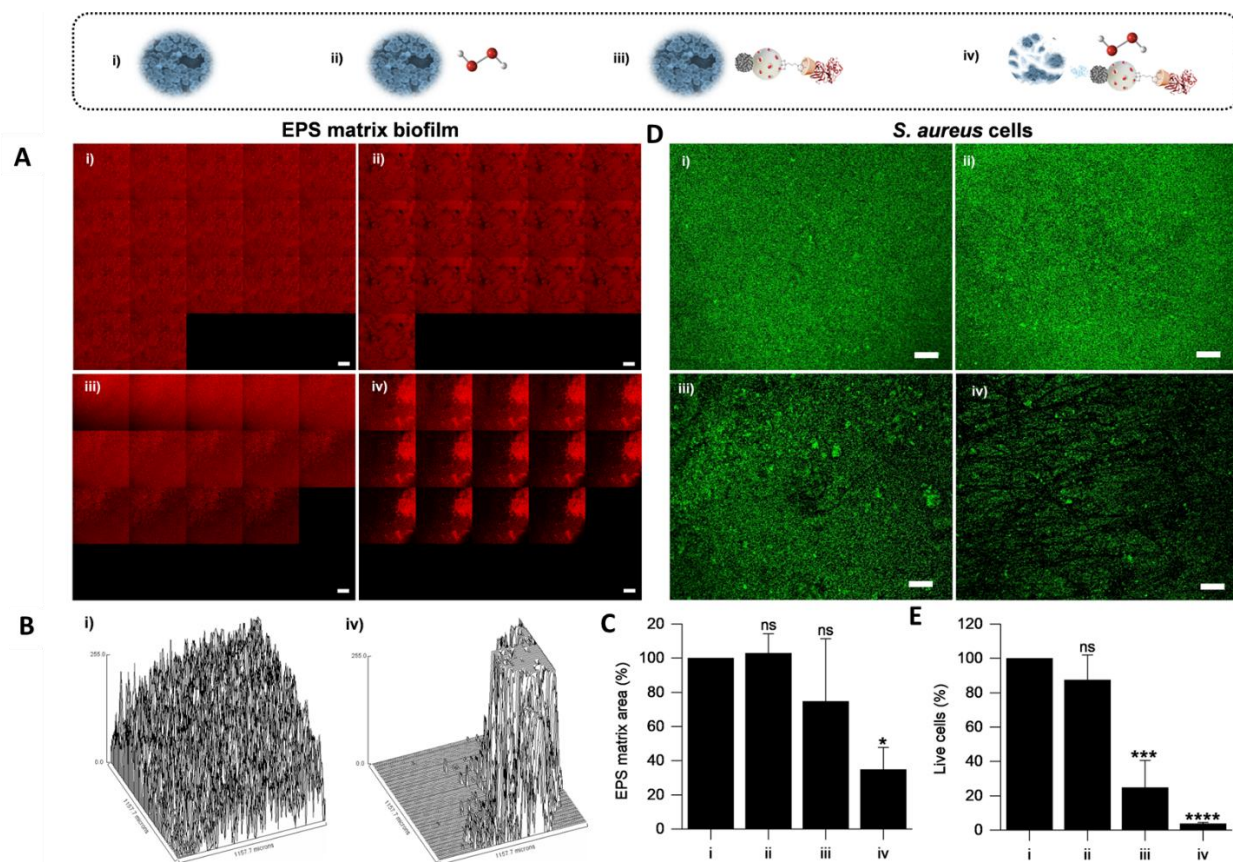


Figure V-4. Disruption of biofilm EPS and quantification of live cells present in pre-formed *S. aureus* biofilms after treatment with self-propelled nanoparticles. Experimental groups are untreated control (i), 0.15% H₂O₂ (ii), 1 mg/mL NM_{vF} (iii) and 1 mg/mL NM_{vF} + 0.15% H₂O₂ (iv). **A** - CLSM analysis of *S. aureus* biofilms labeled with Alexa Fluor 680-dextran conjugate after 24 h of treatment. Each of the 20 images shows the area covered by EPS (in red) in the biofilm stacks, micrographs are taken from top to bottom. **B** - 3D reconstruction of the top biofilm layer of control (i) and H₂O₂ activated NM_{vF} (iv) at 24 h. Biofilm reconstructions were performed using ImageJ software. **C** - Quantification of matrix glucan in the top layer of biofilms after i-iv treatments, expressed as area percentage \pm SE at 24 h. **D** - CLSM images showing viable cells stained with SYTO9 (green) remaining after 24 h of treatment. **E** - Fluorescent-based quantification of live cells, expressed as percentage \pm SE regarding the control. Areas covered by the matrix and live cells' fluorescent intensity were estimated by Image J software (n=3, one-way ANOVA and Dunnett's multiple comparison test, *p<0.05, ****p<0.0001, ns - nonsignificant). Scale bar: 200 μ m.

The ability of self-propelled nanoparticles to eradicate mature staphylococcal biofilms was confirmed using scanning electron microscopy (SEM) after 24h of treatment. SEM micrographs in **Figure V-5** show that the combination of vancomycin and ficin and non-fueled

NM_{VF} had an effect on biofilm architecture by reducing the number of biofilm-embedded bacteria. The larger EPS destruction and the lowest levels of bacterial clusters embedded within the biofilm matrix were seen in the biofilms treated with H₂O₂-fueled NM_{VF}, indicating a strong anti-biofilm capacity.

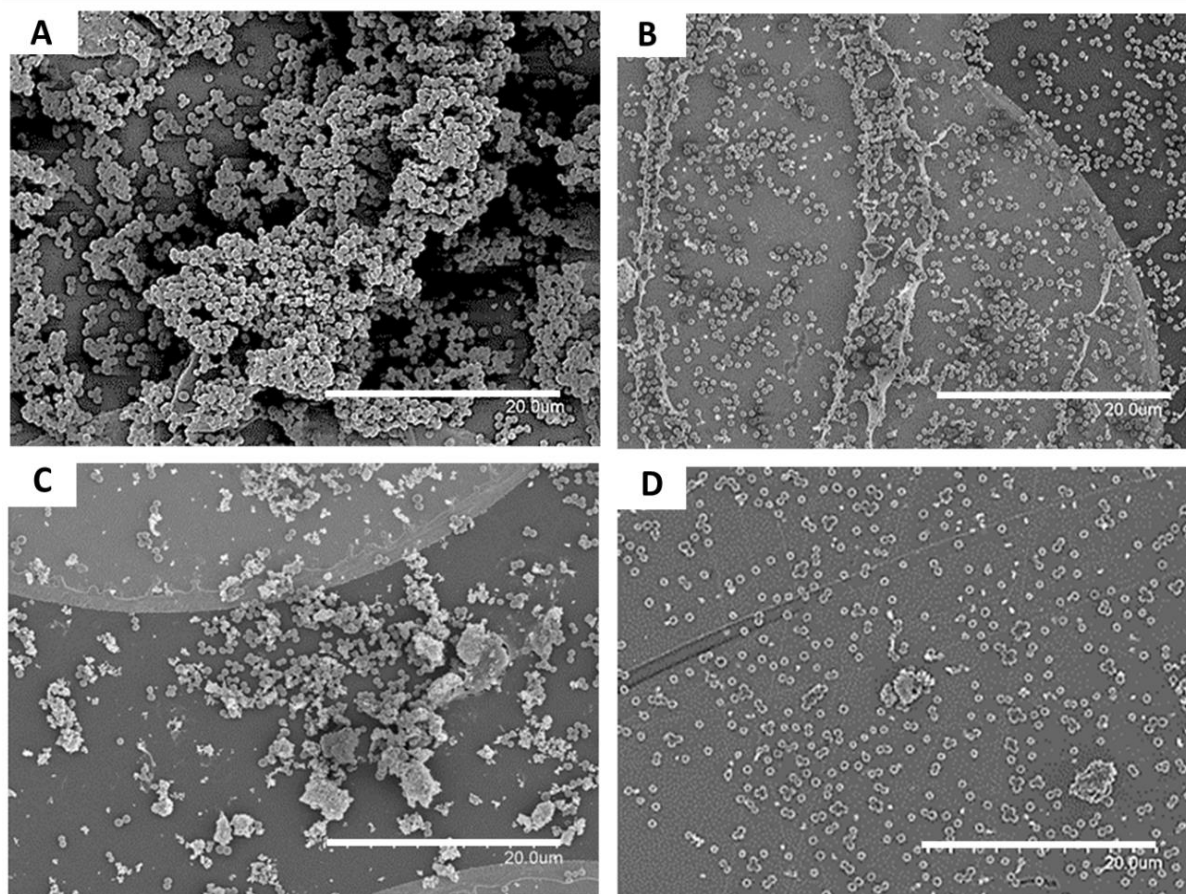


Figure V-5. Scanning electron microscopy (SEM) micrographs of 24h mature *S. aureus* 240 biofilms. **A** - Untreated control, **B** - Biofilms treated with VF, **C** - Biofilms treated with a NM_{VF} in the absence of H₂O₂, **D** - Biofilms treated with NM_{VF} and fueled with 0.15% of H₂O₂. Scale bar: 20 μ m.

DISCUSSION

Many microorganisms grow attached to biotic and abiotic surfaces embedded in a self-produced extracellular matrix and form biological structures called biofilms^{78,412}. In fact, more than 80% of bacterial infections in the human body are associated with biofilms responsible for

increased mortality rates⁴⁰⁹. In addition, bacterial cells encased in a biofilm matrix are highly recalcitrant to antimicrobials and antibiofilm compounds. This recalcitrance is related to the inability of conventional antibiotics to penetrate the biofilm backbone⁸⁸. Although multiple studies have applied many different approaches against bacterial biofilm prevention and eradication, most of them concluded that existing therapies lack the efficacy on pre-formed and mature bacterial biofilms^{107,162,235,242,277}. For this reason, novel works suggested using nanomaterials such as nanowires, microtubes, Janus-based nanoparticles and others as drug delivery vehicles for biofilm elimination and killing^{413–415}. While some of them have been shown to prevent biofilm formation and accumulation, and others could detach pre-formed biofilms, their lack of efficacy against established bacterial biofilms highlights the need to increase their efficacy in biofilm eradication^{240,416,417}.

S. aureus is considered one of the most notorious pathogens capable of forming robust biofilms in clinical settings, especially on indwelling medical devices^{193,418}. Thus, in the current manuscript, we use staphylococcal biofilms as a model to evaluate the efficacy of a novel nanodevice that includes movement, antibacterial activity and matrix disruption capacity. In this proof of principle, we test the self-propelled nanodevice using H₂O₂ as the fuel for the nanomotor, mesoporous Janus nanoparticles loaded with vancomycin and ficin as a biofilm-degrading enzymatic drill as a new anti-biofilm strategy against pre-formed and established staphylococcal biofilms. However, the system developed in this study is highly versatile, and the fuel, the drilling enzyme or the cargo could be changed, depending on the specific application, to other compounds. For instance, our team is currently testing a similar construction containing the antiseptic chlorhexidine to treat endodontic infections, and another one with an antifungal drug and a different protease, with promising results against *Candida* biofilms. The molecular gate can also be modified to respond to other stimuli, ranging from alkaline pH to the attachment to specific targets, paving the way for selective antibiotic treatment. In the current study, impedance measurements in real time showed that self-propelled nanoparticles were capable of disrupting pre-formed *S. aureus* biofilms up to 82%. On the contrary, free vancomycin was incapable of reducing biofilm biomass. To our knowledge, this extent of biofilm mass reduction in *S. aureus* had never been achieved by any existing conventional therapy^{198,410}.

Additionally, the results described in this study suggest that the nanodevice moves toward inner biofilm layers creating channels through the biofilm backbone while releasing vancomycin. In agreement with this, viable colony counting showed that self-propelled nanoparticles result in a decrease in cell viability in both supernatant and residual biofilm over 3-logs when compared to untreated controls, highlighting their biocidal capacity. Moreover, CLSM analysis of different biofilm layers using Alexa Fluor 647-dextran conjugate showed that H₂O₂ inducible nanoparticles significantly reduced the area covered by the EPS matrix, while H₂O₂ alone did not have any significant effect. Similar findings were obtained after the quantification of dead bacterial cells within bacterial biofilms. Thus, CSLM data indicated H₂O₂ activated **NM_{VF}** led to a decrease in viable cells within the biofilm by over 95% when compared to the untreated control, supporting results obtained by impedance measurements and viable colony counts.

Furthermore, we tested the capacity of the self-propelled nanodevice to interfere with mature 24h biofilms using SEM imaging. Obtained results were consistent with those obtained on 6h biofilms. For instance, non-activated nanodevices seemed to detach bacterial cells embedded in biofilms. However, some cell aggregation could be seen after the treatment. On the contrary, H₂O₂ activated **NM_{VF}** completely destroyed biofilm architecture compared to untreated controls and to the free vancomycin-ficin combination. Similar results were seen by Liu and colleagues who tested topic ferumoxytol nanoparticles against oral biofilms and tooth decay *in vitro* and *in vivo*²⁷³.

Taken together, the *in vitro* results performed in this study strongly suggest the use of novel nanoparticles as a targeted approach to treat biofilm-associated infections. These would include tissues in which endogenous H₂O₂ is present or released such as those that occur in the wound inflammatory response or in vaginal infections, where the presence of H₂O₂ producing *Lactobacillus* would facilitate cargo release from the nanodevice. Additionally, self-propelled nanoparticles could also be used to treat oral infections caused by opportunistic pathogens such as different *Candida spp*, with the aid of hydrogen peroxide mouth rinses⁴¹⁹. Another application of these nanoparticles could also be their use in environments where H₂O₂ is widely applied as a potent surface disinfectant in diverse areas, such as the medical and alimentary industries, to improve sterilizing methods in these fields. Besides surface sterilization, nanodevices could be

developed as a new approach to sterilize indwelling medical devices before their implantation in the human body in order to prevent biofilm formation and infection risk, especially in immunocompromised patients⁴²⁰. We hope that the proof of concept of this triple-strategy combination in a single nanodevice will stimulate further research in the field by the implementation of alternative self-propelling fuels, antimicrobial cargos and enzymes and the validation of the system in relevant environments, both *in vitro* and *in vivo*.

CHAPTER V SUPPLEMENTARY INFORMATION

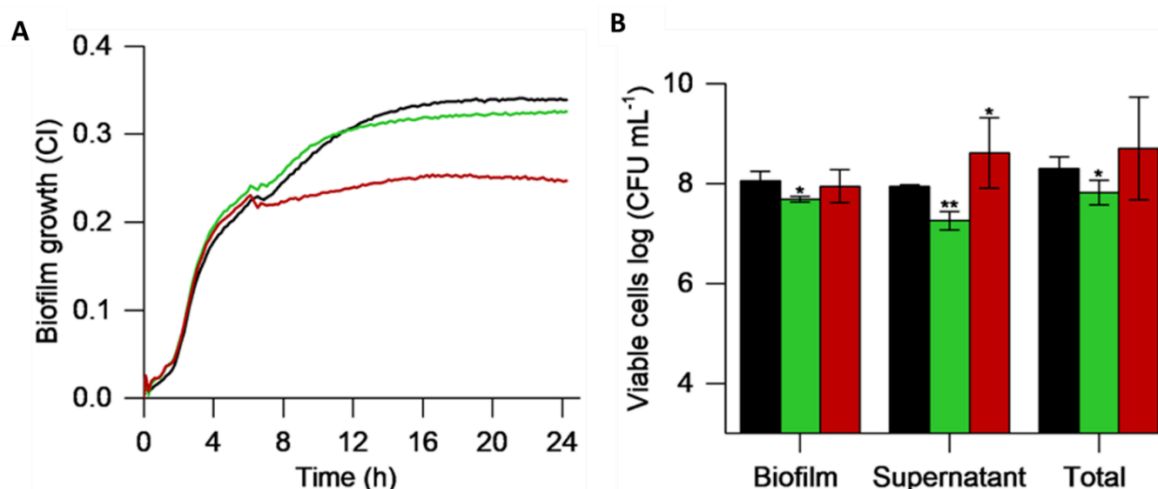


Figure V-S1. Comparative effect of F (red) and V (green) on pre-formed *S. aureus* biofilms **A** Biofilm biomass (CI) (treatments were added at 6 h). All treatments were added at 6h of biofilm growth (indicated by black arrow). SDs are not shown for clarity. **B** - Bacterial cell viability in biofilms and supernatants after different treatments, expressed as log (CFU/mL). (n=3, T-test values *p<0.05, **p<0.01, ***p<0.001, ns - non-significant). Treatment concentrations were 23 $\mu\text{g/mL}$ of vancomycin and 25 $\mu\text{g/mL}$ of ficin, respectively. Black bars indicate untreated controls.

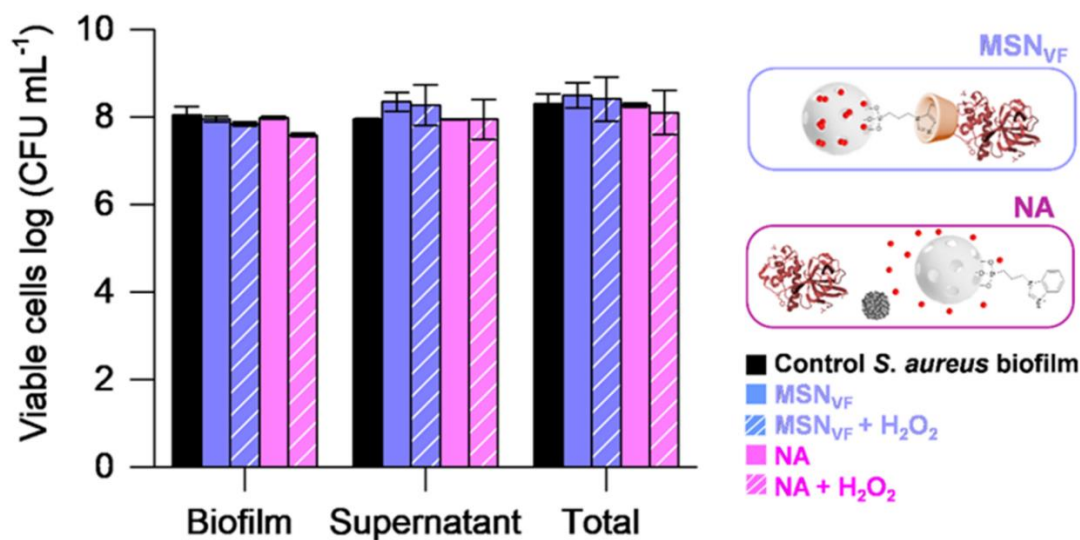


Figure V-S2. Bacterial cell viability in pre-formed *S. aureus* biofilms and supernatants after treatments with control MSN_{VF} (in the absence of H₂O₂, light blue/ in the presence of H₂O₂,

stripped blue) and **NA** (in the absence of H_2O_2 , light purple/ in the presence of H_2O_2 , stripped purple), expressed as log (CFU/mL). The experiment included three biological replicates ($n=3$, $p > 0.05$ (T-test) in all cases). Treatment concentrations: 1 mg/mL **MSN_{vF}** or **NA** in the absence or presence of 0.15% of H_2O_2 .

GENERAL DISCUSSION

1. The challenge of studying and combating biofilms

Bacterial and fungal biofilms not only pose harm to the industry but also are closely related to increased morbidity and mortality rates of infectious diseases as most of the medically relevant microorganisms can grow surrounded by EPS matrix^{1,15}. In fact, different authors have highlighted that more than 80% of infections in the human body are linked to the capacity of gram-positive and gram-negative bacteria and fungi to produce surface-related and tissue-associated biofilms^{64,159}.

Recent studies also underlined that one of the most important features of biofilms is their extreme resistance to antibiotics, antifungals, different antimicrobial compounds and immune system elements, including polymorphonuclear leucocytes and macrophages^{1,306,320,421}. For this reason, numerous efforts and methods have been employed to detect and study microbial biofilms^{28,170,179,422}.

However, the main drawback of most static methods for biofilm examination is based on end-point measurements and need more reproductivity. They also involve various manipulation steps, leading to scattered results, while dynamic methods are costly, time-consuming or even require special training^{169,179}. Thus, the work described in this doctoral thesis comprehensively describes the development of a novel continuous, inexpensive and non-invasive impedance measurements-based xCELLigence system for both mono- and complex polymicrobial biofilm studies. Additionally, the results described in different chapters of this thesis highlight the necessity of studying global biofilm growth dynamics instead of using classical single-end point methods, as biofilm growth patterns play a crucial role in understanding biofilm physiology, behaviour and resistance¹. Additionally, different chapters of this doctoral thesis describe the real-time *in vitro* effect of already existing and new antimicrobial therapies against biofilm formation and disassembly, as well as identify new approaches and the possibility of selecting individualized treatment against biofilm-forming microorganisms, including both bacteria and fungi.

2. Are all biofilms the same?

Traditional end-point methods such as crystal violet staining, viable colony counts, and microscopic techniques are commonly used to analyze gram-positive, gram-negative, and fungal biofilm^{164,170}. However, various authors have concluded that biofilm formation capacity, growth and maturation, along with behavior and architecture of different bacteria and fungi, are highly species- or even strain-specific^{1,102,115,290}. For example, a recent study showed that biofilm features and formation capacity of the same strain could vary depending on the surface properties, including hydrophobicity and topography⁴¹. Additionally, robust differences in gene expression patterns related to surface sensing and hydrophobicity in *P. aeruginosa* were found⁴²³. Another study by Silva and colleagues assessed that *Candida* spp. biofilm formation, development and architecture are highly species dependent⁴²⁴, while Kaneko and colleagues proved that azole group antifungals can provoke robust phenotypical changes in biofilm architecture and its spatial structure¹¹⁵. Thus, to understand and detect this biofilm specificity could also be relevant for addressing strategies to combat biofilms.

Regarding this biofilm heterogeneity, the results described in this doctoral thesis highlight the importance of studying biofilm formation capacity and eradication patterns for each isolate individually, as all tested strains showed differences in biofilm growth dynamics. For instance, CI values observed for gram-positive bacteria (**Chapter I**) were lower compared to those of biofilm-forming *P. aeruginosa* isolates (**Chapter II**) or fungal biofilms (**Chapter III**), suggesting that cell size might influence biofilm formation. Additionally, impedance data showed certain differences in final CI values when different bacterial and fungal growth media were used for biofilm cultivation. For example, *P. aeruginosa* isolates showed higher biofilm formation capacity in LB growth media without additional glucose when compared to BHI or TSB (or even LB supplemented with glucose). In fact, the use of TSB growth media (both supplemented with 0.5% of glucose and without additional glucose) resulted in biofilm growth delay (**Chapter II**), suggesting that nutrient limitation might alter biofilm formation capacity and growth rate. Similarly to these results in **Chapter III**, all tested *Candida* spp. isolates showed a higher ability to form more robust biofilms in YPD growth media than YNB and RPMI1460. These findings suggest that both YNB and RPMI1460 might favor planktonic, and not biofilm form of growth and are in accordance with other authors who concluded that culture media have

a dramatic influence on biofilm architecture and might result in altered resistance to antifungal compounds¹¹¹.

Besides the ability to study biofilm growth patterns of different microorganisms in real time, another important highlight of the xCELLigence system is that impedance data was found to be comparable to standard end-point measures. For example, CI values highly correlated with staphylococcal, *P. aeruginosa* and *Candida spp.* biofilm crystal violet staining data (**Chapters I-III**). Additionally, a reduction in CI values after biofilm treatment with different antimicrobial and anti-biofilms also caused a decrease in viable cell number which was confirmed by CFU counts (**Chapters I, II, III and V**). Furthermore, the capacity of different antibiofilm compounds, such as andrographolide or self-propelled nanoparticles, to cause biofilm eradication and killing was confirmed using both confocal and scanning electron microscopy (**Chapters III and V**). On the other hand, a drawback in impedance measures was observed as some antibiotics and antibiofilm compounds resulted in the drop of CI values, which could derive from an artifact by pH changes or other factors affecting conductivity. Thus, in those cases it is very important to add appropriate controls and to confirm impedance data using standard methods to study biofilms.

In contrast to mono-species biofilms, complex polymicrobial biofilms consist of up to hundreds of different aerobic and anaerobic microorganisms and require powerful approaches for their growth, visualization and study^{31,129}. However, some existing techniques, such as flow cells, bioreactors and others, are expensive, while others, such as FISH, qPCR or DNA-hybridization, consider the presence of specific bacterial species rather than whole biofilm (where different bacterial strains co-existence and interactions can lead to increased resistance to antimicrobial compounds)^{16,425}. Therefore, this doctoral thesis describes subgingival dental plaque growth in real-time using impedance measures for the first time. In detail, the first round of the experiments in **Chapter IV** included transport media for subgingival plaque transport and storage testing. In fact, subgingival plaque samples were stored at room temperature for up to 48h, recovered, and grown in real-time, to study the capacity of periodontal bacteria to form polymicrobial biofilms in real-time. Subsequently, the impedance data obtained using the xCELLigence system was confirmed using 16s rRNA gene sequencing, where the comparison of initial inocula to the biofilms grown in xCELLigence for 8h showed a high similarity between

them. For instance, biofilms grown *in vitro* contained representative periodontal microbiota, including common periodontal pathogens belonging to the genera *Tannerella*, *Treponema*, *Filifactor*, *Fusobacterium*, *Treponema*, *Porphyromonas* and others.

Nevertheless, it is also important to underline that the *Streptococcus* genus was found at a higher abundance in real-time grown subgingival biofilms when compared to the initial inocula in most cases. This overgrowth of *Streptococcus* genera could be explained by the relatively high sugar concentration in BHI growth media⁴²⁶, suggesting that BHI without sugar, artificial saliva, or other bacterial growth media that contain low sugar concentrations could be used in future studies for periodontal biofilm growth⁴⁰². Nevertheless, the results described in **Chapter IV** conclude that the impedance system is an accurate and reliable tool for oral biofilm growth evaluation, and future studies should evaluate its accuracy for polymicrobial samples isolated from different sites and/or tissues.

3. Antibiotic susceptibility tests for biofilms

In order to find an efficient treatment for biofilm-associated infections, it is necessary to determine MIC and MBIC values. Typically, MIC values assessed *in vitro* are lower when compared to MBICs, as biofilm-grown microorganisms tend to show increased resistance to common drugs. Additionally, most of the research characterizing the susceptibility of bacteria and fungi to different antimicrobials is based on growing microorganisms planktonically in liquid media or testing their susceptibility on agar-based tests. However, MIC and MBIC values can vary depending on the growth media they are tested in, and these differences are usually strain-specific. In fact, a recent study concluded that some strains with identical MICs show different resistance profiles when grown in biofilms, where one *P. aeruginosa* strain was susceptible to tobramycin, and another one could tolerate relatively high concentrations of the drug⁴²⁷. Thus, the treatment selection using standard MIC values instead of MBICs often leads to wrong diagnosis and treatment failure, increased healthcare costs, and prolonged hospital stays.

In accordance with these previous findings by other authors, a similar trend was also observed in this doctoral thesis, as MBICs of dalbavancin for the tested *S. aureus* and *S. epidermidis* strains were up to 22 times higher when compared to MICs measured standard by E-

tests (**Chapter I**). Additionally, in **Chapter II**, the resistance to different antibiotics was shown to increase up to 32 times in *P. aeruginosa* biofilms as measured by impedance. Furthermore, a similar tendency was observed in fungal biofilms (**Chapter III**). When MBICs for both *C. albicans* and *C. glabrata* were compared to standard MICs, they were up to 100 times higher for some of the tested antifungals, confirming that biofilm-grown microorganisms tend to be highly resilient to treatment, especially when compared to their planktonic counterparts.

Moreover, an important highlight of the impedance system is its ability to evaluate how conventional and novel antimicrobials could influence biofilm formation and dynamics of different microorganisms, including both bacteria and fungi, and to select efficient antimicrobials in real-time for biofilm treatment.

Furthermore, it is also important to highlight that MIC and MBIC values from *in vitro* assays can differ from those obtained in *ex vivo* or *in vivo* biofilm models. Hence, future studies should investigate the possibility of standardizing antibiotic and antifungal susceptibility assays when bacteria and fungi are grown in the form of biofilms. Nevertheless, the use of appropriate biofilm susceptibility tests, such as those provided by impedance measurements, may offer a more accurate alternative for fast and individualized antibiotic selection, which could result in earlier patient discharge from the hospital and lower treatment failure rates.

In addition to antimicrobial susceptibility testing, in **Chapter IV** of this doctoral thesis, impedance measurements were used for individualized antibiotic selection for patients with periodontal disease. The results described in this chapter strongly suggest that the xCELLigence system can predict the best treatment strategy in a fast (less than 3 hours) and reliable way. Besides the capacity to select the most efficient treatment strategy in each particular case in **Chapter IV**, the impedance system was also capable of predicting the cases where all tested conventional antibiotics resulted in biofilm formation induction instead of its inhibition, suggesting that this treatment might result in treatment failure and indicating the need to test different antibiotics, antiseptics, antimicrobials, or their combinations in these cases. Moreover, the ability of impedance measurements to identify the antibiotics that fail to prevent biofilm formation could also help to assess possible clinical outcomes or even describe the relationship between infection and inflammation, as ineffective treatment results in the regrowth of periodontal pathogens aggravating the disease. Overall, the results in **Chapter IV** propose that an impedance

measurements-based system is a new and reliable approach for testing new treatment strategies against both biofilm prevention and eradication and could be used as a tool to select antimicrobial therapy for other infections that require the use of antibiotics or antifungals. I hope that the positive results obtained in the clinical trial with periodontal patients stimulates further research directed towards an application of impedance measures in real-time cultures for clinical use in hospitals, for example to determine antibiotic susceptibility in biofilm-mediated infections.

4. Conventional therapies against biofilms

Biofilm-forming bacterial and fungal pathogens pose a considerable threat to public health as they exhibit increased resistance to antimicrobials and antibiofilm compounds²⁷. This resilience to therapy usually requires the use of increased antimicrobial concentrations that can be unreachable *in vivo*, subsequently leading to multidrug resistance, serious health complications or even death^{1,15,52}. Hence, new and effective approaches against biofilm-embedded microorganisms must be investigated.

Diverse studies recently concluded that when antibiotics, antifungals or their combinations with suitable antibiofilm compounds are added at the beginning of biofilm formation as a preventive strategy against bacterial and fungal biofilms, they are capable to inhibit biofilm development at relatively low concentrations^{1,228,260}. For instance, a recent study showed that rifampin-impregnated central venous catheters decreased the occurrence of bloodstream infections in intensive care units⁴²⁸. Another study by Hashem and colleagues. showed the efficacy of vancomycin in inhibiting enterococci biofilm formation when the antibiotic was added together with bacterial inoculum⁴²⁹. Finally, Kamble et al, showed increased efficiency of the combinations of ciprofloxacin and vancomycin, daptomycin and vancomycin, and tobramycin and vancomycin against *S. aureus* biofilms when compared to monotherapy⁴³⁰.

In accordance with these studies, the results described in this dissertation confirm that when antibiotics are added at the beginning of biofilm formation, they have a strong potential in preventing further biofilm development, even when administered as monotherapy. For instance,

in **Chapter I**, conventional antibiotics such as vancomycin, linezolid, cloxacillin, and rifampicin showed biofilm inhibition capacity against staphylococcal biofilms in a dose-dependent manner. However, as observed in **Chapter I**, relatively low concentrations of vancomycin, linezolid and cloxacillin resulted in biofilm growth induction in tested *S. aureus* and *S. epidermidis* strains suggesting that these antibiotics can't kill whole bacterial population and highlighting the need to develop and test novel antibiotics. For this reason, assays performed in **Chapter I** evaluated the anti-biofilm efficacy of dalbavancin and concluded that this novel lipoglycopeptide group antibiotic has a strong potential to prevent staphylococcal biofilm formation, especially when compared to existing conventional therapy. The results described in **Chapter I** were confirmed by other authors, who intensively studied the anti-biofilm capacity of dalbavancin and demonstrated that this antibiotic exhibits strong biofilm inhibition properties against gram-positive bacteria both *in vitro* and *in vivo*^{300,431–434}.

Contrary to results observed in **Chapter I**, antibiotics that inhibit bacterial cell wall synthesis lacked the efficiency against *P. aeruginosa* biofilms even when administered at relatively high concentrations (**Chapter II**), highlighting the notorious capacity of this bacterium to resist conventional treatment²³. Similarly, colistin was not able to halt the biofilm development of *P. aeruginosa*, and impedance results suggest that this antimicrobial might result in the overproduction of extracellular biofilm matrix elements, as observed in previous studies^{212,320,332}. In contrast to these results, the largest biofilm prevention and the capacity to disrupt established biofilms were observed when pseudomonas biofilms were treated with ciprofloxacin (inhibits DNA gyrase) and tobramycin (suppresses protein synthesis), suggesting that the efficiency of both antibiotics against *P. aeruginosa* biofilms might be related to their mechanisms of action. Nevertheless, certain concentrations of both of these antibiotics resulted in the induction of biofilm formation when administered at relatively low concentrations, highlighting the need to search for novel compounds that would be capable of entirely suppressing further biofilm formation in *P. aeruginosa*.

In parallel to gram-positive and gram-negative biofilms, the inhibition of *Candida* spp. biofilm formation using two different classes of antifungals (azoles and echinocandins) showed concentration and strain-dependent effect (**Chapter III**). Nevertheless, azole group antifungals provoked biofilm growth induction and resulted in changes in biofilm growth dynamics. Given

that relatively high concentrations of fluconazole and voriconazole induced further biofilm development, these results suggest that azoles might interfere with some components of the EPS matrix leading to changes, such in the biofilm architecture. Additionally, the results described in this doctoral thesis are in accordance with other authors who concluded that azole group antifungals can result in phenotypical changes during biofilm development and maturation^{363–365}. Contrary to fluconazole and voriconazole, echinocandins (micafungin and caspofungin) showed a strong capacity to halt biofilm formation when added with fungal inoculum, confirming findings described elsewhere^{112,115,119,342}. Therefore, the results in **Chapter III** indicate the importance to evaluate the capacity of individual strains to form biofilms in the presence of different antifungals, considering biofilm growth dynamics. Given that biofilm growth dynamics can predict whether the exposure of biofilms to different concentrations of the drug will result in biofilm growth inhibition, or further development, the impedance-based measures are of great interest in selecting the best treatment strategy for the prevention of biofilm formation.

However, most biofilm-related infections are usually diagnosed when biofilms are already established. In these particular cases, conventional drugs can only halt their further development but are incapable of eradicating thick EPS matrix or killing biofilm-embedded bacterial and fungal cells^{6,82,215,408}. In accordance with numerous *in vitro* studies, the results in **Chapter I** indicated that the exposure of established staphylococcal biofilms to vancomycin, linezolid, cloxacillin and rifampicin not only lacked the capacity to prevent new biofilm accumulation in all tested strains, but some concentrations of these antibiotics resulted in biofilm growth induction up to 40% when compared to untreated control. This phenomenon might occur due to limited penetration of the antibiotics into deep biofilm layers, low cell metabolic activity within biofilms, activation of efflux pumps or altered synthesis of different macromolecules in EPS as shown elsewhere^{24,162,306,314,315}. Nevertheless, it should be taken into account when selecting treatment of biofilm-associated infections. For this reason, given that dalbavancin not only showed the capacity to inhibit biofilm formation but also was capable to eradicate pre-formed biofilms, the results described in **Chapter I** suggest that this antibiotic might penetrate established biofilms more efficiently when compared to conventional antibiotics (especially vancomycin and linezolid and cloxacillin) that are commonly used as primary treatment strategies against biofilm-associated staphylococcal infections in clinical practice. In addition, the capacity of dalbavancin to reduce established biofilm biomass indicates that its effect might

be facilitated by the pharmacokinetics of this antibiotic, as dalbavancin not only inhibits bacterial cell wall synthesis but also anchors the pathogen's cell membrane, leading to a prolonged half-life^{295,435}.

Regarding gram-negative pseudomonal biofilms, both ciprofloxacin and tobramycin that showed a strong biofilm inhibition capacity were also capable of eradicating mature pseudomonal biofilms when added at 24 and 48h of biofilm growth. However, certain concentrations of both conventional antibiotics resulted in the appearance of a second peak in the impedance system, suggesting the presence of dormant cell fractions within *P. aeruginosa* biofilms. Phenotypical and genetic analysis of survivor cells confirmed this hypothesis, and the results described in this dissertation suggest that a biofilm-specific environment, which represents nutrient limitations, anaerobic conditions, and other factors, such as the presence of conventional antibiotics, can trigger cell heterogeneity within biofilms. Thus, the findings in **Chapter II** are similar to those recently published by Soares et al., who have generated *P. aeruginosa* persister cell fraction using supra-MIC ciprofloxacin concentrations²⁴⁹. Additionally, these results highlight the inefficiency of existing conventional antibiotics to kill all biofilm-embedded bacteria and indicate the need to search for new approaches against preformed and mature heterogeneous biofilms.

As discussed above, dose-response experiments performed in **Chapter III** of this doctoral thesis indicated that echinocandins micafungin and caspofungin have a strong biofilm inhibition capacity against both *C. albicans* and *C. glabrata*. Nevertheless, the exposure of mature 24h *Candida spp.* biofilms resulted in treatment failure, as any of the tested concentrations of these antifungals could disassemble or halt further biofilm development in any of the tested strains. This lack of efficiency against mature *Candida spp.* biofilms could be related to their inability to reach biofilm embedded fungal cells, the presence of hyphae, or/and changes in cell metabolic activity^{114,363,436}. Besides the inability to halt established biofilms, some of the tested concentrations of micafungin and caspofungin induced further biofilm growth, suggesting that the use of these antifungals to treat fungal biofilm-associated infections could result in the emergence of multidrug-resistant variants or even lead to the aggravation of the disease as suggested by other authors^{115,125}. Therefore, given that any tested conventional therapy could decrease established biofilms, findings from previous studies that highlighted the

drawbacks of antifungal drugs^{126,343,437} and the results described in **Chapter III** emphasize the need to develop new potent strategies to combat mature fungal biofilms¹⁰⁹.

5. Novel strategies against biofilms

As extensively explained above, pre-formed and mature biofilms generally do not respond to conventional antimicrobials. For this reason, recent advances have been made in exploring alternative strategies to eradicate microbial biofilms^{64,67}. For instance, natural antibiofilm compounds, antibiotic and antifungal combinations, antimicrobial peptides, phages and other approaches have been recently proposed to be more efficient than conventional monoteraphies^{21,438,439}. Therefore, different approaches to increase the efficiency of conventional antibiotics and antifungals were undertaken in this doctoral thesis. Firstly, given that dalbavancin showed limited efficacy when administered on mature staphylococcal biofilms in **Chapter I**, an effort was undertaken to increase the efficiency of this novel antibiotic using different anti-biofilm compounds such as N-acetylcysteine (NAC) and a natural plant protease ficin. NAC, besides its antimicrobial effect, was also shown to have an impact on polysaccharides in biofilm matrix^{294,308}, while ficin was recently found to be capable of interfering with EPS proteins¹⁹⁴. Surprisingly, results described in **Chapter I** indicated that *in vitro* interactions between both anti-biofilm compounds with dalbavancin represent a strain and concentration-dependent effect. Additionally, some antagonistic effects were observed when dalbavancin was combined with NAC, suggesting that the combinations between conventional antibiotics used in clinical practice and anti-biofilm compounds should be carefully investigated to anticipate their combined effect and ensure the best clinical outcomes.

Contrary to these results, a natural plant protease ficin was capable of intensifying the effect of dalbavancin, highlighting its ability to detach bacterial cells from the biofilm and therefore making them more susceptible to the antibiotic. Nevertheless, the results in **Chapter I** showed that in contrast to NAC, ficin alone has no antimicrobial capacity, suggesting that an efficient antibiotic should be used in combination with ficin to detach and kill cells released from the biofilm successfully. Therefore, it is also important to mention that *S. aureus* and *S. epidermidis* biofilms are classified as consisting of polysaccharide material and proteinaceous

matrix^{55,82,86}. In fact, several recent studies have indicated that the MRSA strain's biofilm matrix consists of mostly protein-related material. For this reason, the lack of the efficiency of NAC and the strong capacity of ficin to disperse bacterial cells from the biofilms could be explained by their mechanisms of action, as protein-like biofilms are more susceptible to protease-mediated biofilm detachment⁵⁵. Nevertheless, the combination of dalbavancin with this or other biofilm-detaching compounds should be further studied in the future using animal models and/or host-immune system interaction studies in order to predict the efficiency of the therapy. For instance alternatives for matrix degrading enzymes include trypsin, DNaseI, dispersinB and others that were found to be capable of dispersing both preformed and established biofilms^{67,74,85,242,440}.

Comparably to gram-positive staphylococcal biofilms, established fungal biofilms are found to be extremely difficult to eradicate^{107,365}. Recent investigations identified mechanisms involved in this resistance, concluding that fungal biofilm matrix usually impairs azole group antifungals, while hyphae formation and biofilm maturation in *Candida spp.* biofilms were shown to correlate to recalcitrance to different classes of conventional drugs^{441,442}. Findings in this doctoral thesis confirmed that the resistance of 24h *C. albicans* and *C. glabrata* biofilms was significantly increased when compared to the assays where both azole and echinocandin group antifungals were added at the beginning of biofilm formation. In fact, most of the concentrations of these antifungals used in **Chapter III** induced further biofilm formations, suggesting that they might be incapable of penetrating within biofilms or facilitating the synthesis of different EPS matrix components^{118,121,443}. For this reason, a novel natural compound, andrographolide, was tested to assess its effectiveness against fungal biofilms alone and in combination with micafungin. Although this compound has already been shown to have anti-inflammatory, anti-viral and antimicrobial properties against some bacteria and has been shown to affect quorum sensing systems in both *S. aureus* and *P. aeruginosa*³⁵⁰⁻³⁵⁵, the efficiency of this compound against *Candida spp.* biofilms remained elusive. Therefore, although in **Chapter III**, andrographolide showed antagonistic effect when administered together with micafungin, this compound alone was capable to detach fungal biofilms almost completely and reduced the viability of biofilm embedded fungal cells up to 99.9%, showing both anti-biofilm and antimicrobial properties. Moreover, andrographolide was shown to affect biofilm architecture, and combined impedance, viable counting and microscopy results indicate that this compound

represents a considerably higher efficacy when compared to conventional antifungals such as micafungin or caspofungin. Thus, the results described in **Chapter III** promote the use of andrographolide against fungal biofilm-related infections. Given that it is the first study that uses impedance-based measurements to describe the effect of novel antibiofilm (i.e. andrographolide) compounds on fungal biofilm formation and disassembly, future studies should evaluate the *ex vivo* and/or *in vivo* effect of andrographolide in order to conclude whether this compound is suitable for treating fungal infections associated to biofilms. Overall, **Chapter III** highlights the importance of testing new natural compounds with biocidal or antibiofilm properties in order to achieve better clinical outcomes of fungal biofilm-associated infections when compared to existing conventional therapies.

Besides the inability of conventional therapy to penetrate inner biofilm layers, the metabolic state of the bacterial and fungal cells embedded in a biofilm can have an influence on antibiotic and antifungal lethality^{358,444}. For example, the appearance of persister cells with low metabolic rates within microbial biofilms is a crucial factor affecting conventional treatment failure and antibiotic resistance²⁷⁸. Although various strategies to combat dormant persister cell populations, such as the utilization of DNA crosslinking agents, colistin-based antibiotic combinations or glycolysis intermediates, were suggested by recent studies, the ability to study and eradicate them is still limited^{445,446}. Given that in **Chapter II** after the exposure of mature *P. aeruginosa* biofilms to tobramycin, ceftazidime, and ciprofloxacin the appearance of dormant cell populations was successfully identified using impedance measurements, further experiments in **in Chapter II** of this doctoral thesis included testing mannitol's ability to revert dormant cell fractions into actively growing bacteria and to potentiate the killing effect of ciprofloxacin. In order to complete this objective, the capacity of mannitol alone or in combination with ciprofloxacin to eradicate mature *P. aeruginosa* biofilms was tested following the work of Barraud and colleagues, who found that TOB efficiency was potentiated by mannitol by increasing the killing in the biofilm-embedded persister cell population up to three orders of magnitude³³³. Similarly, in this doctoral thesis, mannitol, which showed to have neither antimicrobial nor antibiofilm effect when administered alone, was capable of potentiating ciprofloxacin killing in a dose-dependending manner and led to complete elimination of mature *P. aeruginosa* biofilms. This kind of mature heterogenous biofilm eradication and killing to our knowledge was never described before. In addition, further experiments in **Chapter II** showed

that persister cells inoculated in LB media supplemented with mannitol restored pyocyanin synthesis faster than in LB alone, concluding that this compound is responsible for fast switch from dormant cell population to actively growing bacteria. Nevertheless, given that any specific genomic rearrangements were found to be specific to persister cells in **Chapter II**, future studies should investigate transcriptomic and metabolomic events that might occur during the transition of actively growing bacteria to dormant cells.

Therefore, the results obtained using real time impedance measurements described in **Chapter II** of this doctoral thesis are of both basic and applied interest as it is the first study which investigates the emergence of persister cells in real-time and shows that ciprofloxacin efficacy can be dramatically improved with mannitol without needing to increase the antibiotic concentration. Thus, I hope that these results stimulate the use of mannitol as a combined treatment in future studies related to multi-resistant recurrent biofilm infections both in *vitro* and in *vivo*.

Lastly, besides recent advances in biofilm treatment, the incapacity of novel compounds to completely eliminate mature biofilms highlights the need to keep developing novel approaches for their eradication¹⁷⁹. Nevertheless, a main goal should be not to continuously create new antibiotics or antifungals but to increase the efficiency of already existing drugs. This could be achieved, for instance, by the use of nanomaterials that could reach the infection site and uniquely interact with bacterial and fungal biofilms^{240,256}. Hence, various studies have used mesoporous silica nanoparticles to treat *S. aureus* biofilms. For instance, Devlin et al., used mesoporous nanoparticles functionalized with lysostaphin and other enzymes, achieving a reduction in biofilm biomass⁴⁴⁷. However, the efficiency of the nanoparticles was observed to be significantly lower when they were added on mature 24h and 48h biofilms. Another study by Fulaz and colleagues showed that the use of mesoporous silica nanoparticles loaded with vancomycin and functionalized with amine, carboxyl, or aromatic groups decreased cell viability in both MSSA and MRSA⁴⁴⁸. Nevertheless, although the use of functionalized nanoparticles produced changes in biofilm architecture (especially in MRSA strains) these nanoparticles were also incapable to eradicate mature biofilms. Thus, **Chapter V** of this doctoral thesis describes the use of a novel self-propelled nanodevice on mature *S. aureus* biofilms. This nanomotor consists of a H₂O₂ inducible platinum nanomotor, mesoporous silica nanoparticles loaded with

vancomycin and the plant protease ficin that confers biofilm detaching properties. Given that the nanoparticles release their cargo only when the pH is acidic (inside of biofilm backbone), the results described in **Chapter V** indicate that this controlled vancomycin release can result in more efficient biofilm disruption and killing compared to free vancomycin. In addition, as shown in **Chapter I**, the plant protease ficin has a strong capacity to disperse established biofilms, making them more susceptible to dalbavancin. Significant results were also observed in **Chapter V**, where ficin was shown to potentiate the effect of vancomycin when released from the nanoparticles. Thus, data described in **Chapter V** show the capacity of novel nanodevices to increase vancomycin's efficiency and successfully eliminate pre-formed and mature staphylococcal biofilms (more than 82% of biofilm mass elimination using only 1 mg of these novel nanoparticles). Additionally, biofilm-embedded cell viability was reduced more than 99.9%, demonstrating the biocidal capacity of self-propelled nanoparticles. Therefore, the novel nanodevice could be used for both biofilm prevention and established biofilm treatment and might find an application in environments where H₂O₂ is present naturally, such as the vaginal tract or inflamed tissues⁴¹⁹ or where this compound can be applied easily, for example, in chronic wounds⁴⁴⁹. Nevertheless, future studies should test the efficiency and possible toxicity of the novel nanodevice both *ex vivo* and *in vivo* in order to assure their safety and possible use to treat biofilm-associated infections.

6. Future prospects for biofilm studies

Although biofilm study methods range from simple *in vitro* biofilm mass measurements to complex *in vivo* models, the detection and treatment of biofilm-associated infections remain challenging. Therefore, this doctoral thesis developed and validated a new methodology to study biofilm formation dynamics in real time using impedance measurements with a commercially available system that was originally designed to measure the growth of eukaryotic cells. Overall findings of this doctoral thesis show that an impedance system is an accurate tool to comprehensively assess the capacity of different microorganisms to form biofilms. Although cellular index values varied among tested microorganisms, these differences might be related to cell size, as gram-positive bacteria showed lower CIs when compared to larger-size organisms such as *P. aeruginosa* or *Candida* spp. Nevertheless, most of the laboratory strains and clinical

isolates tested in the current work showed the capacity to form robust biofilms, which were possible to monitor in real time. This biofilm formation capacity was confirmed using standard biofilm methodologies such as CV staining. For instance, CV staining in **Chapter I** demonstrated the capacity of ficin to detach bacterial cells embedded in mature staphylococcal biofilms. Secondly, biofilm staining using CV helped to assess biofilm formation capacity between different *P. aeruginosa* and *Candida* spp. strains and compare these results to those observed using impedance in **Chapters II** and **III**. For example, the results observed in **Chapter II** showed that most of the strains showed similar biofilm formation dynamics in both xCELLigence and Ibidi plates, suggesting that both methodologies are comparable. Nevertheless, some tested strains were able to adhere faster and stronger on Ibidi plate surfaces. These differences confirm that surface properties such as porosity and hydrophobicity can influence biofilm thickness and architecture, as was already described by recent studies^{57,412,450-452}.

Given that CV staining does not provide information on whether biofilm-embedded cells are viable, this thesis compared impedance-based measurements with viable colony counts after biofilms were treated with antibiotics and antifungals, including dalbavancin, ciprofloxacin, vancomycin and micafungin alone or in combination with anti-biofilm compounds such as ficin in **Chapter I** or andrographolide in **Chapter III**. Additionally, viable colony counts confirmed that mannitol was efficient when treating heterogeneous *P. aeruginosa* biofilms in converting dormant cells into actively growing bacteria and potentiating the effect of subinhibitory ciprofloxacin concentrations (**Chapter II**). Similarly, the effect of novel self-propelled nanoparticles besides impedance measurements was assessed using viable colony counts in **Chapter V**, verifying their efficiency against pre-formed *S. aureus* biofilms. Thus, these results are in accordance with other authors and indicate that even though CFU methodology is laborious and might result in scattered results due to bacterial aggregation, it is a powerful quantitative technique to assess biofilm viability after treatment^{161,169}. Thus, classic viability counting provides useful complementary information to the monitoring of biofilm dynamics. For example, it enables to identify whether different antibiofilm compounds only detach bacterial or fungal cells embedded within the biofilm backbone (i.e ficin in **Chapter I** and mannitol in **Chapter II**) or if they also contain antimicrobial properties (i.e. andrographolide **Chapter III**)

In addition to biofilm formation assessment by staining and quantifying viable cells within biofilms, the visualization of biofilm structure is also critical. For this reason, microscopic techniques emerged as a potent tool for biofilm observations. For example, CLSM and SEM are commonly used to study biofilm structure and matrix elements after treatment with different antimicrobials and anti-biofilm compounds. Although CLSM needs fluorophores, it is an effective technique that permits the analysis of biofilm 3D view, quantifying live and dead bacterial cells within treated biofilms and comparing treated biofilms to untreated controls. This technique was also used in **Chapter V** of the thesis to confirm the effect of self-propelled mesoporous platinum nanoparticles loaded with vancomycin and anchored with ficin on *S. aureus* biofilms. For instance, biofilm EPS was labelled using Alexa-Fluor 680-dextran conjugate to observe biofilm 3D structure and assess EPS matrix surface area reduction before and after treatment. In addition, live-dead staining with SYTO9 and propidium iodide was performed to evaluate and quantify live and dead bacterial cells within *S. aureus* biofilms. CLSM images confirmed the results observed using impedance-based measurements where the self-propelled nanomotor showed the extraordinary capacity to detach and kill bacterial cells. In addition, the possibility of labeling the matrix provided a different piece of information to evaluate the effect of the treatment on this portion of the biofilm mass, which could not be assessed by CFU counts nor by impedance measurements.

Instead of using conventional CLSM, other authors have employed confocal microscopy to describe biofilm 3D structure and its spatial distribution over time. Advanced confocal time-lapse microscopy is now commonly used for biofilm growth observations, such as studying how swimming motility and trajectories influence biofilm architecture⁴⁵³. In addition, the utilization of modern microscopy techniques in real-time lead to a better understanding of bacterial interactions and can help to identify heterogenous bacterial populations within biofilms^{454,455}. This was shown by Welch and colleagues who have labelled dental plaque using fluorescence in situ hybridization (FISH). The utilization of ten different rRNA probes labelled with fluorophores (each one for different bacteria) helped to clarify the structure of complex oral biofilms¹⁶⁵. Another recent study by Molina-Santiago et al. applied time-lapse confocal imaging to study colony biofilms on agar substrate for assessing bacterial interactions between different biofilm populations⁴⁵⁶.

Besides CLSM, SEM can be applied to study biofilm matrix elements and their architecture. In addition, it is a powerful technique that permits studying how anti-biofilm compounds interfere with biofilm matrix elements and allows various magnifications, allowing single-cell visualization^{185,189,190,192}. In the current thesis, SEM was also employed to assess the effect of andrographolide on established candida biofilms in **Chapter III**. SEM micrographs showed that andrographolide could disassemble both *C. albicans* and *C. glabrata* biofilms almost completely, confirming the anti-biofilm effect of this compound. Moreover, SEM was undertaken to validate the results obtained in **Chapter IV**, where novel self-propelled platinum nanoparticles could detach established *S. aureus* biofilms up to 82% in less than one hour of exposure. Therefore, 24h *S. aureus* biofilms treated with 1mg/mL of novel nanoparticles resulted in complete biofilm disassembly, with only small separate cell-clusters observed after treatment. Overall, these results suggest that even though sample preparation for SEM imaging is a laborious and time-consuming process, this technique permits validation of the results observed using other biofilm methods, including those obtained using impedance measures in real time.

On the other hand, there exist other methods that allow real-time biofilm analysis. For instance, some of them are based on isothermal microcalorimetry measures that record heat released from the biofilms⁴⁵⁷. Calorimetric assays have already been used to identify heterogeneous populations within biofilms and test antimicrobial susceptibility⁴⁵⁷⁻⁴⁵⁹. However, they require internal controls as different bacterial and fungal strains attribute different metabolic activity. Another technique allowing biofilm studies in real time is a microfluidic platform which can be used to analyze mono-species, dual and complex biofilms¹⁷². This technique allows biofilm analysis using dynamic and static conditions and further biofilm observation using microscopy techniques. Recently, a new advanced microfluidics system (BiofilmChip) was developed⁴²⁵. Besides continuously supplying nutrients for biofilms mimicking the host environment conditions, the novel chip can be connected to an impedance analyzer. This could allow direct biofilm analysis based on the ability of biofilm forming microorganisms to impede electric current. In addition, biofilms grown on Biofilm Chip can be stained and further analyzed using CSML.

Overall, accelerated development of biofilm study methods has not yet achieved a decrease in the appearance of multi-resistant strains associated with bacterial and fungal biofilms. Thus, the development of new methods is necessary in order to evaluate new anti-

biofilm strategies and successfully fight with biofilm associated infections. This doctoral thesis comprehensively described and validated impedance-based bacterial and fungal biofilm analysis system in real-time using static conditions. Although the main disadvantage of this system is the inability to mimic events occurring in the host environment, the results obtained using this system were comparable to classical biofilm testing methodologies, including qualitative staining, quantification of biofilm embedded cells using colony counts and different microscopy techniques. Moreover, impedance measures do not require labeling nor manipulation and give information about biofilm growth dynamics, which can vary between different bacterial species or even strains. Further future studies should concentrate on the analysis of different biofilm-forming microorganisms in real time and validate the obtained results using *ex vivo* and *in vivo* methods. The data obtained in the current thesis conclude that impedance measures are therefore a powerful technique with improved characteristics compared to other methodologies. However, as it happens with other approaches, it does not provide a full information about the biofilm, and I suggest that a combination of impedance measures with viability quantification and microscopy will offer complementary data for a more complete assessment.

Table 1. Methods for assessing biofilm formation

<i>METHOD</i>	<i>ADVANTAGES</i>	<i>DISADVANTAGES</i>
Crystal violet staining	<ul style="list-style-type: none"> • Inexpensive. • Provides information about biofilm formation capacity. 	<ul style="list-style-type: none"> • End-point measurements. • Poor reproducibility. • Does not provide information about cell viability.
Viable cell counting	<ul style="list-style-type: none"> • Quantitative method. • Provides information about cell viability. • Easy to perform. 	<ul style="list-style-type: none"> • Time-consuming. • Might represent poor reproducibility due to bacterial aggregates. • End-point measurement.

Scanning electron microscopy

- High resolution, a wide range of magnifications.
- Permits analysis of biofilm spatial structure and EPS matrix element observation.
- Highly correlates with quantitative techniques.
- Helps to assess the effect of different compounds on biofilm architecture.
- Easy to use.
- Time-consuming sample preparation, which involves dehydration, fixation and metal coating, can destroy the sample.
- Lacks vertical resolution.
- Expensive.
- Sample observation performed in a vacuum.
- Quantification can be subjective and low sample size

Confocal microscopy

- Helps to localize and quantify live-dead bacteria within biofilms.
- 3D biofilm view.
- Provides information about biofilm structure.
- Give real-time information about the metabolic state of bacteria, which can help to identify dormant and unculturable cell fractions.
- Not disruptive.
- No labelling needed.
- Use only a small volume of media and reactivities.
- Requires use of fluorophores.
- Only a limited number of fluorophores exist.
- Overlap of fluorescence signals might result in false positives.
- Need internal controls as all bacteria have metabolic activity.
- Do not provide information about biofilm thickness or EPS elements.
- Difficult to study complex biofilms.

Calorimetric assays

- Provide information about biofilm growth dynamics over time.
- Possible to test many different conditions/antimicrobials or anti-biofilm compounds simultaneously.
- Need no additional manipulation or labelling.
- Do not mimic the host microenvironment and nutrients present *in vivo*.
- Some metabolites or antibiotics can affect conductivity.
- System is static.

Impedance measurements

BiofilmChip

- Allows multiple replicates and objective quantification
- Microfluidics resemble the host environment and events that occur *in vivo*.
- Can detect early biofilm attachment.
- Enables analysis of polymicrobial biofilms.
- Allows further biofilm imaging using CLSM
- Requires use of high volumes of growth media.
- Can be expensive.
- Further biofilm visualization involves biofilm staining and might be time-consuming.

One of the main goals of the current thesis has been to set up an inexpensive, rapid and consistent method to evaluate antibiotic susceptibility. Given that results after just a few hours appear to be representative of the antibiotic response, the application of impedance measures in clinical settings should be seriously considered. We evaluated the use of this method in a specific clinical situation, namely the use of antibiotics in periodontal treatment, which is usually made empirically, or in the best case scenario by DNA hybridization or qPCR or other molecular methods to detect the levels of periodontal pathogens. Our data show that even when compared to the standard technique of antibiotic selection in these cases, the RT-culture methodology provided improved clinical and microbiological outputs. I hope this proof of concept stimulates further studies to evaluate the implementation of this method not only in dentistry but also in hospitals, where the treatment of biofilm-mediated infections could benefit enormously by providing a faster, cheaper and more efficient approach that could in addition contribute to a more rational use of antibiotics.

CONCLUSIONS

1. Impedance-based measures appear to provide a valid system for studying *S. aureus*, *S. epidermidis* and *P. aeruginosa* biofilm formation in real-time and for testing biofilm susceptibility to conventional and novel antimicrobials on both biofilm formation and eradication.
2. Real-time dose-response experiments indicate that dalbavancin and rifampicin were the best therapeutic agents against *S. aureus* and *S. epidermidis* when added at the beginning of biofilm formation.
3. MBIC values of dalbavancin for the tested strains were up to 22 times higher compared to MICs measured standard by E-tests, concluding that biofilm-grown bacteria are considerably more resistant to treatment than their planktonic counterparts.
4. Dalbavancin was the only antibiotic that could prevent new biofilm development when added to established staphylococcal biofilms, while conventional antibiotics such as vancomycin, cloxacillin or linezolid showed no inhibitory effect or even induced biofilm growth when compared to untreated controls.
5. Real-time impedance measurements showed that NAC and ficin had biofilm inhibitory capacity when added at the beginning of staphylococcal biofilm formation. The effect of these compounds on pre-formed biofilms was strain and dose-dependent.
6. When dalbavancin was combined with anti-biofilm compounds, strain and concentration-dependent effects were observed. While NAC and dalbavancin showed an antagonistic effect, the combination of dalbavancin with the natural plant protease ficin efficiently detached and killed bacterial cells embedded in pre-formed biofilms, suggesting the potential of this combination as a new therapeutic strategy against Staphylococcal infections.

7. An impedance system was set up for gram-negative biofilm studies and was validated using standard CV staining. While the most suitable media for gram-negative biofilm growth was LB without additional glucose, the initial bacterial optical density had no influence on final CI values.
8. Real-time biofilm inhibitory effect of eight conventional antibiotics on *P. aeruginosa* biofilm formation was assessed, showing a lack of efficacy for antibiotics affecting cell wall synthesis, and highlighting the potential of both ciprofloxacin and tobramycin to prevent pseudomonal biofilm development.
9. The exposure of mature *P. aeruginosa* biofilms to specific concentrations of ceftazidime, tobramycin and ciprofloxacin resulted in the appearance of persistent cell populations that could be detected by impedance measurements for the first time, confirmed using microbiological assays and full genome-sequencing. Additionally, genetic analysis showed no specific mutations in persister cells, suggesting that dormancy might be related to transcriptomic and metabolomic changes.
10. Impedance measures, microbiological assays and viable cell counts indicate that mannitol reverts dormant cells into actively growing bacteria without killing them in a concentration-dependent manner, and its combination with subinhibitory concentrations of ciprofloxacin results in complete persister cell population eradication.
11. Impedance measurements provide a valid system to study fungal (*Candida* spp.) biofilm growth dynamics and was used to study the effects of conventional azole and echinocandin group antifungals and the new antibiofilm compound andrographolide.
12. YPD growth media without additional glucose was the most suitable for *Candida* spp. to form biofilms in real-time.
13. Azoles showed concentration and species-dependent effects on *Candida* spp. biofilm growth prevention, while echinocandins (micafungin and caspofungin) prevented biofilm formation at relatively low concentrations for all tested strains.

14. Exposure of 24h *C. albicans* and *C. glabrata* biofilms to micafungin and caspofungin indicated that these antifungals could not disrupt mature biofilms, and at some concentrations they even induced further biofilm development.
15. A plant-derived compound, andrographolide, showed extensive antifungal properties on both planktonic and biofilm growth, as determined by impedance measures, colony counting and microscopy. Although this compound showed no synergy when combined with micafungin, andrographolide alone at the concentration of 5 g/L reduced viable counts by up to three orders of magnitude and showed the ability to destroy EPS matrix in both *C. albicans* and *C. glabrata*.
16. VMG III transport media without additional agar and agarose showed the best capacity to preserve bacterial composition and the capacity of periodontitis-associated bacteria to form biofilms for up to 48 hours.
17. The bacterial composition of ex vivo-grown subgingival biofilms is comparable to the initial inocula indicating that a microcosm approach like that provided by the impedance system in the current thesis is a useful tool for studying complex polymicrobial biofilms.
18. While conventional pre-formed *S. aureus* biofilm treatment with vancomycin resulted in treatment failure, the addition of novel nanoparticles on 7h *S. aureus* biofilms reduced biofilm biomass up to 82% in less than one hour of exposure and resulted in a decrease in cell viability in both supernatant and residual biofilm over 3-logs when compared to untreated controls and were capable to detach and eradicate mature 24h biofilms.

ANNEX A – Published version of CHAPTER I

© Frontiers in Microbiology, 2020



ORIGINAL RESEARCH
published: 17 April 2020
doi: 10.3389/fmicb.2020.00553



Effect of Dalbavancin on Staphylococcal Biofilms When Administered Alone or in Combination With Biofilm-Detaching Compounds

Miglė Žiemytė¹, Juan C. Rodríguez-Díaz², María P. Ventero², Alex Mira^{1,2*} and María D. Ferrer^{1,2}

¹ Genomics and Health Department, FISABIO Foundation, Valencia, Spain, ² Servicio de Microbiología, Hospital General Universitario de Alicante, ISABIAL, Alicante, Spain, ³ CIBER Epidemiología y Salud Pública, Madrid, Spain

OPEN ACCESS

Edited by:

Sujogya Kumar Pauda,
KU Louvain, Belgium

Reviewed by:

Pilar Toivola,
University of Minho, Portugal
Fernanda Gomes,
University of Minho, Portugal

*Correspondence:

Alex Mira
mira_alex@fisabio.es

Specialty section:

This article was submitted to
Antimicrobials, Resistance
and Chemotherapy,
a section of the journal
Frontiers in Microbiology

Received: 20 December 2019

Accepted: 13 March 2020

Published: 17 April 2020

Citation:

Žiemytė M, Rodríguez-Díaz JC,
Ventero MP, Mira A and Ferrer MD
(2020) Effect of Dalbavancin on
Staphylococcal Biofilms When
Administered Alone or in Combination
With Biofilm-Detaching Compounds.
Front. Microbiol. 11:553.
doi: 10.3389/fmicb.2020.00553

Microorganisms grown in biofilms are more resistant to antimicrobial treatment and immune system attacks compared to their planktonic forms. In fact, infections caused by biofilm-forming *Staphylococcus aureus* and *Staphylococcus epidermidis* are a large threat for public health, including patients with medical devices. The aim of the current manuscript was to test the effect of dalbavancin, a recently developed lipoglycopeptide antibiotic, alone or in combination with compounds contributing to bacterial cell disaggregation, on staphylococcal biofilm formation and elimination. We used real-time impedance measurements in microtiter plates to study biofilm growth dynamics of *S. aureus* and *S. epidermidis* strains, in the absence or presence of dalbavancin, linezolid, vancomycin, cloxacillin, and rifampicin. Further experiments were undertaken to check whether biofilm-detaching compounds such as *N*-acetylcysteine (NAC) and ficin could enhance dalbavancin efficiency. Real-time dose-response experiments showed that dalbavancin is a highly effective antimicrobial, preventing staphylococcal biofilm formation at low concentrations. Minimum biofilm inhibitory concentrations were up to 22 higher compared to standard *E*-test values. Dalbavancin was the only antimicrobial that could halt new biofilm formation on established biofilms compared to the other four antibiotics. The addition of NAC decreased dalbavancin efficacy while the combination of dalbavancin with ficin was more efficient than antibiotic alone in preventing growth once the biofilm was established. Results were confirmed by classical biofilm quantification methods such as crystal violet (CV) staining and viable colony counting. Thus, our data support the use of dalbavancin as a promising antimicrobial to treat biofilm-related infections. Our data also highlight that synergistic and antagonistic effects between antibiotics and biofilm-detaching compounds should be carefully tested in order to achieve an efficient treatment that could prevent both biofilm formation and disruption.

Keywords: dalbavancin, E-test, biofilm, *Staphylococcus*, ficin, *N*-acetylcysteine, xCELLigence

ANNEX B – Published version of CHAPTER II

© Emerging Microbes & Infections, 2021

Emerging Microbes & Infections
2021, VOL. 10
<https://doi.org/10.1080/22221751.2021.1994355>



ORIGINAL ARTICLE

OPEN ACCESS

Real-time monitoring of *Pseudomonas aeruginosa* biofilm growth dynamics and persister cells' eradication

Miglè Žiemytė ^a, Miguel Carda-Diéguez ^a, Juan C. Rodríguez-Díaz ^b, María P. Ventero ^b, Alex Mira ^{a,c} and María D. Ferrer ^{a,c}

^aGenomics & Health Department, FISABIO Foundation, Valencia, Spain; ^bServicio de Microbiología, Hospital General Universitario de Alicante, ISABAL, Alicante, Spain; ^cQBER of Epidemiology and Public Health, Madrid, Spain

ABSTRACT

Biofilm formation and the appearance of persister cells with low metabolic rates are key factors affecting conventional treatment failure and antibiotic resistance. Using impedance-based measurements, crystal violet staining and traditional culture we have studied the biofilm growth dynamics of 13 *Pseudomonas aeruginosa* strains under the effect of seven conventional antibiotics. Real-time growth quantifications revealed that the exposure of established *P. aeruginosa* biofilms to certain concentrations of ciprofloxacin, ceftazidime and tobramycin induced the emergence of persister cells, that showed different morphology and pigmentation, as well increased antibiotic resistance. Whole-genome sequencing of wildtype and persister cells identified several SNPs, a genomic inversion and a genomic duplication in one of the strains. However, these mutations were not uniquely associated with persisters, suggesting that the persistent phenotype may be related to metabolic and transcriptional changes. Given that mannitol has been proposed to activate bacterial metabolism, the synergistic combination of mannitol and ciprofloxacin was evaluated on clinical 48 h *P. aeruginosa* biofilms. When administered at doses ≥ 320 mg/L, mannitol was capable of preventing persister cell formation by efficiently activating dormant bacteria and making them susceptible to the antibiotic. These results were confirmed using viable colony counting. As the tested ciprofloxacin-mannitol combination appeared to fully eradicate mature biofilms, we conclude that impedance-based biofilm diagnostics, which permits antibiotic susceptibility testing and the identification of persister cells, is of great potential for the clinical practice and could aid in establishing treatment breakpoints for emerging biofilm-related infections.

ARTICLE HISTORY Received 8 July 2021; Revised 16 September 2021; Accepted 12 October 2021

KEYWORDS *P. aeruginosa*; xCELLigence; biofilms; mannitol; persister cells; antibiotic resistance; ciprofloxacin

Introduction

Biofilms can be described as bacterial communities immobilized in a self-secreted biopolymeric matrix. This matrix is mainly composed of macromolecules including DNA, proteins and polysaccharides and has a very selective permeability to nutrients and antimicrobial compounds [1,2]. Thus, biofilms have already been described to be up to 1000 times more resistant to antibiotics compared to their planktonic forms and exhibit a large threat to human health [3]. Although bacterial biofilms have been deeply investigated during the past decades, a major limitation is that most existing methods for biofilm research provide information at a single endpoint, therefore missing relevant features about the growth and persistence dynamics [4–6]. In addition, classical biofilm mass quantification usually provides high standard deviations, and can result in lack of reproducibility due to manipulation steps. For this reason, methods for continued monitoring of biofilm growth where the biofilm does not need to be labelled or manipulated

have been proposed as a powerful alternative to traditional staining procedures [7,8].

Pseudomonas aeruginosa is an opportunistic pathogenic bacterium that causes both acute and chronic infections in severe wounds, urinary tract, or in patients undergoing chemotherapy or any other medical condition related to a weakened immune system like cystic fibrosis [9,10]. The pathogenic success of this bacterium is closely related to quorum sensing systems and the ability to synthesize different metabolites and virulence factors such as pyoverdine, exotoxin A, phospholipase C and elastase [11–13]. Moreover, *P. aeruginosa* infections are extremely difficult to treat, as this bacterium is resistant to many antimicrobial compounds and can easily survive on abiotic and biotic surfaces such as medical equipment even after disinfection [14]. In addition, biofilm formation capacity of *P. aeruginosa* contributes enormously to infection development because biofilms protect this bacterium from immune system attack and conventional antibiotic treatment [15–19].

CONTACT Alex Mira mira_ale@fisabio.es Genomics & Health Department, FISABIO Foundation, Avda. Catalunya 21, 46020 Valencia, Spain

Supplemental data for this article can be accessed at <https://doi.org/10.1080/22221751.2021.1994355>.

© 2021 The Author(s). Published by Informa UK Limited, trading as Taylor & Francis Group, on behalf of Shanghai Shangyixun Cultural Communication Co., Ltd. This is an Open Access article distributed under the terms of the Creative Commons Attribution License (<http://creativecommons.org/licenses/by/4.0/>), which permits unrestricted use, distribution, and reproduction in any medium, provided the original work is properly cited.

REFERENCES

- 1 Bjarnsholt T, Ciofu O, Molin S, Givskov M, Høiby N. Applying insights from biofilm biology to drug development-can a new approach be developed? *Nat. Rev. Drug Discov.* 2013; **12**: 791–808.
- 2 Ciofu O, Tolker-Nielsen T. Tolerance and resistance of pseudomonas aeruginosa biofilms to antimicrobial agents-how P. aeruginosa Can escape antibiotics. *Front Microbiol* 2019; **10**. doi:10.3389/fmicb.2019.00913.
- 3 O’Toole GA, Wong GCL. Sensational biofilms: Surface sensing in bacteria. *Curr. Opin. Microbiol.* 2016; **30**. doi:10.1016/j.mib.2016.02.004.
- 4 Flemming HC, Wingender J. The biofilm matrix. *Nat. Rev. Microbiol.* 2010; **8**: 623–633.
- 5 Costerton WJ, Wilson M. Introducing Biofilms . *Biofilms* 2004; **1**. doi:10.1017/s1479050504001164.
- 6 Gries CM, Kielian T. Staphylococcal biofilms and immune polarization during prosthetic joint infection. In: *Journal of the American Academy of Orthopaedic Surgeons*. Lippincott Williams and Wilkins, 2017, pp S20–S24.
- 7 Stewart PS, Costerton JW. Antibiotic resistance of bacteria in biofilms. *Lancet* 2001; **358**: 135–38.
- 8 Yin W, Wang Y, Liu L, He J. Biofilms: The microbial “protective clothing” in extreme environments. *Int J Mol Sci* 2019; **20**. doi:10.3390/ijms20143423.
- 9 Hall-Stoodley L, Costerton JW, Stoodley P. Bacterial biofilms: From the natural environment to infectious diseases. *Nat. Rev. Microbiol.* 2004; **2**. doi:10.1038/nrmicro821.
- 10 Costerton JW, Geesey GG, Cheng KJ. How bacteria stick. *Sci Am* 1978; **238**. doi:10.1038/scientificamerican0178-86.
- 11 Stewart PS, Costerton JW. Antibiotic resistance of bacteria in biofilms. *Lancet* 2001; **358**: 135–138.
- 12 Lewis K. Riddle of biofilm resistance. *Antimicrob. Agents Chemother.* 2001; **45**. doi:10.1128/AAC.45.4.999-1007.2001.
- 13 Crouzet M, Le Senechal C, Brözel VS *et al.* Exploring early steps in biofilm formation: Set-up of an experimental system for molecular studies. *BMC Microbiol* 2014; **14**. doi:10.1186/s12866-014-0253-z.
- 14 Lebeaux D, Chauhan A, Rendueles O, Beloin C. From in vitro to in vivo models of bacterial biofilm-related infections. *Pathogens.* 2013; **2**. doi:10.3390/pathogens2020288.
- 15 Høiby N, Ciofu O, Johansen HK *et al.* The clinical impact of bacterial biofilms. In: *International Journal of Oral Science*. 2011 doi:10.4248/IJOS11026.

- 16 Bermejo P, Sánchez MC, Llama-Palacios A, Figuero E, Herrera D, Sanz Alonso M. Biofilm formation on dental implants with different surface micro-topography: An in vitro study. *Clin Oral Implants Res* 2019; **30**. doi:10.1111/clr.13455.
- 17 Li X, Kolltveit KM, Tronstad L, Olsen I. Systemic diseases caused by oral infection. *Clin. Microbiol. Rev.* 2000; **13**. doi:10.1128/CMR.13.4.547-558.2000.
- 18 Singh R, Ray P, Das A, Sharma M. Role of persisters and small-colony variants in antibiotic resistance of planktonic and biofilm-associated *Staphylococcus aureus*: An in vitro study. *J Med Microbiol* 2009; **58**: 1067–1073.
- 19 Wu H, Moser C, Wang HZ, Høiby N, Song ZJ. Strategies for combating bacterial biofilm infections. *Int. J. Oral Sci.* 2015; **7**. doi:10.1038/ijos.2014.65.
- 20 Moser C, Pedersen HT, Lerche CJ *et al.* Biofilms and host response – helpful or harmful. *APMIS.* 2017; **125**. doi:10.1111/apm.12674.
- 21 Otto M. Staphylococcal Infections: Mechanisms of Biofilm Maturation and Detachment as Critical Determinants of Pathogenicity. *Annu Rev Med* 2013; **64**: 175–188.
- 22 Høiby N. A short history of microbial biofilms and biofilm infections. *APMIS.* 2017; **125**. doi:10.1111/apm.12686.
- 23 Mulcahy LR, Isabella VM, Lewis K. *Pseudomonas aeruginosa* Biofilms in Disease. *Microb Ecol* 2014; **68**. doi:10.1007/s00248-013-0297-x.
- 24 Sharma D, Misba L, Khan AU. Antibiotics versus biofilm: An emerging battleground in microbial communities. *Antimicrob. Resist. Infect. Control.* 2019; **8**. doi:10.1186/s13756-019-0533-3.
- 25 Uruén C, Chopo-Escuin G, Tommassen J, Mainar-Jaime RC, Arenas J. Biofilms as promoters of bacterial antibiotic resistance and tolerance. *Antibiotics.* 2021; **10**. doi:10.3390/antibiotics10010003.
- 26 Aparna MS, Yadav S. Biofilms: Microbes and disease. *Brazilian J. Infect. Dis.* 2008; **12**. doi:10.1590/S1413-86702008000600016.
- 27 Fux CA, Costerton JW, Stewart PS, Stoodley P. Survival strategies of infectious biofilms. *Trends Microbiol.* 2005. doi:10.1016/j.tim.2004.11.010.
- 28 Simões M, Simões LC, Vieira MJ. A review of current and emergent biofilm control strategies. *LWT.* 2010; **43**. doi:10.1016/j.lwt.2009.12.008.
- 29 O’Toole G, Kaplan HB, Kolter R. Biofilm formation as microbial development. *Annu. Rev. Microbiol.* 2000; **54**. doi:10.1146/annurev.micro.54.1.49.
- 30 Muhammad MH, Idris AL, Fan X *et al.* Beyond Risk: Bacterial Biofilms and Their Regulating Approaches. *Front. Microbiol.* 2020; **11**. doi:10.3389/fmicb.2020.00928.
- 31 Magana M, Sereti C, Ioannidis A *et al.* Options and limitations in clinical investigation of bacterial biofilms. *Clin Microbiol Rev* 2018; **31**: 1–49.
- 32 Deng Y, Lv W. *Biofilms and Implantable Medical Devices: Infection and Control.* 2016.

- 33 Soll DR, Daniels KJ. Plasticity of *Candida albicans* Biofilms. *Microbiol Mol Biol Rev* 2016; **80**. doi:10.1128/mbr.00068-15.
- 34 Sadekuzzaman M, Yang S, Mizan MFR, Ha SD. Current and Recent Advanced Strategies for Combating Biofilms. *Compr Rev Food Sci Food Saf* 2015; **14**. doi:10.1111/1541-4337.12144.
- 35 Belas R. Biofilms, flagella, and mechanosensing of surfaces by bacteria. *Trends Microbiol.* 2014; **22**. doi:10.1016/j.tim.2014.05.002.
- 36 Schultz MP, Bendick JA, Holm ER, Hertel WM. Economic impact of biofouling on a naval surface ship. *Biofouling* 2011; **27**. doi:10.1080/08927014.2010.542809.
- 37 Dunne WM. Bacterial adhesion: Seen any good biofilms lately? *Clin. Microbiol. Rev.* 2002; **15**. doi:10.1128/CMR.15.2.155-166.2002.
- 38 Donlan RM. Biofilms: Microbial life on surfaces. *Emerg. Infect. Dis.* 2002; **8**. doi:10.3201/eid0809.020063.
- 39 Toyofuku M, Inaba T, Kiyokawa T, Obana N, Yawata Y, Nomura N. Environmental factors that shape biofilm formation. *Biosci. Biotechnol. Biochem.* 2016; **80**. doi:10.1080/09168451.2015.1058701.
- 40 Di Ciccio P, Vergara A, Festino AR *et al.* Biofilm formation by *Staphylococcus aureus* on food contact surfaces: Relationship with temperature and cell surface hydrophobicity. *Food Control* 2015; **50**. doi:10.1016/j.foodcont.2014.10.048.
- 41 Guilbaud M, Bruzard J, Bouffartigues E *et al.* Proteomic response of *Pseudomonas aeruginosa* PAO1 adhering to solid surfaces. *Front Microbiol* 2017; **8**. doi:10.3389/fmicb.2017.01465.
- 42 Song F, Koo H, Ren D. Effects of material properties on bacterial adhesion and biofilm formation. *J. Dent. Res.* 2015; **94**. doi:10.1177/0022034515587690.
- 43 Harrison JJ, Almblad H, Irie Y *et al.* Elevated exopolysaccharide levels in *Pseudomonas aeruginosa* flagellar mutants have implications for biofilm growth and chronic infections. *PLoS Genet* 2020; **16**: 1–22.
- 44 Flemming HC, Wingender J, Szewzyk U, Steinberg P, Rice SA, Kjelleberg S. Biofilms: An emergent form of bacterial life. *Nat. Rev. Microbiol.* 2016; **14**. doi:10.1038/nrmicro.2016.94.
- 45 Fernández-Barat L, Ciofu O, Kragh KN *et al.* Phenotypic shift in *Pseudomonas aeruginosa* populations from cystic fibrosis lungs after 2-week antipseudomonal treatment. *J Cyst Fibros* 2017; **16**: 222–229.
- 46 Branda SS, Vik Å, Friedman L, Kolter R. Biofilms: The matrix revisited. *Trends Microbiol.* 2005; **13**. doi:10.1016/j.tim.2004.11.006.
- 47 Decho AW. The EPS matrix as an adaptive bastion for biofilms: Introduction to special issue. *Int. J. Mol. Sci.* 2013; **14**. doi:10.3390/ijms141223297.
- 48 Flemming HC, Neu TR, Wozniak DJ. The EPS matrix: The ‘House of Biofilm Cells’. *J.*

- Bacteriol. 2007; **189**. doi:10.1128/JB.00858-07.
- 49 Jakubovics NS, Goodman SD, Mashburn-Warren L, Stafford GP, Cieplik F. The dental plaque biofilm matrix. *Periodontol 2000* 2021; **86**. doi:10.1111/prd.12361.
- 50 Molloy S. Biofilms: Biofilms take shape. *Nat. Rev. Microbiol.* 2012; **10**. doi:10.1038/nrmicro2756.
- 51 Vitális E, Nagy F, Tóth Z *et al.* Candida biofilm production is associated with higher mortality in patients with candidaemia. *Mycoses* 2020; **63**. doi:10.1111/myc.13049.
- 52 Ciofu O, Moser C, Jensen PØ, Høiby N. Tolerance and resistance of microbial biofilms. *Nat. Rev. Microbiol.* 2022; **20**. doi:10.1038/s41579-022-00682-4.
- 53 Bjarnsholt T, Jensen PØ, Rasmussen TB *et al.* Garlic blocks quorum sensing and promotes rapid clearing of pulmonary *Pseudomonas aeruginosa* infections. *Microbiology* 2005; **151**. doi:10.1099/mic.0.27955-0.
- 54 Alhede M, Bjarnsholt T, Jensen P *et al.* *Pseudomonas aeruginosa* recognizes and responds aggressively to the presence of polymorphonuclear leukocytes. *Microbiology* 2009; **155**. doi:10.1099/mic.0.031443-0.
- 55 Schilcher K, Horswill AR. Staphylococcal Biofilm Development: Structure, Regulation, and Treatment Strategies. *Microbiol Mol Biol Rev* 2020; **84**. doi:10.1128/mubr.00026-19.
- 56 Lejeune P. Biofilm-Dependent Regulation of Gene Expression. In: *Medical Implications of Biofilms*. 2009 doi:10.1017/cbo9780511546297.002.
- 57 Kuchma SL, O'Toole GA. Surface-induced and biofilm-induced changes in gene expression. *Curr. Opin. Biotechnol.* 2000; **11**. doi:10.1016/S0958-1669(00)00123-3.
- 58 Schembri MA, Kjærgaard K, Klemm P. Global gene expression in *Escherichia coli* biofilms. *Mol Microbiol* 2003; **48**. doi:10.1046/j.1365-2958.2003.03432.x.
- 59 Tuson HH, Weibel DB. Bacteria-surface interactions. *Soft Matter*. 2013; **9**. doi:10.1039/c3sm27705d.
- 60 Mulcahy H, Charron-Mazenod L, Lewenza S. Extracellular DNA chelates cations and induces antibiotic resistance in *Pseudomonas aeruginosa* biofilms. *PLoS Pathog* 2008; **4**. doi:10.1371/journal.ppat.1000213.
- 61 Zhang X, Bishop PL, Kupferle MJ. Measurement of polysaccharides and proteins in biofilm extracellular polymers. In: *Water Science and Technology*. 1998 doi:10.1016/S0273-1223(98)00127-9.
- 62 Guzmán-Soto I, McTiernan C, Gonzalez-Gomez M *et al.* Mimicking biofilm formation and development: Recent progress in in vitro and in vivo biofilm models. *iScience*. 2021; **24**. doi:10.1016/j.isci.2021.102443.
- 63 Wille J, Coenye T. Biofilm dispersion: The key to biofilm eradication or opening Pandora's box? *Biofilm*. 2020; **2**. doi:10.1016/j.biofilm.2020.100027.
- 64 Fleming D, Rumbaugh K. Approaches to Dispersing Medical Biofilms. *Microorganisms*

- 2017; **5**: 15.
- 65 Kaplan JB. Biofilm Dispersal: Mechanisms, Clinical Implications, and Potential Therapeutic Uses. *J. Dent. Res.* 2010; **89**: 205–218.
- 66 Liu C, Sun D, Liu J *et al.* cAMP and c-di-GMP synergistically support biofilm maintenance through the direct interaction of their effectors. *Nat Commun* 2022; **13**. doi:10.1038/s41467-022-29240-5.
- 67 Rumbaugh KP, Sauer K. Biofilm dispersion. *Nat Rev Microbiol* 2020; **18**: 571–586.
- 68 Simon-Soro A, Ren Z, Krom BP *et al.* Polymicrobial Aggregates in Human Saliva Build the Oral Biofilm. *MBio* 2022; **13**. doi:10.1128/MBIO.00131-22.
- 69 Kragh KN, Hutchison JB, Melaugh G *et al.* Role of multicellular aggregates in biofilm formation. *MBio* 2016; **7**. doi:10.1128/mBio.00237-16.
- 70 Xu R, Zhang S, Meng F. Large-sized planktonic bioaggregates possess high biofilm formation potentials: Bacterial succession and assembly in the biofilm metacommunity. *Water Res* 2020; **170**. doi:10.1016/j.watres.2019.115307.
- 71 Kaplan JB. Biofilm Dispersal: Mechanisms, Clinical Implications, and Potential Therapeutic Uses. *J Dent Res* 2010; **89**: 205–218.
- 72 Schooling SR, Charaf UK, Allison DG, Gilbert P. A role for rhamnolipid in biofilm dispersion. *Biofilms* 2004; **1**. doi:10.1017/s147905050400119x.
- 73 Davies DG, Marques CNH. A fatty acid messenger is responsible for inducing dispersion in microbial biofilms. *J Bacteriol* 2009; **191**. doi:10.1128/JB.01214-08.
- 74 Solano C, Echeverz M, Lasa I. Biofilm dispersion and quorum sensing. *Curr. Opin. Microbiol.* 2014; **18**. doi:10.1016/j.mib.2014.02.008.
- 75 Saxena P, Joshi Y, Rawat K, Bisht R. Biofilms: Architecture, Resistance, Quorum Sensing and Control Mechanisms. *Indian J. Microbiol.* 2019; **59**. doi:10.1007/s12088-018-0757-6.
- 76 De Kievit TR. Quorum sensing in *Pseudomonas aeruginosa* biofilms. *Environ. Microbiol.* 2009; **11**. doi:10.1111/j.1462-2920.2008.01792.x.
- 77 Zhou L, Zhang Y, Ge Y, Zhu X, Pan J. Regulatory Mechanisms and Promising Applications of Quorum Sensing-Inhibiting Agents in Control of Bacterial Biofilm Formation. *Front. Microbiol.* 2020; **11**. doi:10.3389/fmicb.2020.589640.
- 78 Mukherjee PK, Zhou G, Munyon R, Ghannoum MA. *Candida* biofilm: A well-designed protected environment. *Med. Mycol.* 2005; **43**. doi:10.1080/13693780500107554.
- 79 Schwartz K, Stephenson R, Hernandez M, Jambang N, Boles BR. The use of drip flow and rotating disk reactors for *Staphylococcus aureus* biofilm analysis. *J Vis Exp* 2010. doi:10.3791/2470.
- 80 Moormeier DE, Bayles KW. *Staphylococcus aureus* biofilm: a complex developmental organism. *Mol. Microbiol.* 2017; **104**: 365–376.
- 81 Foster TJ. Surface Proteins of *Staphylococcus epidermidis*. *Front. Microbiol.* 2020; **11**.

- doi:10.3389/fmicb.2020.01829.
- 82 Speziale P, Pietrocola G, Foster TJ, Geoghegan JA. Protein-based biofilm matrices in staphylococci. *Front. Cell. Infect. Microbiol.* 2014; **4**. doi:10.3389/fcimb.2014.00171.
- 83 *Biofilms and Implantable Medical Devices*. 2017 doi:10.1016/c2014-0-04106-8.
- 84 Khatoon Z, McTiernan CD, Suuronen EJ, Mah TF, Alarcon EI. Bacterial biofilm formation on implantable devices and approaches to its treatment and prevention. *Heliyon*. 2018; **4**. doi:10.1016/j.heliyon.2018.e01067.
- 85 Okuda KI, Nagahori R, Yamada S *et al.* The composition and structure of biofilms developed by *Propionibacterium acnes* isolated from cardiac pacemaker devices. *Front Microbiol* 2018; **9**: 1–12.
- 86 O’Gara JP. ica and beyond: Biofilm mechanisms and regulation in *Staphylococcus epidermidis* and *Staphylococcus aureus*. *FEMS Microbiol. Lett.* 2007; **270**. doi:10.1111/j.1574-6968.2007.00688.x.
- 87 Kogan G, Sadovskaya I, Chaignon P, Chokr A, Jabbouri S. Biofilms of clinical strains of *Staphylococcus* that do not contain polysaccharide intercellular adhesin. *FEMS Microbiol Lett* 2006; **255**. doi:10.1111/j.1574-6968.2005.00043.x.
- 88 Zheng Y, He L, Asiamah TK, Otto M. Colonization of medical devices by staphylococci. *Environ. Microbiol.* 2018; **20**. doi:10.1111/1462-2920.14129.
- 89 Bjarnsholt T, Jensen PØ, Fiandaca MJ *et al.* *Pseudomonas aeruginosa* biofilms in the respiratory tract of cystic fibrosis patients. *Pediatr Pulmonol* 2009; **44**. doi:10.1002/ppul.21011.
- 90 Veessenmeyer JL, Hauser AR, Lisboa T, Rello J. *Pseudomonas aeruginosa* virulence and therapy: Evolving translational strategies. *Crit Care Med* 2009; **37**: 1777–1786.
- 91 Chatterjee P, Sass G, Swietnicki W, Stevens DA. Review of Potential *Pseudomonas* Weaponry , Relevant to the *Pseudomonas – Aspergillus* Interplay , for the Mycology Community. 2020.
- 92 Alonso B, Fernández-Barat L, Di Domenico EG *et al.* Characterization of the virulence of *Pseudomonas aeruginosa* strains causing ventilator-associated pneumonia. *BMC Infect Dis* 2020; **20**: 1–8.
- 93 Høiby N. Recent advances in the treatment of *Pseudomonas aeruginosa* infections in cystic fibrosis. *BMC Med.* 2011; **9**. doi:10.1186/1741-7015-9-32.
- 94 Breidenstein EBM, de la Fuente-Núñez C, Hancock REW. *Pseudomonas aeruginosa*: All roads lead to resistance. *Trends Microbiol.* 2011; **19**. doi:10.1016/j.tim.2011.04.005.
- 95 Rasamiravaka T, Labtani Q, Duez P, El Jaziri M. The formation of biofilms by *pseudomonas aeruginosa*: A review of the natural and synthetic compounds interfering with control mechanisms. *Biomed Res. Int.* 2015; **2015**. doi:10.1155/2015/759348.
- 96 Soares A, Alexandre K, Etienne M. Tolerance and Persistence of *Pseudomonas aeruginosa* in Biofilms Exposed to Antibiotics: Molecular Mechanisms, Antibiotic Strategies and

- Therapeutic Perspectives. *Front. Microbiol.* 2020; **11**. doi:10.3389/fmicb.2020.02057.
- 97 Goltermann L, Tolker-Nielsen T. Importance of the exopolysaccharide matrix in antimicrobial tolerance of *Pseudomonas aeruginosa* aggregates. *Antimicrob Agents Chemother* 2017; **61**. doi:10.1128/AAC.02696-16.
- 98 Leid JG, Willson CJ, Shirtliff ME, Hassett DJ, Parsek MR, Jeffers AK. The Exopolysaccharide Alginate Protects *Pseudomonas aeruginosa* Biofilm Bacteria from IFN- γ -Mediated Macrophage Killing . *J Immunol* 2005; **175**. doi:10.4049/jimmunol.175.11.7512.
- 99 Boyd A, Chakrabarty AM. *Pseudomonas aeruginosa* biofilms: role of the alginate exopolysaccharide. *J Ind Microbiol* 1995; **15**. doi:10.1007/BF01569821.
- 100 Billings N, Ramirez Millan M, Caldara M *et al.* The Extracellular Matrix Component Psl Provides Fast-Acting Antibiotic Defense in *Pseudomonas aeruginosa* Biofilms. *PLoS Pathog* 2013; **9**. doi:10.1371/journal.ppat.1003526.
- 101 Colvin KM, Irie Y, Tart CS *et al.* The Pel and Psl polysaccharides provide *Pseudomonas aeruginosa* structural redundancy within the biofilm matrix. *Environ Microbiol* 2012; **14**. doi:10.1111/j.1462-2920.2011.02657.x.
- 102 Colvin KM, Gordon VD, Murakami K *et al.* The pel polysaccharide can serve a structural and protective role in the biofilm matrix of *Pseudomonas aeruginosa*. *PLoS Pathog* 2011; **7**. doi:10.1371/journal.ppat.1001264.
- 103 Keren I, Kaldalu N, Spoering A, Wang Y, Lewis K. Persister cells and tolerance to antimicrobials. *FEMS Microbiol Lett* 2004; **230**. doi:10.1016/S0378-1097(03)00856-5.
- 104 Long Y, Fu W, Li S *et al.* Identification of novel genes that promote persister formation by repressing transcription and cell division in *Pseudomonas aeruginosa*. *J Antimicrob Chemother* 2019; **74**: 2575–2587.
- 105 Silva S, Negri M, Henriques M, Oliveira R, Williams DW, Azeredo J. Adherence and biofilm formation of non-*Candida albicans* *Candida* species. *Trends Microbiol.* 2011; **19**. doi:10.1016/j.tim.2011.02.003.
- 106 Chandra J, Kuhn DM, Mukherjee PK, Hoyer LL, McCormick T, Ghannoum MA. Biofilm formation by the fungal pathogen *Candida albicans*: Development, architecture, and drug resistance. *J Bacteriol* 2001; **183**. doi:10.1128/JB.183.18.5385-5394.2001.
- 107 Lohse MB, Gulati M, Craik CS, Johnson AD, Nobile CJ. Combination of Antifungal Drugs and Protease Inhibitors Prevent *Candida albicans* Biofilm Formation and Disrupt Mature Biofilms. *Front Microbiol* 2020; **11**: 1–12.
- 108 Nett JE, Andes DR. Fungal Biofilms: In Vivo Models for Discovery of Anti-Biofilm Drugs . In: *Microbial Biofilms*. 2015 doi:10.1128/9781555817466.ch2.
- 109 Atriwal T, Azeem K, Husain FM *et al.* Mechanistic Understanding of *Candida albicans* Biofilm Formation and Approaches for Its Inhibition. *Front Microbiol* 2021; **12**. doi:10.3389/fmicb.2021.638609.

- 110 Kuhn DM, Chandra J, Mukherjee PK, Ghannoum MA. Comparison of biofilms formed by *Candida albicans* and *Candida parapsilosis* on bioprosthetic surfaces. *Infect Immun* 2002; **70**. doi:10.1128/IAI.70.2.878-888.2002.
- 111 Serrano-Fujarte I, López-Romero E, Reyna-López GE, Martínez-Gómez MA, Vega-González A, Cuéllar-Cruz M. Influence of culture media on biofilm formation by *Candida* species and response of sessile cells to antifungals and oxidative stress. *Biomed Res Int* 2015; **2015**. doi:10.1155/2015/783639.
- 112 Seneviratne CJ, Jin L, Samaranayake LP. Biofilm lifestyle of *Candida*: A mini review. *Oral Dis*. 2008; **14**. doi:10.1111/j.1601-0825.2007.01424.x.
- 113 Cateau E, Berjeaud JM, Imbert C. Possible role of azole and echinocandin lock solutions in the control of *Candida* biofilms associated with silicone. *Int J Antimicrob Agents* 2011; **37**. doi:10.1016/j.ijantimicag.2010.12.016.
- 114 Galdiero E, de Alteriis E, De Natale A *et al*. Eradication of *Candida albicans* persister cell biofilm by the membranotropic peptide gH625. *Sci Rep* 2020; **10**: 1–12.
- 115 Kaneko Y, Miyagawa S, Takeda O *et al*. Real-time microscopic observation of *Candida* biofilm development and effects due to micafungin and fluconazole. *Antimicrob Agents Chemother* 2013; **57**: 2226–2230.
- 116 Douglas LJ. Medical importance of biofilms in *Candida* infections. *Rev. Iberoam. Micol.* 2002; **19**.
- 117 Sanglard D, Odds FC. Resistance of *Candida* species to antifungal agents: Molecular mechanisms and clinical consequences. *Lancet Infect. Dis.* 2002; **2**. doi:10.1016/S1473-3099(02)00181-0.
- 118 Taff HT, Mitchell KF, Edward JA, Andes DR. Mechanisms of *Candida* biofilm drug resistance. *Future Microbiol.* 2013; **8**. doi:10.2217/fmb.13.101.
- 119 Sanglard D. Emerging threats in antifungal-resistant fungal pathogens. *Front. Med.* 2016; **3**. doi:10.3389/fmed.2016.00011.
- 120 Tits J, Cammue BPA, Thevissen K. Combination therapy to treat fungal biofilm-based infections. *Int J Mol Sci* 2020; **21**: 1–19.
- 121 Cowen LE, Sanglard D, Howard SJ, Rogers PD, Perlin DS. Mechanisms of antifungal drug resistance. *Cold Spring Harb Perspect Med* 2015; **5**: 1–22.
- 122 Salci TP, Negri M, Abadio AKR, Svidzinski TIE, Kioshima ÉS. Targeting *Candida* spp. to develop antifungal agents. *Drug Discov. Today*. 2018; **23**. doi:10.1016/j.drudis.2018.01.003.
- 123 Gonçalves SS, Souza ACR, Chowdhary A, Meis JF, Colombo AL. Epidemiology and molecular mechanisms of antifungal resistance in *Candida* and *Aspergillus*. *Mycoses* 2016; **59**. doi:10.1111/myc.12469.
- 124 Alcazar-Fuoli L, Mellado E. Current status of antifungal resistance and its impact on clinical practice. *Br. J. Haematol.* 2014; **166**. doi:10.1111/bjh.12896.

- 125 Cavalheiro M, Teixeira MC. Candida Biofilms: Threats, challenges, and promising strategies. *Front. Med.* 2018; **5**. doi:10.3389/fmed.2018.00028.
- 126 Gadour E, Kotb A. Systematic Review of Antifungal-Induced Acute Liver Failure. *Cureus* 2021. doi:10.7759/cureus.18940.
- 127 Rosier BT, Marsh PD, Mira A. Resilience of the Oral Microbiota in Health: Mechanisms That Prevent Dysbiosis. *J. Dent. Res.* 2018; **97**. doi:10.1177/0022034517742139.
- 128 Marsh PD. Are dental diseases examples of ecological catastrophes? *Microbiology.* 2003; **149**. doi:10.1099/mic.0.26082-0.
- 129 Kolenbrander PE. Oral microbial communities: Biofilms, interactions, and genetic systems. *Annu. Rev. Microbiol.* 2000; **54**. doi:10.1146/annurev.micro.54.1.413.
- 130 Kuboniwa M, Lamont RJ. Subgingival biofilm formation. *Periodontol 2000* 2010; **52**. doi:10.1111/j.1600-0757.2009.00311.x.
- 131 Checchi V, Pascolo G. Microbiological Response to Periodontal Therapy: A Retrospective Study. *Open Dent J* 2018; **12**. doi:10.2174/1874210601812010837.
- 132 Jiao Y, Hasegawa M, Inohara N. The role of oral pathobionts in dysbiosis during periodontitis development. *J. Dent. Res.* 2014; **93**. doi:10.1177/0022034514528212.
- 133 Mira A, Buetas E, Rosier B *et al.* Development of an in vitro system to study oral biofilms in real time through impedance technology: validation and potential applications. *J Oral Microbiol* 2019; **11**. doi:10.1080/20002297.2019.1609838.
- 134 Ortiz V, Filippi A. Halitosis. *Monogr. Oral Sci.* 2020; **29**. doi:10.1159/000510192.
- 135 Sánchez MC, Alonso-Español A, Ribeiro-Vidal H, Alonso B, Herrera D, Sanz M. Relevance of biofilm models in periodontal research: From static to dynamic systems. *Microorganisms.* 2021; **9**. doi:10.3390/microorganisms9020428.
- 136 Jenkinson HF. Beyond the oral microbiome. *Environ. Microbiol.* 2011; **13**. doi:10.1111/j.1462-2920.2011.02573.x.
- 137 Lasserre JF, Brex MC, Toma S. Oral microbes, biofilms and their role in periodontal and peri-implant diseases. *Materials (Basel)* 2018; **11**.
- 138 Kolenbrander PE, London J. Adhere today, here tomorrow: Oral bacterial adherence. *J Bacteriol* 1993; **175**: 3247–3252.
- 139 Kolenbrander PE, Andersen RN, Blehert DS, Eglund PG, Foster JS, Palmer RJ. Communication among Oral Bacteria. *Microbiol Mol Biol Rev* 2002; **66**: 486–505.
- 140 Rath S, Bal SCB, Dubey D. Oral Biofilm: Development Mechanism, Multidrug Resistance, and Their Effective Management with Novel Techniques. *Rambam Maimonides Med J* 2021; **12**. doi:10.5041/RMMJ.10428.
- 141 Darveau RP. Periodontitis: A polymicrobial disruption of host homeostasis. *Nat. Rev. Microbiol.* 2010; **8**. doi:10.1038/nrmicro2337.
- 142 Chapple ILC, Mealey BL, Van Dyke TE *et al.* Periodontal health and gingival diseases

- and conditions on an intact and a reduced periodontium: Consensus report of workgroup 1 of the 2017 World Workshop on the Classification of Periodontal and Peri-Implant Diseases and Conditions. *J Periodontol* 2018; **89**. doi:10.1002/JPER.17-0719.
- 143 Chapple ILC, Van Der Weijden F, Doerfer C *et al.* Primary prevention of periodontitis: Managing gingivitis. *J. Clin. Periodontol.* 2015; **42**. doi:10.1111/jcpe.12366.
- 144 Marcenes W, Kassebaum NJ, Bernabé E *et al.* Global burden of oral conditions in 1990-2010: A systematic analysis. *J Dent Res* 2013; **92**. doi:10.1177/0022034513490168.
- 145 O’Leary TJ, Drake RB, Naylor JE. The Plaque Control Record. *J Periodontol* 1972; **43**. doi:10.1902/jop.1972.43.1.38.
- 146 Johnston W, Rosier BT, Artacho A *et al.* Mechanical biofilm disruption causes microbial and immunological shifts in periodontitis patients. *Sci Rep* 2021; **11**. doi:10.1038/s41598-021-89002-z.
- 147 Heller D, Varela VM, E Silva-Senem MX, Torres MCB, Feres-Filho EJ, Colombo APV. Impact of systemic antimicrobials combined with anti-infective mechanical debridement on the microbiota of generalized aggressive periodontitis: A 6-month RCT. *J Clin Periodontol* 2011; **38**. doi:10.1111/j.1600-051X.2011.01707.x.
- 148 Mombelli A, Walter C. Antibiotics in Periodontics. *Swiss Dent J* 2019; **129**.
- 149 Griffiths GS, Ayob R, Guerrero A *et al.* Amoxicillin and metronidazole as an adjunctive treatment in generalized aggressive periodontitis at initial therapy or re-treatment: A randomized controlled clinical trial. *J Clin Periodontol* 2011; **38**. doi:10.1111/j.1600-051X.2010.01632.x.
- 150 Elashiry M, Morandini AC, Cornelius Timothius CJ, Ghaly M, Cutler CW. Selective antimicrobial therapies for periodontitis: Win the “battle and the war”. *Int. J. Mol. Sci.* 2021; **22**. doi:10.3390/ijms22126459.
- 151 Zijngé V, Van Leeuwen MBM, Degener JE *et al.* Oral biofilm architecture on natural teeth. *PLoS One* 2010; **5**. doi:10.1371/journal.pone.0009321.
- 152 Algburi A, Comito N, Kashtanov D, Dicks LMT, Chikindas ML. Erratum for Algburi *et al.*, Control of Biofilm Formation: Antibiotics and Beyond. *Appl Environ Microbiol* 2017; **83**. doi:10.1128/aem.00165-17.
- 153 Reddy M, Shetty S, Vannala V. Embracing personalized medicine in dentistry. *J. Pharm. Bioallied Sci.* 2019; **11**. doi:10.4103/JPBS.JPBS_297_18.
- 154 Schulze A, Mitterer F, Pombo JP, Schild S. Biofilms by bacterial human pathogens: Clinical relevance - Development, composition and regulation - Therapeutical strategies. *Microb Cell* 2021; **8**. doi:10.15698/MIC2021.02.741.
- 155 Di Bonaventura G, Pompilio A. In Vitro Antimicrobial Susceptibility Testing of Biofilm-Growing Bacteria: Current and Emerging Methods. In: *Advances in Experimental Medicine and Biology*. 2022 doi:10.1007/5584_2021_641.
- 156 Macià MD, Rojo-Molinero E, Oliver A. Antimicrobial susceptibility testing in biofilm-

- growing bacteria. *Clin. Microbiol. Infect.* 2014; **20**. doi:10.1111/1469-0691.12651.
- 157 Hamilton MA. Testing antimicrobials against biofilm bacteria. *J AOAC Int* 2002; **85**. doi:10.1093/jaoac/85.2.479.
- 158 Brown DFJ, Kothari D. Antimicrobial-susceptibility testing of rapidly growing pathogenic bacteria. *J Antimicrob Chemother* 1978; **4**. doi:10.1093/jac/4.1.19.
- 159 Brackman G, Coenye T. Send Orders for Reprints to reprints@benthamscience.net
Quorum Sensing Inhibitors as Anti-Biofilm Agents. 2015.
- 160 Bahamondez-Canas TF, Heersema LA, Smyth HDC. Current status of in vitro models and assays for susceptibility testing for wound biofilm infections. *Biomedicines*. 2019; **7**. doi:10.3390/biomedicines7020034.
- 161 Wilson C, Lukowicz R, Merchant S *et al*. Quantitative and Qualitative Assessment Methods for Biofilm Growth: A Mini-review. *Res Rev J Eng Technol* 2017; **6**.<http://www.ncbi.nlm.nih.gov/pubmed/30214915><http://www.pubmedcentral.nih.gov/articlerender.fcgi?artid=PMC6133255>.
- 162 Roy R, Tiwari M, Donelli G, Tiwari V. Strategies for combating bacterial biofilms: A focus on anti-biofilm agents and their mechanisms of action. *Virulence*. 2018; **9**: 522–554.
- 163 Castro J, Lima Â, Sousa LGV, Rosca AS, Muzny CA, Cerca N. Crystal Violet Staining Alone Is Not Adequate to Assess Synergism or Antagonism in Multi-Species Biofilms of Bacteria Associated With Bacterial Vaginosis. *Front Cell Infect Microbiol* 2022; **11**. doi:10.3389/fcimb.2021.795797.
- 164 Kragh KN, Alhede M, Kvich L, Bjarnsholt T. Into the well—A close look at the complex structures of a microtiter biofilm and the crystal violet assay. *Biofilm* 2019; **1**: 100006.
- 165 Welch K, Cai Y, Strømme M. A Method for Quantitative Determination of Biofilm Viability. *J Funct Biomater* 2012; **3**. doi:10.3390/jfb3020418.
- 166 Gomes IB, Meireles A, Gonçalves AL *et al*. Standardized reactors for the study of medical biofilms: a review of the principles and latest modifications. *Crit Rev Biotechnol* 2018; **38**: 657–670.
- 167 Sternberg C, Bjarnsholt T, Shirtliff M. Methods for dynamic investigations of surface-attached in vitro bacterial and fungal biofilms. *Methods Mol Biol* 2014; **1147**. doi:10.1007/978-1-4939-0467-9_1.
- 168 Franklin MJ, Chang C, Akiyama T, Bothner B. New Technologies for Studying Biofilms. *Microb Biofilms* 2015; **3**: 1–32.
- 169 Azeredo J, Azevedo NF, Briandet R *et al*. Critical review on biofilm methods. *Crit. Rev. Microbiol.* 2017; **43**. doi:10.1080/1040841X.2016.1208146.
- 170 Castelo-Branco D de SCM, Amando BR, Ocadaque CJ *et al*. Mini-review: from in vitro to ex vivo studies: an overview of alternative methods for the study of medical biofilms. *Biofouling* 2020; **36**: 1129–1148.
- 171 Yassin SA, German MJ, Rolland SL, Rickard AH, Jakubovics NS. Inhibition of

- multispecies biofilms by a fluoride-releasing dental prosthesis copolymer. *J Dent* 2016; **48**. doi:10.1016/j.jdent.2016.03.001.
- 172 Nance WC, Dowd SE, Samarian D *et al.* A high-throughput microfluidic dental plaque biofilm system to visualize and quantify the effect of antimicrobials. *J Antimicrob Chemother* 2013; **68**. doi:10.1093/jac/dkt211.
- 173 Mira A. Oral Microbiome Studies: Potential Diagnostic and Therapeutic Implications. *Adv. Dent. Res.* 2018; **29**. doi:10.1177/0022034517737024.
- 174 Straub H, Eberl L, Zinn M, Rossi RM, Maniura-Weber K, Ren Q. A microfluidic platform for in situ investigation of biofilm formation and its treatment under controlled conditions. *J Nanobiotechnology* 2020; **18**. doi:10.1186/s12951-020-00724-0.
- 175 Camelo-Castillo AJ, Mira A, Pico A *et al.* Subgingival microbiota in health compared to periodontitis and the influence of smoking. *Front Microbiol* 2015; **6**. doi:10.3389/fmicb.2015.00119.
- 176 Griffen AL, Beall CJ, Campbell JH *et al.* Distinct and complex bacterial profiles in human periodontitis and health revealed by 16S pyrosequencing. *ISME J* 2012; **6**. doi:10.1038/ismej.2011.191.
- 177 Bizzarro S, Laine ML, Buijs MJ *et al.* Microbial profiles at baseline and not the use of antibiotics determine the clinical outcome of the treatment of chronic periodontitis. *Sci Rep* 2016; **6**. doi:10.1038/srep20205.
- 178 Chen T, Yu WH, Izard J, Baranova O V., Lakshmanan A, Dewhirst FE. The Human Oral Microbiome Database: a web accessible resource for investigating oral microbe taxonomic and genomic information. *Database (Oxford)* 2010; **2010**. doi:10.1093/database/baq013.
- 179 Coenye T, Nelis HJ. In vitro and in vivo model systems to study microbial biofilm formation. *J. Microbiol. Methods.* 2010; **83**. doi:10.1016/j.mimet.2010.08.018.
- 180 Yasuda H, Koga T, Fukuoka T. In vitro and in vivo models for bacterial biofilms. *Methods Enzymol* 1999; **310**. doi:10.1016/S0076-6879(99)10045-4.
- 181 P. C, A. M. In vivo biofilm has different minimum biofilm eradication concentration than in-vitro biofilm. *J Orthop Res* 2016; **34**.
- 182 Thomas SG, Glover M, Parthasarathy A, O'Hudson A. The Close-Call in Microbiology Labs - Understanding Microbes. *Adv Biol Lab Educ* 2020. doi:10.37590/able.v41.art85.
- 183 Le Norcy T, Faÿ F, Obando CZ, Hellio C, Réhel K, Linossier I. A new method for evaluation of antifouling activity of molecules against microalgal biofilms using confocal laser scanning microscopy-microfluidic flow-cells. *Int Biodeterior Biodegrad* 2019; **139**. doi:10.1016/j.ibiod.2019.03.001.
- 184 Goeres DM, Hamilton MA, Beck NA *et al.* A method for growing a biofilm under low shear at the air-liquid interface using the drip flow biofilm reactor. *Nat Protoc* 2009; **4**: 783–788.
- 185 Relucenti M, Familiari G, Donfrancesco O *et al.* Microscopy methods for biofilm

- imaging: Focus on sem and VP-SEM pros and cons. *Biology (Basel)*. 2021; **10**. doi:10.3390/biology10010051.
- 186 Schlafer S, Meyer RL. Confocal microscopy imaging of the biofilm matrix. *J. Microbiol. Methods*. 2017; **138**. doi:10.1016/j.mimet.2016.03.002.
- 187 Capita R, Vicente-Velasco M, Rodríguez-Melcón C, García-Fernández C, Carballo J, Alonso-Calleja C. Effect of low doses of biocides on the antimicrobial resistance and the biofilms of *Cronobacter sakazakii* and *Yersinia enterocolitica*. *Sci Rep* 2019; **9**: 1–12.
- 188 Welch JLM, Rossetti BJ, Rieken CW, Dewhirst FE, Borisy GG. Biogeography of a human oral microbiome at the micron scale. *Proc Natl Acad Sci U S A* 2016; **113**: E791–E800.
- 189 Gomes LC, Mergulhão FJ. SEM analysis of surface impact on biofilm antibiotic treatment. *Scanning* 2017; **2017**. doi:10.1155/2017/2960194.
- 190 Harrison JJ, Ceri H, Yerly J *et al*. The use of microscopy and three-dimensional visualization to evaluate the structure of microbial biofilms cultivated in the Calgary biofilm device. *Biol Proced Online* 2006; **8**. doi:10.1251/bpo127.
- 191 Sutherland IW. Biofilm exopolysaccharides: A strong and sticky framework. *Microbiology*. 2001; **147**. doi:10.1099/00221287-147-1-3.
- 192 Asahi Y, Miura J, Tsuda T *et al*. Simple observation of *Streptococcus mutans* biofilm by scanning electron microscopy using ionic liquids. *AMB Express* 2015; **5**: 0–8.
- 193 Chatterjee S, Biswas N, Datta A, Dey R, Maiti P. Atomic force microscopy in biofilm study. *Microscopy* 2014; **63**. doi:10.1093/jmicro/dfu013.
- 194 Baidamshina DR, Trizna EY, Holyavka MG *et al*. Targeting microbial biofilms using Ficin, a nonspecific plant protease. *Sci Rep* 2017; **7**. doi:10.1038/srep46068.
- 195 Dongari-Bagtzoglou A, Kashleva H, Dwivedi P, Diaz P, Vasilakos J. Characterization of mucosal *Candida albicans* biofilms. *PLoS One* 2009; **4**. doi:10.1371/journal.pone.0007967.
- 196 Ferrer MD, Rodriguez JC, Álvarez L, Artacho A, Royo G, Mira A. Effect of antibiotics on biofilm inhibition and induction measured by real-time cell analysis. *J Appl Microbiol* 2017; **122**: 640–650.
- 197 Lamarche B, Mira A FM. Studying bacterial biofilms using cellular impedance. xCELLigence @Real-time cell analyzers. 2017; : 1–6.
- 198 Žiemytė M, Rodríguez-Díaz JC, Ventero MP, Mira A, Ferrer MD. Effect of Dalbavancin on Staphylococcal Biofilms When Administered Alone or in Combination With Biofilm-Detaching Compounds. *Front Microbiol* 2020; **11**: 1–11.
- 199 Villanueva-Castellote Á, Llena Puy C, Carda-Diéguez M, Mira Á, Ferrer MD. Ex vivo evaluation of antibiotic sensitivity in samples from endodontic infections. *J Oral Microbiol* 2023; **15**. doi:10.1080/20002297.2022.2160536.
- 200 Rumbaugh KP, Carty NL. In vivo models of biofilm infection. In: *Biofilm Infections*. 2011 doi:10.1007/978-1-4419-6084-9_16.

- 201 Andes D, Nett J, Oschel P, Albrecht R, Marchillo K, Pitula A. Development and characterization of an in vivo central venous catheter *Candida albicans* biofilm model. *Infect Immun* 2004; **72**. doi:10.1128/IAI.72.10.6023-6031.2004.
- 202 Chauhan A, Lebeaux D, Decante B *et al*. A rat model of central venous catheter to study establishment of long-term bacterial biofilm and related acute and chronic infections. *PLoS One* 2012; **7**. doi:10.1371/journal.pone.0037281.
- 203 Stember T, Gaab J. Bacterial Colonization of Two Different Antiseptic-Impregnated Central Venous Catheters in a Rabbit Model. *J Vasc Access* 2014; **15(3)**.
- 204 Chandra J, Pearlman E, Ghannoum MA. Animal models to investigate fungal biofilm formation. *Methods Mol Biol* 2014; **1147**. doi:10.1007/978-1-4939-0467-9_10.
- 205 Anderson GG, Palermo JJ, Schilling JD, Roth R, Heuser J, Hultgren SJ. Intracellular bacterial biofilm-like pods in urinary tract infections. *Science (80-)* 2003; **301**. doi:10.1126/science.1084550.
- 206 Low J Le, Kao PH-N, Tambyah PA *et al*. Development of a polymer-based antimicrobial coating for efficacious urinary catheter protection. *Biotechnol Notes* 2021; **2**. doi:10.1016/j.biotno.2020.12.001.
- 207 Wang S, Wu N. Selecting the swimming mechanisms of colloidal particles: Bubble propulsion versus self-diffusiophoresis. *Langmuir* 2014; **30**. doi:10.1021/la500182f.
- 208 Bottagisio M, Coman C, Lovati AB. Animal models of orthopaedic infections. A review of rabbit models used to induce long bone bacterial infections. *J. Med. Microbiol.* 2019; **68**. doi:10.1099/jmm.0.000952.
- 209 Tran PA, O'Brien-Simpson N, Palmer JA *et al*. Selenium nanoparticles as anti-infective implant coatings for trauma orthopedics against methicillin-resistant *Staphylococcus aureus* and *epidermidis*: In vitro and in vivo assessment. *Int J Nanomedicine* 2019; **14**. doi:10.2147/IJN.S197737.
- 210 Tran PL, Lowry N, Campbell T *et al*. An organoselenium compound inhibits *Staphylococcus aureus* biofilms on hemodialysis catheters in vivo. *Antimicrob Agents Chemother* 2012; **56**. doi:10.1128/AAC.05680-11.
- 211 Keiser NW, Engelhardt JF. New animal models of cystic fibrosis: What are they teaching us? *Curr. Opin. Pulm. Med.* 2011; **17**. doi:10.1097/MCP.0b013e32834b14c9.
- 212 Sweeney E, Sabnis A, Edwards AM, Harrison F. Effect of host-mimicking medium and biofilm growth on the ability of colistin to kill *pseudomonas aeruginosa*. *Microbiol (United Kingdom)* 2020; **166**. doi:10.1099/mic.0.000995.
- 213 Van Heeckeren AM, Schluchter MD. Murine models of chronic *Pseudomonas aeruginosa* lung infection. *Lab Anim* 2002; **36**. doi:10.1258/002367702320162405.
- 214 Pletzer D, Mansour SC, Wuerth K, Rahanjam N, Hancock REW. New mouse model for chronic infections by gram-negative bacteria enabling the study of anti-infective efficacy and host-microbe interactions. *MBio* 2017; **8**. doi:10.1128/mBio.00140-17.

- 215 Matilla-Cuenca L, Gil C, Cuesta S *et al.* Antibiofilm activity of flavonoids on staphylococcal biofilms through targeting BAP amyloids. *Sci Rep* 2020; **10**. doi:10.1038/s41598-020-75929-2.
- 216 Saraswathi P, Beuerman RW. Corneal Biofilms: From Planktonic to Microcolony Formation in an Experimental Keratitis Infection with *Pseudomonas Aeruginosa*. *Ocul Surf* 2015; **13**. doi:10.1016/j.jtos.2015.07.001.
- 217 Tan XW, Goh TW, Saraswathi P *et al.* Effectiveness of antimicrobial peptide immobilization for preventing perioperative cornea implant-associated bacterial infection. *Antimicrob Agents Chemother* 2014; **58**. doi:10.1128/AAC.02859-14.
- 218 Nash EE, Peters BM, Lilly EA, Noverr MC, Fidel PL. A murine model of *Candida glabrata* vaginitis shows no evidence of an inflammatory immunopathogenic response. *PLoS One* 2016; **11**. doi:10.1371/journal.pone.0147969.
- 219 Nett JE. The host's reply to *Candida* biofilm. *Pathogens*. 2016; **5**. doi:10.3390/pathogens5010033.
- 220 FITZGERALD RJ, KEYES PH. Demonstration of the etiologic role of streptococci in experimental caries in the hamster. *J Am Dent Assoc* 1960; **61**. doi:10.14219/jada.archive.1960.0138.
- 221 Bainbridge B, Verma RK, Eastman C *et al.* Role of *Porphyromonas gingivalis* phosphoserine phosphatase enzyme SerB in inflammation, immune response, and induction of alveolar bone resorption in rats. *Infect Immun* 2010; **78**. doi:10.1128/IAI.00703-10.
- 222 Brown JL, Johnston W, Delaney C *et al.* Polymicrobial oral biofilm models: Simplifying the complex. *J. Med. Microbiol.* 2019; **68**. doi:10.1099/JMM.0.001063.
- 223 Jiao Y, Hasegawa M, Inohara N. Emerging roles of immunostimulatory oral bacteria in periodontitis development. *Trends Microbiol.* 2014; **22**. doi:10.1016/j.tim.2013.12.005.
- 224 Tseng BS, Zhang W, Harrison JJ *et al.* The extracellular matrix protects *Pseudomonas aeruginosa* biofilms by limiting the penetration of tobramycin. *Environ Microbiol* 2013; **15**. doi:10.1111/1462-2920.12155.
- 225 Rabin N, Zheng Y, Opoku-Temeng C, Du Y, Bonsu E, Sintim HO. Biofilm formation mechanisms and targets for developing antibiofilm agents. *Future Med Chem* 2015; **7**: 493–512.
- 226 Rossi E, La Rosa R, Bartell JA *et al.* *Pseudomonas aeruginosa* adaptation and evolution in patients with cystic fibrosis. *Nat Rev Microbiol* 2020. doi:10.1038/s41579-020-00477-5.
- 227 Allison KR, Brynildsen MP, Collins JJ. Metabolite-enabled eradication of bacterial persisters by aminoglycosides. *Nature* 2011; **473**. doi:10.1038/nature10069.
- 228 Rodrigues LR. Inhibition of bacterial adhesion on medical devices. *Adv Exp Med Biol* 2011; **715**: 351–367.
- 229 Crnich CJ, Halfmann JA, Crone WC, Maki DG. The Effects of Prolonged Ethanol

- Exposure on the Mechanical Properties of Polyurethane and Silicone Catheters Used for Intravascular Access. *Infect Control Hosp Epidemiol* 2005; **26**. doi:10.1086/502607.
- 230 Siddiq DM, Darouiche RO. New strategies to prevent catheter-associated urinary tract infections. *Nat. Rev. Urol.* 2012; **9**. doi:10.1038/nrurol.2012.68.
- 231 Tîlmaciu CM, Mathieu M, Lavigne JP *et al.* In vitro and in vivo characterization of antibacterial activity and biocompatibility: A study on silver-containing phosphonate monolayers on titanium. *Acta Biomater* 2015; **15**. doi:10.1016/j.actbio.2014.12.020.
- 232 Lara HH, Lopez-Ribot JL. Inhibition of mixed biofilms of candida albicans and methicillin-resistant staphylococcus aureus by positively charged silver nanoparticles and functionalized silicone elastomers. *Pathogens* 2020; **9**. doi:10.3390/pathogens9100784.
- 233 Bak J, Ladefoged SD, Tvede M, Begovic T, Gregersen A. Dose requirements for UVC disinfection of catheter biofilms. *Biofouling* 2009; **25**. doi:10.1080/08927010802716623.
- 234 Chen M, Yu Q, Sun H. Novel strategies for the prevention and treatment of biofilm related infections. *Int. J. Mol. Sci.* 2013; **14**: 18488–18501.
- 235 Guzzo F, Scognamiglio M, Fiorentino A, Buommino E, D’abrosca B. Plant Derived Natural Products against *Pseudomonas aeruginosa* and *Staphylococcus aureus*: Antibiofilm Activity and Molecular Mechanisms. *Molecules* 2020; **25**. doi:10.3390/molecules25215024.
- 236 Karimi A, Karig D, Kumar A, Ardekani AM. Interplay of physical mechanisms and biofilm processes: Review of microfluidic methods. *Lab Chip.* 2015; **15**. doi:10.1039/c4lc01095g.
- 237 Marquez B. Bacterial efflux systems and efflux pumps inhibitors. *Biochimie.* 2005; **87**. doi:10.1016/j.biochi.2005.04.012.
- 238 Zhu X, Rice SA, Barraud N. Nitric oxide and iron signaling cues have opposing effects on biofilm development in *Pseudomonas aeruginosa*. *Appl Environ Microbiol* 2019; **85**. doi:10.1128/AEM.02175-18.
- 239 Yoon SS, Hennigan RF, Hilliard GM *et al.* *Pseudomonas aeruginosa* anaerobic respiration in biofilms: Relationships to cystic fibrosis pathogenesis. *Dev Cell* 2002; **3**: 593–603.
- 240 Pelgrift RY, Friedman AJ. Nanotechnology as a therapeutic tool to combat microbial resistance. *Adv. Drug Deliv. Rev.* 2013; **65**. doi:10.1016/j.addr.2013.07.011.
- 241 Kolderman E, Bettampadi D, Samarian D *et al.* L-arginine destabilizes oral multi-species biofilm communities developed in human saliva. *PLoS One* 2015; **10**. doi:10.1371/journal.pone.0121835.
- 242 Chung PY, Toh YS. Anti-biofilm agents: Recent breakthrough against multi-drug resistant *Staphylococcus aureus*. *Pathog. Dis.* 2014; **70**: 231–239.
- 243 Kiedrowski MR, Horswill AR. New approaches for treating staphylococcal biofilm infections. *Ann N Y Acad Sci* 2011; **1241**. doi:10.1111/j.1749-6632.2011.06281.x.
- 244 Aggarwal S, Stewart PS, Hozalski RM. Biofilm Cohesive Strength as a Basis for Biofilm

- Recalcitrance: Are Bacterial Biofilms Overdesigned? *Microbiol Insights* 2015; **8s2**. doi:10.4137/mbi.s31444.
- 245 Lee JH, Kaplan JB, Lee WY. Microfluidic devices for studying growth and detachment of *Staphylococcus epidermidis* biofilms. *Biomed Microdevices* 2008; **10**. doi:10.1007/s10544-007-9157-0.
- 246 Donelli G, Francolini I, Romoli D *et al.* Synergistic activity of dispersin B and cefamandole nafate in inhibition of staphylococcal biofilm growth on polyurethanes. *Antimicrob Agents Chemother* 2007; **51**. doi:10.1128/AAC.01249-06.
- 247 Roberts ME, Stewart PS. Modelling protection from antimicrobial agents in biofilms through the formation of persister cells. *Microbiology* 2005; **151**. doi:10.1099/mic.0.27385-0.
- 248 Stewart PS. Mechanisms of antibiotic resistance in bacterial biofilms. *Int J Med Microbiol* 2002. doi:10.1078/1438-4221-00196.
- 249 Soares A, Roussel V, Pestel-Caron M *et al.* Understanding Ciprofloxacin Failure in *Pseudomonas aeruginosa* Biofilm: Persister Cells Survive Matrix Disruption. *Front Microbiol* 2019; **10**: 1–10.
- 250 Patra JK, Das G, Fraceto LF *et al.* Nano based drug delivery systems: Recent developments and future prospects 10 Technology 1007 Nanotechnology 03 Chemical Sciences 0306 Physical Chemistry (incl. Structural) 03 Chemical Sciences 0303 Macromolecular and Materials Chemistry 11 Medical and He. *J Nanobiotechnology* 2018; **16**: 1–33.
- 251 Koo H, Allan RN, Howlin RP, Stoodley P, Hall-Stoodley L. Targeting microbial biofilms: Current and prospective therapeutic strategies. *Nat. Rev. Microbiol.* 2017; **15**. doi:10.1038/nrmicro.2017.99.
- 252 Jiang Y, Geng M, Bai L. Targeting biofilms therapy: Current research strategies and development hurdles. *Microorganisms.* 2020; **8**. doi:10.3390/microorganisms8081222.
- 253 Stewart PS. Biophysics of biofilm infection. *Pathog. Dis.* 2014; **70**. doi:10.1111/2049-632X.12118.
- 254 Goodwine J, Gil J, Doiron A *et al.* Pyruvate-depleting conditions induce biofilm dispersion and enhance the efficacy of antibiotics in killing biofilms in vitro and in vivo. *Sci Rep* 2019; **9**. doi:10.1038/s41598-019-40378-z.
- 255 Alvarez-Rueda N, Rouges C, Touahri A, Misme-Aucouturier B, Albassier M, Pape P Le. In vitro immune responses of human PBMCs against *Candida albicans* reveals fungal and leucocyte phenotypes associated with fungal persistence. *Sci Rep* 2020; **10**: 1–16.
- 256 Fulaz S, Vitale S, Quinn L, Casey E. Nanoparticle–Biofilm Interactions: The Role of the EPS Matrix. *Trends Microbiol.* 2019; **27**. doi:10.1016/j.tim.2019.07.004.
- 257 Dai X, Zhao Y, Yu Y *et al.* Single Continuous Near-Infrared Laser-Triggered Photodynamic and Photothermal Ablation of Antibiotic-Resistant Bacteria Using Effective Targeted Copper Sulfide Nanoclusters. *ACS Appl Mater Interfaces* 2017; **9**.

- doi:10.1021/acsami.7b09638.
- 258 Khan I, Saeed K, Khan I. Nanoparticles: Properties, applications and toxicities <https://doi.org/10.1016/j.arabjc.2017.05.011>. *Arab J Chem* 2017; **12**.
- 259 Bernardos A, Piacenza E, Sancenón F *et al*. Mesoporous Silica-Based Materials with Bactericidal Properties. *Small*. 2019; **15**. doi:10.1002/sml.201900669.
- 260 Balaure PC, Grumezescu AM. Recent advances in surface nanoengineering for biofilm prevention and control. Part i: Molecular basis of biofilm recalcitrance. passive anti-biofouling nanocoatings. *Nanomaterials*. 2020; **10**. doi:10.3390/nano10061230.
- 261 Shkodenko L, Kassirov I, Koshel E. Metal oxide nanoparticles against bacterial biofilms: Perspectives and limitations. *Microorganisms*. 2020; **8**. doi:10.3390/microorganisms8101545.
- 262 Yetisgin AA, Cetinel S, Zuvin M, Kosar A, Kutlu O. Therapeutic nanoparticles and their targeted delivery applications. *Molecules*. 2020; **25**. doi:10.3390/molecules25092193.
- 263 Balaure PC, Grumezescu AM. Recent advances in surface nanoengineering for biofilm prevention and control. Part i: Molecular basis of biofilm recalcitrance. passive anti-biofouling nanocoatings. *Nanomaterials* 2020; **10**: 1–30.
- 264 Sánchez-López E, Gomes D, Esteruelas G *et al*. Metal-based nanoparticles as antimicrobial agents: An overview. *Nanomaterials*. 2020; **10**. doi:10.3390/nano10020292.
- 265 Ooi ML, Richter K, Bennett C *et al*. Topical colloidal silver for the treatment of recalcitrant chronic rhinosinusitis. *Front Microbiol* 2018; **9**. doi:10.3389/fmicb.2018.00720.
- 266 Chen YM, Dai AP, Shi Y, Liu ZJ, Gong MF, Yin XB. Effectiveness of silver-impregnated central venous catheters for preventing catheter-related blood stream infections: A meta-analysis. *Int J Infect Dis* 2014; **29**. doi:10.1016/j.ijid.2014.09.018.
- 267 Gilbert RE, Harden M. Effectiveness of impregnated central venous catheters for catheter related blood stream infection: a systematic review. *Curr Opin Intern Med* 2008; **7**. doi:10.1097/mci.0b013e32830c6d26.
- 268 Swidan NS, Hashem YA, Elkhatib WF, Yassien MA. Antibiofilm activity of green synthesized silver nanoparticles against biofilm associated enterococcal urinary pathogens. *Sci Rep* 2022; **12**. doi:10.1038/s41598-022-07831-y.
- 269 Muthamil S, Devi VA, Balasubramaniam B, Balamurugan K, Pandian SK. Green synthesized silver nanoparticles demonstrating enhanced in vitro and in vivo antibiofilm activity against *Candida* spp. *J Basic Microbiol* 2018; **58**. doi:10.1002/jobm.201700529.
- 270 Ikuma K, Decho AW, Lau BLT. When nanoparticles meet biofilms - Interactions guiding the environmental fate and accumulation of nanoparticles. *Front. Microbiol*. 2015; **6**. doi:10.3389/fmicb.2015.00591.
- 271 Qayyum S, Khan AU. Nanoparticles: Vs. biofilms: A battle against another paradigm of antibiotic resistance. *Medchemcomm* 2016; **7**. doi:10.1039/c6md00124f.

- 272 Mu H, Tang J, Liu Q, Sun C, Wang T, Duan J. Potent Antibacterial Nanoparticles against Biofilm and Intracellular Bacteria. *Sci Rep* 2016; **6**. doi:10.1038/srep18877.
- 273 Liu Y, Naha PC, Hwang G *et al*. Topical ferumoxytol nanoparticles disrupt biofilms and prevent tooth decay in vivo via intrinsic catalytic activity. *Nat Commun* 2018; **9**. doi:10.1038/s41467-018-05342-x.
- 274 Tran HM, Tran H, Booth MA *et al*. Nanomaterials for treating bacterial biofilms on implantable medical devices. *Nanomaterials*. 2020; **10**. doi:10.3390/nano10112253.
- 275 Hagens WI, Oomen AG, de Jong WH, Cassee FR, Sips AJAM. What do we (need to) know about the kinetic properties of nanoparticles in the body? *Regul Toxicol Pharmacol* 2007; **49**. doi:10.1016/j.yrtph.2007.07.006.
- 276 Lei R, Wu C, Yang B *et al*. Integrated metabolomic analysis of the nano-sized copper particle-induced hepatotoxicity and nephrotoxicity in rats: A rapid in vivo screening method for nanotoxicity. *Toxicol Appl Pharmacol* 2008; **232**. doi:10.1016/j.taap.2008.06.026.
- 277 Fisher RA, Gollan B, Helaine S. Persistent bacterial infections and persister cells. *Nat. Rev. Microbiol.* 2017; **15**. doi:10.1038/nrmicro.2017.42.
- 278 Wood TK. Combatting bacterial persister cells. *Biotechnol. Bioeng.* 2016; **113**. doi:10.1002/bit.25721.
- 279 Vulin C, Leimer N, Huemer M, Ackermann M, Zinkernagel AS. Prolonged bacterial lag time results in small colony variants that represent a sub-population of persisters. *Nat Commun* 2018; **9**. doi:10.1038/s41467-018-06527-0.
- 280 Moldoveanu AL, Rycroft JA, Helaine S. Impact of bacterial persisters on their host. *Curr. Opin. Microbiol.* 2021; **59**. doi:10.1016/j.mib.2020.07.006.
- 281 Prax M, Bertram R. Metabolic aspects of bacterial persisters. *Front. Cell. Infect. Microbiol.* 2014; **4**. doi:10.3389/fcimb.2014.00148.
- 282 Jermy A. Bacterial physiology: No rest for the persisters. *Nat. Rev. Microbiol.* 2013; **11**. doi:10.1038/nrmicro2969.
- 283 LaFleur MD, Qi Q, Lewis K. Patients with long-term oral carriage harbor high-persister mutants of *Candida albicans*. *Antimicrob Agents Chemother* 2010; **54**. doi:10.1128/AAC.00860-09.
- 284 Baek MS, Chung ES, Jung DS, Ko KS. Effect of colistin-based antibiotic combinations on the eradication of persister cells in *Pseudomonas aeruginosa*. *J Antimicrob Chemother* 2020; **75**. doi:10.1093/jac/dkz552.
- 285 Yang S, Hay ID, Cameron DR *et al*. Antibiotic regimen based on population analysis of residing persister cells eradicates *Staphylococcus epidermidis* biofilms. *Sci Rep* 2015; **5**: 1–11.
- 286 De Groote VN, Verstraeten N, Fauvart M *et al*. Novel persistence genes in *Pseudomonas aeruginosa* identified by high-throughput screening. *FEMS Microbiol Lett* 2009; **297**.

- doi:10.1111/j.1574-6968.2009.01657.x.
- 287 Marques CNH, Nelson SM. Pharmacodynamics of ciprofloxacin against *Pseudomonas aeruginosa* planktonic and biofilm-derived cells. *Lett Appl Microbiol* 2019; **68**: 350–359.
- 288 Torrey HL, Keren I, Via LE, Lee JS, Lewis K. High persister mutants in mycobacterium tuberculosis. *PLoS One* 2016; **11**. doi:10.1371/journal.pone.0155127.
- 289 Pu Y, Zhao Z, Li Y *et al.* Enhanced Efflux Activity Facilitates Drug Tolerance in Dormant Bacterial Cells. *Mol Cell* 2016; **62**: 284–294.
- 290 Klockgether J, Miethke N, Kubesch P *et al.* Intracolonial diversity of the *Pseudomonas aeruginosa* cystic fibrosis airway isolates TBCF10839 and TBCF121838: Distinct signatures of transcriptome, proteome, metabolome, adherence and pathogenicity despite an almost identical genome sequence. *Environ Microbiol* 2013; **15**: 191–210.
- 291 Hall CW, Mah TF. Molecular mechanisms of biofilm-based antibiotic resistance and tolerance in pathogenic bacteria. *FEMS Microbiol. Rev.* 2017; **41**: 276–301.
- 292 Dinicola S, De Grazia S, Carlomagno G, Pintucci JP. N-acetylcysteine as powerful molecule to destroy bacterial biofilms. A systematic review. *Eur. Rev. Med. Pharmacol. Sci.* 2014; **18**: 2942–2948.
- 293 Blasi F, Page C, Rossolini GM *et al.* The effect of N-acetylcysteine on biofilms: Implications for the treatment of respiratory tract infections. *Respir. Med.* 2016; **117**: 190–197.
- 294 Costa F, Sousa DM, Parreira P, Lamghari M, Gomes P, Martins MCL. N-acetylcysteine-functionalized coating avoids bacterial adhesion and biofilm formation. *Sci Rep* 2017; **7**. doi:10.1038/s41598-017-17310-4.
- 295 Chen AY, Zervos MJ, Vazquez JA. Dalbavancin: A novel antimicrobial. *Int. J. Clin. Pract.* 2007; **61**: 853–863.
- 296 Seltzer E, Dorr MB, Goldstein BP *et al.* Once-Weekly Dalbavancin versus Standard-of-Care Antimicrobial Regimens for Treatment of Skin and Soft-Tissue Infections. 2003<http://cid.oxfordjournals.org/>.
- 297 Meeker DG, Beenken KE, Mills WB *et al.* Evaluation Of Antibiotics Active Against methicillin-resistant *Staphylococcus aureus* based on activity in an established biofilm. *Antimicrob Agents Chemother* 2016; **60**: 5688–5694.
- 298 Knafl D, Tobudic S, Cheng SC, Bellamy DR, Thalhammer F. Dalbavancin reduces biofilms of methicillin-resistant *Staphylococcus aureus* (MRSA) and methicillin-resistant *Staphylococcus epidermidis* (MRSE). *Eur J Clin Microbiol Infect Dis* 2017; **36**: 677–680.
- 299 Di Pilato V, Ceccherini F, Sennati S *et al.* In vitro time-kill kinetics of dalbavancin against *Staphylococcus* spp. biofilms over prolonged exposure times. *Diagn Microbiol Infect Dis* 2020. doi:10.1016/j.diagmicrobio.2019.114901.
- 300 Darouiche RO, Mansouri MD. Dalbavancin compared with vancomycin for prevention of *Staphylococcus aureus* colonization of devices in vivo. *J Infect* 2005; **50**: 206–209.

- 301 Baldoni D, Furustrand Taffin U, Aeppli S *et al.* Activity of dalbavancin, alone and in combination with rifampicin, against methicillin-resistant *Staphylococcus aureus* in a foreign-body infection model. *Int J Antimicrob Agents* 2013; **42**: 220–225.
- 302 Kussmann M, Obermueller M, Berndl F *et al.* Dalbavancin for treatment of implant-related methicillin-resistant *Staphylococcus aureus* osteomyelitis in an experimental rat model. *Sci Rep* 2018. doi:10.1038/s41598-018-28006-8.
- 303 EUCAST. Breakpoint tables for interpretation of MICs and zone diameters. Version 8.0, 2018. 2018<http://www.eucast.org>.
- 304 Stepanovic S, Vukovic D, Dakic I, Savic B, Svabic-vlahovic M. A modified microtiter-plate test for quantification of staphylococcal biofilm formation. 2000; **40**: 175–179.
- 305 Calcagno V. Package ‘glmulti’. 2013.
- 306 Jefferson KK, Goldmann DA, Pier GB. Use of confocal microscopy to analyze the rate of vancomycin penetration through *Staphylococcus aureus* biofilms. *Antimicrob Agents Chemother* 2005; **49**: 2467–2473.
- 307 Gutiérrez D, Fernández L, Martínez B, Ruas-Madiedo P, García P, Rodríguez A. Real-time assessment of *Staphylococcus aureus* biofilm disruption by phage-derived proteins. *Front Microbiol* 2017; **8**: 1–10.
- 308 Kundukad B, Schussman M, Yang K *et al.* Mechanistic action of weak acid drugs on biofilms. *Sci Rep* 2017; **7**. doi:10.1038/s41598-017-05178-3.
- 309 Fernández J, Greenwood-Quaintance KE, Patel R. In vitro activity of dalbavancin against biofilms of staphylococci isolated from prosthetic joint infections. *Diagn Microbiol Infect Dis* 2016; **85**: 449–451.
- 310 Campbell EA, Korzheva N, Mustaev A *et al.* Structural mechanism for rifampicin inhibition of bacterial RNA polymerase. *Cell* 2001; **104**. doi:10.1016/S0092-8674(01)00286-0.
- 311 Zimmerli W, Sendi P. Role of rifampin against staphylococcal biofilm infections in vitro, in animal models, and in orthopedic-device-related infections. *Antimicrob. Agents Chemother.* 2019; **63**. doi:10.1128/AAC.01746-18.
- 312 Raad I, Hanna H, Jiang Y *et al.* Comparative activities of daptomycin, linezolid, and tigecycline against catheter-related methicillin-resistant *Staphylococcus bacteremic* isolates embedded in biofilm. *Antimicrob Agents Chemother* 2007; **51**: 1656–1660.
- 313 Zhou W, Shan W, Ma X *et al.* Molecular characterization of rifampicin-resistant *Staphylococcus aureus* isolates in a Chinese teaching hospital from Anhui, China. *BMC Microbiol* 2012; **12**. doi:10.1186/1471-2180-12-240.
- 314 Jacqueline C, Caillon J. Impact of bacterial biofilm on the treatment of prosthetic joint infections. *J Antimicrob Chemother* 2014; **69**. doi:10.1093/jac/dku254.
- 315 Lopatkin AJ, Stokes JM, Zheng EJ *et al.* Bacterial metabolic state more accurately predicts antibiotic lethality than growth rate. *Nat Microbiol* 2019; **4**: 2109–2117.

- 316 Choo EJ, Chambers HF. Treatment of methicillin-resistant *Staphylococcus aureus* bacteremia. *Infect. Chemother.* 2016; **48**: 267–273.
- 317 Cendra M del M, Blanco-Cabra N, Pedraz L, Torrents E. Optimal environmental and culture conditions allow the in vitro coexistence of *Pseudomonas aeruginosa* and *Staphylococcus aureus* in stable biofilms. *Sci Rep* 2019; **9**. doi:10.1038/s41598-019-52726-0.
- 318 Boudarel H, Mathias JD, Blaysat B, Grédiac M. Towards standardized mechanical characterization of microbial biofilms: analysis and critical review. *npj Biofilms Microbiomes* 2018; **4**. doi:10.1038/s41522-018-0062-5.
- 319 Wan N, Wang H, Ng CK *et al.* Bacterial metabolism during biofilm growth investigated by ¹³C tracing. *Front Microbiol* 2018; **9**. doi:10.3389/fmicb.2018.02657.
- 320 Chua SL, Yam JKH, Hao P *et al.* Selective labelling and eradication of antibiotic-Tolerant bacterial populations in *Pseudomonas aeruginosa* biofilms. *Nat Commun* 2016; **7**. doi:10.1038/ncomms10750.
- 321 Khlebodarova TM, Likhoshvai VA. Persister Cells – a Plausible Outcome of Neutral Coevolutionary Drift. *Sci Rep* 2018; **8**: 1–11.
- 322 Miyaue S, Suzuki E, Komiyama Y, Kondo Y, Morikawa M, Maeda S. Bacterial memory of persisters: Bacterial persister cells can retain their phenotype for days or weeks after withdrawal from colony-biofilm culture. *Front Microbiol* 2018; **9**. doi:10.3389/fmicb.2018.01396.
- 323 Wood TK, Knabel SJ, Kwan BW. Bacterial persister cell formation and dormancy. *Appl. Environ. Microbiol.* 2013; **79**. doi:10.1128/AEM.02636-13.
- 324 Bakkeren E, Diard M, Hardt WD. Evolutionary causes and consequences of bacterial antibiotic persistence. *Nat. Rev. Microbiol.* 2020; **18**. doi:10.1038/s41579-020-0378-z.
- 325 Schmieder R, Edwards R. Quality control and preprocessing of metagenomic datasets. *Bioinformatics* 2011; **27**. doi:10.1093/bioinformatics/btr026.
- 326 Bankevich A, Nurk S, Antipov D *et al.* SPAdes: A new genome assembly algorithm and its applications to single-cell sequencing. *J Comput Biol* 2012; **19**. doi:10.1089/cmb.2012.0021.
- 327 Hyatt D, Chen GL, LoCascio PF, Land ML, Larimer FW, Hauser LJ. Prodigal: Prokaryotic gene recognition and translation initiation site identification. *BMC Bioinformatics* 2010; **11**. doi:10.1186/1471-2105-11-119.
- 328 Finn RD, Clements J, Eddy SR. HMMER web server: Interactive sequence similarity searching. *Nucleic Acids Res* 2011; **39**. doi:10.1093/nar/gkr367.
- 329 Stiefel P, Rosenberg U, Schneider J, Mauerhofer S, Maniura-Weber K, Ren Q. Is biofilm removal properly assessed? Comparison of different quantification methods in a 96-well plate system. *Appl Microbiol Biotechnol* 2016; **100**. doi:10.1007/s00253-016-7396-9.
- 330 Kim SK, Lee JH. Biofilm dispersion in *Pseudomonas aeruginosa*. *J. Microbiol.* 2016; **54**.

- doi:10.1007/s12275-016-5528-7.
- 331 Mojsoska B, Cameron D, Bartell J *et al.* The high persister phenotype of *Pseudomonas aeruginosa* is associated with increased fitness and persistence in cystic fibrosis airways. *bioRxiv* 2019. doi:10.1101/561589.
- 332 Bowler LL, Zhanel GG, Ball TB, Saward LL. Mature *Pseudomonas aeruginosa* biofilms prevail compared to young biofilms in the presence of ceftazidime. *Antimicrob Agents Chemother* 2012; **56**: 4976–4979.
- 333 Barraud N, Buson A, Jarolimek W, Rice SA. Mannitol enhances antibiotic sensitivity of persister bacteria in *Pseudomonas aeruginosa* biofilms. *PLoS One* 2013; **8**. doi:10.1371/journal.pone.0084220.
- 334 Loo CY, Lee WH, Lauretani G *et al.* Sweetening Inhaled Antibiotic Treatment for Eradication of Chronic Respiratory Biofilm Infection. *Pharm Res* 2018; **35**. doi:10.1007/s11095-018-2350-4.
- 335 Guérillot R, Kostoulas X, Donovan L *et al.* Unstable chromosome rearrangements in *Staphylococcus aureus* cause phenotype switching associated with persistent infections. *Proc Natl Acad Sci U S A* 2019; **116**. doi:10.1073/pnas.1904861116.
- 336 Irvine S, Bunk B, Bayes HK *et al.* Genomic and transcriptomic characterization of *Pseudomonas aeruginosa* small colony variants derived from a chronic infection model. *Microb Genomics* 2019; **5**: 1–11.
- 337 Pearson JP, Pesci EC, Iglewski BH. Roles of *Pseudomonas aeruginosa* las and rhl quorum-sensing systems in control of elastase and rhamnolipid biosynthesis genes. *J Bacteriol* 1997; **179**. doi:10.1128/jb.179.18.5756-5767.1997.
- 338 Cao H, Lai Y, Bougouffa S, Xu Z, Yan A. Comparative genome and transcriptome analysis reveals distinctive surface characteristics and unique physiological potentials of *Pseudomonas aeruginosa* ATCC 27853. *BMC Genomics* 2017; **18**. doi:10.1186/s12864-017-3842-z.
- 339 Dunn MJ, Fillinger RJ, Anderson LM, Anderson MZ. Automated quantification of *Candida albicans* biofilm-related phenotypes reveals additive contributions to biofilm production. *npj Biofilms Microbiomes* 2020; **6**. doi:10.1038/s41522-020-00149-5.
- 340 Thein ZM, Seneviratne CJ, Samaranayake YH, Samaranayake LP. Community lifestyle of *Candida* in mixed biofilms: A mini review. *Mycoses*. 2009; **52**. doi:10.1111/j.1439-0507.2009.01719.x.
- 341 Mataraci-Kara E, Ataman M, Yilmaz G, Ozbek-Celik B. Evaluation of antifungal and disinfectant-resistant *Candida* species isolated from hospital wastewater. *Arch Microbiol* 2020; **202**. doi:10.1007/s00203-020-01975-z.
- 342 Ghannoum M, Roilides E, Katragkou A, Petraitis V, Walsh TJ. The Role of Echinocandins in *Candida* Biofilm-Related Vascular Catheter Infections: In Vitro and in Vivo Model Systems. *Clin Infect Dis* 2015; **61**: S618–S621.
- 343 Barantsevich N, Barantsevich E. Diagnosis and Treatment of Invasive Candidiasis.

- Antibiotics* 2022; **11**. doi:10.3390/antibiotics11060718.
- 344 Sumiyoshi M, Miyazaki T, Makau JN *et al*. Novel and potent antimicrobial effects of caspofungin on drug-resistant *Candida* and bacteria. *Sci Rep* 2020; **10**. doi:10.1038/s41598-020-74749-8.
- 345 Posteraro B, Sanguinetti M, Fiori B *et al*. Caspofungin activity against clinical isolates of azole cross-resistant *Candida glabrata* overexpressing efflux pump genes. *J Antimicrob Chemother* 2006; **58**. doi:10.1093/jac/dkl237.
- 346 Cannon RD, Lamping E, Holmes AR *et al*. Efflux-mediated antifungal drug resistance. *Clin. Microbiol. Rev.* 2009; **22**. doi:10.1128/CMR.00051-08.
- 347 Rogers PD, Barker KS. Genome-wide expression profile analysis reveals coordinately regulated genes associated with stepwise acquisition of azole resistance in *Candida albicans* clinical isolates. *Antimicrob Agents Chemother* 2003; **47**. doi:10.1128/AAC.47.4.1220-1227.2003.
- 348 Habibzadeh A, Lankarani KB, Farjam M *et al*. Prevalence of Fungal Drug Resistance in COVID-19 Infection: a Global Meta-analysis. *Curr Fungal Infect Rep* 2022; : 154–164.
- 349 Girardot M, Imbert C. Natural sources as innovative solutions against fungal biofilms. *Adv Exp Med Biol* 2016; **931**: 105–125.
- 350 Singha PK, Roy S, Dey S. Antimicrobial activity of *Andrographis paniculata*. *Fitoterapia* 2003; **74**. doi:10.1016/S0367-326X(03)00159-X.
- 351 Mussard E, Cesaro A, Lespessailles E, Legrain B, Berteina-Raboin S, Toumi H. Andrographolide, a natural antioxidant: An update. *Antioxidants*. 2019; **8**. doi:10.3390/antiox8120571.
- 352 Burgos RA, Alarcón P, Quiroga J, Manosalva C, Hancke J. Andrographolide, an Anti-Inflammatory Multitarget Drug: All Roads Lead to Cellular Metabolism. *Molecules*. 2020; **26**. doi:10.3390/molecules26010005.
- 353 Zhang L, Wen B, Bao M *et al*. Andrographolide Sulfonate Is a Promising Treatment to Combat Methicillin-resistant *Staphylococcus aureus* and Its Biofilms. *Front Pharmacol* 2021; **12**. doi:10.3389/fphar.2021.720685.
- 354 Ma L, Liu X, Liang H *et al*. Effects of 14- α -lipoyl andrographolide on quorum sensing in *Pseudomonas aeruginosa*. *Antimicrob Agents Chemother* 2012; **56**. doi:10.1128/AAC.01119-12.
- 355 Xu Y, Marshall RL, Mukkur TKS. An investigation on the antimicrobial activity of *Andrographis paniculata* extracts and andrographolide in vitro. *Asian J Plant Sci* 2006; **5**. doi:10.3923/ajps.2006.527.530.
- 356 Dedhia J, Mukharjee E, Luke AM, Mathew S, Pawar AM. Efficacy of *Andrographis paniculata* compared to *Azadirachta indica*, *Curcuma longa*, and sodium hypochlorite when used as root canal irrigants against *Candida albicans* and *Staphylococcus aureus*: An in vitro antimicrobial study. *J Conserv Dent* 2018; **21**. doi:10.4103/JCD.JCD_118_18.

- 357 Pettygrove BA, Smith HJ, Pallister KB, Voyich JM, Stewart PS, Parker AE. Experimental Designs to Study the Aggregation and Colonization of Biofilms by Video Microscopy With Statistical Confidence. *Front Microbiol* 2022; **12**. doi:10.3389/fmicb.2021.785182.
- 358 Žiemytė M, Carda-Diéguez M, Rodríguez-Díaz JC, Ventero MP, Mira A, Ferrer MD. Real-time monitoring of *Pseudomonas aeruginosa* biofilm growth dynamics and persister cells' eradication. *Emerg Microbes Infect* 2021; **10**: 2062–2075.
- 359 Negri M, Gonçalves V, Silva S, Henriques M, Azeredo J, Oliveira R. Crystal violet staining to quantify *Candida* adhesion to epithelial cells. *Br J Biomed Sci* 2010; **67**. doi:10.1080/09674845.2010.11730308.
- 360 The European Committee on Antimicrobial Susceptibility Testing. Breakpoint tables for interpretation of MICs for antifungal agents, version 10.0, 2020. *Eucast* 2020; : 0–8.
- 361 Douglas LJ. *Candida* biofilms and their role in infection. *Trends Microbiol.* 2003; **11**. doi:10.1016/S0966-842X(02)00002-1.
- 362 Tran VN, Khan F, Han W *et al.* Real-time monitoring of mono- and dual-species biofilm formation and eradication using microfluidic platform. *Sci Rep* 2022; **12**: 1–14.
- 363 Alves R, Kastora SL, Gomes-Gonçalves A *et al.* Transcriptional responses of *Candida glabrata* biofilm cells to fluconazole are modulated by the carbon source. *npj Biofilms Microbiomes* 2020; **6**: 1–11.
- 364 You J, Du L, King JB, Hall BE, Cichewicz RH. Small-molecule suppressors of *Candida albicans* biofilm formation synergistically enhance the antifungal activity of amphotericin b against clinical *Candida* isolates. *ACS Chem Biol* 2013; **8**: 840–848.
- 365 Bruzual I, Riggle P, Hadley S, Kumamoto CA. Biofilm formation by fluconazole-resistant *Candida albicans* strains is inhibited by fluconazole. *J Antimicrob Chemother* 2007; **59**. doi:10.1093/jac/dkl521.
- 366 Zhang L, Bao M, Liu B *et al.* Effect of Andrographolide and Its Analogs on Bacterial Infection: A Review. *Pharmacology* 2020; **105**: 123–134.
- 367 Di Domenico EG, Cavallo I, Guembe M *et al.* The clinical Biofilm Ring Test: A promising tool for the clinical assessment of biofilm-producing *Candida* species. *FEMS Yeast Res* 2018; **18**. doi:10.1093/femsyr/foy025.
- 368 Lu M, Xuan S, Wang Z. Oral microbiota: A new view of body health. *Food Sci Hum Wellness* 2019; **8**: 8–15.
- 369 Lamont RJ, Koo H, Hajishengallis G. The oral microbiota: dynamic communities and host interactions. *Nat Rev Microbiol* 2018; **16**: 745–759.
- 370 Papapanou PN, Sanz M, Buduneli N *et al.* Periodontitis: Consensus report of workgroup 2 of the 2017 World Workshop on the Classification of Periodontal and Peri-Implant Diseases and Conditions. *J Periodontol* 2018; **89**. doi:10.1002/JPER.17-0721.
- 371 Nilsson H, Berglund JS, Renvert S. Periodontitis, tooth loss and cognitive functions among older adults. *Clin Oral Invest* 2018; **22**. doi:10.1007/s00784-017-2307-8.

- 372 Aljehani YA. Risk factors of periodontal disease: Review of the literature. *Int. J. Dent.* 2014; **2014**. doi:10.1155/2014/182513.
- 373 Feres M, Figueiredo LC, Soares GMS, Favari M. Systemic antibiotics in the treatment of periodontitis. *Periodontol 2000* 2015; **67**. doi:10.1111/prd.12075.
- 374 Isola G. Antibiotics and antimicrobials for treatment of the oral microbiota: Myths and facts in research and clinical practice. *Antibiotics*. 2020; **9**. doi:10.3390/antibiotics9020095.
- 375 Ko TJ, Byrd KM, Kim SA. The chairside periodontal diagnostic toolkit: Past, present, and future. *Diagnostics*. 2021; **11**. doi:10.3390/diagnostics11060932.
- 376 Van der Weijden F, Rijnen M, Valkenburg C. Comparison of three qPCR-based commercial tests for detection of periodontal pathogens. *Sci Rep* 2021; **11**. doi:10.1038/s41598-021-85305-3.
- 377 Lu H, He L, Xu J *et al.* Well-maintained patients with a history of periodontitis still harbor a more dysbiotic microbiome than health. *J Periodontol* 2020; **91**. doi:10.1002/JPER.19-0498.
- 378 Irshad M, Alam MK, Alawneh A *et al.* Characterization and antimicrobial susceptibility of pathogens associated with periodontal abscess. *Antibiotics* 2020; **9**. doi:10.3390/antibiotics9100654.
- 379 Dahlén G, Pipattanagovit P, Rosling B, Möller JR. A comparison of two transport media for saliva and subgingival samples. *Oral Microbiol Immunol* 1993; **8**. doi:10.1111/j.1399-302X.1993.tb00614.x.
- 380 Weinberg MA, Eskow RN. Periodontal Terminology Revisited. *J Periodontol* 2003; **74**. doi:10.1902/jop.2003.74.4.563.
- 381 Ainamo J, Bay I. Problems and proposals for recording gingivitis and plaque. *Int Dent J* 1975; **25**.
- 382 Santigli E, Leitner E, Wimmer G *et al.* Accuracy of commercial kits and published primer pairs for the detection of periodontopathogens. *Clin Oral Investig* 2016; **20**. doi:10.1007/s00784-016-1748-9.
- 383 Urbán E, Terhes G, Radnai M, Gorzó I, Nagy E. Detection of periodontopathogenic bacteria in pregnant women by traditional anaerobic culture method and by a commercial molecular genetic method. *Anaerobe* 2010; **16**. doi:10.1016/j.anaerobe.2010.02.005.
- 384 Sanz M, Herrera D, Kebschull M *et al.* Treatment of stage I–III periodontitis—The EFP S3 level clinical practice guideline. *J Clin Periodontol* 2020; **47**. doi:10.1111/jcpe.13290.
- 385 Hojo K, Nagaoka S, Murata S, Taketomo N, Ohshima T, Maeda N. Reduction of vitamin K concentration by salivary Bifidobacterium strains and their possible nutritional competition with Porphyromonas gingivalis. *J Appl Microbiol* 2007; **103**. doi:10.1111/j.1365-2672.2007.03436.x.
- 386 Kapoor A, Malhotra R, Grover V, Grover D. Systemic antibiotic therapy in periodontics.

- Dent Res J (Isfahan)* 2012; **9**. doi:10.4103/1735-3327.104866.
- 387 Foulds G, Shepard RM, Johnson RB. The pharmacokinetics of azithromycin in human serum and tissues. *J Antimicrob Chemother* 1990; **25**. doi:10.1093/jac/25.suppl_A.73.
- 388 Matzneller P, Krasniqi S, Kinzig M *et al*. Blood, tissue, and intracellular concentrations of azithromycin during and after end of therapy. *Antimicrob Agents Chemother* 2013; **57**. doi:10.1128/AAC.02011-12.
- 389 Dzidic M, Collado MC, Abrahamsson T *et al*. Oral microbiome development during childhood: an ecological succession influenced by postnatal factors and associated with tooth decay. *ISME J* 2018; **12**. doi:10.1038/s41396-018-0204-z.
- 390 Callahan BJ, McMurdie PJ, Rosen MJ, Han AW, Johnson AJA, Holmes SP. DADA2: High-resolution sample inference from Illumina amplicon data. *Nat Methods* 2016; **13**. doi:10.1038/nmeth.3869.
- 391 Quast C, Pruesse E, Yilmaz P *et al*. The SILVA ribosomal RNA gene database project: Improved data processing and web-based tools. *Nucleic Acids Res* 2013; **41**. doi:10.1093/nar/gks1219.
- 392 Team RC. R Development Core Team. R: A language and environment for statistical computing. R Foundation for Statistical Computing, Vienna, Austria; 2014. *Google Sch* 2018.
- 393 Lin H, Peddada S Das. Analysis of compositions of microbiomes with bias correction. *Nat Commun* 2020; **11**. doi:10.1038/s41467-020-17041-7.
- 394 Oksanen J, Kindt R, Legendre P *et al*. Community Ecology Package. R package version 2.4-2. *Community Ecol Packag* 2019; **2.5-6**.
- 395 Pérez-Chaparro PJ, Gonçalves C, Figueiredo LC *et al*. Newly identified pathogens associated with periodontitis: A systematic review. *J. Dent. Res.* 2014; **93**. doi:10.1177/0022034514542468.
- 396 Feres M, Retamal-Valdes B, Mestnik MJ *et al*. The ideal time of systemic metronidazole and amoxicillin administration in the treatment of severe periodontitis: Study protocol for a randomized controlled trial. *Trials* 2018; **19**. doi:10.1186/s13063-018-2540-8.
- 397 Hajishengallis G. Periodontitis: From microbial immune subversion to systemic inflammation. *Nat. Rev. Immunol.* 2015; **15**. doi:10.1038/nri3785.
- 398 Vianna ME, Horz HP, Gomes BPF, Conrads G. Microarrays complement culture methods for identification of bacteria in endodontic infections. *Oral Microbiol Immunol* 2005; **20**. doi:10.1111/j.1399-302X.2005.00221.x.
- 399 Horz HP, Conrads G. Diagnosis and anti-infective therapy of periodontitis. *Expert Rev. Anti. Infect. Ther.* 2007; **5**. doi:10.1586/14787210.5.4.703.
- 400 Conrads G, Klomp T, Deng D, Wenzler JS, Braun A, Abdelbary MMH. The Antimicrobial Susceptibility of *Porphyromonas gingivalis*: Genetic Repertoire, Global Phenotype, and Review of the Literature. *Antibiotics* 2021; **10**.

- doi:10.3390/antibiotics10121438.
- 401 Rams TE, Slots J. Antimicrobial Chemotherapy for Recalcitrant Severe Human Periodontitis. *Antibiotics* 2023; **12**: 1–18.
- 402 Naginyte M, Do T, Meade J, Devine DA, Marsh PD. Enrichment of periodontal pathogens from the biofilms of healthy adults. *Sci Rep* 2019; **9**. doi:10.1038/s41598-019-41882-y.
- 403 Lázár V, Snitser O, Barkan D, Kishony R. Antibiotic combinations reduce *Staphylococcus aureus* clearance. *Nature* 2022; **610**: 540–546.
- 404 Mira A, Simon-Soro A, Curtis MA. Role of microbial communities in the pathogenesis of periodontal diseases and caries. *J Clin Periodontol* 2017; **44**. doi:10.1111/jcpe.12671.
- 405 Oteo A, Herrera D, Figuro E, O'Connor A, González I, Sanz M. Azithromycin as an adjunct to scaling and root planing in the treatment of *Porphyromonas gingivalis*-associated periodontitis: A pilot study. *J Clin Periodontol* 2010; **37**. doi:10.1111/j.1600-051X.2010.01607.x.
- 406 Muniz FWMG, De Oliveira CC, De Sousa Carvalho R, Moreira MMSM, De Moraes MEA, Martins RS. Azithromycin: A new concept in adjuvant treatment of periodontitis. *Eur. J. Pharmacol.* 2013; **705**. doi:10.1016/j.ejphar.2013.02.044.
- 407 Haffajee AD, Socransky SS. Microbial etiological agents of destructive periodontal diseases. *Periodontol 2000* 1994; **5**. doi:10.1111/j.1600-0757.1994.tb00020.x.
- 408 Brackman G, Coenye T. In vitro and in vivo biofilm wound models and their application. *Adv Exp Med Biol* 2016; **897**. doi:10.1007/5584_2015_5002.
- 409 Davies D. Understanding biofilm resistance to antibacterial agents. *Nat. Rev. Drug Discov.* 2003; **2**. doi:10.1038/nrd1008.
- 410 Ford CA, Hurford IM, Cassat JE. Antivirulence Strategies for the Treatment of *Staphylococcus aureus* Infections: A Mini Review. *Front. Microbiol.* 2021; **11**. doi:10.3389/fmicb.2020.632706.
- 411 Calcagno V. Package ‘glmulti’. CRAN Repos. 2015.
- 412 Kassinger SJ, van Hoek ML. Biofilm architecture: An emerging synthetic biology target. *Synth. Syst. Biotechnol.* 2020; **5**. doi:10.1016/j.synbio.2020.01.001.
- 413 Kagan D, Laocharoensuk R, Zimmerman M *et al.* Rapid delivery of drug carriers propelled and navigated by catalytic nanoshuttles. *Small* 2010; **6**. doi:10.1002/sml.201001257.
- 414 Van Nguyen K, Minteer SD. DNA-functionalized Pt nanoparticles as catalysts for chemically powered micromotors: Toward signal-on motion-based DNA biosensor. *Chem Commun* 2015; **51**. doi:10.1039/c4cc10250a.
- 415 Sanchez S, Soler L, Katuri J. Chemically powered micro- and nanomotors. *Angew Chemie - Int Ed* 2015; **54**. doi:10.1002/anie.201406096.
- 416 de Faria AF, de Moraes ACM, Alves OL. Toxicity of Nanomaterials to Microorganisms:

- Mechanisms, Methods, and New Perspectives. 2014 doi:10.1007/978-1-4614-8993-1_17.
- 417 De Faria AF, De Moraes ACM, Marcato PD *et al.* Eco-friendly decoration of graphene oxide with biogenic silver nanoparticles: Antibacterial and antibiofilm activity. *J Nanoparticle Res* 2014; **16**. doi:10.1007/s11051-013-2110-7.
- 418 Bassetti M, Peghin M, Carnelutti A, Righi E. The role of dalbavancin in skin and soft tissue infections. *Curr Opin Infect Dis* 2018; **31**: 141–147.
- 419 Balkus JE, Mitchell C, Agnew K *et al.* Detection of hydrogen peroxide-producing *Lactobacillus* species in the vagina: a comparison of culture and quantitative PCR among HIV-1 seropositive women. *BMC Infect Dis* 2012; **12**. doi:10.1186/1471-2334-12-188.
- 420 Josephs-Spaulling J, Singh O V. Medical Device Sterilization and Reprocessing in the Era of Multidrug-Resistant (MDR) Bacteria: Issues and Regulatory Concepts. *Front Med Technol* 2021; **2**. doi:10.3389/fmedt.2020.587352.
- 421 Thurlow LR, Hanke ML, Fritz T *et al.* *Staphylococcus aureus* Biofilms Prevent Macrophage Phagocytosis and Attenuate Inflammation In Vivo . *J Immunol* 2011; **186**. doi:10.4049/jimmunol.1002794.
- 422 Ahmed MN, Abdelsamad A, Wassermann T *et al.* The evolutionary trajectories of *P. aeruginosa* in biofilm and planktonic growth modes exposed to ciprofloxacin: beyond selection of antibiotic resistance. *npj Biofilms Microbiomes* 2020; **6**. doi:10.1038/s41522-020-00138-8.
- 423 Chang CY. Surface sensing for biofilm formation in *Pseudomonas aeruginosa*. *Front. Microbiol.* 2018; **8**. doi:10.3389/fmicb.2017.02671.
- 424 Silva S, Henriques M, Martins A, Oliveira R, Williams D, Azeredo J. Biofilms of non-*Candida albicans* *Candida* species: Quantification, structure and matrix composition. *Med Mycol* 2009; **47**. doi:10.3109/13693780802549594.
- 425 Blanco-Cabra N, López-Martínez MJ, Arévalo-Jaimes BV, Martín-Gómez MT, Samitier J, Torrents E. A new BiofilmChip device for testing biofilm formation and antibiotic susceptibility. *npj Biofilms Microbiomes* 2021; **7**. doi:10.1038/s41522-021-00236-1.
- 426 Klug B, Santigli E, Westendorf C, Tangl S, Wimmer G, Grube M. From mouth to model: Combining in vivo and in vitro oral biofilm growth. *Front Microbiol* 2016; **7**. doi:10.3389/fmicb.2016.01448.
- 427 Thöming JG, Häussler S. *Pseudomonas aeruginosa* Is More Tolerant Under Biofilm Than Under Planktonic Growth Conditions: A Multi-Isolate Survey. *Front Cell Infect Microbiol* 2022; **12**. doi:10.3389/fcimb.2022.851784.
- 428 Bonne S, Mazuski JE, Sona C *et al.* Effectiveness of Minocycline and Rifampin vs Chlorhexidine and Silver Sulfadiazine-Impregnated Central Venous Catheters in Preventing Central Line-Associated Bloodstream Infection in a High-Volume Academic Intensive Care Unit: A before and after Trial. *J Am Coll Surg* 2015; **221**. doi:10.1016/j.jamcollsurg.2015.05.013.
- 429 Hashem YA, Amin HM, Essam TM, Yassin AS, Aziz RK. Biofilm formation in

- enterococci: Genotype-phenotype correlations and inhibition by vancomycin. *Sci Rep* 2017; **7**. doi:10.1038/s41598-017-05901-0.
- 430 Kamble E, Sanghvi P, Pardesi K. Synergistic effect of antibiotic combinations on *Staphylococcus aureus* biofilms and their persister cell populations. *Biofilm* 2022; **4**. doi:10.1016/j.biofilm.2022.100068.
- 431 Knafl D, Tobudic S, Cheng SC, Bellamy DR, Thalhammer F. Dalbavancin reduces biofilms of methicillin-resistant *Staphylococcus aureus* (MRSA) and methicillin-resistant *Staphylococcus epidermidis* (MRSE). *Eur J Clin Microbiol Infect Dis* 2017; **36**: 677–680.
- 432 Jacob B, Makarewicz O, Hartung A, Brodt S, Roehner E, Matziolis G. In vitro additive effects of dalbavancin and rifampicin against biofilm of *Staphylococcus aureus*. *Sci Rep* 2021; **11**. doi:10.1038/s41598-021-02709-x.
- 433 Oliva A, Stefani S, Venditti M, Di Domenico EG. Biofilm-Related Infections in Gram-Positive Bacteria and the Potential Role of the Long-Acting Agent Dalbavancin. *Front. Microbiol.* 2021; **12**. doi:10.3389/fmicb.2021.749685.
- 434 Ferri M, Ranucci E, Romagnoli P, Giaccone V. Antimicrobial resistance: A global emerging threat to public health systems. *Crit Rev Food Sci Nutr* 2017; **57**. doi:10.1080/10408398.2015.1077192.
- 435 Burke SL, Rose WE. New pharmacological treatments for methicillin-resistant *Staphylococcus aureus* infections. *Expert Opin Pharmacother* 2014; **15**: 483–491.
- 436 Dunn MJ, Fillinger RJ, Anderson LM, Anderson MZ. Automated quantification of *Candida albicans* biofilm-related phenotypes reveals additive contributions to biofilm production. *npj Biofilms Microbiomes* 2020; **6**: 1–12.
- 437 Arastehfar A, Gabaldón T, Garcia-Rubio R *et al.* Drug-resistant fungi: An emerging challenge threatening our limited antifungal armamentarium. *Antibiotics*. 2020; **9**. doi:10.3390/antibiotics9120877.
- 438 Taylor PK, Yeung ATY, Hancock REW. Antibiotic resistance in *Pseudomonas aeruginosa* biofilms: Towards the development of novel anti-biofilm therapies. *J Biotechnol* 2014; **191**. doi:10.1016/j.jbiotec.2014.09.003.
- 439 Chen Y, Liu T, Wang K *et al.* Baicalein inhibits *Staphylococcus aureus* biofilm formation and the quorum sensing system in vitro. *PLoS One* 2016; **11**: 1–18.
- 440 Kaplan JB, Mlynek KD, Hettiarachchi H *et al.* Extracellular polymeric substance (EPS)-degrading enzymes reduce staphylococcal surface attachment and biocide resistance on pig skin in vivo. *PLoS One* 2018; **13**. doi:10.1371/journal.pone.0205526.
- 441 Li J, Wang AL, Xu LJ. Biofilm maturation is correlated to drug resistance of *Candida albicans*. *Acta Anat Sin* 2009; **40**. doi:10.3969/j.issn.0529-1356.2009.03.033.
- 442 Seneviratne CJ, Samaranyake LP. Drug resistance mechanisms of fungal biofilms. In: *Biofilms: Formation, Development and Properties*. 2011.
- 443 Pereira R, dos Santos Fontenelle RO, de Brito EHS, de Moraes SM. Biofilm of *Candida*

- albicans: formation, regulation and resistance. *J. Appl. Microbiol.* 2021; **131**. doi:10.1111/jam.14949.
- 444 Lewis K. *Persister cells and infectious disease*. 2019 doi:10.1007/978-3-030-25241-0.
- 445 Song S, Wood TK. Are we really studying persister cells? *Environ. Microbiol. Rep.* 2021; **13**. doi:10.1111/1758-2229.12849.
- 446 Wood TK. Strategies for combating persister cell and biofilm infections. *Microb Biotechnol* 2017; **10**: 1054–1056.
- 447 Devlin H, Fulaz S, Hiebner DW, O’gara JP, Casey E. Enzyme-functionalized mesoporous silica nanoparticles to target *Staphylococcus aureus* and disperse biofilms. *Int J Nanomedicine* 2021; **16**. doi:10.2147/IJN.S293190.
- 448 Fulaz S, Devlin H, Vitale S, Quinn L, O’gara JP, Casey E. Tailoring nanoparticle-biofilm interactions to increase the efficacy of antimicrobial agents against *staphylococcus aureus*. *Int J Nanomedicine* 2020; **15**. doi:10.2147/IJN.S256227.
- 449 Zhu G, Wang Q, Lu S, Niu Y. Hydrogen Peroxide: A Potential Wound Therapeutic Target? *Med. Princ. Pract.* 2017; **26**. doi:10.1159/000475501.
- 450 Ormanci S, Yucel N. Biofilm formation on polystyrene and glass surface by *Aeromonas* species isolated from different sources. *J Food Process Preserv* 2017; **41**. doi:10.1111/jfpp.13223.
- 451 Zheng S, Bawazir M, Dhall A *et al.* Implication of Surface Properties, Bacterial Motility, and Hydrodynamic Conditions on Bacterial Surface Sensing and Their Initial Adhesion. *Front. Bioeng. Biotechnol.* 2021; **9**. doi:10.3389/fbioe.2021.643722.
- 452 Krsmanovic M, Biswas D, Ali H, Kumar A, Ghosh R, Dickerson AK. Hydrodynamics and surface properties influence biofilm proliferation. *Adv. Colloid Interface Sci.* 2021; **288**. doi:10.1016/j.cis.2020.102336.
- 453 Ravel G, Bergmann M, Trubuil A, Deschamps J, Briandet R, Labarthe S. Inferring characteristics of bacterial swimming in biofilm matrix from time-lapse confocal laser scanning microscopy. *Elife* 2022; **11**: 1–41.
- 454 Molina-Santiago C, Pearson JR, Navarro Y *et al.* The extracellular matrix protects *Bacillus subtilis* colonies from *Pseudomonas* invasion and modulates plant co-colonization. *Nat Commun* 2019; **10**. doi:10.1038/s41467-019-09944-x.
- 455 Vlamakis H, Aguilar C, Losick R, Kolter R. Control of cell fate by the formation of an architecturally complex bacterial community. *Genes Dev* 2008; **22**. doi:10.1101/gad.1645008.
- 456 Molina-Santiago C, Pearson JR, Berlanga-Clavero MV, Pérez-Lorente AI, de Vicente A, Romero D. A Noninvasive Method for Time-Lapse Imaging of Microbial Interactions and Colony Dynamics. *Microbiol Spectr* 2022; **10**. doi:10.1128/spectrum.00939-22.
- 457 Butini ME, Abbandonato G, Di Rienzo C, Trampuz A, Di Luca M. Isothermal microcalorimetry detects the presence of persister cells in a *Staphylococcus aureus* biofilm

- after vancomycin treatment. *Front Microbiol* 2019; **10**. doi:10.3389/fmicb.2019.00332.
- 458 Butini ME, Gonzalez Moreno M, Czuban M *et al*. Real-Time Antimicrobial Susceptibility Assay of Planktonic and Biofilm Bacteria by Isothermal Microcalorimetry. In: *Advances in Experimental Medicine and Biology*. 2019 doi:10.1007/5584_2018_291.
- 459 Sultan AR, Tavakol M, Lemmens-Den Toom NA *et al*. Real time monitoring of *Staphylococcus aureus* biofilm sensitivity towards antibiotics with isothermal microcalorimetry. *PLoS One* 2022; **17**. doi:10.1371/journal.pone.0260272.